TKI resistance in CML cell lines: Investigating resistance pathways

Carine Tang

The Melissa White Laboratory
Centre for Cancer Biology and
SA Pathology
&
The Faculty of Health Sciences
Department of Medicine
The University of Adelaide
South Australia

Thesis submitted to the University of Adelaide
in candidature for the degree of Doctor of Philosophy
2011

Supervisors: Prof. Timothy Hughes[1,2] & A/Prof. Deborah White[1,2]

1 The Melissa White Laboratory, Division of Haematology, IMVS

2 Centre for Cancer Biology, Adelaide, Australia

Table of Contents

Declaration 12
Acknowledgements 13
Glossary 15
Abstract 18

Chapter 1: **20**
Introduction **20**
1.1 Chronic myeloid leukaemia 21
1.2 The Philadelphia chromosome and BCR-ABL 21
1.2.1 BCR-ABL is sufficient to cause CML 21
1.3 CML treatment 25
1.3.1 Non-specific therapies 25
1.3.2 Imatinib mesylate 26
1.3.3 Nilotinib & Dasatinib 29
1.4 IC50 and Intracellular Uptake and Retention assay (IUR) 29
1.5 OCT-1 32
1.6 ABCB1 and ABCG2 35
1.6.1 TKI interaction with ABCB1 and ABCG2 38
1.6.1.1 Imatinib 38
1.6.1.2 Nilotinib 39
1.6.1.3 Dasatinib 40
1.7 Haematopoietic Stem Cells 40
1.8 Mechanisms of resistance to TKIs 41
1.8.1 BCR-ABL expression induces genomic instability 41
1.8.2 BCR-ABL kinase domain mutations 44
1.8.3 Upregulation of TKI efflux proteins 49
1.8.4 BCR-ABL overexpression 50
1.8.4.1 Homogeneously staining regions and double minutes 51
1.8.5 BCR-ABL independent resistance 51
1.9 Generation of TKI resistance in vitro, and investigating the kinetics and interplay of resistance mechanism emergence 53
1.10 Hypothesis 55
1.11 Aims 55

Chapter 2: **56**
Materials and Methods **56**
2.1 Commonly used reagents 57
2.2 Solutions, buffers and media 57
2.2.1 Cell culture media 57

2.2.2 Tyrosine kinase inhibitors 58
2.2.2.1 Imatinib mesylate 58
2.2.2.2 Nilotinib 58
2.2.2.3 Dasatinib 58
2.2.2.4 100µM 14C-Imatinib mixture (50%) 58
2.2.2.5 100µM 14C-Dasatinib mixture (50%) 58
2.2.3 Prazosin hydrochloride – inhibits OCT-1 58
2.2.4 PSC833 – inhibits ABCB1 59
2.2.5 Ko143 – inhibits ABCG2 59
2.2.6 Flow cytometry Fixative (FACS Fix) 59
2.2.7 Freeze Mix 59
2.2.8 Laemmli's Buffer 59
2.2.9 Membrane blocking solution (2.5%) 60
2.2.10 SDS-Polyacrylamide Gel 60
2.2.11 1×TBS 60
2.2.12 1×TBST 60
2.2.13 dNTP set (N = A, C, G, T) 60
2.2.14 Random Hexamer Primer 61
2.3 Cell lines 61
2.3.1 K562 61
2.3.2 K562 Dox 61
2.3.3 KU812 61
2.4 General Techniques 61
2.4.1 Tissue culture 61
2.4.2 Cell counts 62
2.4.3 Cryopreservation of cells 62
2.4.4 Thawing cells 62
2.5 Specialised Techniques 62
2.5.1 Generation of TKI resistant cell lines 62
2.5.1.1 Sampling intermediate lines for analysis 63
2.5.2 DNA extraction 63
2.5.3 Quantitative DNA PCR 64
2.5.4 mRNA extraction 65
2.5.5 cDNA synthesis 65
2.5.6 RQ-PCR: BCR-ABL transcript quantitation 66
2.5.7 Sequencing the BCR-ABL kinase domain 67
2.5.7.1 Conventional sequencing 69
2.5.7.2 MassARRAY sequencing (Sequenom) 69
2.5.8 RQ-PCR: Lyn transcript quantitation 71
2.5.9 IC50 assay and Western blot 73
2.5.10 Flow cytometry 73

2.5.10.1 Measurement of ABCB1/ABCG2 cell-surface expression. 73
2.5.10.2 Cell viability 74
2.5.11 Intracellular Uptake and Retention (IUR) assay 75
2.5.12 Cytogenetic analysis 75
2.5.12.1 Fluorescence in situ hybridisation (FISH) 75
2.5.12.2 Karyotyping 77
2.5.13 Statistics 77

Chapter 3: 78
Imatinib resistance in the K562 cell line is mediated by BCR-ABL overexpression 78
3.1 Introduction 79
3.1.1 Adherence and dose-interruptions 79
3.1.2 Suboptimal kinase inhibition 79
3.1.3 Generation of imatinib-resistant cell lines 80
3.1.4 BCR-ABL overexpression 81
3.1.5 The K562 cell line 82
3.2 Approach 83
3.2.1 Generation of imatinib-resistant cell lines 83
3.2.2 Analysis of imatinib-resistant cell lines 88
3.3 Results 90
3.4 Discussion 107

Chapter 4: 111
Imatinib resistance in the K562 Dox cell line is mediated by ABCB1 overexpression 111
4.1 Introduction 112
4.1.1 The multidrug resistance protein, ABCB1 112
4.1.2 ABCB1 expression in CML 113
4.1.3 The breast cancer resistance protein, ABCG2 115
4.1.4 The K562 Dox cell line 116
4.2 Approach 117
4.2.1 Generating imatinib resistance in the K562 Dox cell line 117
4.2.2 Analysis of imatinib-resistant cell lines 118
4.3 Results 119
4.4 Discussion 134

Chapter 5: 137
BCR-ABL kinase domain mutations arise in the setting of BCR-ABL overexpression, in imatinib- and dasatinib-resistant cell lines 137
5.1 Introduction 138
5.1.1 BCR-ABL kinase domain mutations 138
5.1.2 BCR-ABL expression and kinase domain mutations 139

5.1.3 Conventional sequencing and the MassARRAY technique....140
5.1.4 The KU812 cell line....141
5.2 Approach....143
5.2.1 Generating dasatinib resistance in the K562 and K562 Dox cell lines....143
5.2.2 Generating imatinib resistance in the KU812 cell line....145
5.2.3 Re-escalation of intermediates in imatinib, dasatinib or nilotinib....146
5.2.4 Analysis of dasatinib- and imatinib-resistant cell lines....147
5.3 Results....150
5.3.1 Dasatinib resistance in the K562 cell line....150
5.3.2 Dasatinib-resistance in K562 Dox cell lines....156
5.3.2.1 The K562 Dox 200nM DAS1 cell line....156
5.3.2.2 The K562 Dox 200nM DAS2 cell line....164
5.3.3 Imatinib-resistance in KU812 cell lines....172
5.3.3.1 The KU812 2µM IM1 cell line....172
5.3.3.2 The KU812 3µM IM2 cell line....176
5.3.3.3 The KU812 2µM IM3 cell line....182
5.4 Discussion....192
5.4.1 BCR-ABL overexpression precedes the emergence of KD mutations....192
5.4.2 BCR-ABL expression levels significantly decrease upon the emergence of KD mutations 194
5.4.3 Kinetics of DAS-resistance development in the K562 200nM DAS cell line....195
5.4.4 A V299L-carrying clone emerged early on in DAS exposure in the K562 Dox cell line....198
5.4.5 Multiple KD mutations emerged in imatinib-resistant KU812 cell cultures....199

Chapter 6:....202
TKI cross-resistance and differential resistance in imatinib- and dasatinib-resistant CML cell lines....202
6.1 Introduction....203
6.1.1 TKI cross-resistance and differential resistance....203
6.1.2 BCR-ABL independent resistance: Src family kinases....203
6.2 Approach....205
6.3 Results....206
6.3.1 TKI cross-resistance in the K562 200nM DAS cell line....206
6.3.2 Differential TKI resistance and cross-resistance in the K562 Dox 200nM DAS1 and 2 cell lines....206
6.3.3 ABCB1 overexpression confers TKI cross-resistance in the K562 Dox 2µM IM1, IM2 and IM3 cell lines....210
6.3.4 BCR-ABL overexpression and KD mutations in the KU812 2µM IM1, 3µM IM2 and 2µM IM3 cell lines conferred differential or cross-resistance to TKIs....213
6.3.5 BCR-ABL and Lyn overexpression in the K562 2µM IM1 and IM2 cell lines conferred differential or cross-resistance to TKIs....213
6.4 Discussion....222

6.4.1 TKI-cross resistance 222
6.4.2 Differential resistance 224
6.4.3 Lyn overexpression in the K562 2µM IM2 cell line: Is it really a BCR-ABL-independent resistance mechanism? 225

Chapter 7: 226
Discussion 226
7.1 Introduction 227
7.2 TKI resistance mechanisms 227
7.3 Studying the kinetics of TKI resistance mechanism emergence 228
7.4 Major findings of this study 229
7.4.1 Kinase domain mutations arise in the setting of BCR-ABL overexpression 229
7.4.2 Resistance mechanism emergence is stochastic 230
7.4.3 Different TKIs may foster different resistance mechanisms 231
7.4.4 Different cell lines responded differently to a given TKI 232
7.4.5 TKIs share the same broad resistance susceptibilities 233
7.4.6 Src kinase overexpression may not be a BCR-ABL *independent* resistance mechanism 233
7.5 Future directions 234
7.6 Summary & Conclusion 234

Appendix I 236
AI.1 Quantitative DNA PCR setup sheet 237
AI.2 RQ-PCR for BCR-ABL quantitation setup sheet 238
AI.3 BCR-ABL mRNA quantitation setup sheet 239
AI.4 DNA sequence of the Abl gene 240
AI.5 Kinase domain mutations included in the MassARRAY sequencing screen 242
AI.6 Lyn quantitation setup sheet 243
AI.7 Western blots for Table 6.1: Dasatinib IC50s for the K562 Dox 200nM DAS1 cell line and intermediates 244
AI.8 Western blots for Table 6.1: Nilotinib IC50s for the K562 Dox 200nM DAS1 cell line and intermediates 245
AI.9 Western blots for Table 6.1: Imatinib IC50s for the K562 Dox 200nM DAS1 cell line and intermediates 246
AI.10 Western blots for Figure 6.4: Nilotinib IC50s for the K562 Dox 2µM IM1, IM2 and IM3 cell lines and Naïve controls 247
AI.11 Western blots for Figure 6.4: Nilotinib IC50s with PSC833 for the K562 Dox 2µM IM1, IM2 and IM3 cell lines and Naïve controls 248
AI.12 Western blots for Figure 6.4: Dasatinib IC50s for the K562 Dox 2µM IM1, IM2 and IM3 cell lines and Naïve controls 249
AI.13 Western blots for Figure 6.4: Dasatinib IC50s with PSC833 for the K562 Dox 2µM IM1, IM2 and IM3 cell lines and Naïve controls 250

AI.14 Western blots for Table 6.2: Imatinib IC50s for the KU812 2µM IM1 and 3µM IM2 cell lines and KU812 Naïve control 251
AI.15 Western blots for Table 6.2: Nilotinib IC50s for the KU812 2µM IM1 and 3µM IM2 cell lines and KU812 Naïve control 252
AI.16 Western blots for Table 6.2: Dasatinib IC50s for the KU812 2µM IM1 and 3µM IM2 cell lines and KU812 Naïve control 253
AI.17 Western blots for Table 6.3: Imatinib IC50s for the KU812 2µM IM3 cell line and intermediates 254
AI.18 Western blots for Table 6.3: Nilotinib IC50s for the KU812 2µM IM3 cell line and intermediates 255
AI.19 Western blots for Table 6.3: Dasatinib IC50s for the KU812 2µM IM3 cell line and intermediates 256
AI.20 Western blots for Figure 6.5 & 6.6: Nilotinib and dasatinib IC50s for the K562 2µM IM1 and IM2 cell lines 257

Appendix II

Publication arising from this thesis 258

References 268

List of Figures and Tables

Figure 1.1: The Philadelphia Chromosome 22
Figure 1.2: The Philadelphia chromosome and the BCR-ABL oncoprotein....23
Figure 1.3: Signal transduction pathways affected by BCR-ABL....24
Figure 1.4: Molecular structure of imatinib mesylate 27
Figure 1.5: Mechanism of action of imatinib 28
Figure 1.6: Molecular structure of nilotinib 30
Figure 1.7: Molecular structure of dasatinib....31
Figure 1.8: Protein structure of OCT-1 (SLC22A1)....34
Figure 1.9: Protein structure of ABCB1 (MDR1; P-glycoprotein)....36
Figure 1.10: Protein structure of ABCG2 (BCRP)....37
Figure 1.11: Mechanisms of resistance to TKIs....42
Figure 1.12: The effects of BCR-ABL on mutagenesis....45
Figure 1.13: Map of BCR-ABL KD mutations....46
Figure 1.14: Nilotinib and dasatinib have different critical binding residues in the ABL kinase domain, compared to imatinib....47
Figure 1.15: Differential sensitivity of kinase domain mutations to the three TKIs – imatinib, nilotinib and dasatinib....48

Figure 3.1: The K562 Naïve cell line does not carry any BCR-ABL kinase domain mutations 84
Figure 3.2: ABCB1 cell-surface expression in the IM1 and IM2 resistant cell lines....86
Figure 3.3: ABCG2 cell-surface expression in the IM1 and IM2 resistant cell lines 87
Figure 3.4: Viability assay by trypan blue analysis: K562 Naïve versus K562 2µM IM1 & IM2 cell lines 91
Figure 3.5: Viability by Annexin V and 7AAD staining: K562 Naïve versus K562 2µM IM1 & IM2 cell lines 92
Figure 3.6: Example of a K562 Naïve $IC50^{imatinib}$ Western blot quantification....93
Figure 3.7: $IC50^{imatinib}$ of the K562 Naïve, K562 2µM IM1 and K562 2µM IM2 cell lines 95
Figure 3.8: Average IC50 imatinib for K562 Naïve, K562 2µM IM1 and K562 2µM IM2 96
Figure 3.9: Imatinib IUR assay: K562 Naïve cell line versus K562 2µM IM1 cell line 97
Figure 3.10: Imatinib IUR assay: K562 Naïve cell line versus K562 2µM IM2 cell line 98
Figure 3.11: Intermediate BCR-ABL expression in the IM1 and IM2 resistant cell lines 100
Figure 3.12: Interphase FISH to identify BCR-ABL fusion genes 101
Figure 3.13: Karyotype of the K562 Naïve cell line....102
Figure 3.14: Karyotype of K562 2µM IM1 and IM2 cell lines 103
Figure 3.15: Metaphase FISH to identify markers carrying Bcr-Abl....105
Figure 3.16: Bcr-Abl copy number in the IM1 and IM2 resistant cell lines....106

Figure 4.1: The development of a multidrug resistant (MDR) cancer 114
Figure 4.2: Intermediate BCR-ABL mRNA expression in the K562 Dox 2µM IM1, IM2 and IM3 cell lines 120
Figure 4.3: ABCG2 cell surface expression in IM-resistant K562 Dox cell lines....121
Figure 4.4: ABCB1 cell surface expression increased in the K562 Dox IM-resistant cell lines 122
Figure 4.5: K562 Dox IM-resistant cell lines have a reduced imatinib intracellular uptake and retention (IUR) compared to K562 Dox Naïve control cells 123
Figure 4.6: Example of a K562 Dox Naïve $IC50^{imatinib}$ Western blot quantification 127
Figure 4.7: K562 Dox IM-resistant cell lines have increased $IC50^{imatinib}$ compared to K562 Dox Naïve control cells 129
Figure 4.8: In the presence of PSC833, K562 Dox IM-resistant cell lines have similar $IC50^{imatinib}$ values compared to K562 Dox Naïve control cells 131
Figure 4.9: PSC833 removes the significant difference in $IC50^{imatinib}$ values between the three IM-resistant K562 Dox lines and Naïve controls 133

Figure 5.1: Karyotype of KU812 cell line when first established 142
Figure 5.2: Src-mediated pathways contribute to cancer progression....144
Figure 5.3: K562 DMSO $IC50^{dasatinib}$ Western blot quantification 148
Figure 5.4: The K562 200nM DAS cell line has an increased $IC50^{DAS}$ compared to the K562 Naïve and DMSO control cell lines 151
Figure 5.5: The average $IC50^{DAS}$ for K562 200nM DAS was significantly greater than that of the K562 Naïve and DMSO control cell lines 152
Figure 5.6: The K562 200nM DAS cell line does not express ABCB1 or ABCG2 153
Figure 5.7: Dasatinib IUR does not differ between the K562 200nM DAS cell line and the K562 Naïve and DMSO control cell lines 154
Figure 5.8: BCR-ABL expression levels and KD mutation status in the K562 200nM DAS cell line ...155
Figure 5.9: Bcr-Abl copy number in intermediates of the K562 200nM DAS cell line....157
Figure 5.10: Cell surface expression of ABCB1 or ABCG2 in the K562 Dox 200nM DAS1 cell line...158
Figure 5.11: Dasatinib IUR does not differ between the K562 Dox 200nM DAS1 cell line and the K562 Dox Naïve control cell line 160
Figure 5.12: BCR-ABL expression increased until the emergence of the V299L mutation in a DAS-resistant K562 Dox cell line 161
Figure 5.13: Bcr-Abl copy number in selected intermediates of the K562 Dox 200nM DAS1 cell line 162
Figure 5.14: Interphase FISH to identify Bcr-Abl fusion genes 163
Figure 5.15: Cell surface expression of ABCB1 or ABCG2 in the K562 Dox 40nM and 55nM dasatinib re-escalation cell lines 165
Figure 5.16: The V299L mutation emerged when the K562 Dox 55nM DAS1 intermediate was re-escalated in dasatinib 166
Figure 5.17: The V299L mutation emerged when the K562 Dox 40nM DAS1 intermediate was re-escalated in dasatinib 167

Figure 5.18: There was no change in cell surface expression of ABCB1 or ABCG2 in the K562 Dox 500nM NIL re-escalation cell lines 168
Figure 5.19: Re-escalation of the K562 Dox 55nM intermediate in NIL resulted in the emergence of the G250E mutation or increased BCR-ABL expression 169
Figure 5.20: Cell surface expression of ABCB1 or ABCG2 in the K562 Dox 200nM DAS2 cell line 170
Figure 5.21: Intermediate BCR-ABL expression levels in the K562 Dox 200nM DAS2 cell line 171
Figure 5.22: Cell surface expression of ABCB1 and ABCG2 in the KU812 2µM IM1 cell line 173
Figure 5.23: The imatinib IUR in the KU812 2µM IM1 cell line was not significantly different from the KU812 Naïve cell line, and was not affected by blocking ABCG2 174
Figure 5.24: BCR-ABL expression increased until the emergence of three KD mutations in the KU812 2µM IM1 cell line 175
Figure 5.25: Bcr-Abl DNA copy number was significantly increased in the KU812 2µM IM1 cell line compared to the KU812 Naïve cell line 177
Figure 5.26: Karyotype of the KU812 Naïve cell line 178
Figure 5.27: Karyotypes of the heterogeneous KU812 2µM IM1 population 179
Figure 5.28: Interphase FISH to identify Bcr-Abl fusion genes 180
Figure 5.29: BCR-ABL expression and KD mutation status in the KU812 3µM IM2 cell line 181
Figure 5.30: Bcr-Abl DNA copy number was significantly increased in the KU812 3µM IM2 cell line compared to the KU812 Naïve cell line 183
Figure 5.31: Interphase FISH to identify Bcr-Abl fusion genes 184
Figure 5.32: Cell surface expression of ABCB1 and ABCG2 in the KU812 3µM IM2 cell line 185
Figure 5.33: Cell surface expression of ABCB1 and ABCG2 in the KU812 2µM IM3 cell line 186
Figure 5.34: BCR-ABL expression increased until the emergence of the F359C mutation KU812 2µM IM3 cell line 187
Figure 5.35: Bcr-Abl DNA copy number did not significantly change in the KU812 2µM IM3 intermediates or final cell line compared to the KU812 Naïve cell line 188
Figure 5.36: Interphase FISH to identify Bcr-Abl fusion genes 189
Figure 5.37: The F359C mutation emerged when the KU812 200nM IM3 intermediate was re-escalated in imatinib 191
Table 5.1: Summary of resistance mechanisms detected in three TKI-resistant cell lines exposed to IM or DAS, as well as those detected in the re-escalated cell cultures. 193
Figure 5.38: Representations of possible clonal kinetics of resistance emergence 196

Figure 6.1: The K562 200nM DAS cell line displayed overt resistance to imatinib and nilotinib despite previous exposure to dasatinib only 207
Figure 6.2: The average $IC50^{IM}$ and $IC50^{NIL}$ for K562 200nM DAS was significantly greater than that of the K562 Naïve and DMSO control cell lines 208
Table 6.1: The K562 Dox 200nM DAS1 cell line has differential resistance to DAS, NIL and IM 209
Figure 6.3: The K562 Dox 200nM DAS2 cell line displayed overt resistance to dasatinib, imatinib and nilotinib despite previous exposure to dasatinib only 211

Figure 6.4: ABCB1 inhibition ablates NIL and DAS resistance in the three IM-resistant K562 Dox cell lines 212
Table 6.2: The $IC50^{IM}$, $IC50^{NIL}$ and $IC50^{DAS}$ of the KU812 2µM IM1 and 2µM IM2 cell lines compared to the KU812 Naïve cell line 214
Table 6.3: The KU812 2µM IM3 cell line exhibits differential resistance to IM, NIL and DAS 215
Figure 6.5: Nilotinib IC50 and viability of the K562 2µM IM1 and IM2 cell lines 216
Figure 6.6: Dasatinib IC50 and viability of the K562 2µM IM1 and IM2 cell lines 219
Figure 6.7: Lyn kinase expression was significantly increased in the K562 2µM IM2 cell line 221
Table 6.4: Summary of resistance mechanisms detected in the eleven imatinib- or dasatinib-resistant cell lines generated in this study 223

Declaration

I, Carine Tang, certify that this thesis contains no material which has been accepted for the award of any other degree or diploma in any university or other tertiary institution and, to the best of my knowledge and belief, contains no material previously published or written by another person, except where due reference has been made in the text.

I give consent for this copy of my thesis, when deposited in the University Library, to be available for loan and photocopying, subject to the provisions of the Copyright Act 1968. I also give permission for the digital version of my thesis to be made available on the web, via the University's digital research repository, the Library catalogue and also through web search engines, unless permission has been granted by the University to restrict access for a period of time.

Carine Tang

1st September 2011

Acknowledgements

Romans 13:7 *Render therefore to all their dues: tribute to whom tribute is due; custom to whom custom; fear to whom fear; honour to whom honour.*

The past three and a half years have gone surprisingly fast! Time flies when you're having fun, and although I'm not sure 'fun' is the word I would use to describe doing a Phd, it has been a mostly enjoyable and incredibly rewarding experience.

Firstly I must thank Tim and Deb – my fantastic supervisors who have been consistently encouraging and supportive from day one. Your guidance, critique and ideas were essential for all of my achievements (exciting results, conference attendance, poster presentations and a publication……or two?).

Many thanks also to the tireless team that is the Melissa White Laboratory: Eva, Chung, Tamara, Verity, Amity, Phuong, Kelvin, Jarrad, Jenny, Stephanie Z. You have all taught me something, helped me in some way, and patiently answered my many questions. Thanks also to Bron, Ljiljana, Sasha and especially Steph A. for all your work behind the scenes. I must also thank all the MWL students, past and present: Devendra, Jane, Jackie, Laura, Dale, Lisa, Oi-Lin and Liu. Thanks for the support, advice, camaraderie, and for the laughs (you know who you are).

My many tireless hours down in Molecular Pathology would have been much more difficult (and dull) if it wasn't for Susan Branford, Wendy, Jodi and Chani. Thank you so very much for teaching me many useful techniques, for being patient with me, and thanks to Sarah Moore for the incredibly useful karyotyping and FISH results!

Thanks to you Mum for getting me this far – for never giving up on my education, and for instilling in me a strong work ethic and drive for success.

What can I say about my darling Neptune? You have been there with me for many-a weekend tissue culture and late-night Western transfer, and you've never complained. I could not ask for anyone more encouraging, supportive and patient. Thank you for making me laugh whenever I needed it (which was all the time), and for just being you.

Lastly and most importantly, I thank the Lord Jesus Christ, my Creator and personal Saviour. To You belongs all the credit and glory.

Psalms 18:30 *As for God, His way is perfect: the word of the LORD is tried: He is a buckler to all those that trust in Him.*

Glossary

ABCB1/ABCG2	ATP binding cassette (ABC) transporter proteins B1 and G2
ALL	Acute lymphoblastic leukaemia
AP	Accelerated phase
APS	Ammonium persulfate
ATP	Adenosine triphosphate
BC	Blast crisis
BCR	Breakpoint cluster region
BCR-ABL	Breakpoint cluster region-Ableson kinase fusion transcript/protein
Bcr-Abl	Breakpoint cluster region-Ableson kinase fusion gene
C	Celcius
CCR	Complete cytogenetic response
CD	Cluster of differentiation
cDNA	Complementary deoxyribonucleic acid
CHO	Chinese hamster ovary
CHR	Complete haematologic response
CML	Chronic myeloid leukaemia
CP	Chronic phase
Crkl	CT10 regulator of kinase-like
DABCO	1,4-diazabicyclo[2.2.2]octane
DAS	Dasatinib
ddNTP	Dideoxynucleotide triphosphate
DEPC	Diethyl pyrocarbonate
DMSO	Dimethyl sulphoxide
dmin	Double minutes
DNA	Deoxyribonucleic acid
dNTP	Deoxynucleotide triphosphates
DTT	Dithiothreitol
FACS	Fluorescence activated cell sorting
FISH	Fluorescent *in situ* hybridisation

GUSB	Beta-glucuronidase
HBSS	Hanks Balanced Salt Solution
Hck	Haemopoietic cell kinase
HCl	Hydrochloric acid
HSR	Homogenously staining region
IC50	Inhibitory concentration 50%
IgG	Immunoglobulin G
IM	Imatinib mesylate
JAK	Janus kinase
KD	Kinase domain
kD	Kilo Dalton
KDR	Kinase insert domain protein receptor
L	Litre
Lyn	V-yes-1 Yamaguchi sarcoma viral related oncogene homolog
M	Molar (Moles per litre)
Mbq	Mega Becquerel (10^{6} Becquerel)
MCR	Major cytogenetic response
MDR	Multidrug resistance
µCi	Micro Curie (10^{-6} Curie)
µg	Micro gram (10^{-6} gram)
µM	Micro molar (10^{-6} Molar)
MMR	Major molecular response
mM	Milli molar (10^{-3} Molar)
mRNA	Messenger ribonucleic acid
NHEJ	Non-homologous end-joining
NIL	Nilotinib
nM	Nano molar (10^{-9} Molar)
OCT-1	Organic cation transporter 1
PBS	Phosphate buffered saline
PCR	Polymerase chain reaction
Ph	Philadelphia chromosome

PI3-K	Phosphatidylinositol – 3-kinase
P-loop	Phosphate binding loop
PVDF	Polyvinylidene Fluoride
P-value	Probability value
RANKL	Receptor activator of nuclear factor kappa-b ligand
RNA	Ribonucleic acid
ROC	Receiver operating characteristic
RPMI	Roswell Park Memorial Institute (-1640 medium)
RT	Room temperature
RQ-PCR	Real-time quantitative polymerase chain reaction
SD	Standard deviation
SDS-PAGE	Sodium dodecyl sulphate polyacrylamide gel electrophoresis
SEM	Standard error of the mean
SH	Src Homology domain
SN	Supernatant
Src	Sarcoma
SSC	Saline-Sodium Citrate buffer
TBS	Tris buffered saline
TBST	Tris buffered saline with 0.1% Tween20
TKI	Tyrosine kinase inhibitor
Tris	Tris(hydroxymethyl)aminomethane
UV	Ultra violet

Abstract

Chronic myeloid leukaemia (CML) is characterised by the presence of the Philadelphia chromosome which harbours the Bcr-Abl oncogene. BCR-ABL is a constitutively active tyrosine kinase that can be inhibited by rationally designed tyrosine kinase inhibitors (TKIs) such as imatinib, nilotinib and dasatinib. Although TKI therapy is an effective treatment for many patients, resistance can arise. There are currently four identified resistance mechanisms. These are 1) overexpression of drug-efflux proteins (ABCB1 and ABCG2), 2) BCR-ABL kinase domain (KD) mutations, 3) increased BCR-ABL expression and 4) BCR-ABL independent mechanisms such as Lyn kinase expression. In this study the interplay between these four recognised modes of TKI resistance is investigated.

Imatinib- and dasatinib-resistant cell lines were established and used to investigate TKI resistance *in vitro*. Viability and IC50 assays were used to demonstrate TKI sensitivity/resistance. Flow cytometry was used to screen for ABCB1 and ABCG2 cell surface expression, while conventional sequencing and the MassARRAY method were used to determine the mutation status of the BCR-ABL KD. Fluorescence *in situ* hybridisation (FISH) and quantitative DNA PCR were used to investigate Bcr-Abl DNA copy number, and RQ-PCR was used to investigate expression levels of BCR-ABL and Lyn mRNA.

These studies revealed that IM-resistant K562 cell lines exhibited increased BCR-ABL expression at the onset of resistance. Interestingly, these cell lines had increased viability and IC50s for IM and NIL, while the DAS IC50s were variable. Further investigation revealed Lyn overexpression in the cell line which was more sensitive to DAS. The development of a DAS-resistant K562 culture resulted in the emergence of the T315I mutation. Studies of the intermediate stages of resistance of this DAS-resistant cell line revealed that increased BCR-ABL expression occurred gradually, preceding the emergence of the mutation, at which time the BCR-ABL expression decreased and plateaued. Thus, it appears that increased BCR-ABL expression may be the initial mechanism of resistance, followed by the emergence of a KD mutation which has a clear selective advantage. This phenomenon was observed a further four times (in a DAS-resistant K562 Dox culture, and in three IM-resistant KU812 cultures) each time with the emergence of different KD mutations. Different KD mutations resulted in differential resistance to the three TKIs used in this study.

In contrast, three IM-resistant K562 Dox cell lines were not found to have any KD mutations, nor BCR-ABL overexpression. Instead, the primary cause of resistance in these lines appeared to be an increase in ABCB1 expression. The addition of PSC833 (an ABCB1 inhibitor) decreased the IM, NIL, and DAS IC50s for all three resistant lines to the level of the naïve control. This indicated that ABCB1 expression, facilitating active efflux of the drugs, is the primary mechanism of resistance in these lines.

This study demonstrates that KD emergence is a stochastic event, as the same mutation did not always occur twice when exposed to the same TKI. However, increased ABCB1 expression was more likely to arise recurrently in the predisposed K562 Dox cell line. Notably, different TKIs elicited different resistant mechanisms, and all but one (the Lyn overexpressing K562 cell line) were BCR-ABL dependent. Furthermore, all resistant cell lines showed cross-resistance (at least to some extent) to the three TKIs tested, suggesting that currently available TKIs share the same susceptibilities to drug resistance.

Chapter 1:

Introduction

1.1 Chronic myeloid leukaemia

Chronic myeloid leukaemia (CML) is a cancer of haematopoietic progenitors and is characterised by the increased, unregulated growth of predominantly myeloid cells in the bone marrow[1]. These cells include neutrophils, basophils, eosinophils and monocytes[2], and although they are present in abnormally high numbers in CML patients, they retain relatively normal function[3]. Symptoms of CML include fatigue, weight loss, sweating, anaemia, haemorrhaging and splenomegaly, however approximately 20-40% of patients are asymptomatic at diagnosis, which often occurs as the result of a routine blood test[3]. CML accounts for approximately 15-20% of all leukaemias, and has an annual incidence of 0.001%[4]. Untreated, the disease is tri-phasic progressing from a chronic phase (CP) lasting 3-5 years, to an accelerated phase (AP) lasting up to 12 months, and lastly a 3-6 month terminal phase known as blast crisis (BC)[5].

1.2 The Philadelphia chromosome and BCR-ABL

The cytogenetic hallmark of CML is the Philadelphia chromosome, which is present in almost all CML patients, and is the result of a reciprocal translocation between chromosomes 9 and 22[6] **(Figure 1.1)**. This results in fusion of the Abelson kinase gene (ABL) from chromosome 9, with the breakpoint cluster region (BCR) gene of chromosome 22. The resultant Bcr-Abl fusion gene transcribes a novel, chimeric 8.5kb mRNA, which in turn encodes a hybrid 210kDa protein (p210)[4] **(Figure 1.2)**. Depending on the break-point, the fusion protein may be 230, 210 or 185/190kD[7]. The BCR-ABL protein is a constitutively active tyrosine kinase[6] which activates various signal transduction pathways (such as the JAK/STAT, Raf/MEK/ERK, and PI3K/Akt pathways[8], **Figure 1.3**) leading to enhanced proliferation, resistance to apoptosis, cytokine-independent survival[8], altered protein trafficking and suppression of granulocytic differentiation[7]. These characteristics result in the overproduction of leukocytes (and progressively, the presence of more immature leukocytes/blasts in the blood) leading to the CML phenotype[5].

1.2.1 BCR-ABL is sufficient to cause CML

Various CML mouse models have been generated and have provided an experimental system to investigate CML pathogenesis and progression[9-13]. Huettner *et. al.*[9] created transgenic mice that expressed p210 BCR-ABL under the control of a tetracycline-off system. When tetracycline (tet) was

Figure 1.1

Figure 1.1: The Philadelphia Chromosome
The Philadelphia Chromosome arises from the reciprocal translocation of the long arms of chromosomes 9 and 22[1]. (CML Society of Canada, 2007, http://www.cmlsociety.org/?q=node/14)[14].

Figure 1.2

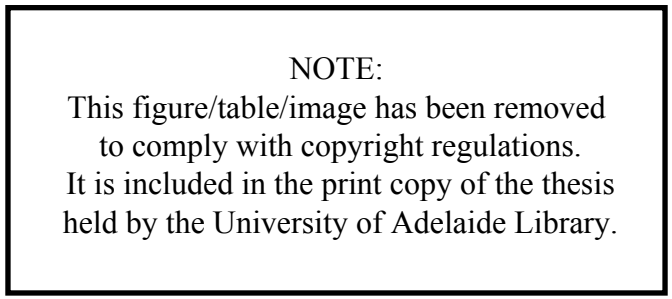

Figure 1.2: The Philadelphia chromosome and the BCR-ABL oncoprotein
The Ph chromosome encodes the BCR-ABL fusion oncoproptein, which is transcribed into messenger RNA (mRNA) molecules with e13a2 or e14a2 junctions, which are then translated, producing p210 BCR-ABL. BCR-ABL contains functional domains from the N-terminus of BCR (dimerization [DD], SRC-homology 2 [SH2]–binding, and the Rho GTP–GDP exchange-factor [GEF] domains) and the C-terminal end of ABL. Tyrosine 177 (Y177) in the BCR portion, and tyrosine 412 (Y412) in the ABL portion, are important for the docking of adapter proteins and for BCR-ABL autophosphorylation, respectively. P-S/T denotes phosphoserine and phosphothreonine (Goldman & Melo, 2003, New England Journal of Medicine)[15].

Figure 1.3

Figure 1.3: Signal transduction pathways affected by BCR-ABL
The key pathways implicated so far are those involving RAS, mitogen-activated protein (MAP) kinases, signal transducers and activators of transcription (STAT), phosphatidylinositol 3-kinase (PI3K), and MYC. Most of the interactions are mediated through tyrosine phosphorylation and require the binding of BCR-ABL to adapter proteins such as growth factor receptor–bound protein 2 (GRB-2), DOK, CRK, CT10 regulator of kinase-like protein (Crkl), SRC-homology–containing protein (SHC), and casitas-B-lineage lymphoma protein (CBL). Downstream effects of BCR-ABL activity include increased proliferation, survival signals and cytokine-independent survival, as well as reduced apoptotic signals (Goldman & Melo, 2003, New England Journal of Medicine)[15].

present in the drinking water of the mice, expression of p210 BCR-ABL was suppressed and the mice remained healthy. However when tet was removed from their drinking water, the mice developed leukaemia and died within 4-11 weeks. It was further discovered that mice, even in advanced stages of the disease (which exhibited leukocytosis, splenomegaly and in some cases lymphadenopathy) could be cured by addition of tet back into the drinking water, which resulted in a drop in their white cell count and normalisation within 48-72hrs. Other leukaemic symptoms disappeared within 5 days of tet re-introduction. Mice could undergo multiple rounds of induction and reversion of the disease, indicating that BCR-ABL is both necessary and sufficient to cause CML, and that silencing of this oncogene may be the key to curing the disease[9]. To date, methods of inhibition of BCR-ABL in humans have been the focus of much research, and resulted in the development of tyrosine kinase inhibitors (TKIs) such as imatinib mesylate[16].

1.3 CML treatment

1.3.1 Non-specific therapies

Prior to the mid-nineties, CML patients were treated with hydroxyurea and busulfan (chemotherapy agents) to alleviate symptoms. However, neither drug could elicit lasting cytogenetic responses, and neither significantly affected the rate of progression to fatal blast crisis[17]. Interferon-α was the first agent proven capable of modifying the biological course of CML by prolonging survival in patients[7] by a median of 20 months (57% survival rate at 5 years after diagnosis, compared with 42% survival on hydroxyurea or busulfan chemotherapy)[18]. However, interferon treatment only resulted in complete and partial cytogenetic remissions[a] in 0-16% and 0-38% of patients respectively, and progression from chronic phase to accelerated or blast phase was merely delayed[18]. Allogeneic bone marrow transplant (BMT) can be curative, however there are limitations to eligibility for this procedure (*e.g.* limitations of age and matched donor availability). Furthermore, there is ~50% probability of survival at 10 years after receiving a BMT in chronic phase – which is reduced to 25% and 15% for patients transplanted in AP or BC respectively[19].

[a] Complete cytogenetic response (CCR) indicates the absence of the Philadelphia chromosome in 20 metaphases on classical karyotyping performed on the bone marrow, and portends favourable prognosis. Partial cytogenetic response indicates 1-34% Ph-positive metaphases[6].

1.3.2 Imatinib mesylate

In the mid-nineties a process of rational design lead to the development of imatinib mesylate (otherwise known as Glivec, produced by Novartis Pharmaceuticals)[20]. Originally, it was noted that 2-phenylaminopyrimidines were potent inhibitors of the Abl kinase. Random screening (utilising large libraries of different molecular combinations) resulted in the modification of the original 2-phenylaminopyrimidine back-bone, and the creation of imatinib mesylate[20] **(Figure 1.4)**.

Imatinib acts by competitively binding at the adenosine tri-phosphate (ATP)-binding site of both the normal Abl and BCR-ABL proteins, stabilising the protein in the inactive conformation and thus preventing ATP hydrolysis and subsequent phosphorylation of substrates[4,21,22] **(Figure 1.5)**. Shortly after its development, imatinib was shown to suppress the proliferation of BCR-ABL-expressing cells *in vitro* and *in vivo*[23]. In colony-forming assays of blood and bone marrow from CML patients, imatinib caused a 92-98% decrease in the number of Bcr-Abl positive colonies, while the colony potential of Bcr-Abl negative cells was unaffected[23]. Since 1998 imatinib has been used in clinical trials on humans[20]. The introduction of imatinib has given new hope for curing CML, as 87% of patients treated with the drug achieved a complete cytogenetic response by 5 years, and 93% did not progress to accelerated phase or blast crisis[24]. Furthermore, patients receiving long-term imatinib treatment had significantly reduced levels of BCR-ABL transcript present in their blood[25]. The ultimate goal of CML therapy is to induce complete molecular remission, *i.e.* elimination of BCR-ABL transcripts by real-time quantitative PCR (RQ PCR)[6]. Despite the success of imatinib therapy to date, several issues require addressing in order to make CML treatment more universally effective. For example, some patients exhibit resistance to imatinib (either primary or acquired), which may be mediated by mutations in the BCR-ABL kinase domain (KD) and thus prevent imatinib from binding and inhibiting the enzyme[7]. Furthermore, only 4% of patients taking imatinib achieve complete molecular remission at 30 months[26]. Lastly, cessation of imatinib treatment leads to a rapid relapse into chronic phase in approximately 50% of patients, even when complete molecular remission had been previously achieved and maintained for a minimum of two years[27-29]. It is therefore theorised that a population of leukaemic haematopoietic stem cells is responsible for relapse, and that these progenitors are insensitive to imatinib therapy. Due to these limitations, and increasing incidence of resistance to imatinib, alternative TKIs were developed including nilotinib (AMN107, Novartis Pharmaceuticals) and dasatinib (BMS-354825, Bristol Myers Squibb)[30].

Figure 1.4

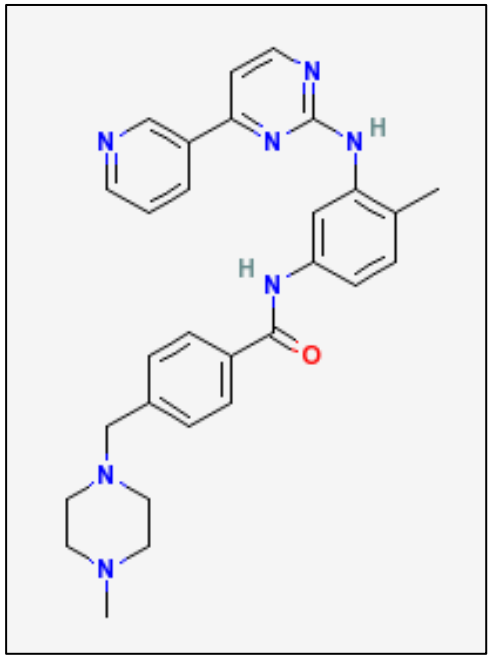

Figure 1.4: Molecular structure of imatinib mesylate
The chemical structure of imatinib mesylate (4-[(4-Methyl-1-piperazinyl) methyl]-N-[4-methyl-3-[[4-(3-pyridinyl)-2-pyrimidinyl]amino] phenyl]-benzamide monomethanesulfonate) is shown above. Molecular weight = 589.7 g/mol (NCBI, PubChem Compound; 2011)[31].

Figure 1.5

Figure 1.5: Mechanism of action of imatinib
A) BCR-ABL activity in the absence of imatinib is shown. Substrates are constitutively phosphorylated, resulting in activation of downstream effector molecules and cell proliferation *i.e.* the CML phenotype. **B)** Imatinib binds BCR-ABL in the ATP binding pocket of the kinase domain. This binding stabilises BCR-ABL in the inactive conformation, thereby preventing ATP binding, and preventing substrate phosphorylation and disease phenotype (Mughal & Goldman, 2006, Frontiers in bioscience)[32].

1.3.3 Nilotinib & Dasatinib

Through molecular, chemical and crystallography studies the detailed structure of BCR-ABL was elucidated, enabling improved design of TKIs that are able to bind the BCR-ABL kinase domain more efficiently[30].

Nilotinib **(Figure 1.6)** and dasatinib **(Figure 1.7)** are approximately 30 and 300 times more potent, respectively, in inhibiting BCR-ABL than imatinib[30,33,34]. Both are effective against many cell lines exhibiting imatinib resistance due to KD mutations. For example, mutations M244V, G250E and Q252H all render BCR-ABL insensitive to imatinib binding, but do not hinder binding with nilotinib or dasatinib. Of the 16 mutations tested by O'Hare *et. al.*[33], the only exception was the T315I mutation, which is insensitive to all three TKIs.

Nilotinib is a more selective Abl inhibitor, while dasatinib was designed to bind with less specificity, thereby having a broader spectrum of action including activity against the Sarcoma (Src) family of tyrosine kinases[30,33]. A recent study showed that Src kinases activated by BCR-ABL remained fully active in imatinib-treated mice, suggesting a deficiency in imatinib's ability to inactivate all BCR-ABL signalling pathways. However, dasatinib, which inhibits both BCR-ABL and the Src kinases, was able to afford complete remission of acute lymphoblastic leukaemia (ALL) in mice[35]. It has also been shown that dasatinib targets an earlier progenitor population than imatinib in primary CML, but does not eliminate the elusive quiescent fraction[26]. Both nilotinib and dasatinib have been approved for patient use, and offer hope to patients who exhibit resistance, or who have a poor primary response, to imatinib. Studies have shown that initial patient sensitivity to imatinib treatment varies, and that this is a major determinant of patient response[36].

1.4 IC50 and Intracellular Uptake and Retention assay (IUR)

Patient response to imatinib is determined by how well imatinib is able to bind and inhibit BCR-ABL in Ph+ cells. In an effort to investigate this intrinsic sensitivity in patients, an assay was developed to test BCR-ABL inactivation by imatinib *in vitro*. The 50% inhibitory concentration for imatinib ($IC50^{imatinib}$) assay measures the decrease of CT10 regulator of kinase like (Crkl) in its phosphorylated form, otherwise known as p-Crkl. Crkl is a BCR-ABL adaptor protein, and is the predominant phosphorylated protein in K562 cells (a BCR-ABL–expressing erythroblastoid cell line)[37,38].

Figure 1.6

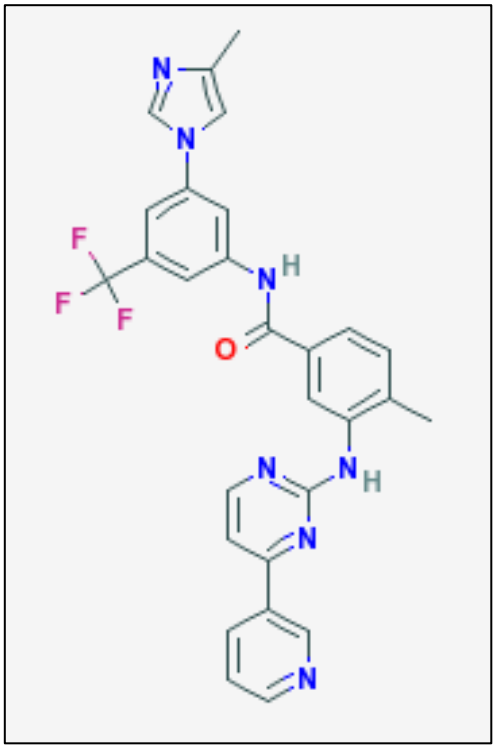

Figure 1.6: Molecular structure of nilotinib
The chemical structure of nilotinib (4-methyl-N-(3-(4-methylimidazol-1-yl)-5-(trifluoromethyl)phenyl)-3-((4-pyridin-3-ylpyrimidin-2-yl)amino) ben-zamide) is shown above. Molecular weight = 529.51579 g/mol (NCBI, PubChem Compound; 2011)[31].

Figure 1.7

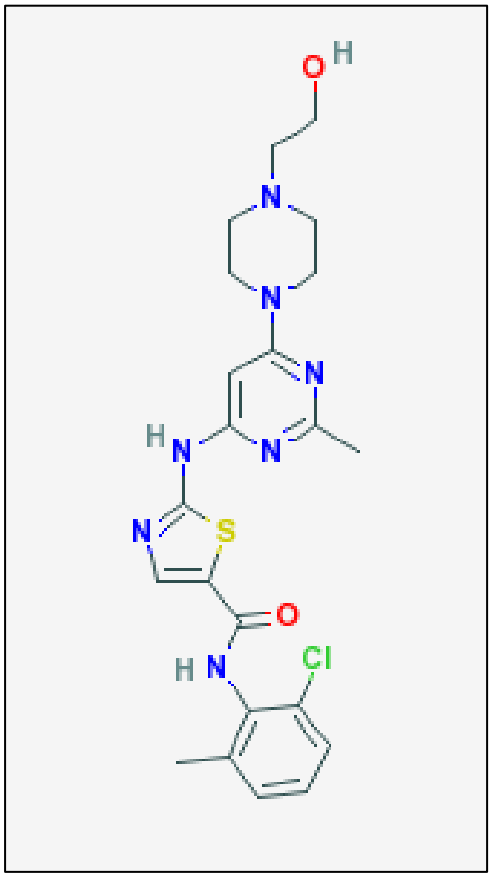

Figure 1.7: Molecular structure of dasatinib
The chemical structure of dasatinib (N-(2-chloro-6-methylphenyl)-2-[[6-[4-(2-hydroxyethyl)-1-piperazinyl]-2-methyl-4-pyrimidinyl]amino]-5-thia-zolecarboxamide, monohydrate) is shown above. Molecular weight = 488.00554 g/mol (NCBI, PubChem Compound; 2011)[31].

Importantly, p-Crkl levels correlate well with levels of BCR-ABL, and p-Crkl is not detectable by Western blot in Bcr-Abl–negative cells[36,37]. The $IC50^{imatinib}$ is therefore defined as the *in vitro* concentration of drug required to reduce phosphorylation of Crkl (*i.e.* p-Crkl levels) by 50%[39]. Patients with a high $IC50^{imatinib}$ (low sensitivity to imatinib) were found to have a significantly lower probability of achieving cytogenetic and molecular remissions by 12 months, thus providing evidence that the degree of BCR-ABL inhibition achieved in patients is a critical determinant of response to imatinib[36]. Less interpatient variability was observed in IC50 with nilotinib, and values were on average 14-fold lower than for imatinib, confirming that nilotinib is a more potent inhibitor of BCR-ABL activity[39].

It has been shown that interpatient variability observed in $IC50^{imatinib}$ assays is mainly due to differences in the efficiency of intracellular uptake and retention (IUR) of the drug[39]. In an IUR assay, ^{14}C-imatinib is added to patient cells and incubated at 37ºC/5%CO_2 for a set time (*e.g.* 2 hrs) before being washed and analysed by a scintillation counter for presence of radioactivity. In this way it is possible to measure the nanograms of drug present in the cell after 2hrs of incubation. It was found that $IC50^{imatinib}$ correlated well with imatinib IUR[39], indicating that a major determinant of patient response to imatinib was the ability of the drug to enter and remain in Ph+ cells. Investigation then turned to mechanisms of imatinib uptake, which was found to be temperature dependent, and therefore likely to be an active process requiring ATP[40]. Thomas *et. al.*[40] conducted experiments inhibiting members of the organic cation transporter (OCT) family, which implicated the OCT-1 transporter in imatinib uptake.

1.5 OCT-1

The largest superfamily of transporters, the solute carrier (SLC) superfamily, contains a subgroup known as SLC22. In humans, this subgroup consists of 12 family members of OCTs[41,42]. While most plasma membrane transporters are substrate specific, the polyspecific OCT family recognises compounds with different sizes and molecular structures. Furthermore, OCTs translocate organic cations in an electrogenic[b] manner, and can do so in either direction across the plasma membrane. These transporters are generally involved in drug uptake in the small intestine and in drug export in

[b] Electrogenic transport is an active, coupled transport process driven by electric potentials that alters the transmembrane electrical gradient.

the liver and kidney. Various compounds are known to inhibit OCTs, but are not transported themselves[42].

OCT-1 **(Figure 1.8)** was first identified in 1994[43] and in humans is principally expressed in the liver[42,44], although it is also expressed in the large and small intestine, stomach, lungs, kidneys and heart[42]. Although not well understood, regulation of human OCT-1 cell surface expression/function is thought to be mediated by calmodulin/calmodulin-dependent kinase II and Src-like kinases (*e.g.* $p56^{lck}$ tyrosine kinase) which stimulate expression, and by protein kinase A (PKA) which is inhibitory[42,44]. Interestingly, regulation of OCTs may affect their affinity for certain substrates, thereby altering their selectivity. For example, when PKA is activated, or Ca^{2+}/CaM inhibited, hOCT-1 affinity for tetraethylammonium decreases six-fold. This is because regulation by phosphorylation/dephosphorylation induces conformational changes in the transporter, thus altering substrate affinity[45,46].

Imatinib is a substrate of OCT-1, and this transporter is known to be the primary mode of active uptake of imatinib in haematopoietic cells[39,40]. Furthermore, OCT-1 mRNA expression has been linked to patient response to imatinib[47,48]. When Crossman *et. al.*[47] categorised patients as either 'responders' (achieving complete cytogenetic response to imatinib within 12 months of treatment) or 'non-responders' (retaining >65% Ph+ karyotypes in the first 10 months of imatinib treatment), RQ-PCR revealed that responders expressed roughly eight-fold more OCT-1 mRNA than non-responders[47]. This suggested that OCT-1 mRNA expression may enable prediction of imatinib response in patients. Indeed, Wang *et. al.*[48] examined OCT-1 mRNA levels in patients prior to imatinib treatment, and found that those with 'high' expression (levels above the median value) had superior cytogenetic responses and progression free survival compared to patients with 'low' OCT-1 expression levels (below the median). However, these studies were not conducted at diagnosis, nor did they examine OCT-1 function. Other influences such as post-transcriptional regulation, membrane localisation and polymorphisms in OCT-1 may play a greater role in determining imatinib response[42,49,50].

Figure 1.8

Figure 1.8: Protein structure of OCT-1 (SLC22A1)
The OCT-1 protein is thought to contain 12 transmembrane domains. Both the N and C termini are located intracellularly. The first large extracellular loop contains three putative *N*-linked glycosylation sites, indicated by branches (Jonker & Schinkel, 2004, The Journal of Pharmacology and Experimental Therapeutics)[51].

An assay was therefore developed to assess OCT-1 activity, and this was investigated in newly diagnosed CML patients. OCT-1 activity was defined as the IUR of ^{14}C-imatinib, minus the IUR in the presence of prazosin (a potent OCT-1 inhibitor)[52]. A significant correlation was observed between $IC50^{imatinib}$ and OCT-1 activity, where patients with a low $IC50^{imatinib}$ had significantly greater OCT-1 activity than patients with high $IC50^{imatinib}$. The same correlation was not observed between $IC50^{imatinib}$ and OCT-1 mRNA expression. Thus it was concluded that OCT-1 functional activity is a significant indicator of imatinib response in *de novo* CML patients[52,53]. Studies suggest that uptake of nilotinib and dasatinib is not mediated by OCT-1, but is primarily passive (*i.e.* by diffusion)[39,54,55]. As well as active influx, the efflux of TKIs is also an important factor in efficacy.

1.6 ABCB1 and ABCG2

Present in almost all living organisms[56], the ATP binding cassette (ABC) transporter proteins are involved in the ATP-fuelled efflux of a wide range of substrates[57]. Substrates include lipids, organic anions, amino acids, carbohydrates, vitamins, glucoronide, glutathione conjugates and xenobiotics/toxins which are transported across the plasma membrane[58]. In doing so, these transporters are able to guard vital body compartments, such as the brain, the fetus, the germ line and haematopoietic stem cells, against invading xenobiotics[57]. Based on their structural similarity, the 48 known ABC transporters have been categorised into seven families named ABC(A-G)[58]. All functionally active ABC transporters contain a minimum of two ABC units and two transmembrane domains (TMDs). These four elements are usually present in a single polypeptide chain, known as a 'full-length' transporter. Members of the ABCG family possess only a single ABC and a single TMD - such 'half-length' transporters must form homo- or heterodimers (via a disulfide bridge) in order to become functional[56,58].

In recent years, multidrug resistance (MDR) has been observed in many cancer patients undergoing chemotherapy. MDR occurs when cancerous cells develop resistance to a chemotherapeutic agent during the course of treatment. In many cases, when resistance develops against a single drug, the resulting phenotype is a cancer that is resistant to a wide range of drugs. In humans, the three major types of MDR proteins include members of the ABCB, ABCC and the ABCG subfamily[56]. Of these, ABCB1 (MDR1, p-glycoprotein (P-gp)) (**Figure 1.9**) and ABCG2 (breast cancer resistance protein

Figure 1.9

Figure 1.9: Protein structure of ABCB1 (MDR1; P-glycoprotein)
The 170-180kD protein consists of 12 transmembrane domains, and two large cytoplasmic domains which contain ATP binding sites. The N-terminal region is modified by 10-15kD glycosylation (indicated by branching)[59]. ABCB1 is known to be responsible for the efflux of various chemotherapeutic drugs (see blue box) (adapted from Sorrentino, 2002, Nature Reviews[60]).

Figure 1.10

Figure 1.10: Protein structure of ABCG2 (BCRP)
One ABCG2 polypeptide is shown, which forms a homodimer bridged by disulfide bonds to facilitate transport function. Green bars represent the 6 transmembrane domains, while yellow branching on extracellular domains indicates glycosylation sites. The purple circle represents the ABC domain (ABC: ATP Binding Cassette), located at the N-terminus (adapted from Sarkadi *et. al.* 2011, Drug Metabolism Tech Review)[61].

(BCRP)) (**Figure 1.10**) are known to interact with imatinib mesylate[62-65], nilotinib[66-70], and dasatinib[55,67-69] and are therefore of greatest interest in this study.

1.6.1 TKI interaction with ABCB1 and ABCG2

1.6.1.1 Imatinib

Contention remains as to whether imatinib merely inhibits ABCB1 and ABCG2[62-65], or whether the drug is actually effluxed by these transporters[40,71-76]. Some argue that both inhibition and transport occurs in the ABCB1-imatinib interaction[73]. Jordanides *et. al.*[62] used primitive CML $CD34^+$ cells (which were found to express 6.8-fold more ABCG2 than normal CD34+ cells) to investigate imatinib efflux. The addition of imatinib to cells resulted in a dose-dependent decrease in efflux of BODIPY-prazosin (B-P), a known ABCG2 substrate. However, this experiment did not distinguish between imatinib acting as an inhibitor or a competitive substrate. It was reasoned that if imatinib were a substrate for ABCG2, then co-treatment with a known ABCG2 inhibitor, fumitremorgin (FTC), would enhance the effect of imatinib and cause increased cell death. As the combination of imatinib and FTC did not result in a decrease of viable cells, it was concluded that imatinib was an inhibitor, but not a substrate, of ABCG2[62]. Similarly, Houghton *et. al.*[63] found that in the human osteosarcoma cell line (Saos2), imatinib sensitivity was unaltered by the expression of ABCG2, but topotecan[c] resistance was reversed by imatinib[77]. It was therefore concluded that imatinib is a potent inhibitor of ABCG2, but not a substrate. Imatinib was also found to be a poor substrate of ABCB1 in a study conducted by Ferrao *et. al*[65]. It was found that imatinib sensitivity of K562 cells was similar regardless of ABCB1 expression. Conversely, Burger *et. al.*[72] demonstrated that, in a panel of well-defined ABCG2-overexpressing cell lines, the accumulation of ^{14}C-imatinib was significantly decreased as compared to parental cell lines. Furthermore, imatinib was found to compete with mitoxantrone (a known ABCG2 substrate) for export, and Ko-143 (an ABCG2 inhibitor) prevented imatinib efflux. In 2005 the same group demonstrated that imatinib accumulation was significantly decreased in KB-8-5 cells (a human epidermoid carcinoma cell line overexpressing ABCB1) compared with the parental cell line which lacked ABCB1 expression[71]. Burger *et. al.* ascribed their results (which conflicted with Jordanides *et. al.*[62], Houghton *et. al.*[63] and Ferrao *et. al.*[65]) to methodological differences, including the time and temperature at which imatinib was incubated with the cells[72]. Illmer *et. al.*[74], and Ozvegy-Laczka *et.*

[c] Topotecan is a chemotherapeutic agent that inhibits DNA topoisomerase I and is effluxed by ABCG2.

al.[75] supported these results, while Hamada *et. al.*[73] concluded that imatinib is a substrate *as well as* a modulator of human ABCB1. Although intracellular imatinib accumulation decreased upon ABCB1 expression in a porcine kidney cell line, it was also found that the imatinib inhibitory effect on ABCB1 was slightly weaker than cyclosporin A, but stronger than verapamil (K_i values for the inhibition of ABCB1 function by cyclosporin A, imatinib and verapamil were calculated as 6.1, 18.3 and 540µM respectively)[73].

Lastly, it has been shown that some polymorphisms in ABCB1 (*e.g.* 1236T) are associated with an increased incidence of imatinib treated patients achieving MMR (85% vs 47.7% for other genotypes). Furthermore the 1236C-2677G-3435C haplotype was statistically linked to less frequent MMR (70% vs 44.6%). This finding implicates a role for ABCB1 in CML outcome – likely to be mediated by its efflux of imatinib[76].

1.6.1.2 Nilotinib

Nilotinib transport is also controversial, as various studies have come to different conclusions regarding this drug's interaction with ABCB1 and ABCG2. Davies *et. al.*[78] found that nilotinib (1-5µM) was not transported by ABCB1 or ABCG2 in CML CD34+ cells. In contrast, Brendel *et. al.*[66] showed that nilotinib interacts with ABCG2 in murine KSL cells, as Hoechst efflux was inhibited in the presence of the drug. Furthermore, ABCG2 expression in K562 cells conferred protection from cell death when exposed to nilotinib (10-25nM), and prevented Crkl dephosphorylation. In 200nM nilotinib, K562-ABCG2 cells had significantly decreased intracellular concentrations of nilotinib compared to the K562-parental line. Blocking ABCG2 with an inhibitor (FTC) increased intracellular nilotinib concentration back to levels of the parental line[66].

Hegedus *et. al.*[69] used K562 Dox (a cell line derived from K562 which expresses ABCB1 due to selection with doxorubicin[79]) and K562-ABCG2 cells (retrovirally transduced with ABCG2[80]) and showed ABCG2, but not ABCB1, conferred protection against the cytotoxic effects of nilotinib. However, nilotinib was able to reduce levels of phospho-BCR-ABL when ABCB1 or ABCG2 was blocked in the respective cell lines[69]. Tiwari *et. al.*[70] found nilotinib was an inhibitor of both ABCB1 and ABCG2 at a concentration of 2.5µM. However, this does not exclude that nilotinib may be transported by these proteins at nanomolar concentrations which may be more pharmacologically relevant. Mahon *et. al.*[81] found that the K562 Dox cell line had increased resistance to nilotinib (1-100nM) compared to the K562 parental line, but that this resistance could be reversed by blocking ABCB1 with verapamil or

PSC833. Furthermore, nilotinib-resistant LAMA84[d] cells (generated by long-term nilotinib culture reaching 20nM) over-expressed BCR-ABL and ABCB1, and blocking ABCB1 with verapamil partially restored sensitivity to nilotinib[81]. Together, these studies clearly indicated some interaction between nilotinib and the efflux proteins ABCB1 and ABCG2. Whether this TKI acts as an inhibitor, or is actually transported, may be concentration dependent. However, it appears that at pharmacologically relevant concentrations, nilotinib is transported[66,81].

1.6.1.3 Dasatinib

Dasatinib transport is less controversial, as several groups have shown the drug is effluxed by both ABCB1 and ABCG2. Hegedus *et. al.*[69] demonstrated that ABCB1 and ABCG2 conferred protection against the cytotoxic effects of dasatinib using K562 Dox and K562-ABCG2 cells. Similarly, Hiwase *et. al.*[55] showed that $IC50^{DAS}$ could be reduced in the K562 Dox and K562-ABCG2 cell lines by the addition of PSC833 or Ko143 (ABCB1 and ABCG2 inhibitors respectively). Furthermore, dasatinib IUR was significantly lower in the K562 Dox, VBL-100, K562-ABCG2 and Mef-BCRP1 cell lines, compared to their non-ABCB1/ABCG2-expressing counterparts[55]. These studies indicate that dasatinib is indeed effluxed by ABCB1 and ABCG2.

It has been suggested that a narrow concentration range exists, within which TKIs may be transported by the efflux transporters, while above this concentration TKIs act as inhibitors[56]. Although debate on clinical relevance continues, it is known that CML haematopoietic stem cells (HSCs) exhibit resistance to imatinib, and may use efflux transport as a mechanism to achieve this[82].

1.7 Haematopoietic Stem Cells

CML haematopoietic stem cells (HSCs) are thought to be responsible for patient relapse when imatinib treatment is discontinued[6]. HSCs exhibit resistance to imatinib and use several mechanisms to achieve this, for example, increased BCR-ABL expression. Some of the most primitive haematopoietic cells ($lin^-CD34^+CD38^-$) express the highest levels of BCR-ABL mRNA, and differentiation is accompanied by decreasing expression[82]. In HSCs, intracellular BCR-ABL concentration may be high enough such that physiologically achievable TKI concentrations are too low to effectively inhibit BCR-ABL[7,83]. Additionally, BCR-ABL is thought to stimulate growth factor expression (*e.g.* IL-3 and G-CSF), thereby conferring resistance against the apoptotic effects of

[d] The LAMA84 cell line is a human, BCR-ABL positive, CML cell line that was established from a CML patient in accelerated phase.

imatinib[7,82]. Furthermore, CML HSC's have significantly increased expression of ABCB1 and ABCB2 (but low expression of the imatinib-influx protein, OCT-1) and differentiation is accompanied by decreased expression of efflux proteins and increased expression of OCT-1[56,82]. This phenomenon may simply be a measure by which stem cells protect themselves, and the body thereby retains integrity of the reparative stem cell population. However, HSC resistance to imatinib (and therefore failure to cure CML) may be an unfortunate consequence.

1.8 Mechanisms of resistance to TKIs

Primary resistance is defined as the inability of a patient to achieve a landmark response[84], for example a major cytogenetic response by 6 months, a complete cytogenetic response by 12 months, or a major molecular response by 18 months[52]. Approximately 2% of patients fail to achieve a haematologic response (normalisation of white blood cell counts), while 8-13% fail to achieve a major or complete cytogenetic response[84]. Primary resistance to imatinib is thought to be conferred by decreased OCT-1 activity in the patient, thereby preventing adequate imatinib uptake and function[52]. Primary resistance to nilotinib and dasatinib (for which cellular uptake is predominantly passive[39,54,55]) is much less common.

Secondary resistance is defined as the loss of recovery benchmarks while on treatment, for example the loss of cytogenetic or haematologic response and disease progression while taking imatinib. After 2 years of treatment, approximately 10% of patients in CP will exhibit resistance to imatinib mesylate (increasing to 40-50% for patients in AP and 80% in BC)[7]. There are several molecular mechanisms contributing to this phenomenon **(Figure 1.11)**.

1.8.1 BCR-ABL expression induces genomic instability

BCR-ABL is both a result, and cause, of genomic instability. The fusion gene is itself a product of two double-stranded breaks that have been repaired aberrantly resulting in the t(9;22) reciprocal translocation. Double stranded breaks are caused by a number of factors, such as ionizing radiation, chemicals, DNA replication stresses and free radicals (*i.e.* reactive oxygen species (ROS)). Endogenous ROS are normally produced in the cell by the electron transport chain in the mitochondria, and the majority are quenched by superoxide dismutase or glutathione peroxidases[85,86]. ROS include superoxide (O_2^-), hydrogen peroxide (H_2O_2) and the hydroxyl free radical (•OH). These

Figure 1.11

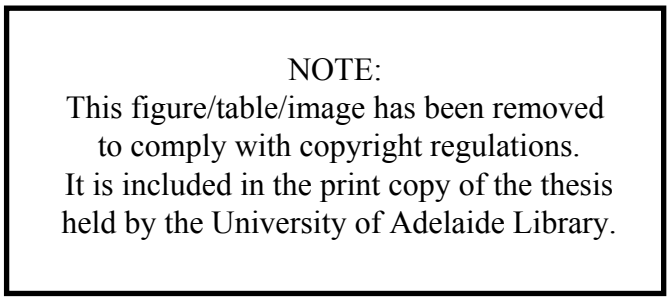

Figure 1.11: Mechanisms of resistance to TKIs
A) Efflux proteins (MDR-1/ABCB1 or ABCG2) can decrease the intracellular concentration of drug in the cell. **B)** Plasma protein binding (*e.g.* binding with α_1-acidic glycoprotein) may decrease the extracellular concentration of the drug. **C)** KD mutations may prevent TKI binding and inhibiting BCR-ABL (*e.g.* T315I). **D)** Down-stream mutations rendering the cell independent of BCR-ABL survival signals (*e.g.* constitutive activation of a Src family member). **E)** Amplification of the BCR-ABL gene, leading to tyrosine kinase overexpression. (Krause & Van Etten, 2005, New England Journal of Medicine)[87].

intermediates of oxygen reduction are reactive and potentially damaging to all molecules, including DNA[85,86]. During DNA synthesis, oxidatively modified bases may be incorporated into the DNA by unfaithful polymerases, resulting in nucleotide mismatches, substitutions or strand breaks[86,88].

BCR-ABL expression in haematopoietic cell lines induces production of ROS[89-91], likely through a PI3K/mTOR pathway-dependent mechanism[92]. Sattler *et. al.*[89] first demonstrated that transfecting the Ba/F3, 32Dc13, and MO7e cell lines with Bcr-Abl resulted in an increase in ROS levels (by flow cytometry) compared to untransformed controls. ROS production is directly due to BCR-ABL, as both imatinib and anti-oxidants abrogate these effects[89,91,93]. Interestingly, Y177F mutated BCR-ABL fails to increase ROS levels, suggesting this residue is critical for ROS generation[92].

Normally, DNA damage activates cell cycle checkpoints and repair mechanisms, however if the damage is too great, cells commit to apoptosis[94]. BCR-ABL kinase activity promotes cell survival and inhibits apoptosis through the Ras/Raf and PI3K/Akt pathways[8,95]. Furthermore, Keeshan *et. al.*[96] have shown that translocation of apoptotic signals Bax and Bad to the mitochondria is blocked in cells expressing high levels of BCR-ABL, and that BCR-ABL prevents late mitochondrial depolarization and caspase 9 and 3 cleavage. Thus, BCR-ABL promotes survival and proliferation in cases when normal cells would apoptose due to DNA damage.

BCR-ABL expressing cell lines have consistently increased genetic and chromosomal abnormalities[97,98] and have been shown to have an increased incidence of sister chromatid exchange and chromosomal translocations after DNA damage[99]. The increase in genetic abnormalities observed in Bcr-Abl positive cells indicates a loss of fidelity in DNA repair. Stoklosa *et. al.*[100] observed a decrease in mismatch repair in both murine haematopoietic cells expressing BCR-ABL, as well as primary CD34+ CML cells compared to control cells, however the mechanism by which this occurs remains unclear. Another study has shown that BCR-ABL down-regulates BCRA1[99] – a protein involved in genome surveillance and repair[101]. Furthermore, BCR-ABL expression increases repair of DNA double-stranded breaks through the error-prone non-homologous end-joining (NHEJ) mechanism up to five-fold, with compromised repair fidelity[102-104]. Nowicki *et. al.*[93] found that BCR-ABL kinase activity enhanced NHEJ activity, and was responsible for a statistically significant loss of DNA during NHEJ (35% of repair products lost more than 100bp) compared to cells not expressing BCR-ABL. In summary, BCR-ABL generates ROS which damages DNA. Instead of undergoing apoptosis,

the cell survives due to BCR-ABL driving survival signals, and low-fidelity repair is promoted resulting in the accumulation of mutations and genomic instability (**Figure 1.12**).

1.8.2 BCR-ABL kinase domain mutations

Imatinib mesylate binds BCR-ABL at the ATP-binding pocket of the kinase domain (KD), stabilising it in the inactive conformation. Specific residues in the KD are necessary for this interaction, as they facilitate the inactive conformation of the tyrosine kinase, and also provide hydrogen bonds for binding[22,105].

Residues in the kinase domain of BCR-ABL may mutate such that the TKI can no longer bind BCR-ABL[105-108] **(Figure 1.13)**. It was once thought that such mutations would render the kinase non-functional, as the ATP-binding site would be compromised. However, it is now known that the TKI and ATP binding sites only party overlap, so a mutation that prevents drug binding may still be enzymatically active[22,109]. KD mutations are selected for in the leukaemic population, as cells harbouring the mutations survive therapy and expand, resulting in a cancer that is resistant to the TKI. In studies using imatinib, KD mutations have been observed to occur after commencing treatment, and may be present at very low levels prior to treatment[107,110-113]. Drug therapy therefore selects and expands clones that may already be present, and when selective pressure is removed (ie. TKI therapy stopped) the mutant clone often decreases as wild-type outgrows[114-116].

KD mutations may be differentially sensitive to different TKIs, as critical binding residues differ between the drugs. That is, patients who have developed imatinib-resistant KD mutations may find a second-generation TKI, such as nilotinib or dasatinib, is effective against the mutated BCR-ABL, as these potent drugs do not require the same residues for binding as imatinib[117,118] **(Figure 1.14)**. Thus, although a KD mutation may prevent imatinib binding to BCR-ABL, nilotinib or dasatinib may still be able to effectively bind and inhibit BCR-ABL kinase activity[119-121] **(Figure 1.15)**. The T315I mutation however, is a notable exception, as this mutation confers resistance to all three drugs[33,107,122,123]. Thr315 is therefore known as the 'gatekeeper' residue, as this is a critical binding residue for all three drugs, and mutations at this site confer overt resistance to all three[124]. *In vitro* mutagenesis screens of BCR-ABL reveal that mutations may also occur outside of the KD (*e.g.* in the neighbouring linker, SH3-SH2 and Cap domains), influencing conformation and leading to imatinib resistance through

Figure 1.12

Figure 1.12: The effects of BCR-ABL on mutagenesis
A) BCR-ABL causes DNA damage through its generation of ROS. **B)** BCR-ABL activity promotes cell survival, despite the presence of DNA damage which would cause most cells to apoptose. **C)** BCR-ABL interacts directly and indirectly with repair proteins contributing to rapid but low fidelity repair. Overall, the activity of BCR-ABL results in the accumulation of mutations and destabilisation of the genome (Burke & Carroll, 2010, Leukemia)[97].

Figure 1.13

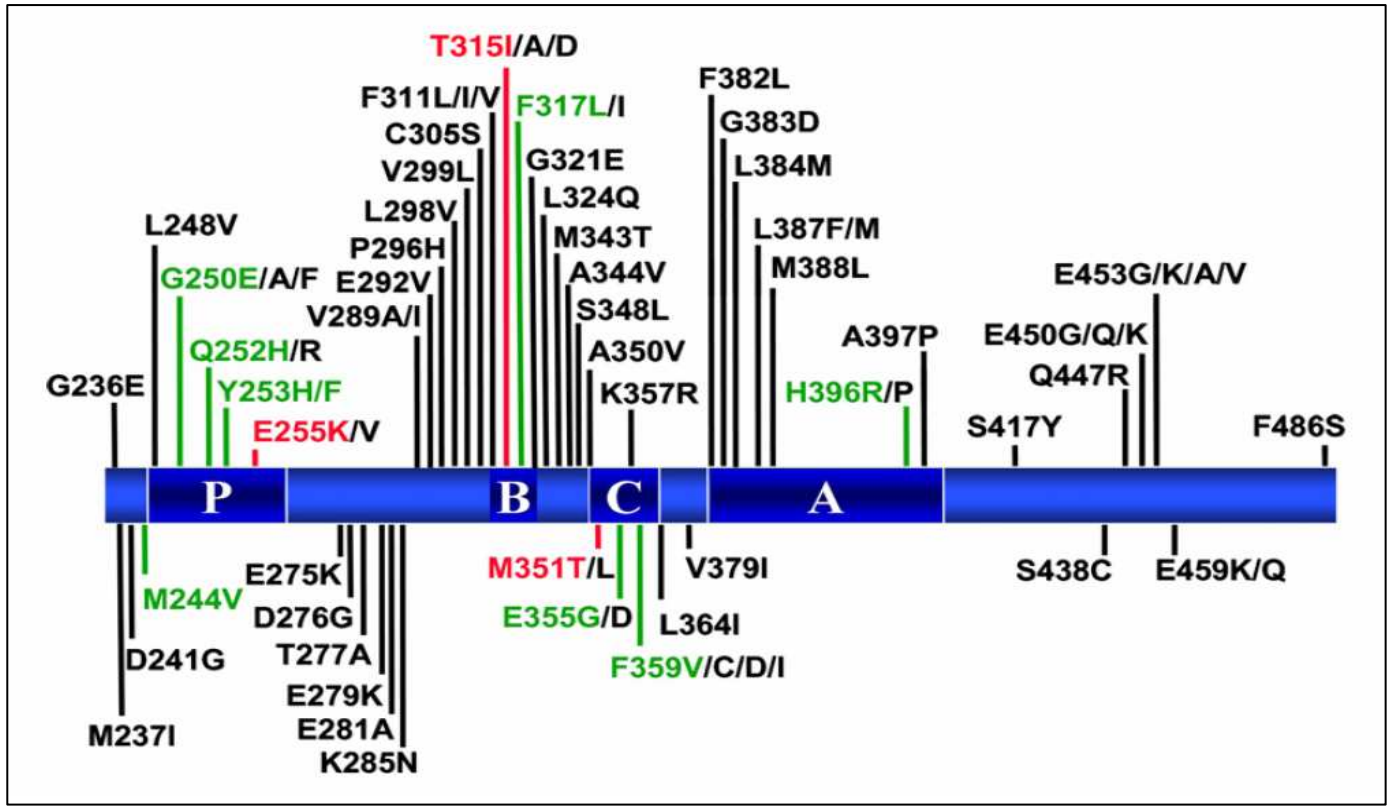

Figure 1.13: Map of BCR-ABL KD mutations
BCR-ABL kinase domain mutations associated with clinical resistance to imatinib are shown. Abbreviations: P, P-loop; B, imatinib binding site; C, catalytic domain; A, activation loop. Amino-acid substitutions in green indicate mutations detected in 2–10% and in red in >10% of patients with mutations (Melo *et. al.* 2007, Cancer Letters)[125].

Figure 1.14

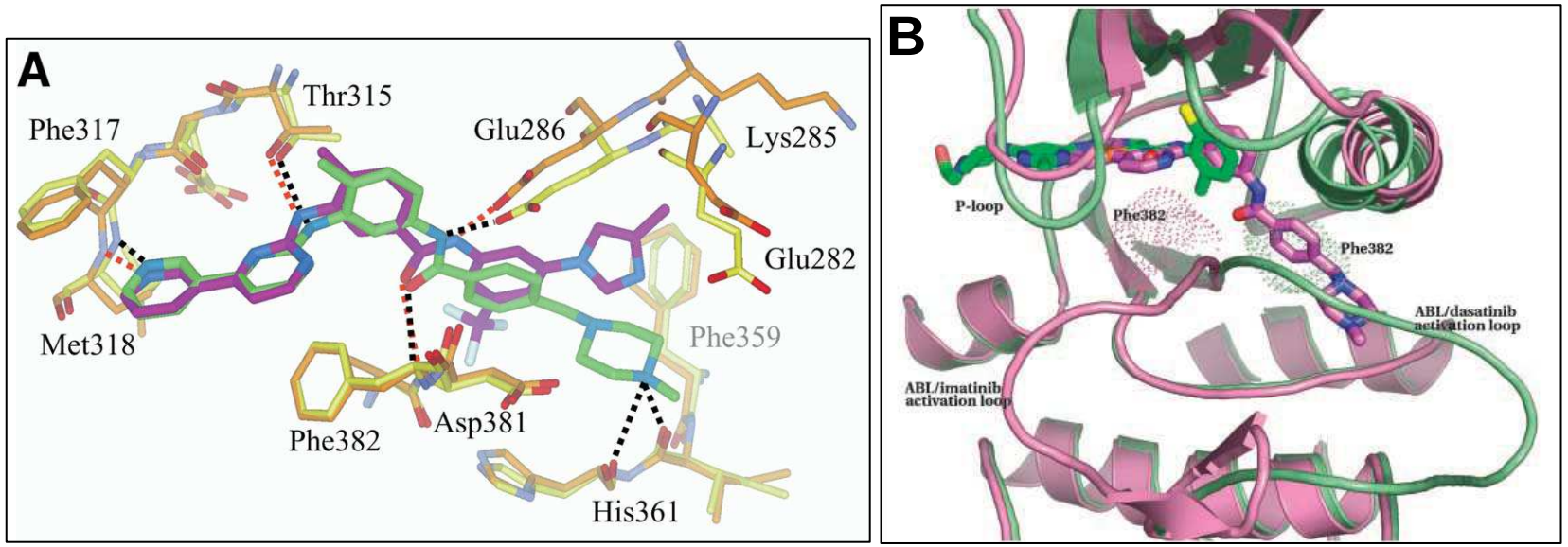

Figure 1.14: Nilotinib and dasatinib have different critical binding residues in the ABL kinase domain, compared to imatinib

A) Superimposition of nilotinib (purple) bound to AblM351T (orange), and imatinib (green) bound to Abl (yellow). Hydrogen bonds within the nilotinib-AblM351T complex are depicted as dashed red lines, whereas those in the imatinib complex are shown in black. The variability in the positions of side chains from the C-helix (top right corner) is due to crystal contacts that influence the position of the N-terminal lobe of the kinase. The methyl-imidazole group of nilotinib packs in a hydrophobic pocket formed by these residues with the nitrogen exposed to solvent (adapted from Weisberg *et. al.* 2005). **B)** A comparison of the dasatinib-ABL complex (protein and dasatinib carbons, green) and imatinib-ABL complex (protein and imatinib carbons, pink). Note the different positions of the drugs themselves, and the activation loop in the two structures. The Phe382 residue in the activation loop (in a dot surface representation for each complex) shows that imatinib would not be able to bind the active conformation of ABL because of a clash with Phe382 (as well as other activation loop residues). Dasatinib, however, is able to bind ABL in both the inactive and active conformations (Tokarski *et. al.* 2006, Cancer Letters)[118].

Figure 1.15

Figure 1.15: Differential sensitivity of kinase domain mutations to the three TKIs – imatinib, nilotinib and dasatinib
The IC50 value was defined as the concentration of inhibitor resulting in a 50% reduction in cell viability. Imatinib: sensitive (≤1000nM), intermediate (≤3000nM), insensitive (>3000nM). Nilotinib: sensitive (≤50nM), intermediate (≤500nM), insensitive (>500nM). Dasatinib: sensitive (≤3nM), intermediate (≤60nM), insensitive (>60nM). Note that the three drugs have different sensitivities to different KD mutations (O'Hare *et. al.* 2007, Blood)[119].

allosteric mechanisms[108]. A study of 98 CML patients taking imatinib revealed that 7% had regulatory domain mutations, while 30% had KD mutations. The T212R mutation in the SH2 domain was found to decrease imatinib sensitivity by 2.4-fold compared to native BCR-ABL[126].

1.8.3 Upregulation of TKI efflux proteins

Resistance may also be caused by upregulation of TKI-export proteins such as ABCB1 and ABCG2[71-75,127]. If the drug is being effluxed from a cell, such that BCR-ABL is not being effectively targeted and inhibited, then survival and proliferation of the leukaemic cell will continue. Upregulation of ABCB1 and ABCG2 may be mediated by established cellular mechanisms in response to the TKI, by gain of function mutations in the promoter region of genes encoding the transporters, or by fusion with constitutively active enhancer elements as a result of genetic instability[128].

ABCB1 and ABCG2 levels respond to stress signals such as heat shock, inflammation, hypoxia, exposure to xenobiotics, toxic metabolites, and ultraviolet (UV) radiation[56]. Hypoxia causes genomic instability and is linked to metastasis and tumour growth and the induction of stress-associated genes. ABCB1 and ABCG2 expression increases under hypoxic conditions, which is mediated by the hypoxia-inducible factor 1 (HIF-1)[56,129,130]. HIF-1 binds to a site in the *ABCB1* promoter (which overlaps with the GC site playing a role in constitutive expression[130]), and in the *ABCG2* promoter (at the proximal hypoxia response element, HRE) leading to the recruitment of transcription factors and thus gene expression[56,129,130]. BCR-ABL induces the expression of functionally active HIF-1 via the PI3-kinase pathway[131]. Thus it is possible that increased BCR-ABL expression in a cell may lead to upregulation of ABCB1 and ABCG2 through this mechanism. Nakanishi *et. al.*[132] found that decreasing BCR-ABL activity with imatinib caused reduced PI3K-Akt signalling, and decreased ABCG2 cell-surface expression in a dose dependent manner.

It has also been demonstrated that ABCB1 is up-regulated by cyclooxygenase-2 (COX-2)[133,134] – an enzyme that catalyses the conversion of arachidonic acid to prostaglandins and other eicosanoids. COX-2 is induced by growth factors, cytokines and carcinogens, and its expression is associated with various cancers. Celecoxib inhibits COX-2, and causes anti-leukaemic effects in K562 cells such as cell cycle arrest, caspase-3 activation, down-regulation of COX-2 and also down-regulation of ABCB1[133-135]. It has been previously shown that bone marrow COX-2 expression is elevated in

chronic-phase CML and is associated with reduced survival[136], which may in part be due to upregulation of ABCB1.

The genomic instability associated with CML may also lead to increased efflux protein expression. Knutsen *et. al.*[128] used fluorescence *in situ* hybridisation (FISH) in drug refractory ALL-patient samples to reveal breakpoints between ABCB1 and sequences 500-1,000kb telomeric to it. These rearrangements resulted in the capture of ABCB1 by (apparently) random, constitutively expressed genes, and led to increased expression of ABCB1. It was concluded that chromosomal rearrangement (which was often also followed by gene amplification) may therefore be a mechanism for TKI resistance observed in drug-selected cell lines, and ALL patients acquiring drug resistance[128].

An intriguing interplay exists between some MDR-ABC transporters, which are able to compensate for the loss of similar efflux pumps. Several cases exist where the reduction of one transporter modifies expression of another related proton pump. This has been observed in studies with ABCB1 and ABCG2, which have overlapping substrate specificities[56]. It was found that ABCG2 was greatly up-regulated in the blood brain barrier of ABCB1-knock-out mice[137]. It is therefore assumed that some redundancy of function exists between these transporters, and that expression of one may influence expression of the other.

1.8.4 BCR-ABL overexpression

Another mechanism of resistance is increased expression of BCR-ABL[107,138,139]. This may occur due to mutations in the promoter region of Bcr-Abl[140], duplication of the Ph chromosome[107,141], or the emergence of double minutes carrying Bcr-Abl[142]. This leads to increased Bcr-Abl transcription and translation such that pharmacologically achievable TKI concentrations are too low to effectively inhibit BCR-ABL[7,40,83].

Bcr-Abl is under the control of the BCR promoter, and mutations affecting expression could be '*in trans*' (affecting both Bcr-Abl and BCR expression) or '*in cis*' (affecting only Bcr-Abl)[140]. Mutations in miRNA203 (which down-regulates both BCR-ABL and ABL by a direct interaction with the 3' untranslated region), may also result in BCR-ABL up-regulation[143].

BCR-ABL overexpression has also been observed to occur through duplication of the Ph chromosome, and emergence of homogenously staining regions (HSR) or double minutes (dmin)

carrying Bcr-Abl[107,141]. The mechanisms by which such duplications arise are likely to involve genomic instability, errors in DNA repair and errors in mitosis, in part facilitated by BCR-ABL expression[97,110].

1.8.4.1 Homogeneously staining regions and double minutes

A HSR is a region of chromosome that contains highly amplified (repeating) DNA sequences[144]. The term was coined as these regions are observable by FISH as broadly staining regions that can span large areas of a chromosome[144]. HSR are frequently observed in solid tumour cells, where an amplified oncogene (facilitating oncogene overexpression) stains uniformly in FISH[145,146]. Dmin are small, circular, acentric fragments of DNA and are thought to be closely related to HSR[147]. Dmin frequently carry oncogenes (*e.g.* KRAS1, MYC, MYCN, NRAS, EGFR, ERBB2 and GLI) and are transcriptionally active, hence facilitating oncogene overexpression in human cancers[145,146,148,149]. As double minutes do not have a centromere, they cannot attach to the mitotic spindle. Consequently, they segregate randomly into the two daughter cells during mitosis, meaning that the number of double minutes per cell will vary in a population. If the double minute carries an oncogene conferring some survival/proliferation benefit, the daughter cell with the most double minutes will have the selective advantage, and thus the number of double minutes per cell can rapidly increase in a population[145]. Double minutes carrying ABCB1 have been observed in colchicine-selected multidrug resistant KB cells (a human epidermoid carcinoma cell line)[149], while double minutes carrying Bcr-Abl have been identified as a cause of imatinib resistance in CML blast crisis patients[142]. Some groups believe that dmin are formed by the breakdown of HSR[145,148,150], while others believe HSR are formed by the integration of dmin[151-153].

1.8.5 BCR-ABL independent resistance

Lastly, resistance may be due to the accumulation of other mutations (due to increased proliferation and genetic instability) that promote proliferation independently of BCR-ABL. Thus, imatinib treatment may eliminate cells that are dependent on BCR-ABL for survival, leaving those that are BCR-ABL-independent to thrive[7,83]. For example, mutations leading to a constitutively active PI3K/AKT pathway[154], or overexpression of Src kinases (*e.g.* Hck or Lyn)[81,125,155,156] may cause resistance to BCR-ABL inhibition.

It was recently found that conditioned media from imatinib-resistant LAMA84 cell clones was found to substantially protect imatinib naïve LAMA84 cells and primary CML progenitors from imatinib or nilotinib-induced cell death[157]. This 'protection' was found to be mediated by paracrine signalling, as resistant cells were secreting granulocyte-macrophage colony-stimulating factor (GM-CSF). This cytokine acted via BCR-ABL-independent activation of the JAK-2/STAT-5 pathway, such that imatinib-sensitive cells survived drug treatment. AG490 (an inhibitor of JAK-2) prevented STAT-5 phosphorylation, and negated the protective effects of GM-CSF[157]. Interestingly, elevated mRNA and protein levels of GM-CSF were found in several imatinib-resistant patient samples, however GM-CSF up-regulation was independent from the BCR-ABL kinase domain mutation status, and was not related to the CML disease phase at time of resistance. The authors of this study argue that changes in cytokine expression are easier to achieve in tumour cells than 'strategic' mutations, thus paracrine signalling (in response to imatinib selection) could be an early resistance mechanism before other mutations arise[157].

Another mechanism of BCR-ABL-independent resistance may involve down-regulation of the suppressor of cytokine signalling 1 (SOCS1) gene. Saudemont *et. al.*[158] found that dormant tumour cells show a progressive decrease of SOCS1 expression (*in vitro* and *in vivo*) caused by progressive methylation of the SOCS1 promoter. As SOCS1 inhibits JAK-2, its down-regulation is accompanied by increased JAK/STAT signalling, which results in resistance to cytotoxic T cell-mediated apoptosis, as well as resistance to imatinib. Increased JAK/STAT signalling (which is also stimulated by BCR-ABL) induces interleukin-3 (IL-3) overproduction in dormant cells, thus creating an autocrine loop that stimulates survival. Saudemont's findings (confirmed by Liu *et. al.*[159]) suggest that long-term persistance of dormant tumour cells may generate more aggressive subclones, which could escape the immune system and imatinib treatment.

Lastly, it has been demonstrated that imatinib stimulates the PI3K/Akt pathway in BCR-ABL positive LAMA84 cells, as well as primary leukaemia cells *in vitro* and in a CP CML patient *in vivo*[160]. It is thought that this occurs as cells attempt to compensate for the loss of signalling when BCR-ABL is inhibited, and enables cells to survive in the presence of TKI treatment before developing overt resistance mutations. Thus, this process appears to be involved in the development of resistance *in*

vivo. However, the mechanism by which imatinib activates PI3K/Akt (and whether this is BCR-ABL dependent) is unknown. Rapamycin (an mTOR inhibitor) and other PI3K inhibitors were found to synergise with imatinib, causing apoptosis in Bcr-Abl positive cell lines, and in imatinib-resistant cell lines where KD mutations were present[160].

1.9 Generation of TKI resistance in vitro, and investigating the kinetics and interplay of resistance mechanism emergence

Le Coutre *et. al.*[139] generated an imatinib-resistant line by culturing LAMA84 cells (human, Ph+ cell line) in gradually increasing concentrations of imatinib, initiated at 50nM, then increased by 100nM every 3-4 weeks until reaching 600nM imatinib. The cell line did not harbour any KD mutations, and ABCB1 mRNA expression had not changed. However, BCR-ABL overexpression was observed, and FISH analysis confirmed the presence of HSR carrying the fusion gene. Quantitation software revealed Bcr-Abl copy number had increased from 4 to 14, however no studies were conducted on the intermediates of resistance development[139].

Mahon *et. al.*[127] and Barnes *et. al.*[161] generated imatinib-resistant cell lines by culturing human or murine (respectively) Bcr-Abl positive cells in gradually increasing concentrations of IM at a rate of 100nM every 10 days until reaching 1μM. In the first study, BCR-ABL and ABCB1 overexpression were noted as mechanisms of resistance, however the kinetics of resistance mechanism emergence were not investigated[127]. Barnes *et. al.*[161] investigated how BCR-ABL expression levels determined the rate of resistance development in the 32D murine myeloid cell line. These cells were transfected to express graded amounts of BCR-ABL, and imatinib-resistance was generated by culture in gradually escalating drug concentrations. They noted that peak BCR-ABL expression preceded kinase domain mutations in three imatinib-resistant cell lines, however these murine cell lines were already expressing high levels of transfected BCR-ABL prior to resistance development. It should be noted that *in vivo* studies by Branford *et. al.*[162] and Press *et. al.*[163] found that a 2–2.6 fold rise in BCR-ABL expression correlated with the emergence of KD mutations, however, it has never been clear whether this is a result of an increase in the number of circulating leukaemic cells, or increased expression of BCR-ABL per cell, or both.

A more recent study by Yuan *et. al.*[164] generated imatinib-resistance by exposing KCL-22 cells (human, CML blast crisis cell line) to a single dose of 1, 1.5 or 10μM IM. After 2 weeks, surviving cells repopulated the culture. Due to the rapid nature of this resistance production, no intermediate stages of resistance were examined, and final resistant cultures were found to have kinase domain mutations, but not BCR-ABL overexpression. Efflux protein expression was not investigated.

A study of 44 patients conducted by White *et. al.*[165] observed that 7 patients developed KD mutations, and of these, the majority (6/7) had high levels of ABCB1 expression (*i.e.* ABCB1 expression levels above the 75th percentile) prior to the detection of the mutation. Interestingly, ABCB1 overexpression was reduced when the mutation developed. This raises the interesting possibility that efflux protein overexpression, resulting in lower intracellular drug concentrations, creates a favourable environment for KD mutation development.

1.10 Hypothesis

In human, Bcr-Abl positive CML, resistance mechanism emergence is complex, involving the interplay of several mechanisms which compete and influence the development of each-other.

1. Partially-protective mechanisms (*e.g.* efflux protein expression) create an environment that selects for further mutations (*e.g.* KD mutations) causing overt TKI resistance *in vitro*.
2. The kinetics of resistance mechanism emergence *in vitro* is different for different TKIs
3. Resistance mechanism emergence is stochastic *in vitro i.e.* different resistant mechanisms/KD mutations will emerge each time an identical cell line is cultured in escalating TKI

1.11 Aims

1. To investigate the interplay and kinetics of three currently identified resistance mechanisms – BCR-ABL overexpression, KD mutations, and ABCB1/ABCG2 overexpression.
2. To determine the dynamics of resistance emergence
3. To determine whether different TKIs elicit different resistant mechanisms in the same cell line.
4. To determine if specific TKIs predispose cell lines to certain resistance mechanisms

To achieve these aims, imatinib and dasatinib-resistant cultures of human, Bcr-Abl positive cell lines were generated, by gradually-increasing exposure of the cells to TKIs. Eleven TKI-resistant cell lines were generated (eight imatinib-resistant and three dasatinib-resistant), as well as six cell lines that were re-escalated in imatinib, dasatinib or nilotinib from key “intermediate” cultures. Intermediate stages of resistance-development were sampled and analysed to determine the mechanisms conferring resistance. Using this approach, trends in resistance mechanism emergence were observed that have therapeutic implications for CML patients.

Chapter 2:

Materials and Methods

2.1 Commonly used reagents

Table 2.1 Suppliers of commonly used reagents

Reagent	Supplier	Catalogue number
0.1M DTT	Invitrogen	18064-014
Acrylamide/Bis solution 40% 37.5:1 ratio	Bio Rad	161-0148
Anti-Crkl antibody	SantaCruz	SC-319
Anti-hBcrp1/ABCG2	R & D systems	FAB995P
Anti-rabbit immunoglobulin (alkaline-phosphatase-conjugated)	SantaCruz	SC2007
CD243-PE (ABCB1)	Beckman Coulter	PN IM 2370U
Chloroform	Merck	100776B
DABCO	Sigma-Aldrich	D-2522
DEPC H_2O	MP Biomedicals Inc.	821739
Dimethyl sulphoxide (DMSO)	Merck	K39661852
dNTP set (N = A, C, G, T)	GE Healthcare	27-2035-02
ECF substrate *Attaphos*	GE Healthcare	RPN 5785
Ethanol	Merck	4.10230.2511
Foetal Bovine Serum (FBS)	JRH Bioscienes	12003-500M
Hanks Buffered Saline Solution (HBSS)	Sigma-Aldrich	H9394
HEPES 1M	Sigma-Aldrich	H0887
High Pure DNA Isolation Kit	Roche	117 968 28001
IgG2a/2b PE control antibodies	Dako Cytomation	X0950 / X095101
Isopropanol	Ajax Finechem	425-2.5L PL
L-glutamine 200mM	SAFC Biosciences	59202C-100ML
Lymphoprep	Axis Shield	1114547
Membrane blocking agent	GE Healthcare	RPN 2125V
Methanol	Chem Supply	MA004-P
Microscint-20 scintillation fluid	Perkin Elmer	6013621
Phosphate Buffered Saline (PBS)	SAFC Bioscieces	59331C
Penicillin Streptomycin 5000µg/mL	Sigma-Aldrich	P4458
Prazosin Hydrochloride	Sigma-Aldrich	P7791
PVDF (Western blot membrane)	GE Healthcare	PRN 303F
Random Hexamer Primer	Geneworks	RP-6
RPMI-1640 Medium w/o glutamine	Sigma-Aldrich	R0883
Sodium Chloride (NaCl)	Ajax Finechem Pty Ltd	1128
Superscript II Reverse Transcriptase	Invitrogen	18064-014
SYBR Green ROX	Qiagen	PA-012-24
Taqman Master Mix	Applied Biosystems	4318157
Tris	Merck	1.08382.0500
Trizol reagent	Invitrogen	15596-018
Trypan Blue Solution (0.4%)	Sigma-Aldrich	T8154
Trypsin	SAFC Biosciences	59417C
Tween20	Sigma-Aldrich	P9416
Vysis Bcr-Abl dual fusion probe	Meta Systems	D-5007-100-OG

2.2 Solutions, buffers and media

2.2.1 Cell culture media

500mL RPMI 1640 Medium

5mL L-Glutamine (200mM)

5mL Penicillin 5000µg/mL / Streptomycin Sulphate 5000µg/mL

50mL Foetal Bovine Serum (FBS) (10%)

Stored at 4℃; heated in 37℃ water bath prior to u se

2.2.2 Tyrosine kinase inhibitors

2.2.2.1 Imatinib mesylate

Imatinib mesylate (imatinib; Glivec) and ^{14}C-imatinib (specific activity 3.394 MBq/mg) were provided by Novartis Pharmaceuticals (Basel, Switzerland). Stock solutions of imatinib were prepared at 10mM with distilled water, sterile filtered and stored at -70℃. Stock solutions of ^{14}C-imatinib were prepared at 1mg/mL with distilled water and stored at -70℃.

2.2.2.2 Nilotinib

Nilotinib (Tasigna) was provided by Novartis Pharmaceuticals. Stock solutions were prepared at 10mM in DMSO and stored at 4℃.

2.2.2.3 Dasatinib

Dasatinib (Sprycel) and ^{14}C-dasatinib (specific activity 31.9µCi/mL) were provided by Bristol-Myers Squibb (Victoria, Australia). Stock solutions of dasatinib were prepared at 10mM in DMSO and stored at 4℃. Stock solutions of ^{14}C-dasatinib were prepared at 1mg/mL in ethanol and stored at -70℃.

2.2.2.4 100µM 14C-Imatinib mixture (50%)

29.5µL ^{14}C-imatinib, 1695.72µM

5µL 10mM imatinib

966µL RPMI medium

Made fresh on the day of use.

2.2.2.5 100µM 14C-Dasatinib mixture (50%)

24.4µL ^{14}C-dasatinib, 2049µM

5µL 10mM dasatinib

970.6µL RPMI medium

Made fresh on the day of use.

2.2.3 Prazosin hydrochloride – inhibits OCT-1

Used at 100µM from 10mM stock

10mM stock = 4.2mg/mL methanol

Made fresh on the day of use.

2.2.4 PSC833 – inhibits ABCB1

Used at 10µM from 8.23mM stock (kindly provided by Novartis Pharmaceuticals).

8.23mM stock = 10mg/mL = 10mg / 500µl 9:1 Ethanol:Tween20, + 500µl water

Made fresh on the day of use.

2.2.5 Ko143 – inhibits ABCG2

Used at 0.5µM from 1mM stock (kindly provided by Dr. John Allen)

Made fresh on the day of use.

2.2.6 Flow cytometry Fixative (FACS Fix)

500mL PBS

5mL 40% w/v Formaldehyde

10g D-glucose

0.1g NaN_3

Stored at 4℃.

2.2.7 Freeze Mix

70% Hanks BSS

20% FBS

10% DMSO

Made fresh on the day of use.

2.2.8 Laemmli's Buffer

50 mMol/L Tris-HCl, pH 6.8

10% glycerol

2% SDS

5% β-mercaptoethanol

0.1% bromophenol blue

1mM NaVanadate

10mM NaFluoride

Stored in 1mL aliquots at -20℃, thawed at RT or br iefly in 100℃ heating block before use

2.2.9 Membrane blocking solution (2.5%)

12.5g Membrane Blocking agent (GE Healthcare, Little Chalfont, Buckinghamshire, United Kingdom)

500mL 1xTBS

2.2.10 SDS-Polyacrylamide Gel

	Resolving gel (12%)	Stacking gel (5%)
MQ H2O	12.9mL	6mL
40% Acrylamide	9mL	1.26mL
1.5M Tris-HCl	7.5ml	2.52mL
10% SDS	300µL	100µL
10% APS	300µL	100µL
TEMED	18µL	10µL

2.2.11 1×TBS

20 mMol/L Tris-HCl, pH 7.5

150 mMol/L NaCl

2.2.12 1×TBST

20 mMol/L Tris-HCl, pH 7.5

150 mMol/L NaCl

0.1% Tween20

2.2.13 dNTP set (N = A, C, G, T)

40µL of each dNTP (25mM stock)

2.2.14 Random Hexamer Primer

500µg/mL stock

Working stock: 100µg in 200µL DEPC water

2.3 Cell lines

2.3.1 K562

The continuous cell line K562 was established by Lozzio and Lozzio[166] from the pleural effusion of a 53-year-old female with CML in terminal blast crisis. Cells were obtained from the American Type Culture Collection (Manassas, VA, USA).

2.3.2 K562 Dox

The ABCB1-overexpressing cell line was derived from the K562 line by exposure to doxorubicin[79]. Cells were provided by Prof. Leonie Ashman (University of Newcastle).

2.3.3 KU812

The KU812 cell line was established from the peripheral blood of a 38-year-old male with CML in blast crisis[167]. Cells were obtained from the American Type Culture Collection (Manassas, USA).

2.4 General Techniques

2.4.1 Tissue culture

All tissue culture was performed in a Class two "biohazard" laminar flow hood (Gelman Sciences).

Cell lines were maintained at a cell density between 8.0×10^4 and 2×10^5 cells/mL, depending on the rate of proliferation, in $25cm^2$, $75cm^2$ or $175cm^2$ tissue culture flasks (Greiner, Frickenhausen, Germany). Culture media was RPMI (Sigma-Aldrich, Castle Hill, Australia) supplemented with penicillin/streptomycin (Sigma-Aldrich), L-glutamine (SAFC Bioscience) and FBS (Trace Biosciences, Sydney Australia) as detailed in *2.2 Solutions, buffers and media*. Cell cultures were kept in a 37℃/5%CO_2 incubator, and were counted, and seeded at the above concentrations three times a week with fresh media (warmed prior to use).

2.4.2 Cell counts

Cell cultures were gently agitated to ensure cells were suspended throughout media. In a laminar flow hood, cells were mixed further by pipetting before a 1-2mL aliquot was taken in 2mL tube (Eppendorf, North Ryde, NSW, Australia). A 10µl aliquot of cells was then mixed with 10µl Trypan Blue (Sigma-Aldrich), and 10µl of this mixture was loaded onto a haemocytometer counting chamber (Neubauer Improved, Assistant, Germany) and cell concentration calculated accordingly.

2.4.3 Cryopreservation of cells

Cells were cryopreserved in a "Freeze Mix" of 70% Hanks BSS, 20% FBS and 10% DMSO as detailed in *2.2 Solutions, buffers and media*. Cells were pelleted, resuspended in Freeze Mix at 2×10^6 cells/mL, and transferred quickly to cryoampoules (Nalgene, Rochester, NY, USA) before being cryopreserved using a "Mr. Frosty" container (Nalgene) for a minimum of 4 hours at -70℃. Cryoampoules were finally stored in liquid nitrogen (-196℃).

2.4.4 Thawing cells

Cells were removed from liquid nitrogen and thawed rapidly in a 37℃ water bath. In a laminar flow hood, cells were transferred to a 50mL tube (BD Biosciences, North Ryde, NSW, Australia) and 30mL warmed culture media was added drop-wise, slowly, with constant mixing. A further 10mL media was added drop-wise quickly, with constant mixing, and a further 10mL media was poured in. Cells were then pelleted at 1200rpm for 10mins, and the supernatant discarded. Cells were again resuspended in 50mL warmed culture media, slowly for the first 30mL, and quickly for the last 20mL (as above). Cells were again pelleted and 40mL of the supernatant discarded. Cells were resuspended in the remaining 10mL, before being counted and placed in incubator.

2.5 Specialised Techniques

2.5.1 Generation of TKI resistant cell lines

Cell lines maintained in liquid culture, as described above (*2.4.1*), were gradually exposed to increasing concentrations of imatinib or dasatinib. Imatinib culture was initiated at 100nM, and the concentration was increased at a rate of 100-200nM every 10-20 days (depending on cell proliferation and viability) until reaching 2µM (approximately 6.5 month duration). Dasatinib culture was initiated

and maintained at varying concentrations/rates (K562 Dox initiated in 6nM, and subsequently 12nM, 20nM, 30nM, 40nM, 55nM, 75nM, 100nM, 150nM; K562 initiated in 0.5nM, and subsequently 1nM, 2nM, 3.5nM, 5nM, 10nM, 15nM, 25nM, 50nM, 75nM, 100nM, 150nM) until reaching 200nM (approximately 9 months). Dasatinib concentration was escalated every 10-30 days, depending on cell proliferation and viability.

Serial dilutions of imatinib (in Milli-Q water) or dasatinib (in DMSO) were made from 10mM stocks such that no more than 20µl of drug was ever added to a 50mL cell culture – thus DMSO concentration never exceeded 0.04%. Parental, 'naïve' cell lines, and dasatinib solvent DMSO (0.1%) lines were maintained in parallel cultures as controls.

2.5.1.1 Sampling intermediate lines for analysis

Prior to drug escalation, cells would be harvested from the culture as follows:

2×10^6 cells for DNA preparation

3×10^7 cells to make three TRIzol (Invitrogen Life Technologies, Carlsbad, CA) preparations, frozen for later RNA extraction.

1.4×10^7 cells for cryopreservation of 6 ampoules of cells at 2×10^6 cells/mL

DNA and RNA were stored until all intermediates of a resistant cell line had been collected before analysis using quantitative DNA-PCR and RQ-PCR

2.5.2 DNA extraction

The High Pure PCR Template Preparation Kit (Roche Diagnostics, Mannheim, Germany) was used to isolate genomic DNA. Briefly, 2×10^6 cells were pelleted, and all but 200µl of supernatant (culture media) aspirated. Cells were resuspended in the remaining 200µl, and transferred to a new, labelled tube. To this, 200µL of Binding Buffer and 40µL proteinase K solution was added, and the tubes vortexed. The samples were then incubated for at least 30 minutes in a 72℃ heating block. Next, 100µL of isopropanol was added and the tube vortexed (at this stage, some samples were stored at -70℃). The mixture was then pipetted into a HighPure filter in a collection tube, and centrifuged at 8,000rpm for 1 minute. Flow-through was discarded, and 500µL of Inhibitor Removal Buffer was added before centrifugation at 8000 rpm for 1 minute. The HighPure filter was then transferred to a clean collection tube, and washed twice with 500µL Wash Buffer (centrifuge at 8,000 rpm for 1 minute). The HighPure filter was then transferred to a clean collection tube, and dried by centrifugation

at 13,000rpm for 1 minute. The filter was transferred once more to a clean, labelled tube, and 100µL of pre-warmed Elution Buffer was added to the filter and left for 5 minutes. Tubes were centrifuged at 8,000rpm for 1 minute to collect DNA eluate. The concentration of DNA was then measured using a NanoDrop Spectrophotometer (Thermo Scientific, Wilmington, DE, USA), and DNA was stored at -20℃.

2.5.3 Quantitative DNA PCR

Master mixes were made for both the GUSB control gene, and Bcr-Abl. The primers and probes used were as follows:

GUSB Forward primer: 5' GAA AAA ATG AGG ACG GGT ACG T 3'

GUSB Reverse primer: 5' ATT TTG CCG ATT TCA TGA CTG A 3'

GUSB probe: 5'ATC CCA TGA GCC AAA CTG CCA CTT ACA C 3'

K562 Forward primer: 5' TGA CCA CGG GAC ACC TTT G 3'

K562 Reverse primer: 5' TTA GTG CAA TCA GAG AAG AAA ATC CTT 3'

K562 probe: 5' CTG GCC GCT GTG GAG TGG GTT TTA TC 3'

KU812 Forward primer: 5' CCC CTA GCC TGT CTC AGA TCC T 3'

KU812 Reverse primer: 5' AAC ATG TCA CTT TCT TCT GCA TGA A 3'

KU812 probe: 5' CTG GTG AGC TGC CCC CTG CTT AAA 3'

GUSB	1 PCR
Master Mix	12.5
DEPC H_2O	9.35
Forward Primer 50µM	0.2
Reverse Primer 50µM	0.2
GUSB probe	0.25

Bcr-Abl	1 PCR
Master Mix	12.5
DEPC H_2O	8.85
Forward Primer 50µM	0.2
Reverse Primer 50µM	0.2
K562/KU812 Probe	0.75

Once master mixes were made, 22.5µL was pipetted into a 96-well PCR plate as per a setup sheet (see *Appendix I.1*). GUSB and Bcr-Abl standards were prepared in-house and run in every batch (copy number 10-10^5 for GUSB plasmid, and 10^{-3}-10^2 for specific cell-line DNA). Salmon sperm diluent and normal DNA (Bcr-Abl negative) were also used as controls.

In a UV'd cabinet, 2.5µL of standards, cell-line standards, and samples (DNA extractions made above) were added to the correct wells, and capped with optical cap strips. Samples were run on the ABI 7500 Sequence Detector Instrument with the following cycler conditions:

Cycle Number	Temperature (℃)	Duration (mins)
1	50	2:00
1	95	10:00
45	95	00:15
	60	1:00

After completion of the run, wells were checked for evaporation and the plate discarded. Results were analysed using 7900HT version 2.3 Sequence Detection Systems software (Applied Biosystems).

2.5.4 mRNA extraction

In a laminar flow hood, 350µl chloroform was added to thawed TRIzol (Invitrogen Life Technologies) preparations and shaken vigorously for 15 seconds. Samples were then incubated on ice for 3mins before centrifugation at 13,000rpm for 15 minutes. Subsequently, 350µl of the clear, upper layers were removed into new, labelled tubes. To this, 350µl of ice-cold isopropanol was added, and the tubes were gently inverted and checked visually for DNA contamination. The samples were then incubated on ice for 10 minutes, then centrifuged at 13,000 rpm for 10 minutes. The supernatants were then discarded, and the pellets were washed with 1mL of 75% ethanol and vortexing for 10 seconds. The samples were then centrifuged again at 6,500rpm for 5 minutes. The supernatants were discarded, and finally tubes were centrifuged to remove the last traces of ethanol. The pellets were air dried in the hood for 10-20mins, before 40µl of DEPC water was added to each tube to dissolve the pellets (15 minutes in 55℃ heat block, or 1 hour at room tempe rature). The concentration of RNA of each sample was then measured using a NanoDrop Spectrophotometer (Thermo Scientific) and DEPC water was added to achieve a desired concentration of between 1 and 2µg/µl. RNA was stored at -70℃.

2.5.5 cDNA synthesis

Two PCR master mixes were made as follows (see setup sheet in *Appendix I.2*):

	RQ-PCR Master Mix	1 sample (µL)
Mix 1 (2.4µL)	25mM dNTP	0.4
	500µg/mL Random Hexamers	2
Mix 2 (6µL)	5x 1st Strand Buffer	4
	0.1M DTT	2

2.4µL of Mix 1 was placed in flat-top PCR tubes, and the volume required for 2µg of RNA was calculated and added. DEPC water was added to make the volume up to 12µL. PCR tubes were heated at 65℃ for 5 minutes in a thermal cycler with heated cover. Tubes were then placed on ice, and 6µL of Mix 2 was added to each tube. Tubes were then heated at 25℃ for 2 minutes in thermal cycler, before placing the tubes on ice and adding 2µL of Superscript II (Invitrogen Life Technologies). The samples were reloaded into the thermal cycler with the following program:

Cycle number	Temperature (℃)	Duration (mins)
1	25	10:00
1	42	50:00
1	70	15:00
1	4	∞

cDNA was stored at -20℃.

2.5.6 RQ-PCR: BCR-ABL transcript quantitation

The cells lines used in this study contain the b3a2 transcript of BCR-ABL, so primers and probes for b3a2 and BCR were designed as previously described[168]. These are as follows:

BCR Forward bF primer: 5' CCT TCG ACG TCA ATA ACA AGG AT 3'

Reverse bR primer: 5' CCT GCG ATG GCG TTC AC 3'

TaqMan BCR probe: 5' TCC ATC TCG CTC ATC ATC ACC GAC A 3'

b3a2 Forward b3 primer: 5' GGG CTC TAT GGG TTT CTG AAT G 3'

Reverse 3a2 primer: 5' CGC TGA AGG GCT TTT GAA CT 3'

TaqMan b3a2 probe: 5' CAT CGT CCA CTC AGC CAC TGG ATT TAA GC 3'

The standards for each transcript (copy number 10-10^6 for b3a2, and 10^3-10^6 for BCR) were prepared in-house, and run in every batch. Master mixes were made using the TaqMan Universal PCR Master Mix (Applied Biosystems, Foster City, CA) as follows:

BCR	1 sample (µL)
TaqMan Universal PCR Master Mix	12.5
DEPC H_2O	9.55
Forward primer 50µM	0.1
Reverse primer 50µM	0.1
BCR probe	0.25

B3A2	1 sample (µL)
TaqMan Universal PCR Master Mix	12.5
DEPC H_2O	9.55
Forward primer 50µM	0.1
Reverse primer 50µM	0.1
B3A2 probe	0.25

22.5µL of Master mix was pipetted into the appropriate wells of a 96-well PCR plate (on ice), before adding 2.5µL of standards (in duplicate) (see setup sheet in *Appendix I.3*). Standard wells were capped before the addition of 2.5µL of cDNA (prepared as above) to the appropriate wells. The PCR was run in the ABI Prism 7500 Sequence Detection System (Applied Biosystems) with the following cycler conditions:

Cycle number	Temperature (℃)	Duration (mins)
1	50	2:00
1	95	10:00
45	95	15:00
	60	1:00

After completion of the run, wells were checked for evaporation and the plate discarded. Results were analysed using the ABI Prism 7500 software (Applied Biosystems).

2.5.7 Sequencing the BCR-ABL kinase domain

Previously designed primers were used for a Long PCR reaction – these are as follows:

ABL kinase Forward primer: 5' CGC AAC AAG CCC ACT GTC T 3'

Exo Reverse primer: 5'CAG GAA TCC AGT ATC TCA GAC GAA 3'

See *Appendix I.4* for the position of these primers in relation to the kinase domain of Abl. Master mix was made for the Long PCR reaction as follows:

Reagent	1 sample (µL)
25mM dNTP	0.75
DEPC H_2O	18.325
10xBuffer 3	2.5
25mM MgCl	0.75
ABL kinase Forward primer	0.15
Exo Reverse primer	0.15
Expand Enzyme Mix	0.375

Expand Enzyme Mix and 10xBuffer 3 were used from a kit (Expand Long Template PCR System; Roche Diagnostics). 23µL of Master mix was placed in flat-topped PCR tubes, and 2µL cDNA (prepared above) was then added for each sample to be sequenced. Cycler conditions were as follows:

Cycle number	Temperature (℃)	Duration (mins)
1	94	2:00
10	94	0:10
	60	0:30
	68	2:00
30	94	0:10
	60	0:30
	68	2:00
1	68	7:00
1	4	∞

* Increase time after cycle 1 by 20 seconds after every cycle.

Long PCR products (1µL aliquot) were visualised on a 2% agarose gel (stained with ethidium bromide) to confirm success of the reaction. The PCR products were then cleaned using an UltraClean™ PCR Clean-up DNA purification kit (Mo Bio Laboratories, Inc., Carlsbad, CA, USA) and diluted 1:4 before being used as template for conventional sequencing, or chip-based MALDI-TOF mass spectrometry (Sequenom, San Diego, CA, USA) described previously[169].

2.5.7.1 Conventional sequencing

For conventional sequencing, Master mixes for the forward and reverse reactions were made as follows:

Forward reaction

Component	1 sample (µl)
Big Dye	1
Sequencing Buffer	2
Forward primer (50µM)	0.15
DEPC H_2O	5.85

Reverse reaction

Component	1 sample (µl)
Big Dye	1
Sequencing Buffer	2
Reverse primer (50µM)	0.15
DEPC H_2O	5.85

Primers are ABL kinase Forward and Exo Reverse (same as for Long PCR, above). 9µL of master mix was placed in flat-topped PCR tubes, before adding 1µL of purified Long PCR product. Cycler conditions were as follows:

Cycle number	Temperature (℃)	Duration (mins)
25	96	0:10
	50	0:05
	60	4:00
1	4	∞

The sequencing reaction was then cleaned using the BigDye® XTerminator™ Purification Kit (Applied Biosystems). Briefly, 45µL of SAM™ Solution and 10µL of Xterminator™ Solution was added to each sample and vortexed for 30 minutes. Tubes were then centrifuged for 2 minutes at 1000g before being sent to the sequencing department for in-house sequencing. Results were analysed using Mutation Surveyor Version 3.24 (© SoftGenetics LLC, 2006).

2.5.7.2 MassARRAY sequencing (Sequenom)

For more sensitive mutation detection (to a level of 1-2% mutant) the Sequenom MassARRAY method was used. MassARRAY Assay Designer 3.1 (Sequenom) was used to design amplification and extension primers for 4 multiplex genotyping assays to detect 31 BCR-ABL mutations (see *Appendix I.5* for comprehensive list of mutations). An assay was designed for a region of ABL exon 7 that contains no known sequence variations (primer extension onto nucleotide 1263, GenBank:

M14752.1). This assay acts as a control for each multiplex to ensure sample was added to the well. Rather than using a mixture of 4 terminator dNTPs (*i.e.* ddNTPs) (iPLEX, Sequenom) in the primer extension reaction, specific mixes of 2 to 3 ddNTPs were used for each multiplex primer extension reactions according to the SABER protocol[170]. This restricts the generation of extension products to the mutant allele(s) only, increasing assay sensitivity compared to the standard protocol. Reactions were carried out essentially as described by the manufacturer using TypePLEX reagents (Sequenom). Briefly, 1µl of PCR product (previously analysed by conventional sequencing, described above) was used as template in each of the 4 multiplex PCR reactions that amplify an approximately 100 bp region targeting the mutations of interest (5 µl reaction). PCR cycler conditions were as follows:

Cycle number	Temperature (℃)	Duration (mins)
1	94	4:00
35	94	0:20
	60	0:30
	72	1:00
1	72	3:00

Unincorporated ddNTPs were inactivated using shrimp alkaline phosphatase prior to single base extension onto the mutation site using the extension primers and assay-specific iPLEX terminator mixes. PCR conditions were as follows:

Cycle number		Temperature (℃)	Duration (mins)
1		94	0:30
40		94	0:05
	5	58	0:05
		80	0:05
1		72	3:00

All reactions were carried out in a 384-well plate using a C1000 ThermoCycler (Bio-Rad Laboratories, Hercules, CA, USA). Extension products were desalted using CleanSeq resin and approximately 20nL was loaded onto each position of a 384-well SpectroCHIP II preloaded with matrix. SpectroCHIPs were analysed by a MassARRAY Analyser Compact MALDI-TOF Mass Spectrometer (Sequenom). Typer4 software (Sequenom) was used to analyse the resulting mass spectra, generating automated mutation calls using the default computational algorithms for genotyping diploid samples; however as extension products were not generated for the wild-type allele, manual calling was necessary in some instances. Manual mutation calling was performed in a blinded fashion, and selected experiments were analysed by 2 independent operators, with a correlation of greater than 98%. Plasmids containing mutant BCR-ABL for each of the 23 nucleotides investigated were included in each experiment as internal standards to monitor assay sensitivity and enable manual calling of low level mutants. Assay-specific mixes of mutant BCR-ABL plasmids were diluted in plasmid containing wild-type BCR-ABL to 2, 0.5, 0.2 and 0.05% mutant which were amplified using PCR and included in each experiment for comparison with experimental samples. The following controls were also included in each experiment: no template, BCR-ABL amplicons of plasmid containing wild-type BCR-ABL, and the ABL kinase domain amplified from cDNA of normal donors and HeLa cells (BCR-ABL-negative cell line). Precautions were taken to avoid false positive results; reagents were prepared in a BCR-ABL naive laboratory using new reagents, primers, water, pipettes, pipette tips and tubes. Reagent mixes and PCR products generated from experimental samples and controls were added to the reaction plate in a UV-irradiated hood. Manual calling was performed by optical inspection of the Typer4 Yield Call Cluster Plot, and patient samples were called positive if the following criteria were met: negative control samples were clustered close to the origin, mutant plasmid samples showed expected yields and were positioned discrete from the negative samples, and the yield of the experimental sample was higher than the lowest mutant plasmid sample with a yield higher than the negative samples, i.e. mutant plasmid samples may not all be called positive for each experiment - the assay sensitivity of each particular experiment was estimated by the lowest dilution mutant plasmid called positive.

2.5.8 RQ-PCR: Lyn transcript quantitation

Lyn transcript levels were quantified as a ratio of GUSB transcript levels. The primers used for Lyn amplification were as follows:

Forward primer: 5' AAG TTG GTG AAA AGG CTT GG 3'

Reverse primer: 5' GCC ACC TTG GTA CTG TTG TTA 3'

The primers used for GUSB amplification were as follows:

Forward primer: 5' GAA AAA ATG AGG ACG GGT ACG T 3'

Reverse primer: 5' ATT TTG CCG ATT TCA TGA CTG A 3'

Primers used for the RANKL control were as follows:

Forward primer: 5' TCA GCC TTT TGC TCA TCT CAC TAT 3'

Reverse primer: 5' CCA CCC CCG ATC ATG GT 3'

Master mixes were made for each primer set using the SYBR Green ROX mix (Qiagen, Venlo, Netherlands) as follows:

Reagent	**1 sample (µL)**
SYBR Green ROX mix	5
Forward primer	0.5
Reverse primer	0.5
DEPC water	2

8µL of Master mix was pipetted into the appropriate 0.1mL PCR tube (in cold rack), before adding 2µL of cDNA (prepared as above, diluted 1/10 in DEPC water) to the appropriate wells. Note, only 1uL of RANKL cDNA was added to the RANKL control reactions. All samples were run in triplicate, and 'no template' controls were run for each primer set. The PCR was run in the Rotor-Gene 3000 PCR cycler machine (Corbett Research, Cambridgeshire, UK) with the following cycler conditions:

Cycle number	**Temperature (℃)**	**Duration (mins)**
1	50	2:00
1	95	15:00
48	95	00:15
	60	00:26
	72	00:10
1	72	00:30
Melt: Ramp from 72℃ – 99℃, rising by 1℃ each ste p. Wait for 15 seconds on first step, then wait for 5 seconds for each step afterwards.		

After completion of the run, PCR tubes were discarded. Results were analysed using the Rotor-Gene 6.1.93 software (Corbett Research) and a standard curve previously generated was used for analysis each time.

2.5.9 IC50 assay and Western blot

Western blot assays for p-Crkl were performed as previously described[36]. Briefly, 2×10^5 Bcr-Abl positive cells were incubated for 2 hours at 37℃ with concentrations of imatinib ranging from 0μM to 200μM, dasatinib ranging from 0μM to 30,000μM or nilotinib ranging from 0μM to 50,000μM. Following incubation, cells were washed once with cold phosphate-buffered saline (PBS) and lysed in Laemmli's buffer by boiling for 12 minutes. Lysates were clarified by microfugation and stored at –20℃. Protein lysates were resolved on a sodium dodecyl sulfate (SDS)/10% polyacrylamide gel and electrophoretically transferred to polyvinylidenefluoride (PVDF) (GE Healthcare). Following blocking, the membrane was probed with anti-Crkl antibody (Santa Cruz Biotechnology, Santa Cruz, CA), then anti-rabbit IgG secondary antibody (alkaline-phosphatase conjugated)(Santa Cruz). Protein bands were detected with ECF substrate (GE Healthcare) and analyzed by Fluor Imager analysis (Molecular Dynamics. Sunnyvale, CA). Signals were quantified using Image Quant software (Molecular Dynamics), and the ratio of p-Crkl to Crkl was determined using Image Quant analysis. IC50 values were determined as the dose of drug required to reduce levels of p-Crkl by 50%. To determine the IC50 when ABCB1 is blocked, assays were conducted in the presence or absence of 10μM PSC833 (provided by Novartis Pharmaceuticals).

2.5.10 Flow cytometry

2.5.10.1 Measurement of ABCB1/ABCG2 cell-surface expression.

1×10^5 cells (for isotype control) or 5×10^5 cells (for experimental samples) were incubated for 40mins on ice in 250μl Hanks Balanced Salt Solution (Ca^{++} and Mg^{++} free; Sigma-Aldrich) medium supplemented with 10mM Hepes (Sigma-Aldrich) with either 5μL of the mouse IgG2a/2b PE control antibodies (Dako), 20μL of ABCB1 PE (Beckman Coulter) or 20μL of ABCG2 PE (Jomar Bioscience) antibodies. Cells were then washed twice with the Hanks-Hepes solution, before being resuspended in 250μl FACS Fix (as described in *2.2.9*). Cells were protected from light and refrigerated until analysis on flow cytometer.

2.5.10.2 Cell viability

Cell viability was measured by staining cells with both 7-Amino-actinomycin D (7-AAD) and Annexin V, and analysing using a flow cytometer. 7-AAD is excluded by viable cells, but can penetrate cell membranes of dying or dead cells where it intercalates into double-stranded nucleic acids. Annexin V is a Ca^{++}-dependant phospholipid-binding protein that binds to phosphatidylserine residues on the cell membrane. In normal cells, these residues are located on the inner surface of the cell membrane, and are therefore inaccessible to Annexin V. However, at an early stage of apoptosis, the phosphatidylserine residues are translocated to the outside of the cell, marking irreversible commitment to death by apoptosis. The residues are then available to be bound by Annexin V[171].

Cells were washed and resuspended in fresh culture media to remove traces of drug, before being cultured in quadruplicate in a 24-well plate. 1mL cultures were seeded at 1×10^5 cell/mL, and TKI was added. Imatinib, dasatinib and nilotinib were serially diluted in an appropriate solvent (water and DMSO respectively) before being added to each well. It should be noted that the volume of TKI added never exceeded 5µL, as this volume of DMSO is toxic to cells in 1mL media. A zero drug control (in sextuplet) was always included, as well as a 5µL DMSO only control where appropriate. The 24-well plates were placed in sterilised cake-boxes, and incubated (37℃/5%CO_2) for three days before staining to observe cell-death.

The probes were thawed in darkness on ice, before being diluted in Staining Buffer (Hanks BSS, 10mM Hepes). 7-AAD (Invitrogen) was used at 0.1µL in 39.9µL Staining Buffer per sample, while Annexin V (BD Biosciences) was used at 1µL in 9µL Staining Buffer per sample.

To make the Annexin V positive control, 1mL of zero drug culture was added to an equal volume of DMSO in a 5mL FACS tube, and incubated at room temperature (RT) for 10 minutes. The cells were then washed twice in 2mL PBS (all centrifugation in this method was at 2700rpm for 2 minutes). The cells were then washed once in 2mL Staining Buffer, supernatant (SN) was removed, 10µL Annexin V (made above) was added, and the tube was incubated at RT for 15 minutes in darkness. Lastly, the cells were resuspended in 400µL Staining buffer and the tube stored on ice. To make the 7-AAD positive control, 1mL of zero drug culture was added to 2mL cold ethanol (70%) in a 5mL FACS tube, and incubated on ice for 10 minutes. The cells were then washed twice in 2mL PBS, and once more in 2mL Staining Buffer. Finally, SN was removed, 40µL 7-AAD (made above) was added, and the tube was incubated at RT for 15 minutes in darkness. Lastly, the cells were resuspended in 400µL Staining

Buffer and the tube stored on ice. For the negative staining control, 1mL of zero drug culture was washed with 1mL of Staining Buffer in a 5mL FACS tube. The SN was removed, and cells were resuspended in 400µL Staining Buffer before placing the tube on ice.

For the experimental samples, 1mL of cell culture for each drug concentration (including zero drug control) was transferred to individual FACS tubes, centrifuged and SN removed. Cells were washed once in 1mL Staining Buffer, and SN removed. Next, 40µL of 7-AAD and 10µL of Annexin V (made earlier) were added to each tube. Tubes were incubated at RT for 15 minutes in darkness. Cells were resuspended in 400µL Staining Buffer and tubes were kept on ice before flow cytometry analysis (within an hour).

2.5.11 Intracellular Uptake and Retention (IUR) assay

The IUR assay was performed as previously described[172]. In brief, 200,000 cells (washed and resuspended in fresh media to remove traces of drug) were incubated for 2 hours at 37℃/5%CO_2 in the presence of varying concentrations of imatinib or dasatinib (50% ^{14}C-mixtures), ranging from 0µM to 2µM. After incubation the cellular and aqueous phases were separated and incorporation determined using a Top Count Microplate Beta Scintillation counter (Perkin Elmer, Boston, MA) following the addition of Microscint20 scintillation fluid (Perkin Elmer). All assays were performed in triplicate and repeated if the assay demonstrated nonconcordance. The IUR was analyzed in K562 cells as a control for reproducibility in all assays. Where the K562 assays fell outside of the 95% confidence limits, the assay results were not included and the assay was repeated. To measure OCT-1 activity, and the IUR when ABCB1 was blocked, the assay was conducted in the presence of 100µM prazosin or 10µM PSC833 respectively.

2.5.12 Cytogenetic analysis

2.5.12.1 Fluorescence in situ hybridisation (FISH)

FISH was performed using Vysis LSI BCR-ABL dual colour, dual fusion probes according to the manufacturer's instructions. Briefly, 1×10^6-1×10^7 cells were harvested from culture, centrifuged for 5 minutes at 1400 rpm, and all but 1mL SN aspirated. Cells were resuspended in remaining 1mL media, and to this 100µL of 10µg/mL colcemid (GIBCO KaryoMAX, Invitrogen) was added. The cells were then incubated (37℃/5%CO_2) for 30 minutes. Note: for Metaphase FISH, cells were first incubated in

100µL ethidium bromide for 40 minutes before the addition of coldemid. Fresh fixative (3:1 methanol:glacial acetic acid) was prepared and refrigerated, while fresh 0.075M KCl was prepared and warmed in 37℃ heating bath. Cells were pelleted (10 minutes at 1000rpm) and SN aspirated. Cells were resuspended in 8mL of warmed KCl, before incubation for 30 minutes (37℃/5%CO_2). Next, 1mL of cold fixative was added to each tube and mixed by inverting several times. Cells were pelleted (10 minutes at 1000rpm) and SN aspirated. Cells were then washed three times in 10mL of cold fixative, and finally resuspended in 1mL of cold fixative. Using a Pasteur pipette, approximately 20µL of cells were dropped from a height of approximately 20cm onto labelled glass slides (polysine coated) and allowed to air-dry before storage at 4℃ in darkness. Each chamber of the Hybaid Omnislide Humidity Chamber (Pegasus Scientific Inc.; Rockville, MD, USA) was filled with 10mL MQ H_2O, and temperature set to 37℃. Next, 20×Saline-Sodium Citrate buffer (SSC; 3M NaCl, 0.3M sodium citrate, pH 7) was diluted with MQ H_2O 1:10 to make 2×SSC. RNase (stock concentration 1mg/mL) was diluted in 2×SSC to make a 100µg/mL working stock. 100µL of the RNase treatment was placed on the fixed cells on the glass slides, and a 22×50mm coverslip was placed on top. Slides were incubated for 1 hour at 37℃ in the Omnislide Humidity Chamber (Pegasus Scientific Inc.). After incubation, coverslips were removed from the slides, and the slides were washed with 2×SSC in a Coplin jar. Slides were then dehydrated by brief rinses in ice-cold 70%, 90% and finally 100% ethanol. The slides were then air-dried on an Omnislide rack (Pegasus Scientific, Inc.). The Omnislide Humidity Chamber (Pegasus Scientific, Inc.) was warmed to 70℃ while probe mix was prepared. To make 10µL probe mix per slide: 7µL Hybridisation mix, 2µL MQ H_2O, 1µL probe. Probe mix was flicked to mix ingredients, and microfuged. 10µL of probe mix was then added to each slide, and covered with a 22×22mm coverslip avoiding air bubbles. Slides were placed in the Humidity Chamber (Pegasus Scientific Inc.) and incubated for 10 minutes at 70℃, then 37℃ overnight (O/N). Coverslips were removed, and slides were washed thrice for 10 minutes in 0.1%SSC at 60℃ in the Hybaid Omnislide Wash Module (Pegasus Scientific Inc.). Next, slides were rinsed in MQ H_2O in a Coplin jar, and air-dried on a slide rack in darkness. Lastly, a Pasteur pipette was used to add one drop of Antifade (0.018g DABCO, 100µL Tris 20mM, 900µL glycerol) onto the slides, and a 22×50mm coverslip was applied. Slides were kept in darkness at 4℃ until analysis with a fluorescence microscope.

2.5.12.2 Karyotyping

For conventional cytogenetic analysis, log phase cultures were treated with 0.1µg/mL colcemid (GIBCO KaryoMAX, Invitrogen) and 0.075M KCl, followed by fixation in 3:1 methanol:acetic acid. The fixed cell suspension was dropped onto microscope slides and the metaphase cells were analysed by microscopy after G-banding using trypsin and Leishman's solution.

2.5.13 Statistics

Figures were developed using GraphPad Prism 5.01 © software (GraphPad Software Inc.) or Microsoft Office Excel 2003 (Microsoft Corporation). Column graphs represent the mean plus the standard error of the mean (SEM), or plus the standard deviation (SD) as indicated. The Student's T-test was used to determine statistical differences between experimental groups where the data sets passed the normality and equal variance tests. Differences were deemed statistically significant when the probability value (*P*-value) was less than 0.05.

Chapter 3:

Imatinib resistance in the K562 cell line is mediated by BCR-ABL overexpression

3.1 Introduction

3.1.1 Adherence and dose-interruptions

Imatinib mesylate was specifically designed to inhibit the ABL kinase domain of BCR-ABL. However, it is also known to bind and inhibit the normal Abelson (ABL) protein, Arg (ABL-related gene) protein, stem cell factor receptor (Kit), the macrophage colony stimulating factor receptor, c-fms, and platelet-derived growth factor receptor α and β (PDGFRα and PDGFRβ) tyrosine kinases[16,23,173,174]. As these and other targets are inhibited by imatinib, patients taking this drug may experience various side-effects, including epiphora and periorbital edema (excessive tear production and fluid retention around the eyes)[175], severe nausea and vomiting[176], or various dermatological conditions[177]. Due to the discomfort imatinib mesylate causes in many patients, compliance (that is, adherence to an imatinib dosage regime) may be affected. Economic and social factors, as well as complacency, may also result in non-adherence[178], while pregnancy will cause some female patients to stop treatment[28].

The ADAGIO study (Adherence Assessment with Glivec: Indicators and Outcomes) assessed adherence in 169 patients (recruited from centres in Belgium) prospectively over a 90-day period. One third of patients were considered to be non-adherent, and only 14.2% of patients were perfectly adherent (taking 100% of prescribed imatinib)[179]. Furthermore, this study revealed that of the patients who achieved a suboptimal response (defined as incomplete haematologic[e] response at 3 months; minor cytogenetic response[f] at 6 months; and less than major molecular response[g] at 18 months, or loss of major molecular response) significantly more were non-adherent (23.2%) compared with patients with optimal response (7.3%, *P*=0.005). Thus, dose interruptions frequently occur during imatinib therapy, and there is evidence for a correlation of non-adherence with suboptimal response[179].

3.1.2 Suboptimal kinase inhibition

In patients receiving imatinib therapy, the median peak and trough plasma concentrations of imatinib are approximately 4μM and 2μM respectively, and these levels are variable between patients[180]. This

[e] Complete haematological remission/response (CHR) is defined by normalization of the white blood cell counts.
[f] Complete cytogenetic remission (CCyR) indicates the absence of the Philadelphia chromosome (Ph) in 20 metaphases on classical karyotyping performed on the bone marrow, and portends favourable prognosis if achieved within 18–24 months of starting therapy with tyrosine kinase inhibitors. Partial cytogenetic remission indicates 1–34% Ph-positive metaphases, and minor cytogenetic remission is 35–90% Ph-positive metaphases.
[g] Major molecular remission (MMR) is defined as a ≥3 log10 reduction of BCR–ABL transcripts by real-time quantitative PCR.

variation may be due to a combination of factors such as imatinib absorption, distribution, metabolism and elimination[180]. Cytochrome P450 (CYP) 3A4 is the main enzyme responsible for imatinib metabolism, and expression/activity of this enzyme varies greatly between patients[180]. Furthermore, protein plasma binding (for example, to albumin and especially α1-acid glycoprotein) also affects bioavailability of imatinib[181].

Patient response is determined by how well imatinib is able to bind and inhibit BCR-ABL. The $IC50^{imatinib}$ assay was developed to measure BCR-ABL kinase inhibition *in vitro*, and is defined as the concentration of imatinib required to reduce levels of the BCR-ABL adapter protein, p-Crkl, by 50%. In a study by White *et. al.*[36], patients with a high $IC50^{imatinib}$ (*i.e.* low sensitivity to imatinib) had a significantly lower probability of achieving cytogenetic and molecular remissions by 12 months. It was also found that $IC50^{imatinib}$ results inversely correlated with intracellular uptake and retention (IUR) of imatinib in patient mononuclear cells (as measured by the IUR assay; *2.5.11*)[39]. Low IUR of imatinib may be mediated by factors intrinsic to the patient, such as drug metabolism, protein plasma binding[180,181], or low OCT-1 activity, as OCT-1-mediated transport is the primary mode of active uptake of imatinib into cells[39]. Indeed, OCT-1 activity has been shown to be predictive of long-term patient outcome[182]. Low IUR may also be mediated by ABCB1 and/or ABCG2 cell surface expression, as these proteins are responsible for imatinib efflux[71,73-75,127]. Non-adherence to the prescribed imatinib dosage would also lower peak imatinib plasma levels, thereby likely contributing to suboptimal IUR in leukaemic cells.

Thus, inadequate BCR-ABL kinase inhibition causes suboptimal response, and evidence suggests this may lead to resistance development.

3.1.3 Generation of imatinib-resistant cell lines

The generation of drug-resistant sub-clones has long been observed in the context of antibiotic-resistant bacteria[183]. Overuse and suboptimal dosage of antibiotics in the human population has led to the development of multi-resistant bacteria. Suboptimal dosage often results when patients cease a therapy regimen prematurely due to complacency or because they “feel better”[184]. In agriculture, animal food is often supplemented with low dose antibiotics[185]. Suboptimal dosage is therefore a

known method of resistance generation, and has been used extensively in the generation of chemotherapy-resistant cell lines (eg. ovarian cancer cell lines resistant to cisplatin and Taxol, epidermoid carcinoma cell lines resistant to colchicine *etc.*)[79,186-189].

Several groups (Le Coutre *et. al.*[139], Mahon *et. al.*[127] and Barnes *et. al.*[161]) have previously generated imatinib resistance in human or murine Bcr-Abl positive cell-lines, by exposing cultures to low-level (*e.g.* 100nM), increasing concentrations of imatinib for a prolonged period of time. By gradually increasing the imatinib concentration in a step-wise fashion (*e.g.* an additional 100nM every 10 days), cells became resistant to up to 1μM imatinib[127,139,161]. Although this method does not mimic imatinib dose fluctuations that patient cells may experience through therapy interruptions or non-adherence, it may reflect the intracellular conditions of a patient with suboptimal IUR (due to plasma protein binding or low OCT-1 activity) who eventually has dosage escalation to improve his/her IUR[52]. Regardless, the resulting imatinib resistant cell lines generated *in vitro* displayed resistance mechanisms similar to those observed in imatinib-resistant patients[127,139,161]. In each of these studies, BCR-ABL overexpression was noted as a mechanism of imatinib resistance.

3.1.4 BCR-ABL overexpression

BCR-ABL overexpression may occur due to altered regulation of the Bcr-Abl promoter[140], duplication of the Ph chromosome[107,141], or through the emergence of double minutes carrying Bcr-Abl[142]. When imatinib-resistance was generated *in vitro* by Le Coutre *et. al.*[139], Mahon *et. al.*[127], and Barnes *et. al.*[161], BCR-ABL overexpression was always accompanied by an increase in Bcr-Abl DNA copy number. In these studies, Bcr-Abl gene amplification was shown by either Southern blots or fluorescence *in situ* hybridisation (FISH). FISH can be used to count Bcr-Abl copy number by using a dual fusion probe that contains probes labelled in red (spanning the Abl locus) and green labelled probes (which bind the Bcr locus). Overlaying these signals can reveal the presence of Bcr-Abl fusion genes. However, only the study by Le Coutre *et. al.*[139] showed that Bcr-Abl amplification was due to HSR and not dmin.

HSR are regions of a chromosome that contain highly amplified (repeating) DNA sequences[144], and are frequently observed in solid tumour cells where an amplified oncogene stains uniformly in

FISH[145,146]. HSR and dmin are closely related, as they are both facilitate oncogene overexpression by amplification[145,146]. Dmin are small, circular fragments of DNA that frequently carry oncogenes and are observed in many different types of human cancers[146,148-150]. As dmin do not have a centromere, they cannot attach to the mitotic spindle, and are distributed to daughter cells randomly during mitosis. The amplification of an oncogene due to dmin can therefore occur rapidly in a population, as cells carrying high numbers will have a selective advantage and outgrow other clones[145]. Dmin carrying Bcr-Abl have been identified in imatinib-resistant CML patients[142]. It is unclear whether the breakdown of HSR gives rise to dmin[145,148,150], or if chromosomal insertion of dmin gives rise to HSR[151-153].

3.1.5 The K562 cell line

The erythroleukaemia K562 cell line was established by Lozzio and Lozzio[166] in 1975 from the pleural effusion of a 53-year-old female with CML in terminal blast crises. The woman was in her fourth year from CML diagnosis, and had previously been treated with busulfan for 3 years and pipobroman for 1 year. Busulfan and pipobroman are both alkylating agents that slow tumour growth by cross-linking guanine bases in DNA double-helix strands, preventing DNA replication and cell division. Both drugs provide symptomatic relief, but are not curative[190,191].

The pleural fluid was collected with heparin, and aliquots of $1.5\text{-}2\times10^7$ cells were diluted with Eagle's minimal essential medium (MEM) plus additional amino acids and 15% foetal bovine serum (FBS). All cultures were kept at 37℃/5%CO_2, and were counted and diluted in fresh media weekly. The cell line was named CML-1 K-562[166].

This was the first human, CML cell line in which the Ph chromosome persisted after prolonged *in vitro* culture (3½ years, 175 serial passages). K562 cells also contain a second reciprocal translocation between the long arms of chromosome 15 and 17 (acrocentric chromosome t(15;17))[166] and an unidentified marker chromosome composed almost entirely of Bcr-Abl fusion genes[192,193]. Additional Bcr-Abl copies are harboured on a der(2)add(2)(q33) chromosome[193]. K562 cells were successfully grafted into nude mice, where they formed solid tumours. Analysis of the tumours revealed cells were near triploid and retained the Ph chromosome[194].

3.2 Approach

3.2.1 Generation of imatinib-resistant cell lines

In general, this study aims to investigate the mechanisms of resistance development (and the kinetics of these events) in human, Bcr-Abl positive cell lines. Therefore, imatinib resistant cell lines were generated *in vitro*, and the intermediate stages of resistance were analysed.

Imatinib resistance was generated using the principle that suboptimal dosage (*i.e.* chronic low intracellular drug concentrations and inadequate kinase inhibition) will allow leukaemic cells to survive and proliferate in the presence of imatinib[127,139,161]. If dosage is escalated slowly enough, this will allow enough time for the emergence of mutant clones (that are mildly resistant to imatinib) and their selection and expansion. A subset of this mildly-resistant population may harbour further mutations/resistance mechanisms that make them more resistant than the bulk population. Thus, every dose escalation will, in theory, select and expand the most imatinib-resistant clones, resulting in the generation of an overtly resistant cell line.

The K562 cell line was chosen for this study, as it has no kinase domain mutations (**Figure 3.1**), nor overexpression of ABCB1 and ABCG2 **(Figure 3.2 & 3.3)**. The K562 cell line is also the parental line of the K562 Dox (ABCB1 overexpressing) cell line. Thus, to be able to compare resistance mechanism emergence in the presence or absence of a drug efflux protein (such as ABCB1), both the K562 and K562 Dox cell lines (see Chapters 4 and 5) were used for tyrosine kinase inhibitor (TKI)-resistance generation

Cultures of K562 cells (obtained from the American Type Culture Collection (Manassas, VA, USA) were passaged in our laboratory for no more than 4 months before resistance generation was commenced. K562 cultures were initiated in 100nM IM, or maintained long-term in the absence of drug as a control (named K562 Naive cells). IM was serially diluted in Milli-Q water from a 10mM stock solution. Drug concentration was increased by 100-200nM approximately every 20 days, until reaching 2µM IM (approximately 7 month total duration). In patient plasma, peak and trough concentrations of imatinib are approximately 4µM and 2µM respectively[180]. Therefore, 2µM imatinib was chosen as the final ‘resistant’ concentration, as this is pharmacologically relevant.

Figure 3.1: The K562 Naïve cell line does not carry any BCR-ABL kinase domain mutations
1×10^7 K562 cells (passage 44) were harvested, pelleted and resuspended in TRIzol reagent. RNA was extracted from the TRIzol solution and used as a template for cDNA synthesis. A Long PCR was then conducted to amplify the product, and conventional sequencing of the BCR-ABL kinase domain was conducted. Shown is an example "screen shot" of Mutation Surveyor Version 3.24, where the kinase domain of the K562 Naïve cell line was sequenced and analysed from residue 309 to 338. Each peak represents a DNA base (A = Adenine; C = Cytosine; G = Guanine; or T = Thymine) in the 5'-3' direction of the ABL sequence. Note the sequence from the K562 Naïve cell line exactly matches exactly with the ABL reference sequence, indicating the lack of mutations in this cell line.

Figure 3.1

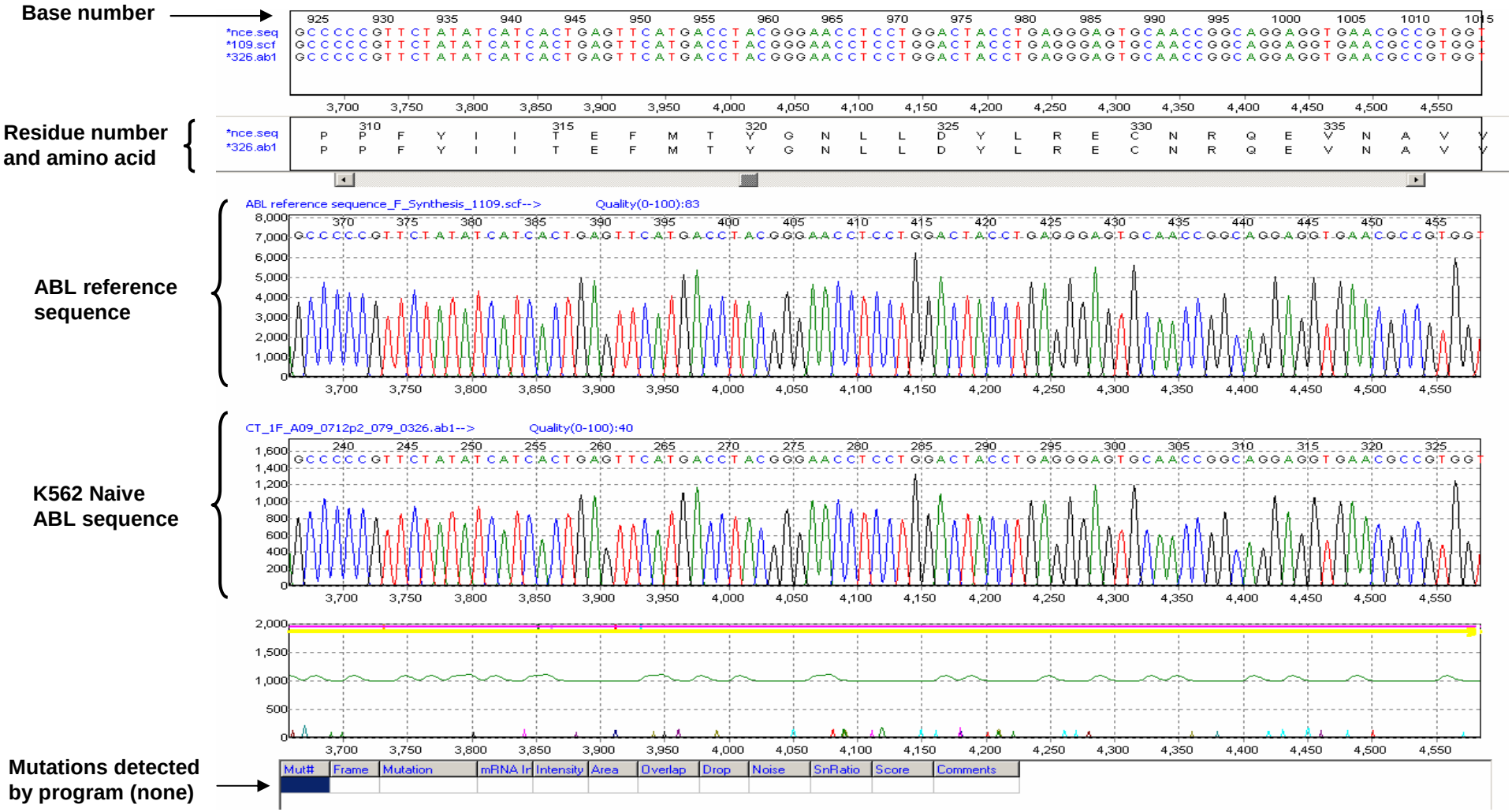
Base number
Residue number and amino acid
ABL reference sequence
K562 Naive ABL sequence
Mutations detected by program (none)
ABL reference sequence_F_Synthesis_1109.scf--> Quality(0-100):83
CT_1F_A09_0712p2_079_0326.ab1--> Quality(0-100):40
Mut# Frame Mutation mRNA Ir Intensity Area Overlap Drop Noise SnRatio Score Comments

Figure 3.2

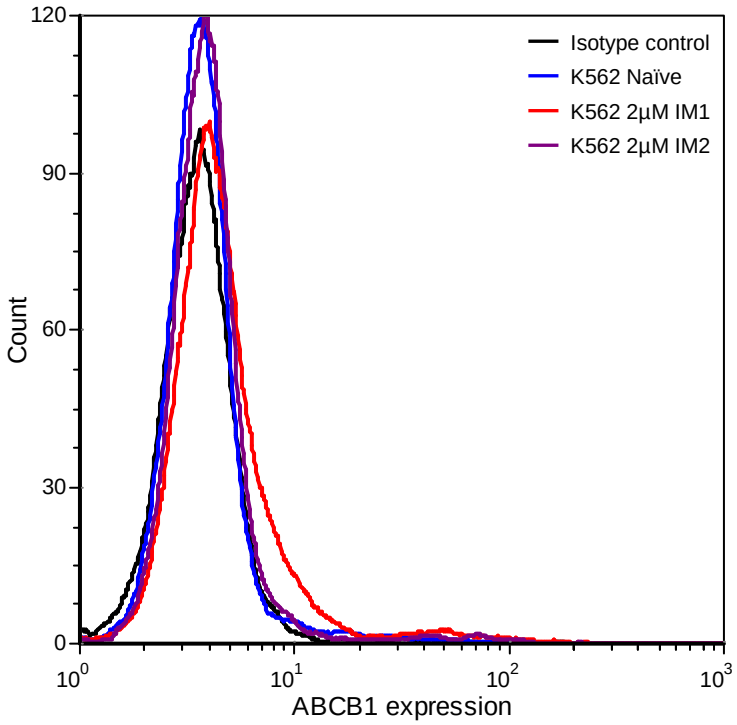

Figure 3.2: ABCB1 cell-surface expression in the IM1 and IM2 resistant cell lines
K562 Naive and resistant cells were harvested and stained with either an isotype control antibody or the PE ABCB1 antibody. After a 45 minute incubation with the antibody, the cells were washed and analysed by flow cytometry. No ABCB1 expression could be detected in either the Naïve or resistant cell lines. Histogram is representative of 3 experiments.

Figure 3.3

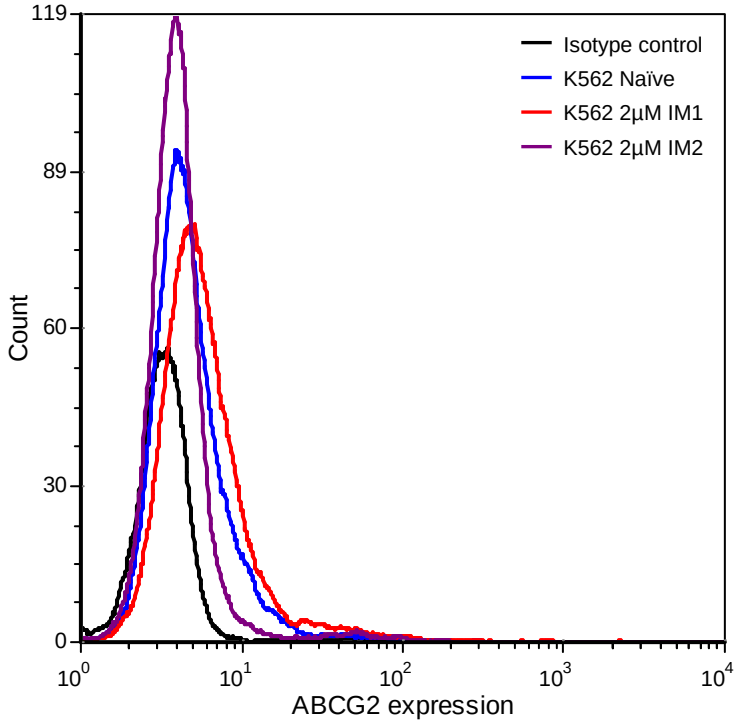

Figure 3.3: ABCG2 cell-surface expression in the IM1 and IM2 resistant cell lines
K562 Naive and resistant cells were harvested and stained with either an isotype control antibody or the PE ABCG2 antibody. After a 45 minute incubation with the antibody, the cells were washed and analysed by flow cytometry. No change in ABCG2 expression could be detected when comparing Naïve and resistant cell lines. Histogram is representative of 3 experiments.

Two imatinib-resistant K562 cell lines were generated. The first IM-resistant K562 cell line (named K562 2µM IM1) was escalated as follows: 100nM, 200nM, 300nM, 400nM, 500nM, 700nM, 900nM, 1.1µM, 1.5µM, 2µM. At the 400-500nM intermediate stages, it was noted that proliferation rate was increasing and cells became able to withstand larger increases in drug concentration. Accordingly, dose escalations became larger (eg. 200nM, 400nM, and finally 500nM) to reach the final concentration of 2µM IM after 7 months.

The second IM-resistant K562 cell line (named K562 2µM IM2) was escalated as follows: 100nM, 200nM, 300nM, 450nM, 600nM, 800nM, 1.4µM, 2µM. Fewer intermediates and larger dose escalations resulted in the 2µM IM2 concentration being reached sooner (less than 6 months). A parental, imatinib-naïve culture was maintained in parallel as a control, named K562 Naïve.

3.2.2 Analysis of imatinib-resistant cell lines

As the study progressed, the kinetics of resistance-mechanism emergence became of great interest. Thus, samples were collected at each point of dose escalation to make DNA and RNA for later analysis. BCR-ABL expression in intermediates could therefore be measured by RQ-PCR, as could the mutation status of the kinase domain.

Viability of these cells in the presence of imatinib was measured by trypan blue analysis, and flow cytometry. Cells were washed to remove traces of imatinib from media, and cultured in a range of imatinib concentrations for three days, before counting or staining dying and apoptotic cells with Annexin V and 7AAD. This enabled direct comparison of the viability in the IM-resistant cell lines with the K562 Naïve control, when exposed to imatinib. $IC50^{imatinib}$ assays were conducted to measure the extent of BCR-ABL kinase activity inhibition occurring by measuring levels of p-Crkl. Crkl is a direct BCR-ABL target, and it has been demonstrated that there is a direct correlation between the presence of BCR-ABL and the phosphorylation status of Crkl[37]. The $IC50^{imatinib}$ is therefore defined as the concentration of imatinib required to reduce levels of p-Crkl by 50%. Intracellular uptake and retention (IUR) assays were used to investigate the amount of imatinib being internalised and retained in the cells. By the addition of prazosin (a potent OCT-1 inhibitor) the OCT-1 activity was also measured. The resistant cell lines were also screened for ABCB1 and ABCG2 cell surface expression by flow cytometry. Furthermore, interphase fluorescence *in situ* hybridisation (FISH) using a dual fusion Bcr

and Abl probe enabled copies of the fusion gene to be visualised in fixed cells. Metaphase FISH and karyotyping was used to determine the presence of Bcr-Abl on specific chromosomes, while DNA PCR allowed for quantification of Bcr-Abl DNA copy number.

3.3 Results

Two K562 2μM IM-resistant cell lines were generated by long-term culture in gradually increasing concentrations of imatinib. Viability of these cells in the presence of imatinib was measured by trypan blue analysis, and flow cytometry. Cells were washed by centrifugation in fresh media and cultured in a range of imatinib concentrations for three days, before counting or staining the dying and apoptotic cells. Both the IM-resistant cell lines had significantly increased survival compared to the K562 Naïve control (reaching significance at 250nM imatinib for both methods; P<0.02)(**Figure 3.4 and 3.5**).

The IC50 assay measures levels of BCR-ABL kinase inhibition in the presence of a tyrosine kinase inhibitor (**Figure 3.6**). This assay has been shown to be predictive of molecular response in *de novo* CML patients, and a high IC50 is indicative of imatinib refractoriness[36]. In both the K562 IM1 and IM2 resistant lines, the IC50 for imatinib ($IC50^{imatinib}$) increased significantly from an average of 6.6μM (naïve control) to 37μM (P<0.0002) and 48μM (P<0.000002) respectively (**Figure 3.7 and 3.8**).

Studies have shown that an increase in the cell-surface expression of ABCB1 (an imatinib efflux protein) increases the $IC50^{imatinib}$ of Bcr-Abl positive cell lines[127,195]. As both ABCB1 and ABCG2 are known to efflux imatinib, the cell-surface expression of these proteins was investigated as a possible cause of the increased $IC50^{imatinib}$. However, flow cytometry could not detect any cell-surface expression of either ABCB1 (**Figure 3.2**) or ABCG2 (**Figure 3.3**).

OCT-1 is the major active influx protein responsible for imatinib transport into cells[39,40]. It has been shown that increased $IC50^{imatinib}$ in CML patient mononuclear cells is mediated by reduced OCT-1 activity[39,52]. Intracellular uptake and retention (IUR) assays were therefore conducted to determine whether imatinib IUR or OCT-1 activity had decreased in the K562 IM-resistant cell lines. However, there was no decrease in the IUR or OCT-1 activity in these cells (**Figure 3.9 and 3.10**). Furthermore, the addition of PSC833 (an ABCB1 inhibitor) or Ko143 (an ABCG2 inhibitor) did not significantly increase the imatinib IUR in either cell line (P>0.3), supporting the finding that no ABCB1 or ABCG2 cell-surface expression was present (**Figure 3.9 and 3.10**).

Figure 3.4

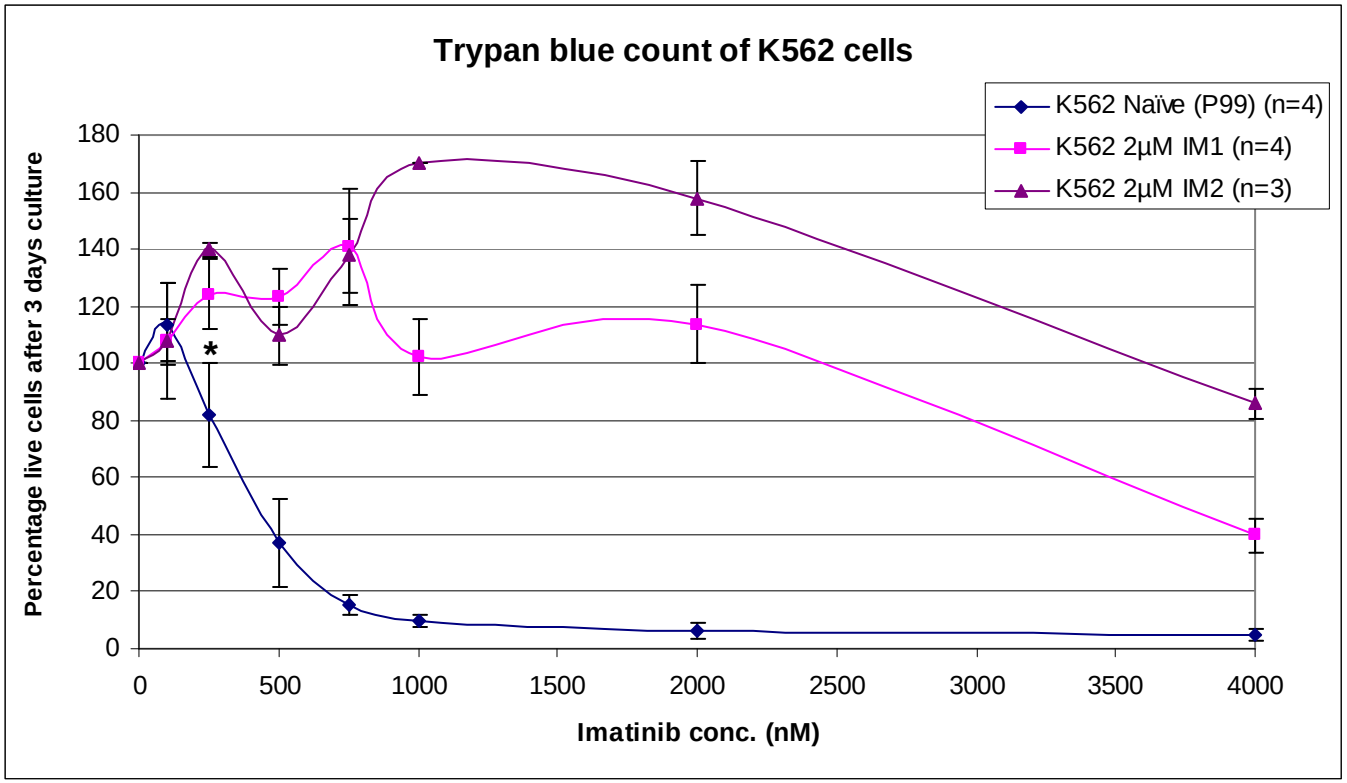

Figure 3.4: Viability assay by trypan blue analysis: K562 Naïve versus K562 2µM IM1 & IM2 cell lines
Cells were washed and resuspended in fresh culture media to remove traces of drug, before being cultured in a 24-well plate. 1×10^5 cells were seeded in 1mL culture medium, and different concentrations of imatinib (serially diluted in water) were added to each well. A no drug control was always included. The 24-well plates were incubated at 37℃/5%CO_2 for three days before trypan blue cell counts were performed. Counts were normalised to viable cells in 0nM drug control well (100%). Data are presented as mean ±SD of at least 3 independent experiments. *P<0.02.

Figure 3.5

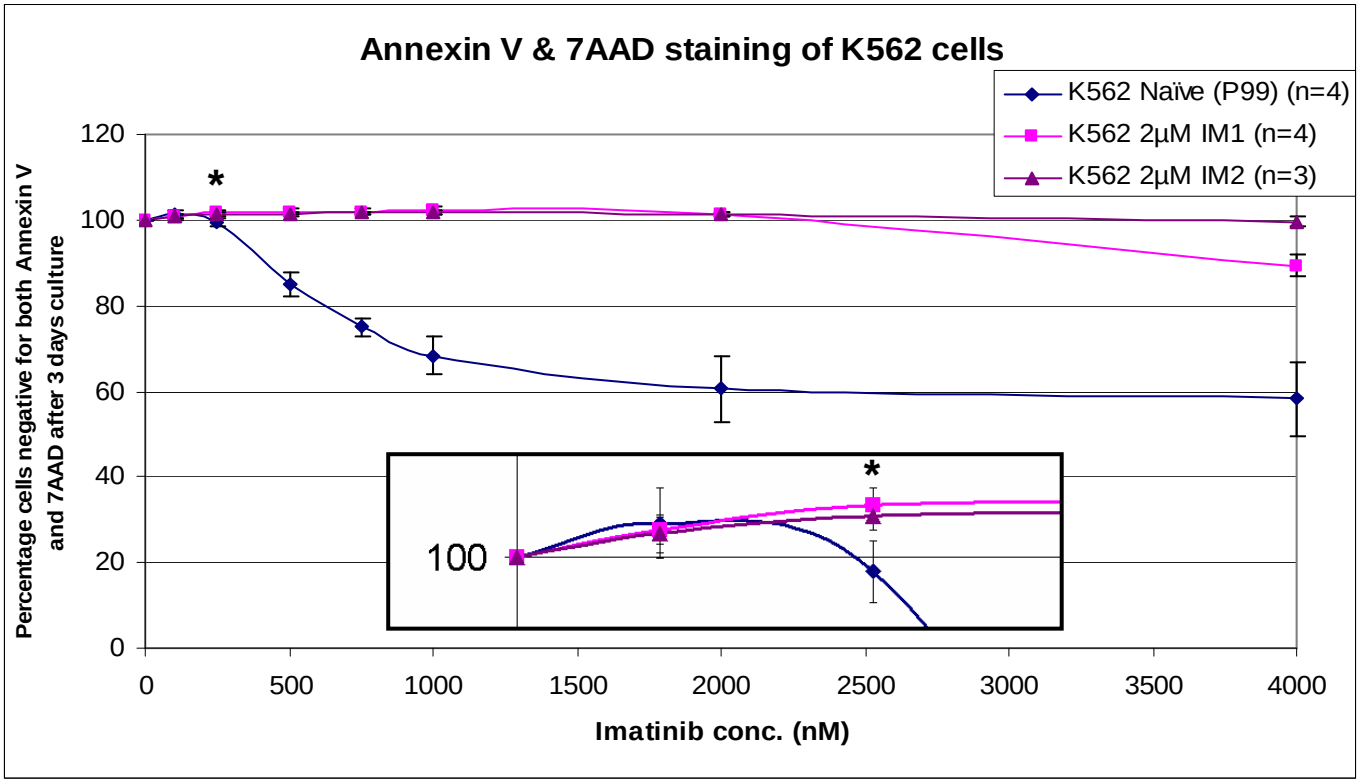

Figure 3.5: Viability by Annexin V and 7AAD staining: K562 Naïve versus K562 2µM IM1 & IM2 cell lines
Cells treated as in figure 3.4. Dying and apoptotic cells were stained with both Annexin V and 7AAD, before being analysed by flow. Live cells were defined as those negative for both Annexin V and 7AAD staining. Counts were normalised to live cells in the 0nM drug control (100%). Data are presented as mean ±SD of at least 3 independent experiments. Inset shows a magnified image of the first three value points. *P<0.01.

Figure 3.6: Example of a K562 Naïve IC50^{imatinib} Western blot quantification
Cells were incubated for 2 hours at 37℃/5%CO_2 with IM concentrations ranging up to 100µM. Western blot analysis for p-Crkl was performed as previously described[36]. Signals were quantified using Image Quant software (Molecular Dynamics), and the ratio of p-Crkl to Crkl was determined using Image Quant analysis. **(A)** Polygons were drawn around each Crkl and p-Crkl band, and blank membrane was also sampled as a background control. **(B)** Bands of p-Crkl were measured and graphed as a percentage of the intensity of total Crkl (*i.e.* p-Crkl + Crkl intensity = 100%). **(C)** These percentages are normalised (0µM imatinib is 100% p-Crkl, 100µM imatinib is 0% p-Crkl). The IC50 value is then taken as the concentration of imatinib when normalised p-Crkl reaches 50% (*i.e.* IC50^{imatinib} = 9µM in this case). This blot is shown again in Figure 3.7.

Figure 3.6

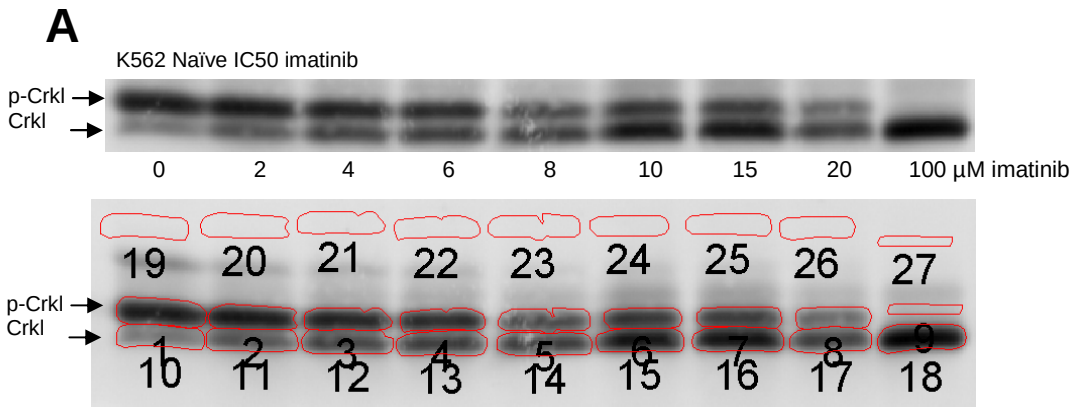
A
K562 Naïve IC50 imatinib
p-Crkl
Crkl
0
2
4
6
8
10
15
20
100 µM imatinib
19
20
21
22
23
24
25
26
27
1
2
3
4
5
6
7
8
9
10
11
12
13
14
15
16
17
18

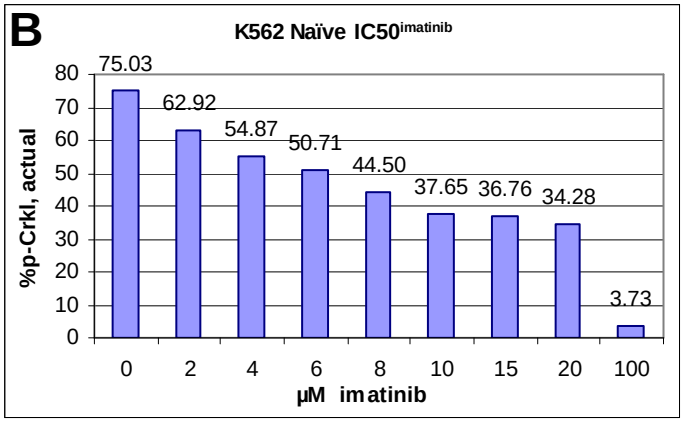
B
K562 Naïve IC50imatinib
%p-Crkl, actual
75.03
62.92
54.87
50.71
44.50
37.65
36.76
34.28
3.73
µM imatinib

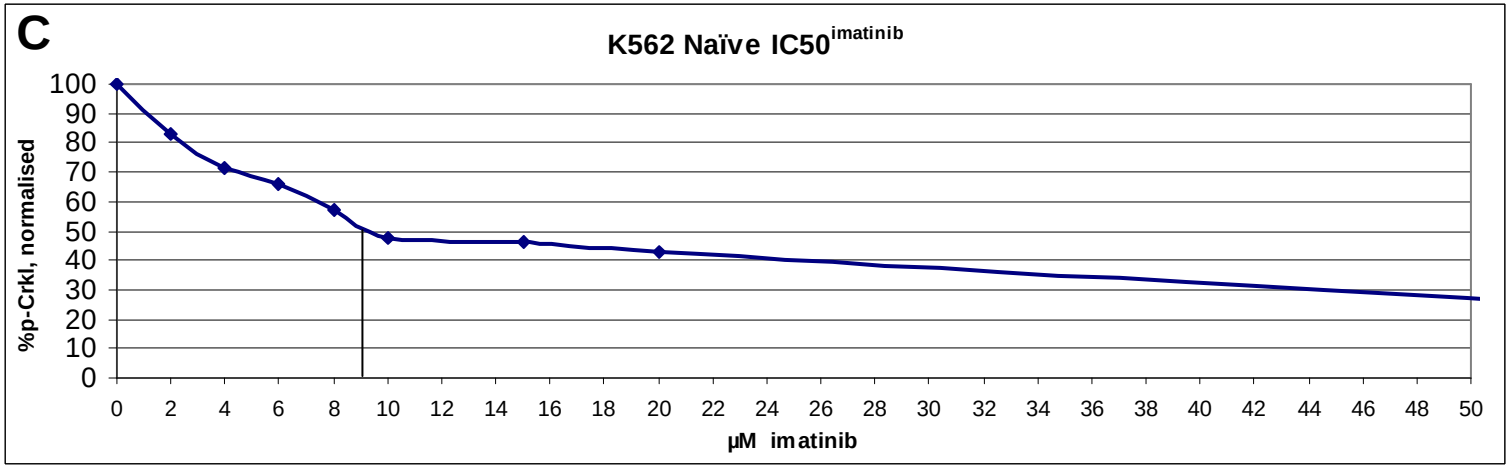
C
K562 Naïve IC50imatinib
%p-Crkl, normalised
µM imatinib

Figure 3.7

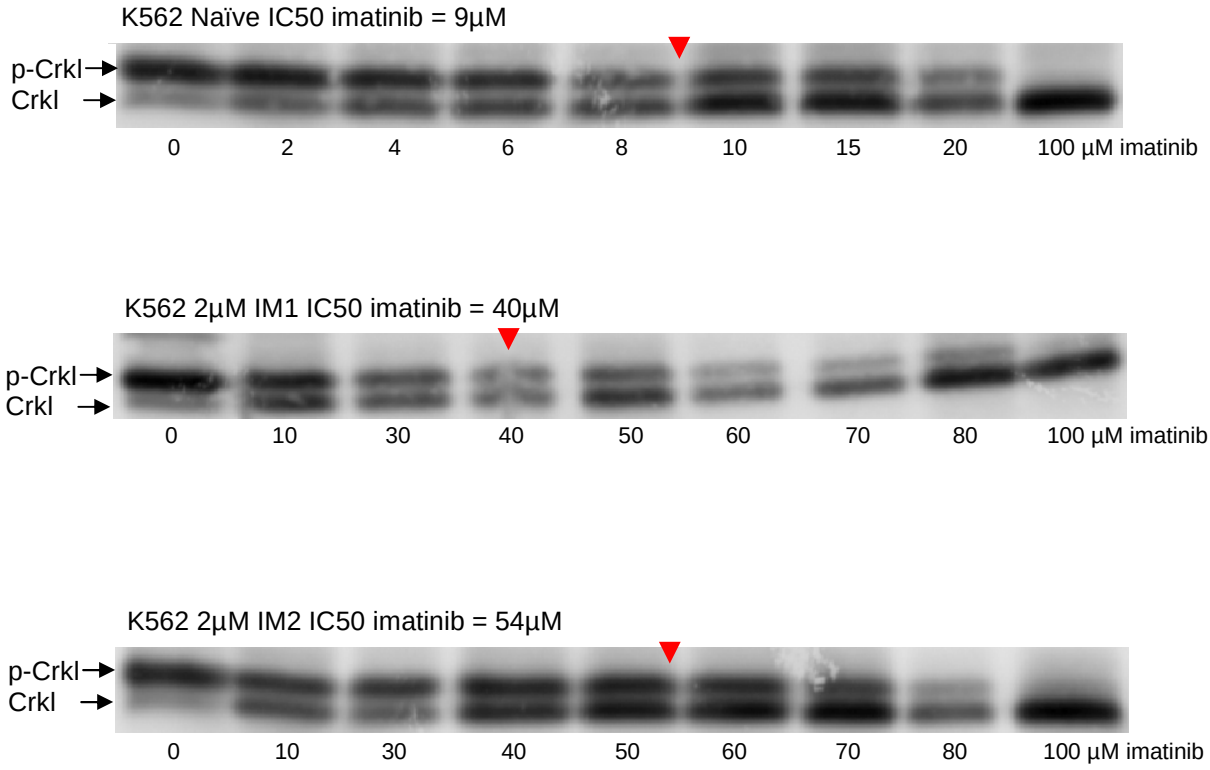

Figure 3.7: IC50^{imatinib} of the K562 Naïve, K562 2µM IM1 and K562 2µM IM2 cell lines

Cells were incubated for 2 hours at 37℃/5%CO_2 with IM concentrations ranging up to 100µM. Western blot assays for p-Crkl were performed as previously described[36]. Signals were quantified using Image Quant software (Molecular Dynamics), and the ratio of p-Crkl to Crkl was determined using Image Quant analysis. The IC50 value for each blot (determined as the dose of drug required to reduce levels of p-Crkl by 50%) is indicated above each blot (and with red arrow). IC50 assays were conducted at least four times, and one representative blot is shown for each of the three cell lines.

Figure 3.8

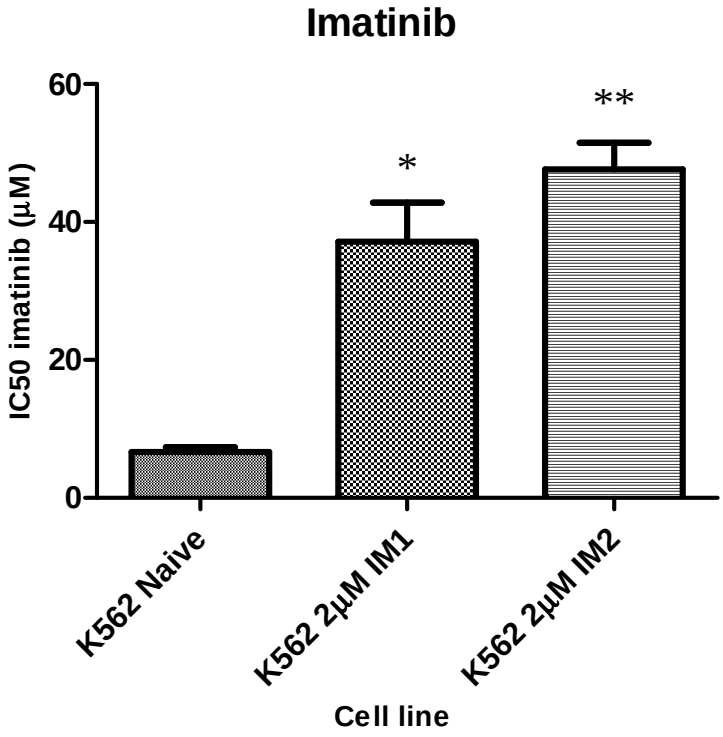

Figure 3.8: Average IC50 imatinib for K562 Naïve, K562 2µM IM1 and K562 2µM IM2

IC50 assays determine the concentration of imatinib required to reduce levels of p-Crkl (a BCR-ABL adapter protein) by 50%. A higher IC50 value indicates greater resistance to imatinib, while a lower IC50 value indicates more sensitivity. Data are presented as mean +SEM of data from at least 4 independent experiments. The $IC50^{IM}$ for both K562 2µM IM1 and IM2 were significantly greater than the Naïve control (**P*<0.0002; ***P*<0.000002).

Figure 3.9

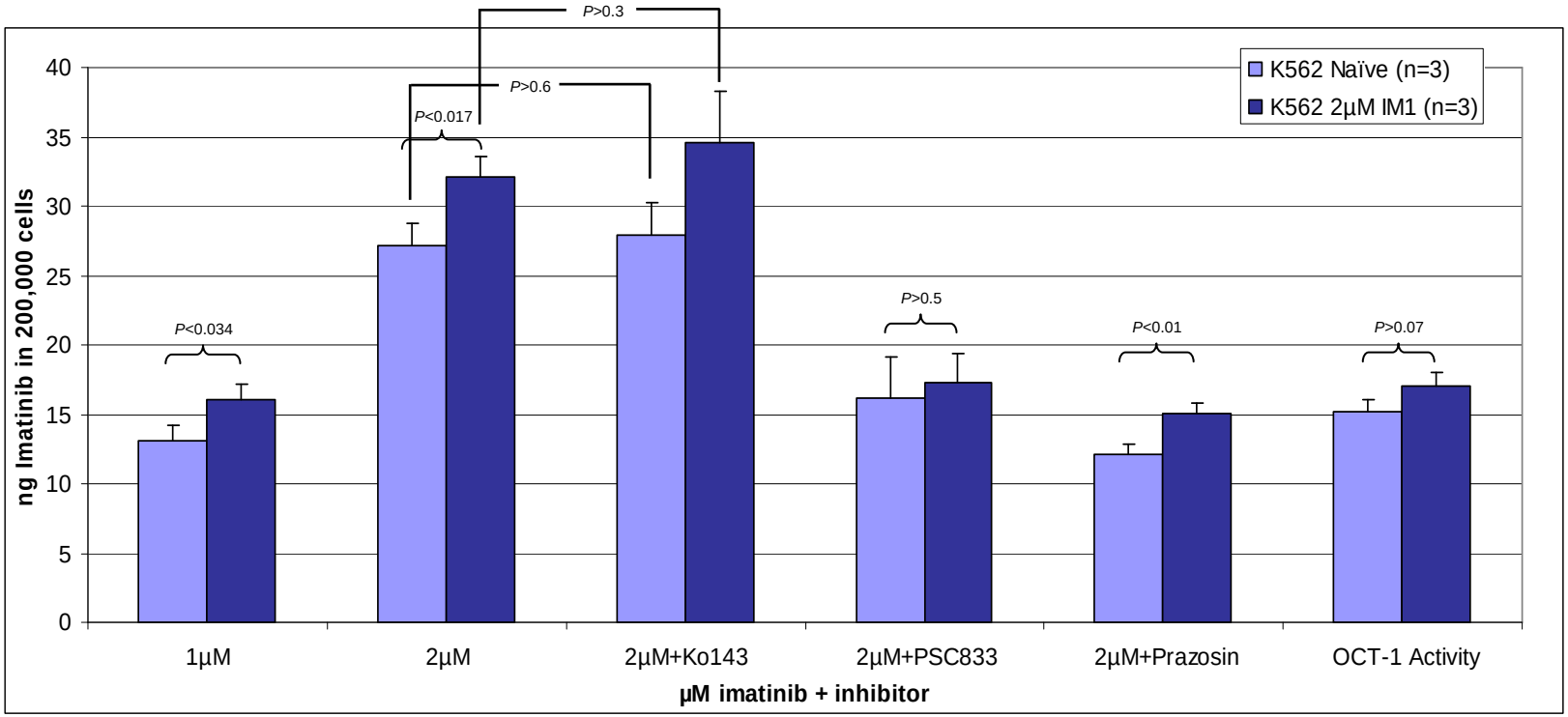

Figure 3.9: Imatinib IUR assay: K562 Naïve cell line versus K562 2µM IM1 cell line
The IUR assay was performed as previously described[172]. Ko143 (0.5µM) inhibits ABCG2, while PSC833 (10µM) inhibits ABCB1. Prazosin (100µM) is a potent inhibitor of OCT-1, so the OCT-1 activity is calculated by subtracting the IUR in the presence of prazosin from the IUR in the absence of prazosin. The IM1-resistant cell line had neither a decreased IUR, nor a decreased OCT-1 activity compared to the Naïve control. Furthermore, blocking ABCB1 or ABCG2 did not result in an increased IUR for either cell line, indicating imatinib efflux by these proteins is not facilitating resistance. Data are presented as mean +SD calculated from at least three independent experiments.

Figure 3.10

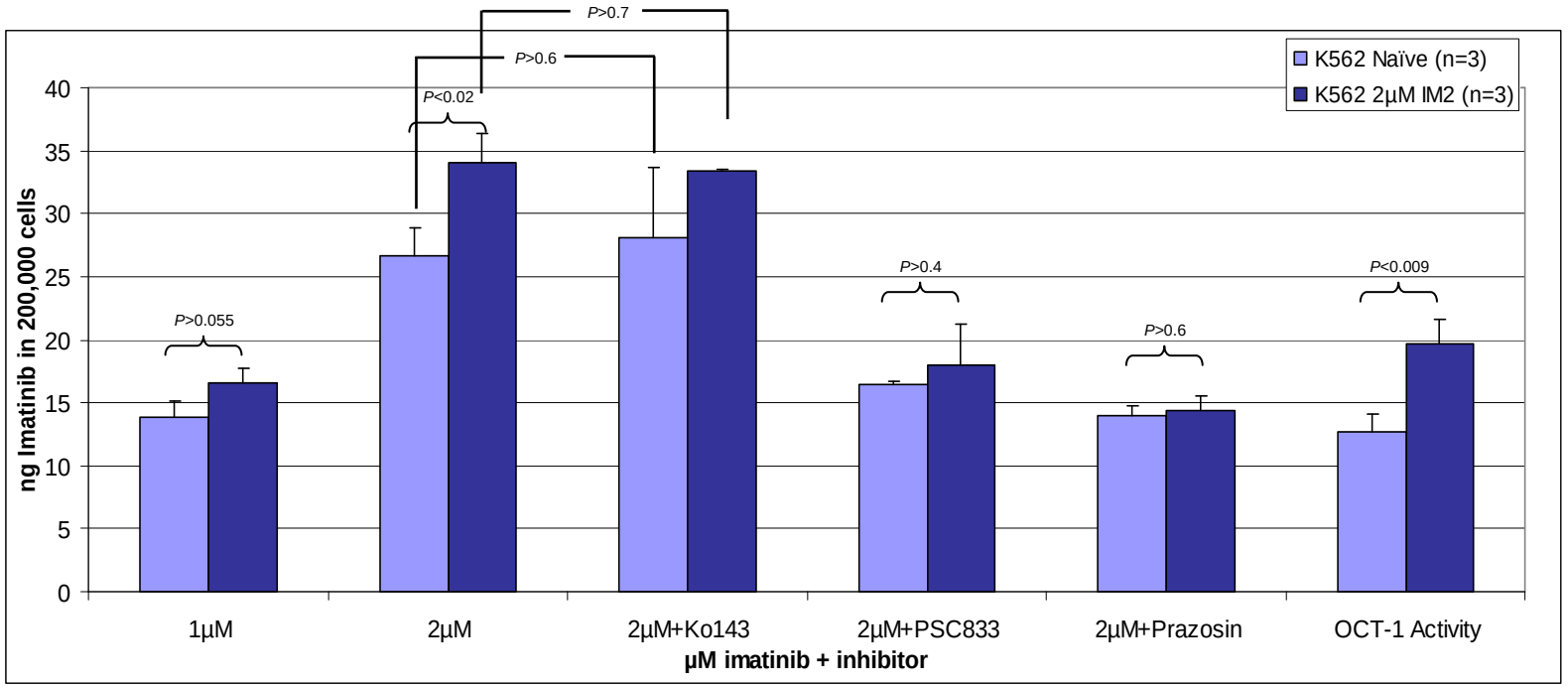

Figure 3.10: Imatinib IUR assay: K562 Naïve cell line versus K562 2µM IM2 cell line
The IUR assay was performed as previously described[172]. Ko143 (0.5µM) inhibits ABCG2, while PSC833 (10µM) inhibits ABCB1. Prazosin (100µM) is a potent inhibitor of OCT-1, so the OCT-1 activity is calculated by subtracting the IUR in the presence of prazosin from the IUR in the absence of prazosin. The IM2-resistant cell line had neither a decreased IUR, nor a decreased OCT-1 activity compared to the Naïve control. Unexpectedly, OCT-1 activity is significantly increased in the IM2-resistant cell line. Blocking ABCB1 or ABCG2 did not result in an increased IUR for either cell line, indicating imatinib efflux by these proteins is not facilitating resistance. Data are presented as mean +SD calculated from at least three independent experiments.

Increased BCR-ABL expression may also increase the concentration of imatinib required to halve kinase activity[7,40,83]. To investigate whether BCR-ABL expression had increased in the IM-resistant cell lines, RQ-PCR was conducted to quantitatively measure BCR-ABL transcript number (with respect to the BCR control gene[196]). RQ-PCR revealed that BCR-ABL/BCR transcript levels significantly increased in both lines from 178% in naïve cells, to approximately 1200% (P<0.0002) and 400% (P<0.002) in the 2µM IM1 and IM2 cell lines respectively (**Figure 3.11**). Studies of the intermediates of resistance development showed a step-wise increase of BCR-ABL expression, before reaching a plateau (**Figure 3.11**). The increase in BCR-ABL expression may have been due to a mutation in the promoter of Bcr-Abl, or an increase in the Bcr-Abl DNA copy number. To distinguish which had occurred, interphase FISH was conducted using a dual colour probe to visualise the number of Bcr-Abl fusion genes in naïve cells compared to the resistant cell lines (**Figure 3.12**). From these results, it appears that the Bcr-Abl copy number has increased in the IM-resistant cell lines compared to the Naïve control, and the spread of fusion signals indicates the presence of dmin. To confirm that amplification had occurred due to double minutes, the cell lines were karyotyped (**Figures 3.13 & 3.14**). However, no double minutes were observed in the IM-resistant cell lines. Instead, HSR harbouring the Bcr-Abl fusion gene were observed using metaphase FISH (**Figure 3.15**). It was found that two marker chromosomes carried additional copies of Bcr-Abl in the K562 Naïve cell line (**Figure 3.13 & 3.15**), while a large HSR on chromosome 14 was responsible for amplification in the K562 2µM IM1 cell line (**Figure 3.14 & 3.15**). A new marker chromosome with HSR in the K562 2µM IM2 cell line was the source of Bcr-Abl amplification in these cells.

To quantify Bcr-Abl copy number, quantitative DNA PCR was conducted using the house-keeping gene, Beta-glucuronidase (GUSB), as a reference gene[196]. These experiments confirmed that Bcr-Abl copy number had significantly increased in both the IM1 and IM2 cell lines from 101% in naïve cells to 721% (P<0.0000003) and 187% (P<0.0005) respectively (**Figure 3.16**). Sequencing of the kinase domain did not reveal the presence of any mutations in either of the IM-resistant cell lines, or in the Naïve control cell line.

Figure 3.11

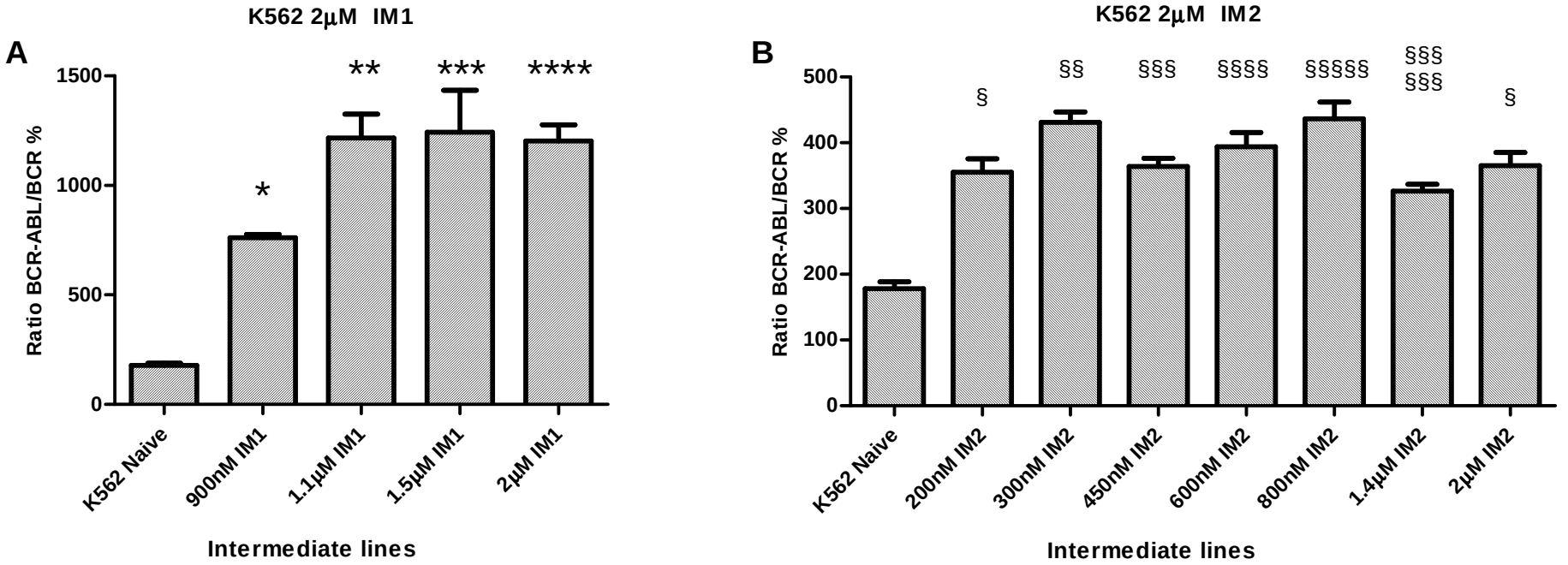

Figure 3.11: Intermediate BCR-ABL expression in the IM1 and IM2 resistant cell lines
BCR-ABL expression increased as IM concentration was escalated in the two IM-resistant K562 cell lines, K562 2µM IM1 **(A)** and K562 2µM IM2 **(B)**. Samples were taken at intermediate stages of resistance development, and cDNA was synthesised using the RNA extracted from 1×10^7 cells. RQ-PCR was conducted using cDNA as the template, and BCR-ABL expression was determined as a ratio of BCR expression. Data are presented as mean +SEM from at least 3 independent experiments. All intermediates are significantly different from the Naïve line (*P<0.000006; **P<0.0007; ***P<0.006; ****P<0.0002; $^{\S}P$<0.002; $^{\S\S}P$<0.0002; $^{\S\S\S}P$<0.0004; $^{\S\S\S\S}P$<0.0009; $^{\S\S\S\S\S}P$<0.0007; $^{\S\S\S\S\S\S}P$<0.0006).

Figure 3.12

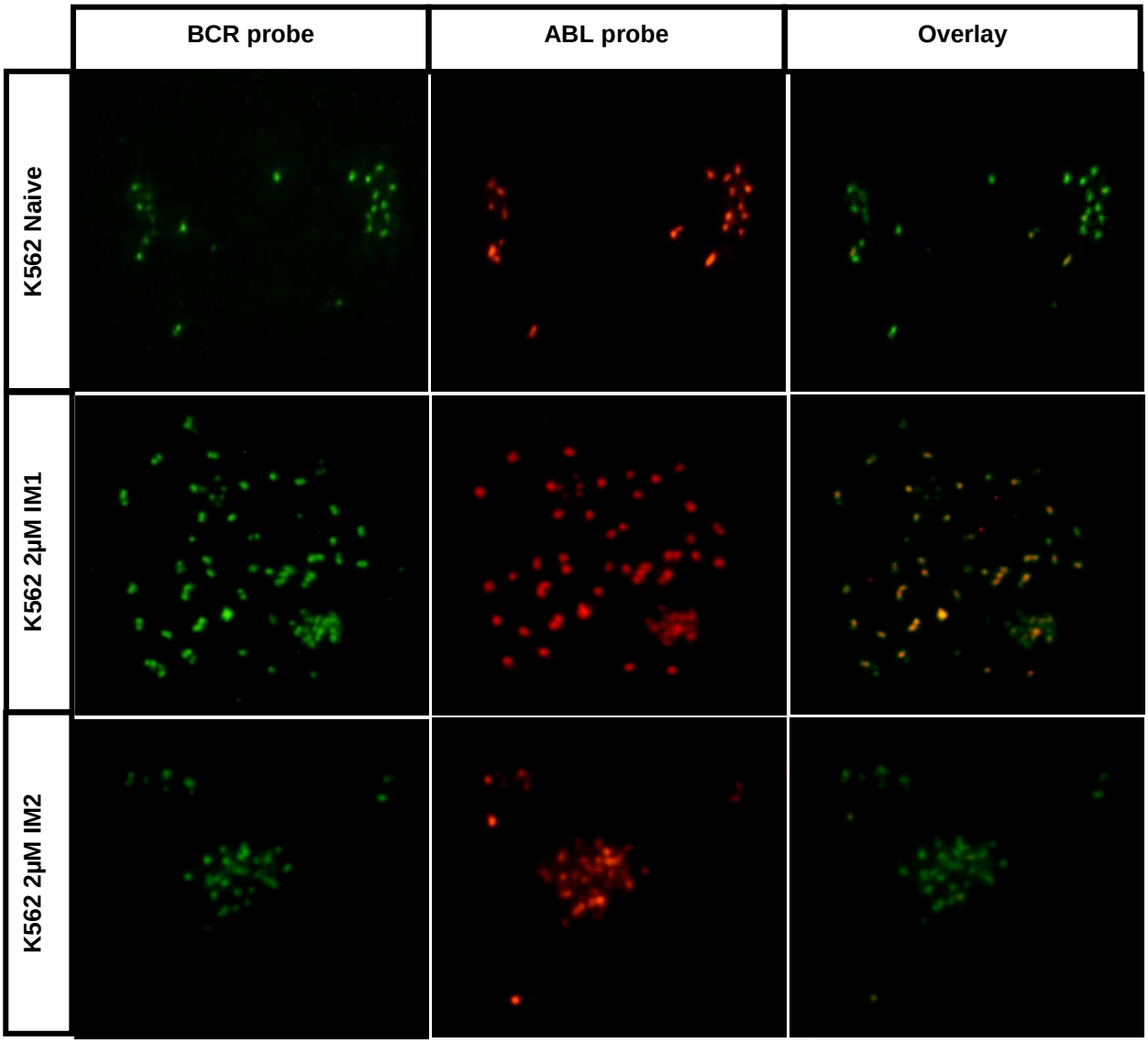

Figure 3.12: Interphase FISH to identify BCR-ABL fusion genes
1×10^6 cells were harvested from culture and incubated in 100µL colcemid before being fixed onto glass slides. After RNase treatment, cells were probed with a dual fusion probe and analysed with a fluorescence microscope. Shown above are a single, representative K562 Naïve cell (top panel), K562 2µM IM1 cell (middle panel), and K562 2µM IM2 cell (bottom panel). Bcr-Abl amplification in the IM-resistant lines, especially the IM1 cell line, is evident due to numerous co-localising BCR (green) and ABL (red) signals.

Figure 3.13

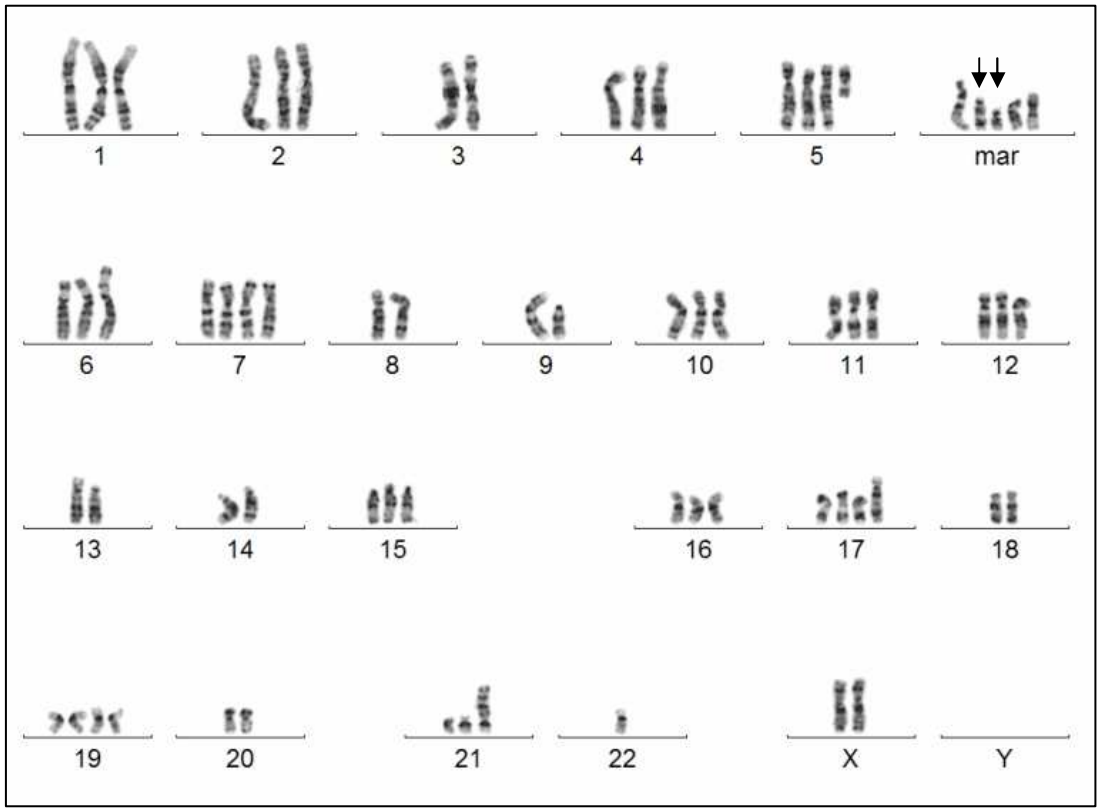

Figure 3.13: Karyotype of the K562 Naïve cell line
The K562 Naïve cell line had undergone over 100 passages as a control culture. This cell line is believed to harbour multiple copies of Bcr-Abl on the marker chromosomes indicated with arrows. Also note ploidy of chromosome 7 which harbours the GUSB reference gene. Karyotyping conducted by Sarah Moore.

Figure 3.14: Karyotype of K562 2µM IM1 and IM2 cell lines
Note multiple marker chromosomes, and large homogeneously staining region on chromosome 14 in the K562 2µM IM1 karyotype (top). Also note a new marker chromosome (which may contain a homogeneously staining region) and additional material on chromosome 7 in the K562 2µM IM2 karyotype (bottom). These abnormalities may harbour additional copies of Bcr-Abl. Karyotyping conducted by Sarah Moore.

Figure 3.14

K562 2μM IM1

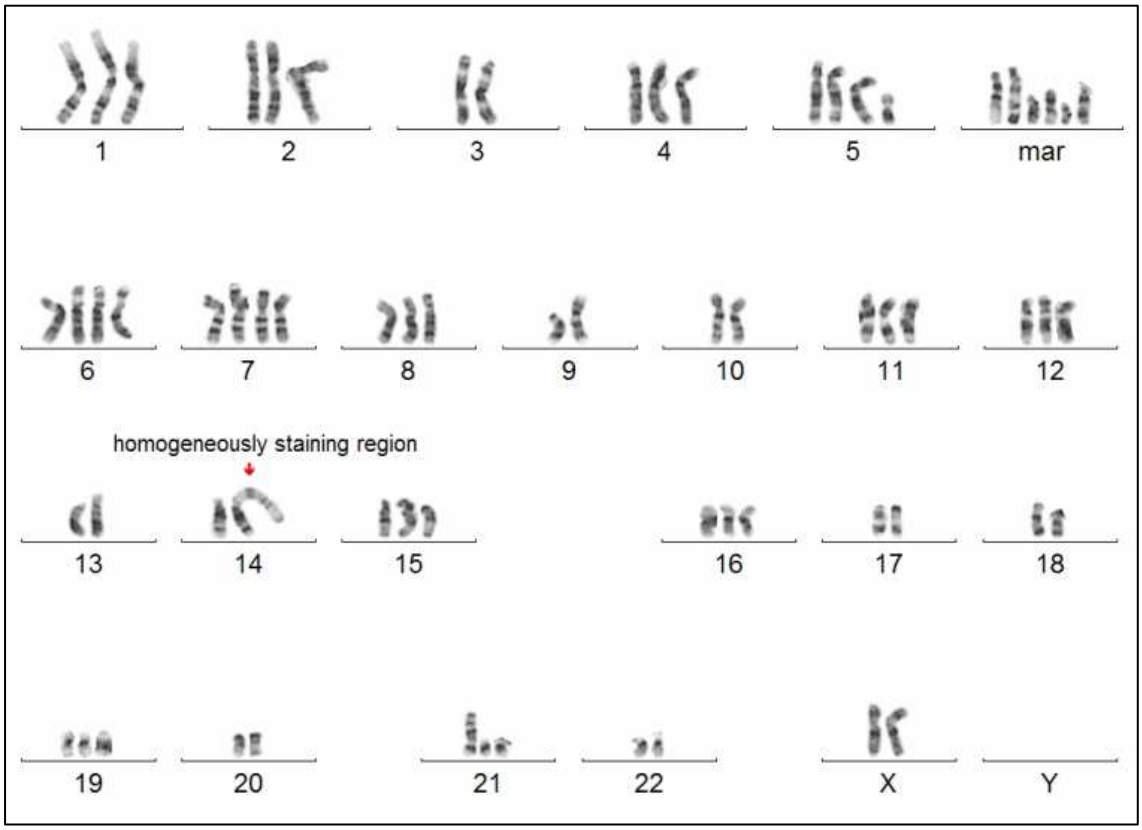

K562 2μM IM2

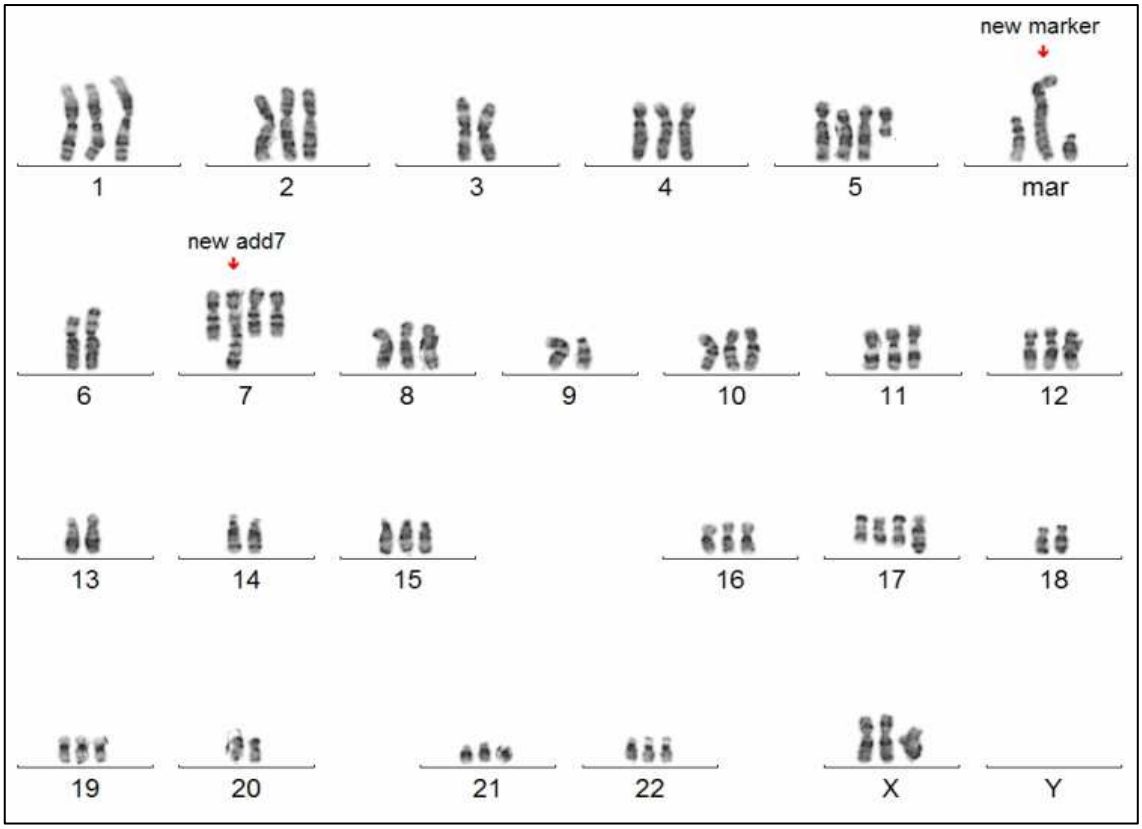

Figure 3.15

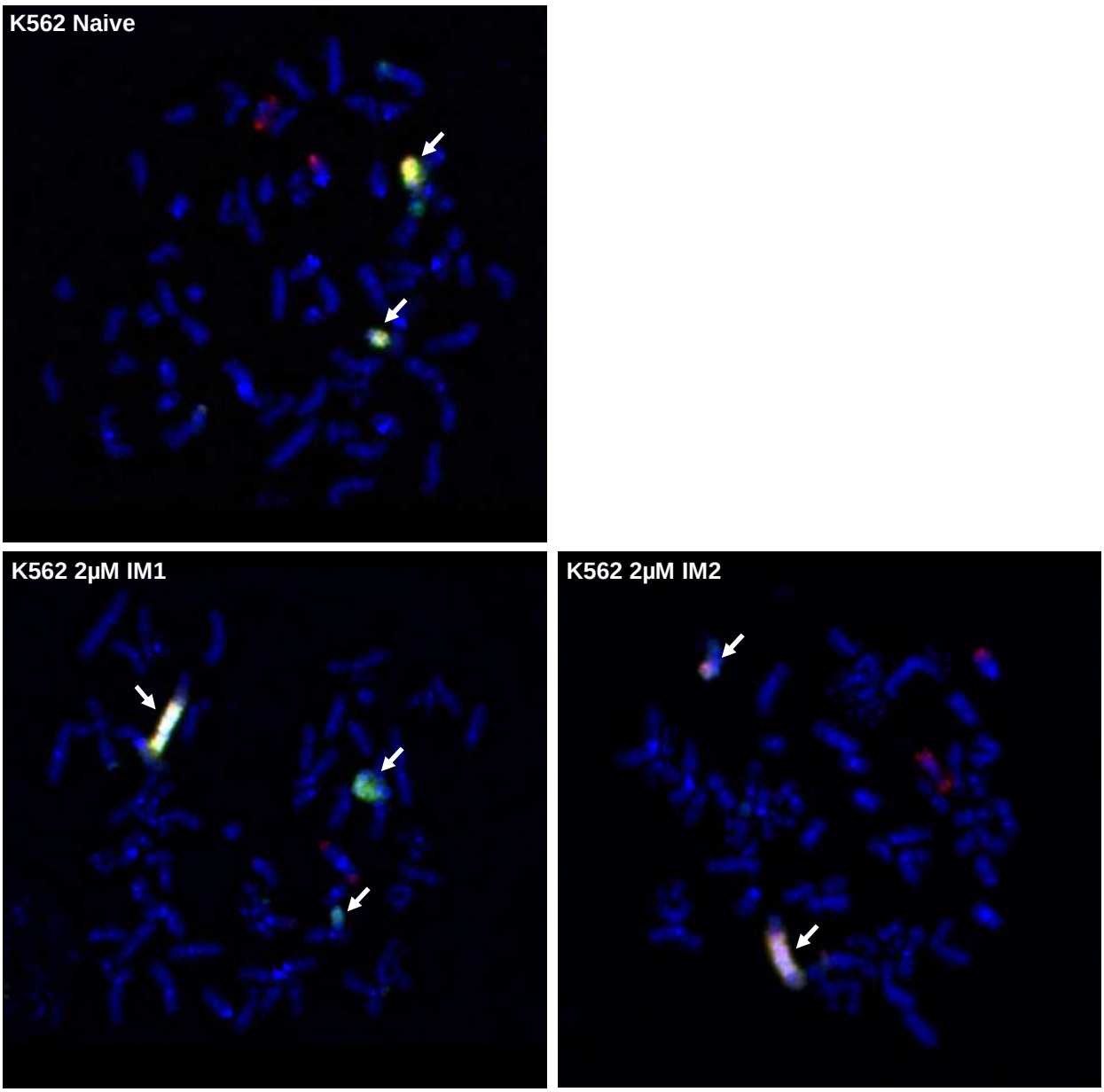

Figure 3.15: Metaphase FISH to identify markers carrying Bcr-Abl
1×10^{7} cells were harvested from culture and incubated in 100μL ethidium bromide, and subsequently 100μL colcemid, before being fixed onto glass slides. After RNase treatment, cells were probed with a dual fusion probe and analysed with a fluorescence microscope. Shown above are a single, representative K562 Naïve cell (top), K562 2μM IM1 cell (bottom left), and K562 2μM IM2 cell (bottom right). Arrows indicate homogeneously staining regions (HSR) carrying the Bcr-Abl fusion gene. In the K562 Naïve line, the two markers indicated in Figure 3.12 are identified here as harbouring Bcr-Abl. In the K562 2μm IM1 cell line, two marker chromosomes as well as a large HSR on chromosome 14 are found to carry Bcr-Abl (see Figure 3.13). In the K562 2μM IM2 cell line, the large marker chromosome and one small marker carry Bcr-Abl (see Figure 3.13). Metaphase FISH conducted by Sarah Moore.

Figure 3.16

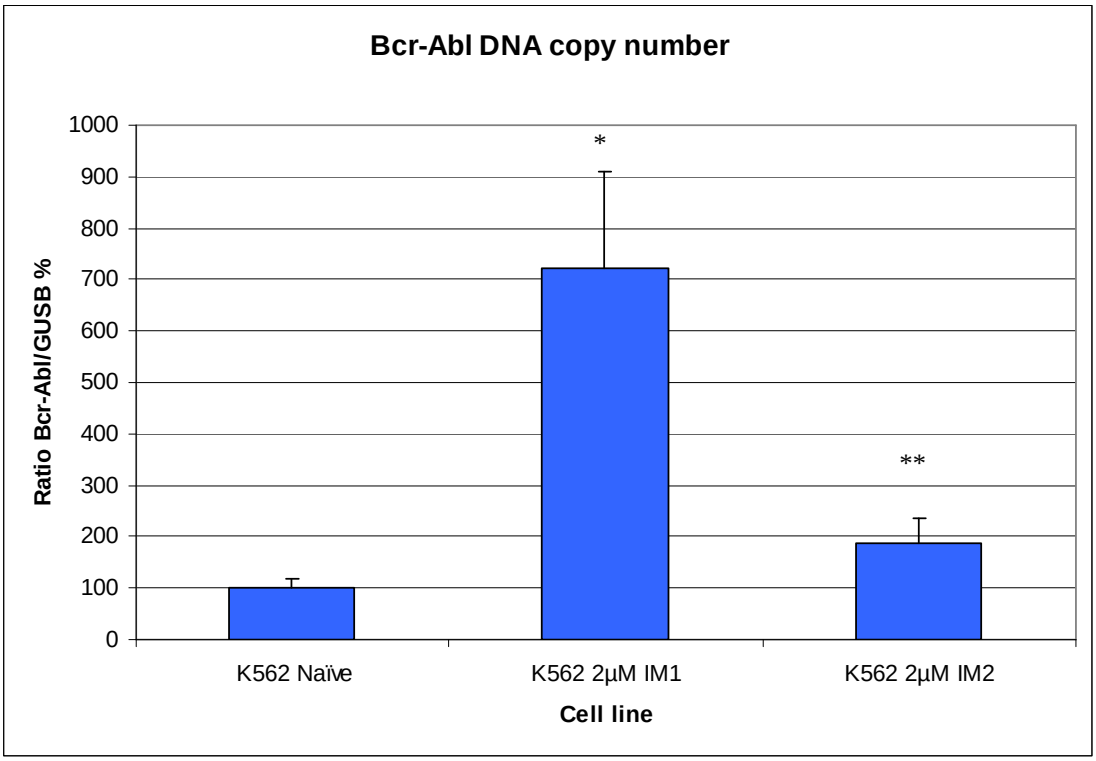

Figure 3.16: Bcr-Abl copy number in the IM1 and IM2 resistant cell lines

Bcr-Abl copy number (with respect to the GUSB control gene) had increased in the two IM-resistant K562 cell lines. DNA was extracted from the three cell lines using a High Pure PCR Template Preparation Kit (Roche Diagnostics, Mannheim, Germany). The DNA was used as a template in quantitative DNA PCR, performed in duplicate for each experiment. Data are presented as mean +SD from at least 3 independent experiments. Both IM-resistant lines were significantly different from the Naïve line (*P<0.0000003; **P<0.0005).

3.4 Discussion

Two IM-resistant K562 cell lines were generated by long-term exposure to gradually increasing concentrations of imatinib. Several mechanisms of resistance were considered and systematically excluded.

Firstly, to determine whether resistance was BCR-ABL dependent or independent, IC50 assays were conducted. In BCR-ABL-independent resistance, alternative oncogenic pathways have emerged that drive proliferation and inhibit apoptosis independently of BCR-ABL kinase activity and its downstream effects[154,156,197]. In theory, the BCR-ABL kinase may be effectively inhibited by a TKI in such cases (ie. cells appear to be sensitive when measured by the IC50 assay which measures the level of kinase inhibition via the BCR-ABL surrogate, p-Crkl), yet the cells would still survive due to mutations in other genes that have accumulated. Therefore, if the resistance mechanism in the K562 2µM IM1 and IM2 lines was exclusively BCR-ABL-independent (*e.g.* Src kinase overexpression) then we would expect no change (or a decrease) in the $IC50^{imatinib}$ despite increased viability in imatinib. However, both IM-resistant lines had an increased viability in imatinib compared with the Naïve control (shown with both trypan blue analysis and flow cytometry) as well as a 5-7 fold increase in $IC50^{imatinib}$. This indicated that the mechanism of resistance was dependent on BCR-ABL, and may therefore include KD mutations, overexpression of the tyrosine kinase, or alteration of imatinib influx/efflux proteins.

It should be noted that IC50 values obtained by the p-Crkl assay (*e.g.* 6.6µM, 37µM and 48µM for K562 Naïve, 2µM IM1 and 2µM IM2 respectively, **Figure 3.8**) are much higher than the concentration required to reduce the number of live cells by 50% in a 3-day viability experiment (*e.g.* approximately 400nM, 3700nM and >4000nM for K562 Naïve, 2µM IM1 and 2µM IM2 respectively, **Figure 3.4**). This is because lower concentrations are sufficient to induce cell death when there is prolonged drug exposure (*i.e.* low level but 'long term' BCR-ABL kinase-inhibition can kill cells)[198,199]. There was also a notable disconcordance between trypan blue analysis and flow cytometry analysis of 3-day viability experiments (compare **Figure 3.4 & 3.5**). By trypan blue analysis, the K562 Naïve cell line was below 10% viability in the presence of 2000nM imatinib, but by flow cytometry the K562 Naïve cells had reached a plateau of 60% in the presence of 2000nM imatinib. This is likely due to aberrant counting of dead cell fragments by the flow sorter machine.

To investigate whether mutations in the kinase domain of BCR-ABL were preventing imatinib from binding, the kinase domain was sequenced (see Chapter 2, section 2.5.7). However, no mutations were detected in either cell line. Mutations in other domains (*e.g.* Linker, SH3-SH2 or Cap domains) cannot be excluded, but these are much rarer.

Blockade of OCT-1 activity with prazosin (a potent OCT-1 inhibitor) allows for determination of the amount of active imatinib uptake and retention for which OCT-1 is responsible. This is termed OCT-1 activity, which is calculated as the (IUR in 2μM imatinib) – (IUR in 2μM imatinib with prazosin). In patients, low OCT-1 activity is predictive of suboptimal response, as less imatinib is entering and being retained in the cells to mediate kinase inhibition[52]. To determine whether the two IM-resistant cell lines had acquired a resistance mechanism involving the OCT-1 transporter, IUR assays were conducted. If the high IC50 values were due to suboptimal IUR, we would expect to see a decrease in imatinib IUR in the resistant cells, coupled with a decrease in the OCT-1 activity. There was no decrease in the IUR or OCT-1 activity in these cells (**Figures 3.9 and 3.10**). Furthermore, if ABCB1 or ABCG2 efflux was playing a role in imatinib resistance, we would expect that blocking these proteins (with PSC833 and Ko143 respectively) would cause an accumulation of intracellular imatinib *i.e.* an increased IUR. However, no significant increase in IUR could be detected in either the IM-resistant lines or the Naïve control, confirming that neither influx nor efflux of imatinib was playing a role in imatinib resistance. This was supported by the fact that no expression of ABCB1 and/or ABCG2 was detectable by flow cytometry.

Notably, the imatinib IUR was significantly higher in the K562 2μM IM1 cell line (at 1μM and 2μM) compared to K562 Naïve cells, even though the OCT-1 activity was not significantly different (**Figure 3.9**). Therefore, this increase in imatinib IUR may be due to passive uptake in the K562 2μM IM1 cell line. As BCR-ABL is overexpressed in the K562 2μM IM1 line, more intracellular imatinib will be bound, and the passive movement of imatinib across the plasma membrane may be skewed toward influx, resulting in increased intracellular concentrations of imatinib. Conversely, the K562 2μM IM2 cell line had significantly higher OCT-1 activity than the Naïve control, which likely mediated the significantly increased imatinib IUR in these cells at 2μM (**Figure 3.10**). Although this is unexpected in

a cell line with a high $IC50^{imatinib}$, it illustrates that whatever mechanism is conferring resistance, is able to tolerate an increased intracellular imatinib concentration.

Next, BCR-ABL/BCR expression was investigated as a possible resistance mechanism. Here we found a significant increase in both lines from 178% in naïve cells, to approximately 1200% and 400% in the resistant cell lines. This overexpression was found to be due to a significantly increased copy number of Bcr-Abl/GUSB, and could be visualised by observing the number of fusion signals in interphase FISH. In interphase, the chromatin is loosely structured and 'spread out' to enable transcription of genes. This usually allows the number of probe signals to be counted when interphase cells are observed in FISH. In metaphase FISH, chromatin is condensed allowing individual chromosomes to be identified. However, because the DNA is so densely packaged, multiple signals (*e.g.* due to the amplification of a gene) will not be visible individually, but as a homogeneously staining region. This may explain why it appeared that dmin were present in the IM-resistant cell lines using interphase FISH (as the multiple gene copies of a HSR were spread out in the nucleus: **Figure 3.12**), whereas karyotyping and metaphase FISH confirmed the presence of HSR rather than dmin (**Figures 3.13, 3.14 & 3.15**). Alternatively, it may be that Bcr-Abl amplification was originally due to dmin, and that some of these integrated into chromosomes forming the HSR. However, this is unlikely because unless every single dmin is integrated, dmin retention would be selected for in the presence of imatinib.

The K562 2µM IM1 cell line karyotype revealed a large HSR present on chromosome 14, as well as several unidentified marker chromosomes (**Figure 3.14**). To determine whether the HSR, or any other chromosomes carried Bcr-Abl, metaphase FISH was conducted. These experiments revealed that chromosome 14 was indeed a carrier of Bcr-Abl, as were two of the small marker chromosomes (**Figure 3.15**). Furthermore, the K562 2µM IM2 cell line was found to have a large new marker chromosome, and extra genetic material on one chromosome 7 (**Figure 3.14**). Metaphase FISH revealed that chromosome 7 was not the site of Bcr-Abl amplification, but rather the large marker chromosome (and another small marker chromosome) (**Figure 3.15**). The GUSB reference gene is located on chromosome 7, therefore the additional material on this chromosome (in the K562 2µM IM2 cell line) potentially harbours duplicate copies of GUSB. If this were the case, it would result in a

decreased ratio of Bcr-Abl/GUSB, making the DNA copy number of Bcr-Abl appear lower than it really is. However, this is unlikely, as BCR-ABL transcript levels mirror Bcr-Abl copy number (both DNA and transcript levels have approximately doubled in the K562 2µM IM2 cell line) and BCR-ABL transcript is measured using a different reference gene (BCR).

The 1200% BCR-ABL/BCR expression observed in the K562 2µM IM1 cell line is likely sufficient to cause resistance to 2µM imatinib, and the 7-fold increase in $IC50^{imatinib}$. Notably, the IM2 cell line had only one third of the BCR-ABL expression present in the IM1 cell line, yet both thrived in the presence of 2µM imatinib, and its $IC50^{imatinib}$ had increased 5-fold above the Naïve line. It is unlikely that 400% BCR-ABL/BCR expression is sufficient to mediate resistance to 2µM imatinib, because if it were there would be no need for the K562 2µM IM1 cell line to express an excessive 1200%. It has been previously postulated that excessive expression of active BCR-ABL is detrimental to the cell[161], and BCR-ABL is known to generate cell-damaging agents such as reactive oxygen species (ROS)[89-91]. It is therefore unlikely that a cell would overexpress BCR-ABL if it was not absolutely necessary for survival. I therefore conclude that the BCR-ABL/BCR expression of 1200% in K562 2µM IM1 cell line is necessary for survival in 2µM imatinib, and that the K562 2µM IM2 cell line (with only 400% BCR-ABL/BCR expression) may harbour another, as yet unidentified, resistance mechanism that compensates for its lower, insufficient expression of BCR-ABL. Other BCR-ABL-dependent resistance mechanisms may include mutations outside of the kinase domain of BCR-ABL, or an unidentified imatinib efflux transporter which may be overexpressed in the IM2 cell line (although this is less likely as imatinib IUR was significantly higher than Naïve cells; **Figure 3.10**). This concept is further discussed in *Chapter 6: TKI cross-resistance*.

Chapter 4:

Imatinib resistance in the K562 Dox cell line is mediated by ABCB1 overexpression

4.1 Introduction

Effective treatment of CML with imatinib mesylate requires sufficient intracellular concentrations of the TKI to bind and inhibit BCR-ABL molecules[39]. The intracellular uptake and retention of imatinib in leukaemic cells (*i.e.* its net influx) is dependent upon the activity of OCT-1, an influx transporter[39,40], and ABCB1 and ABCG2 – efflux transporters[71,73-75]. Cellular transport of imatinib is a critical factor in CML outcome, as OCT-1 activity is predictive of patient response[52,53]. The role of efflux proteins such as ABCB1 and ABCG2 is therefore also of interest, as these transporters negatively affect imatinib IUR. Suboptimal dosage of chemotherapy is known to foster the emergence of resistant clones[79,186-189], and in this study resistance mechanism emergence was investigated in the context of ABCB1 expression.

4.1.1 The multidrug resistance protein, ABCB1

ABCB1 is a member of the ATP-binding cassette (ABC) family of transporters. The protein consists of two homologous halves, each with 6 transmembrane domains and an ABC domain, joined by a linker region. Together, the two halves form a 'pore', enabling translocation of substrates across a plasma membrane by the hydrolysis of ATP[56] (**Figure 1.9**). ABCB1 is highly expressed in epithelial cells lining the lower gastrointestinal tract, in proximal tubule cells of the kidney, in the canalicular membranes of hepatocytes and in capillary epithelial cells in the brain and testes. Lower levels of expression can be found in the placenta, adrenal cortex and CD34+ haematopoietic stem cells[56]. In these compartments, ABCB1 (which has the broadest substrate specificity of all ABC transporters[56]) effluxes undesirable and toxic compounds, thereby protecting these systems[57].

ABCB1 was first identified as a cell surface glycoprotein that decreased the rate of drug uptake in colchicine selected Chinese hamster ovary (CHO) cells. The cells displayed a multidrug resistance (MDR) phenotype, as sensitivity to vinblastine, colcemid, daunomycin, puromycin, cytochalasin B and other drugs was reduced, even though the CHO cells had only ever been exposed to colchicine[200]. Since that time, ABCB1 expression has been identified in various MDR cancers[56].

By facilitating the efflux of cytotoxic drugs, ABCB1 expression allows cells to survive in the presence of such compounds. ABCB1 has been implicated in both primary and secondary drug resistance in

human cancers[201]. Expression of this efflux protein may occur in tumours from tissues that inherently express ABCB1 (*e.g.* colon cancers, resulting in primary resistance[202]) and in tumours from tissues in which it is not normally expressed (*e.g.* breast cancer). In the latter scenario, ABCB1 expression in the tumour results from exposure to, and selection by, chemotherapeutic agents – this leads to relapse/secondary resistance (**Figure 4.1**). ABCB1 expression has been detected in relapsed breast cancer patients after treatment with mitoxantrone, tamoxifen, vincristine, mitomicin, epirubicin, vindesine or combinations thereof[203]. B-cell lymphomas and metastatic melanomas have also been found to express ABCB1 in response to chemotherapy[204,205].

4.1.2 ABCB1 expression in CML

To effectively treat CML, imatinib must be present at a sufficient intracellular concentration in order to adequately inhibit BCR-ABL and cause leukaemic cell death. Intracellular concentrations of imatinib are determined by the net influx of the drug into cells. OCT-1 is responsible for the active influx of imatinib into CML cells[39,40], while ABCB1 has been implicated in imatinib[71,73,74], dasatinib[55,69] and nilotinib[69,81] efflux.

In a study in 1999 by Giles *et. al.*[206], 198 CML patients were screened for ABCB1 expression in peripheral blood by Western blot. Of these, 127 patients were in “early” chronic phase (ECP; less than one year from time of diagnosis), 31 patients were in “late” chronic phase (LCP; greater than one year from diagnosis), 27 patients were in accelerated phase (AP), and 13 were in blast crisis (BC). ABCB1 protein expression levels were compared to 36 normal control samples, and defined as ‘high’ or ‘low‘ about the control median. 57% of ECP patients, 65% of LCP patients, 30% of AP patients, and 62% of BC patients had high ABCB1 expression. Notably, all patients in this study were on interferon-α-based therapy regimens (not transported by ABCB1[207]), and no difference in survival based on ABCB1 expression was observed[206]. In contrast, other studies (also conducted before the introduction of imatinib) noted expression of ABCB1 in up to 70% of blast crisis CML patients, and increased expression in those who relapsed on chemotherapies such as doxorubicin, cytarabine and hydroxyurea[208-210].

Figure 4.1

Figure 4.1: The development of a multidrug resistant (MDR) cancer
A tumour may harbour many different sub-clones (e.g. the green circle represents a clone not expressing ABCB1, the blue circle represents a clone expressing ABCB1 (red circle with arrow)). Cells that do not express ABCB1 are sensitive to chemotherapy (black dots) and die, while those which express ABCB1 are selected and expanded in the population. In the course of chemotherapy, further mutations and selection may greatly increase the expression of ABCB1, which protect the tumour cells against various chemotherapies. The result may be relapse with an MDR cancer despite initial response to the chemotherapy (Sarkadi *et. al.* 2006, Physiological Reviews)[56].

In 2005 Galimberti *et. al.*[211] studied 33 CML patients (30 in CP, 3 in AP) taking imatinib for 18 months. RQ-PCR was used to measure ABCB1 and BCR-ABL expression in the bone marrow at baseline, after 4 weeks of first imatinib dose, and every 3 months during imatinib therapy. 22 patients (66.7%) achieved a complete cytogenetic response (CCR; the absence of the Ph chromosome in 20 metaphases on classical karyotyping of the bone marrow), and 3 (9.1%) achieved a major cytogenetic response (MCR; less than 34% Ph-positive metaphases). 8 patients (including the 3 patients in AP; 24.2%) did not achieve any cytogenetic response milestones. These patients had 10-fold higher ABCB1 expression than those who did achieve a cytogenetic response (P=0.02). Despite an initial complete haematologic response (CHR; normalisation of white blood cell count) the three patients in AP showed disease progression after 8, 12, and 17 months of imatinib treatment respectively. All three patients displayed a concomitant increase in BCR-ABL and ABCB1 expression before relapsing[211]. These observations indicate a role for ABCB1 expression in TKI resistance in CML.

In a study of 44 *de novo* CP CML patients by White *et. al.*[165], 7 patients developed kinase domain mutations, and of these, 6/7 had high levels of ABCB1 expression (above the 75th percentile) prior to the detection of the mutation. This suggested that ABCB1 was involved in resistance-development by interplay with other mechanisms. It may be that low intracellular levels of imatinib (mediated by ABCB1 expression) create an environment conducive to kinase domain mutation development. To investigate this possibility, the K562 Dox cell line was utilised in imatinib resistance generation.

4.1.3 The breast cancer resistance protein, ABCG2

Between 1990 and 1999 a number of mitoxantrone-resistant cell lines were generated that had transporter activity without overexpression of ABCB1 or ABCC1. The cell lines used for these studies included a human gastric carcinoma cell line[212], human colon cancer and multiple myeloma cell lines[213,214], and the MCF-7 breast cancer cell line[213,215,216]. In all cases, the cell lines were cross-resistant to doxorubicin and daunorubicin, but not vinblastine[217]. In 1998, the transporter responsible for this cross-resistance was identified in the MCF-7 cell line, and named the breast cancer resistance protein (BCRP, later ABCG2)[218]. ABCG2 is highly expressed in the placenta, liver, colon, testis, ovary and brain microvessels[217]. A study in 2001 found ABCG2 was also highly expressed in haematopoietic

stem cells (CD34+38- or CD34+KDR+ populations; KDR: kinase insert domain protein receptor) but much lower levels in committed progenitors (CD34+38+, CD34+33+, or CD34+10+)[219].

ABCG2 expression in CML CD34+ cells has been found to be 6.8-fold higher than in their normal counterparts[62], and ABCG2 has been implicated in imatinib[71,72,75], dasatinib[55,69] and nilotinib[66,69] transport in human CML cell lines. For this reason, expression of ABCG2 was also investigated as a possible mode of TKI resistance in all resistant cell lines generated.

4.1.4 The K562 Dox cell line

In 1986 Tsuruo *et. al.*[79] published a study on adriamycin (doxorubicin) resistance-generation in K562 cells. The K562 cells were first exposed to gradually increasing concentrations of vincristine for 1 month, before further treatment with gradually increasing concentrations of doxorubicin. These cells were finally cultured for 4 months in 500nM doxorubicin, and named K562/ADM. Initial studies revealed overexpression of a 180kD glycoprotein (later identified as ABCB1) and the presence of HSR and double minutes, thought to carry amplified ABCB1. None of these traits are present in the parental K562 cell line[79]. In later studies, the cell line became known as K562 Dox[220,221]. It has also been shown that verapamil or PSC833 can block ABCB1 in the K562 Dox cell line, increasing its sensitivity to doxorubicin[222], imatinib[195], nilotinib[81] and dasatinib[55].

4.2 Approach

4.2.1 Generating imatinib resistance in the K562 Dox cell line

The K562 Dox cell line was chosen for this study, as it is an ABCB1 overexpressing variant of the K562 line. One of the hypotheses at the outset of this study was that 'partially-protective mechanisms (*e.g.* efflux protein expression) create an environment that selects for further mutations (eg. KD mutations) causing overt TKI resistance *in vitro*'. Therefore, to compare the resistance mechanisms that emerge in the presence and absence of efflux protein expression, imatinib resistance generation in the K562 cell line was compared with imatinib resistance generation in the K562 Dox cell line.

The first imatinib culture of K562 Dox cells was initiated in 100nM, and subsequently escalated to 200nM, 300nM, 400nM, 500nM, 600nM, 700nM, 800nM, 900nM, 1.1µM, 1.2µM and 2µM. This cell line was named K562 Dox 2µM IM1, and was analysed for resistance mechanisms. It appeared that further expression of ABCB1 was responsible for conferring resistance to imatinib. Due to the theory of clonal selection, it was hypothesised that a different resistance mechanism may emerge each time a cell line is escalated in imatinib. It may be that one clone, expressing higher levels of ABCB1, happened to emerge and out-compete other clones – perhaps harbouring BCR-ABL kinase domain mutations or BCR-ABL overexpression. If the emergence of clones with particular advantages/mutations was stochastic, we would expect a different resistance mechanism to emerge each time a cell line is cultured in imatinib. To determine whether this was the case, the generation of imatinib resistance in the K562 Dox cell line was done in triplicate.

The second imatinib culture was escalated as follows: 100nM, 200nM, 300nM, 400nM, 600nM, 800nM, 1.1µM, 1.5µM and 2µM. This cell line was named K562 Dox 2µM IM2. The third imatinib culture was initiated in 200nM, and subsequently escalated to 400nM, 600nM, 800nM, 1.4µM and 2µM. This cell line was named K562 Dox 2µM IM3. On average, IM-resistance took approximately 4 months to generate in the K562 Dox cell line. Parental 'Naïve' cells were maintained in parallel cultures as controls.

4.2.2 Analysis of imatinib-resistant cell lines

To investigate the cause of imatinib resistance in the three K562 Dox cell lines, samples for RNA and DNA isolation were collected at each intermediate stage of imatinib concentration escalation. Thus, we could observe the mechanisms of resistance as they emerged in each step-wise drug escalation. As the K562 Dox 2µM IM1 and IM2 cell lines were two of the first cell lines generated in this study as a whole (and due to the rapidity with which the K562 Dox cell line can be escalated in imatinib) few intermediate samples were collected for these cell lines.

RNA isolated from all collected intermediate samples was used in RQ-PCR reactions to investigate levels of BCR-ABL expression in the three imatinib resistant K562 Dox cell lines. RNA was also converted to cDNA for use in sequencing reactions to determine the mutation status of the BCR-ABL kinase domain. Additionally, flow cytometry was used to investigate the level of cell-surface expression of ABCB1 and ABCG2. Intracellular uptake and retention (IUR) assays were used to determine the amount of imatinib being internalised and retained in the cells over a 2hr incubation period. By the addition of PSC833 (a potent ABCB1 inhibitor), the amount of imatinib being effluxed due to ABCB1 activity could also be measured. IC50 assays were used to measure the concentration of imatinib that was required to reduce levels of the BCR-ABL adaptor protein, p-Crkl, by 50%, thus giving an indication of how resistant the 2µM IM cell lines were compared to the imatinib-naïve control. Furthermore, the IC50 in the presence of PSC833 was also investigated, to observe how blockade of ABCB1 affects imatinib resistance.

4.3 Results

Three imatinib-resistance K562 Dox cell lines were generated, and were named K562 Dox 2μM IM1, IM2 and IM3. All three cultures thrived in the presence of 2μM imatinib, indicating that they were overtly resistant to imatinib. In order to determine the mechanisms of resistance present in these cell lines, the cells were screened for BCR-ABL expression, kinase domain mutations, ABCB1 and ABCG2 expression, intracellular uptake and retention (IUR) of imatinib, and $IC50^{imatinib}$.

BCR-ABL overexpression is an imatinib resistance mechanism observed in patients[107,138,139], and was the mode of the resistance for the K562 2μM IM1 and IM2 cell lines (**Figures 3.10 & 3.15**). Therefore, RNA isolated from all collected intermediate samples was used in RQ-PCR reactions to investigate levels of BCR-ABL expression in the three imatinib resistant K562 Dox cell lines. Strikingly, there was no significant difference between the BCR-ABL expression levels of the K562 Dox Naïve cell line and the K562 Dox 2μM IM1, IM2 and IM3 cell lines (**Figure 4.2**). Sequencing the BCR-ABL kinase domain did not reveal the presence of any mutations.

ABCB1 and ABCG2 have been implicated in imatinib efflux and resistance *in vitro*[71,72,74,75]. Therefore, overexpression of either of these proteins may have been responsible for the imatinib resistance observed in the K562 Dox 2μM IM1, IM2 and IM3 cell lines. To investigate this possibility, samples of the IM-resistant cell lines were incubated with ABCB1 or ABCG2 antibodies, and analysed using flow cytometry. It was found that cell surface expression of ABCG2 was absent in all three IM-resistant cell lines, as well as in the K562 Dox Naïve control (**Figure 4.3**). However, cell-surface expression of ABCB1 was at least double that of the K562 Dox Naïve control in all three resistant cell lines (199%, 253% and 204% for the IM1, IM2 and IM3 cell lines respectively) (**Figure 4.4**).

As ABCB1 cell-surface overexpression had been identified in the three IM-resistant cell lines, the functionality of the overexpressed protein was then investigated. To determine whether the increased ABCB1 expression was affecting the intracellular levels of imatinib, IUR assays were conducted to measure imatinib uptake and retention over a 2hr period. In all three IM-resistant cell lines imatinib IUR was decreased compared to the K562 Dox Naïve control at both the 1μM and 2μM experimental conditions (**Figure 4.5**). In the IM1 and IM2 cell lines, this decrease in IUR was significant (P<0.03)

Figure 4.2

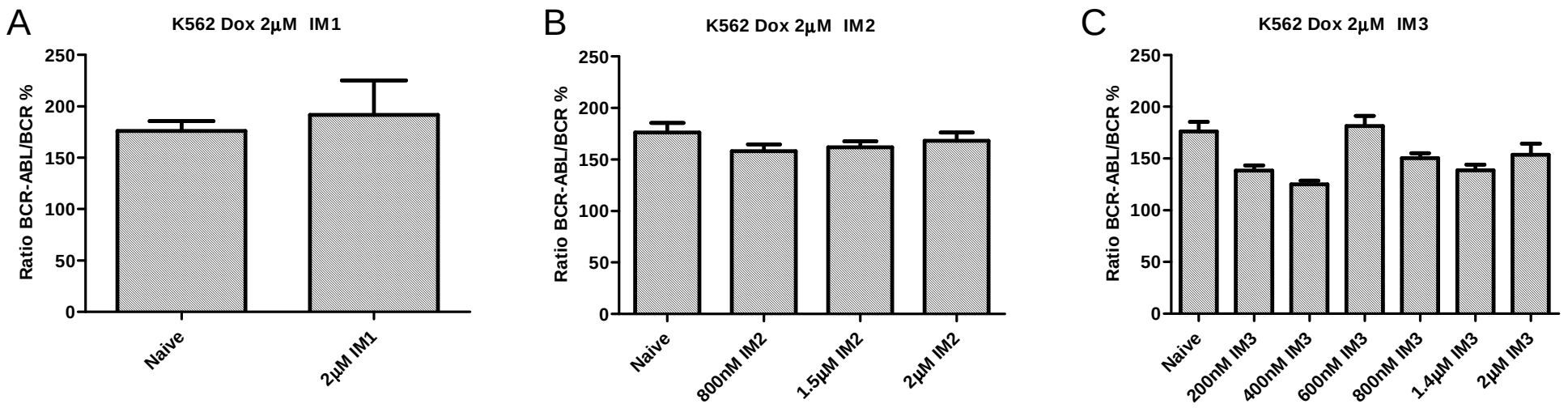

Figure 4.2: Intermediate BCR-ABL mRNA expression in the K562 Dox 2µM IM1, IM2 and IM3 cell lines
BCR-ABL/BCR mRNA expression levels did not significantly change in the **A)** K562 Dox 2µM IM1 **B)** K562 Dox 2µM IM2 or **C)** K562 Dox 2µM IM3 cell lines compared to the Naïve control. Samples were taken at intermediate stages of resistance development, and cDNA synthesised from RNA extracted from 1×10^7 cells. RQ-PCR was conducted using cDNA as the template, and BCR-ABL mRNA expression was determined as a ratio of BCR mRNA expression. Data are presented as mean +SEM from at least 3 independent experiments.

Figure 4.3

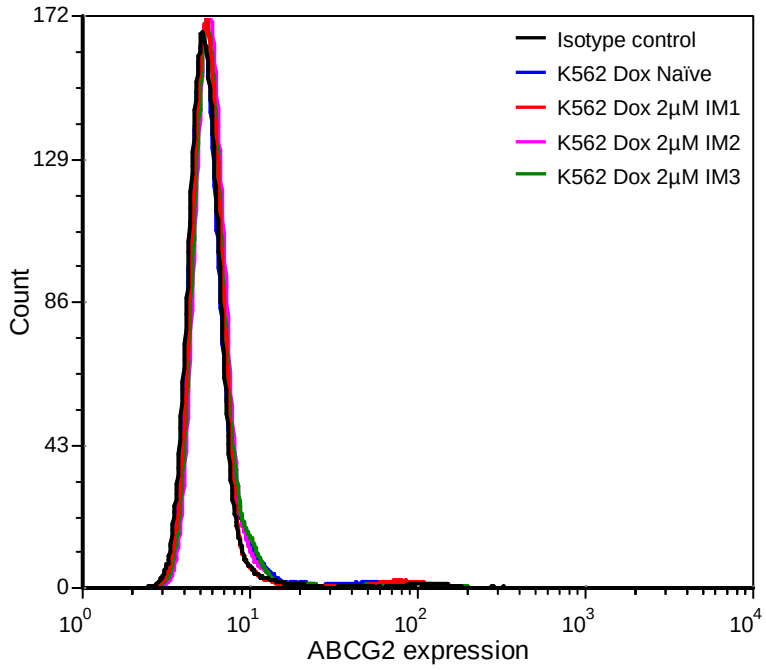

Figure 4.3: ABCG2 cell surface expression in IM-resistant K562 Dox cell lines

K562 Dox Naive and IM-resistant cells were harvested and stained with either an isotype control antibody or the PE ABCG2 antibody. After a 45 minute incubation with the antibody, the cells were washed and analysed by flow cytometry. No ABCG2 expression could be detected in either the Naïve or 2µM IM-resistant cell lines. Histogram is representative of 3 experiments.

Figure 4.4

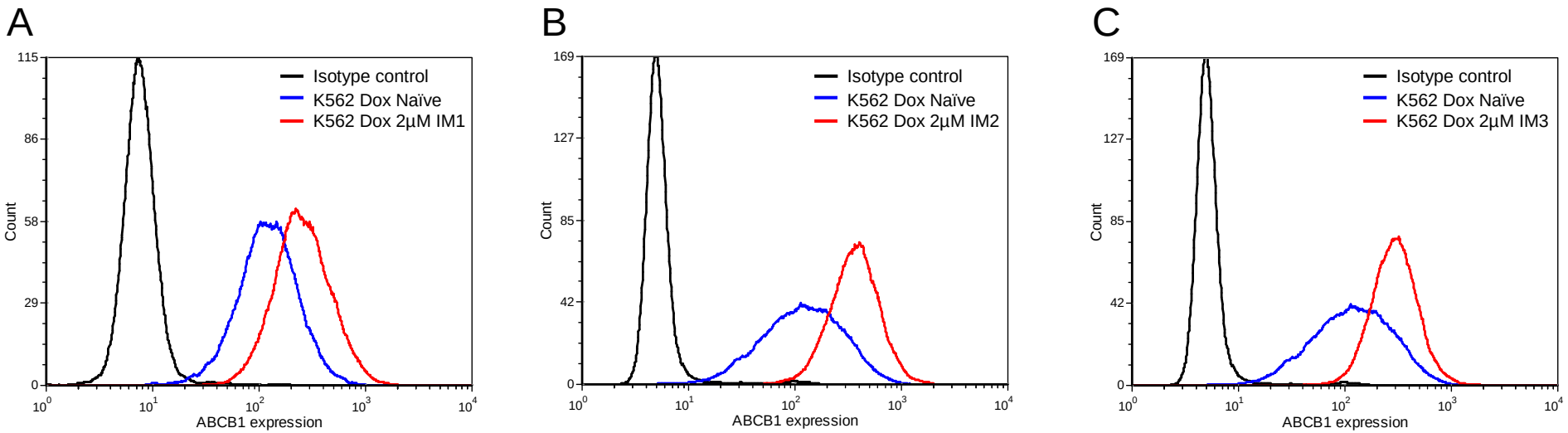

Figure 4.4: ABCB1 cell surface expression increased in the K562 Dox IM-resistant cell lines
K562 Dox Naive and IM-resistant cells were harvested and stained with either an isotype control antibody or the PE ABCB1 antibody. After a 45 minute incubation with the antibody, the cells were washed and analysed by flow cytometry. ABCB1 cell-surface expression was seen to increase to 199% in the K562 Dox IM1 cell line **(A)**, 253% in the K562 Dox IM2 cell line **(B)**, and 204% in the K562 Dox IM3 cell line **(C)** above that of IM-Naïve K562 Dox cells (100%). Histograms are representative of 3 experiments.

Figure 4.5: K562 Dox IM-resistant cell lines have a reduced imatinib intracellular uptake and retention (IUR) compared to K562 Dox Naïve control cells

The IUR assay was performed as previously described[39]. PSC833 (10µM) inhibits ABCB1. "ABCB1-mediated imatinib efflux" is calculated as [IUR of 2µM imatinib + PSC833] minus [IUR of 2µM imatinib]. It is therefore a measure of the amount of imatinib effluxed that is attributable to ABCB1 activity. These data demonstrate that the K562 Dox 2µM IM1 **(A)**, IM2 **(B)** and IM3 **(C)** cell lines have a lower imatinib IUR than the K562 Dox Naïve control, and significantly higher ABCB1-mediated imatinib efflux. Data are presented as mean +SD calculated from at least three independent experiments.

Figure 4.5

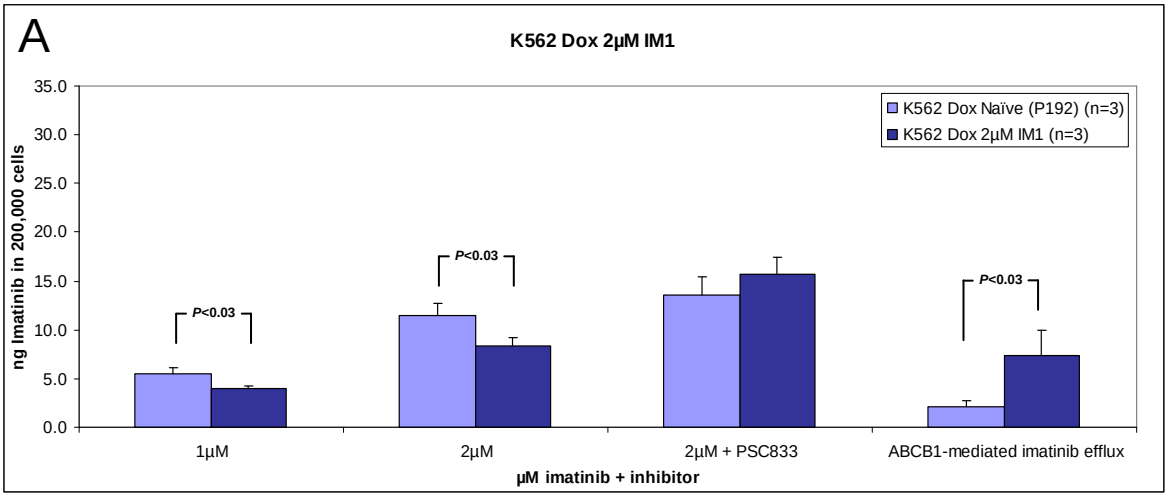
A
K562 Dox 2μM IM1
ng Imatinib in 200,000 cells
35.0
30.0
25.0
20.0
15.0
10.0
5.0
0.0
K562 Dox Naïve (P192) (n=3)
K562 Dox 2μM IM1 (n=3)
P<0.03
P<0.03
P<0.03
1μM
2μM
2μM + PSC833
ABCB1-mediated imatinib efflux
μM imatinib + inhibitor

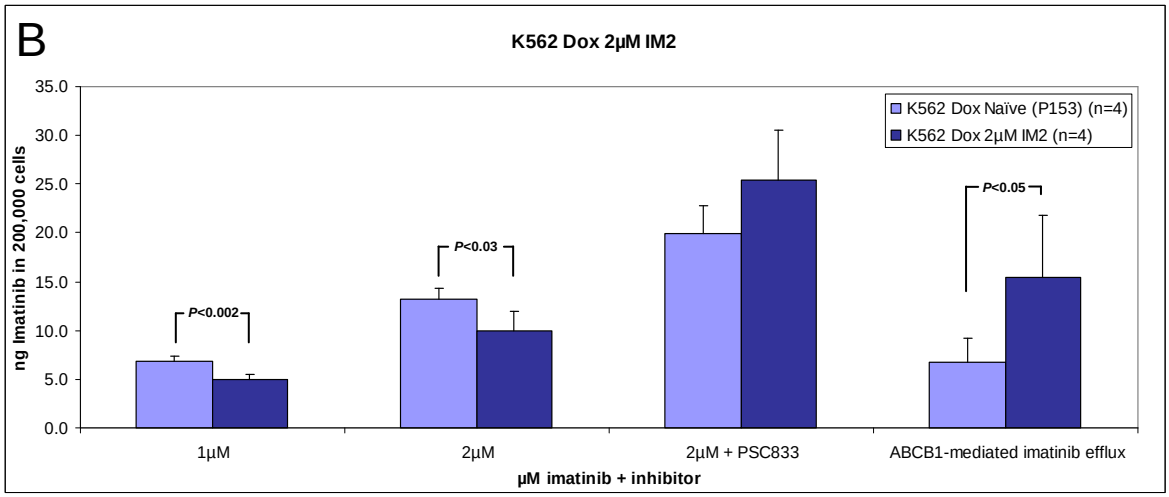
B
K562 Dox 2μM IM2
ng Imatinib in 200,000 cells
35.0
30.0
25.0
20.0
15.0
10.0
5.0
0.0
K562 Dox Naïve (P153) (n=4)
K562 Dox 2μM IM2 (n=4)
P<0.002
P<0.03
P<0.05
1μM
2μM
2μM + PSC833
ABCB1-mediated imatinib efflux
μM imatinib + inhibitor

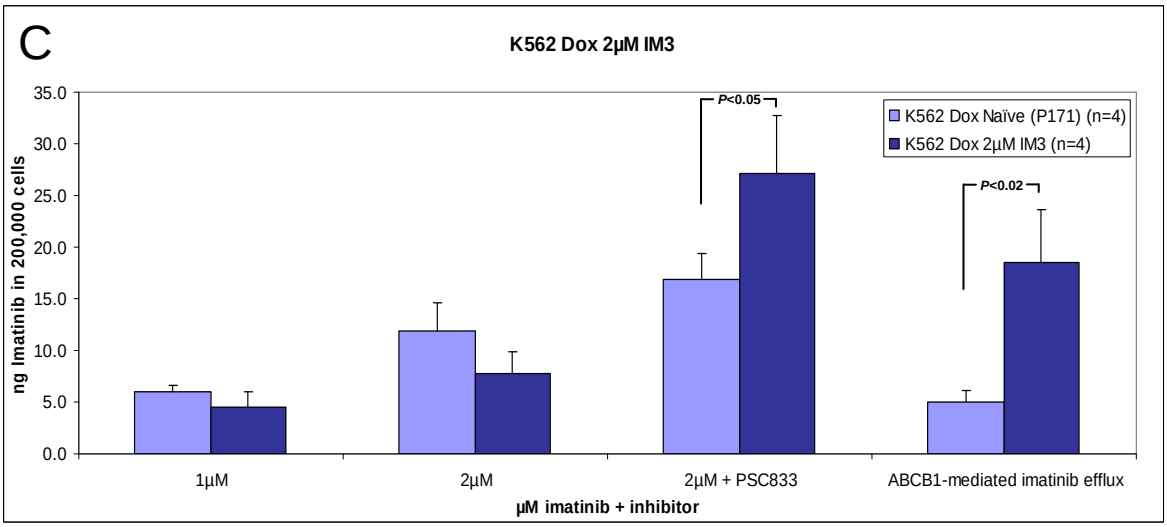
C
K562 Dox 2μM IM3
ng Imatinib in 200,000 cells
35.0
30.0
25.0
20.0
15.0
10.0
5.0
0.0
K562 Dox Naïve (P171) (n=4)
K562 Dox 2μM IM3 (n=4)
P<0.05
P<0.02
1μM
2μM
2μM + PSC833
ABCB1-mediated imatinib efflux
μM imatinib + inhibitor

(**Figure 4.5 A & B**). Blockade of ABCB1 with PSC833 resulted in an increased IUR in all three IM-resistant cell lines above the Naïve control, which was significant in the K562 Dox 2μM IM3 cell line (P<0.05) (**Figure 4.5 C**). ABCB1-mediated imatinib efflux is a measure of [the IUR when ABCB1 is blocked with PSC833] minus [the IUR in the absence of PSC833]. It is therefore a measure of the amount of imatinib efflux that is attributable to ABCB1. In all three IM-resistant cell lines, the amount of ABCB1-mediated imatinib efflux was significantly greater than in the Naïve control (P<0.03, P<0.05, P<0.02 for K562 Dox 2μM IM1, IM2 and IM3 respectively) (**Figure 4.5**).

Notably, viability (cell culture) experiments were attempted to demonstrate that imatinib sensitivity in the K562 Dox 2μM IM1, IM2 and IM3 cell lines could be restored by the inhibition of ABCB1. 1×10^5 cells were seeded in 1mL cultures in a 24-well plate for both K562 Dox Naïve cells and K562 Dox 2μM IM1 cells, in the presence or absence of 10μM PSC833. After 72hrs, cells were harvested and counted with a haemocytometer. 207 live K562 Dox Naïve cells were counted in the absence of PSC833, but only 49 live cells were counted in the presence of PSC833; while 131 live K562 Dox 2μM IM1 cells were counted in the absence of PSC833, but only 36 live cells counted in the presence of PSC833. It appeared that 72hrs of culture with 10μM PSC833 alone caused cell death at an unacceptable level for viability experiments with imatinib. Thus, the IC50 assay was used instead to demonstrate imatinib resistance and sensitivity in the presence or absence of PSC833, as this assay only involves a 2hr incubation period which does not result in significant cell death (see *Materials and Methods, 2.5.8*).

The $IC50^{imatinib}$ (**Figure 4.6**) was measured in the IM-resistant cell lines, to quantify and compare their level of imatinib resistance with the Naïve control. All three cell lines had a significantly increased $IC50^{imatinib}$ (28.7μM, 30.5μM, 28.3μM in IM1, IM2 and IM3 respectively) compared to the K562 Dox Naïve control (10.7μM) (P<0.001) (**Figure 4.7 & 4.9**). In fact, the IM-resistant lines were three-fold more resistant to imatinib than the Naïve control, as almost three times the concentration of imatinib was required to reduce levels of p-Crkl by 50%. If ABCB1 overexpression was the only mechanism of imatinib resistance present in these cell lines, inhibition of ABCB1 should restore sensitivity of the cell lines back to the level of the K562 Dox Naïve control. To confirm this, the $IC50^{imatinib}$ was measured in the presence of 10μM PSC833 (an ABCB1 inhibitor). It was found that the significant difference

between the IC50s of the IM1, IM2 and IM3 resistant cell lines and the K562 Dox Naïve cell line was removed when ABCB1 was blocked (P>0.2). In the presence of PSC833, the $IC50^{imatinib}$ of the IM1, IM2 and IM3 cell lines was 3.6µM, 3.4µM, and 2.4µM respectively, while the K562 Naïve K562 Dox Naïve cell line was 3.3µM and 3.5µM respectively (**Figure 4.8 & 4.9**).

Figure 4.6: Example of a K562 Dox Naïve IC50^{imatinib} Western blot quantification
Cells were incubated for 2 hours at 37℃/5%CO_2 with IM concentrations ranging up to 100µM. Western blot analysis for p-Crkl was performed as previously described[36]. Signals were quantified using Image Quant software (Molecular Dynamics), and the ratio of p-Crkl to Crkl was determined using Image Quant analysis. **(A)** Polygons were drawn around each Crkl and p-Crkl band, and blank membrane was also sampled as a background control. **(B)** Bands of p-Crkl were measured and graphed as a percentage of the intensity of total Crkl (*i.e.* p-Crkl + Crkl intensity = 100%). Note the 40µM imatinib value has been removed as an outlier. **(C)** These percentages are normalised (0µM imatinib is 100% p-Crkl, 100µM imatinib is 0% p-Crkl). The IC50 value is then taken as the concentration of imatinib when normalised p-Crkl reaches 50% (*i.e.* IC50^{imatinib} = 10.5µM in this case). This blot is shown again in Figure 4.7.

Figure 4.6

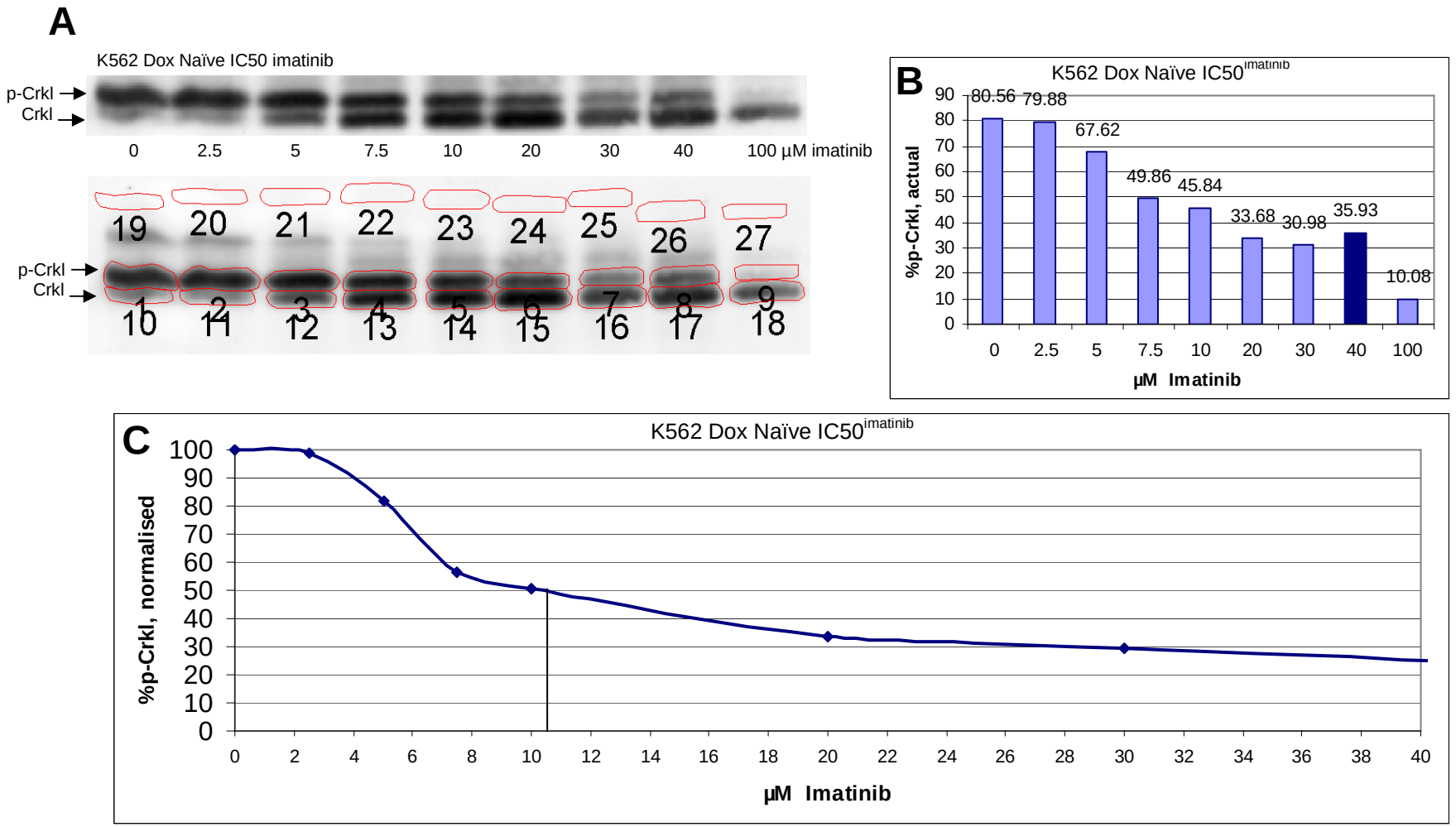
A
K562 Dox Naïve IC50 imatinib
p-Crkl
Crkl
0 2.5 5 7.5 10 20 30 40 100 µM imatinib
19 20 21 22 23 24 25 26 27
1 2 3 4 5 6 7 8 9
10 11 12 13 14 15 16 17 18
B
K562 Dox Naïve IC50imatinib
%p-Crkl, actual
80.56 79.88 67.62 49.86 45.84 33.68 30.98 35.93 10.08
0 2.5 5 7.5 10 20 30 40 100
µM Imatinib
C
K562 Dox Naïve IC50imatinib
%p-Crkl, normalised
0 2 4 6 8 10 12 14 16 18 20 22 24 26 28 30 32 34 36 38 40
µM Imatinib

Figure 4.7: K562 Dox IM-resistant cell lines have increased $IC50^{imatinib}$ compared to K562 Dox Naïve control cells

Cells were incubated for 2 hours at 37℃/5%CO_2 with IM concentrations ranging up to 100μM. Western blot analysis for p-Crkl was performed as previously described[36]. Signals were quantified using Image Quant software (Molecular Dynamics), and the ratio of p-Crkl to Crkl was determined using Image Quant analysis. The IC50 value for each blot (determined as the dose of drug required to reduce levels of p-Crkl by 50%) is indicated above each blot (and with red arrow). IC50 assays were performed at least four times. One representative blot is shown for each of the five cell lines.

Figure 4.7

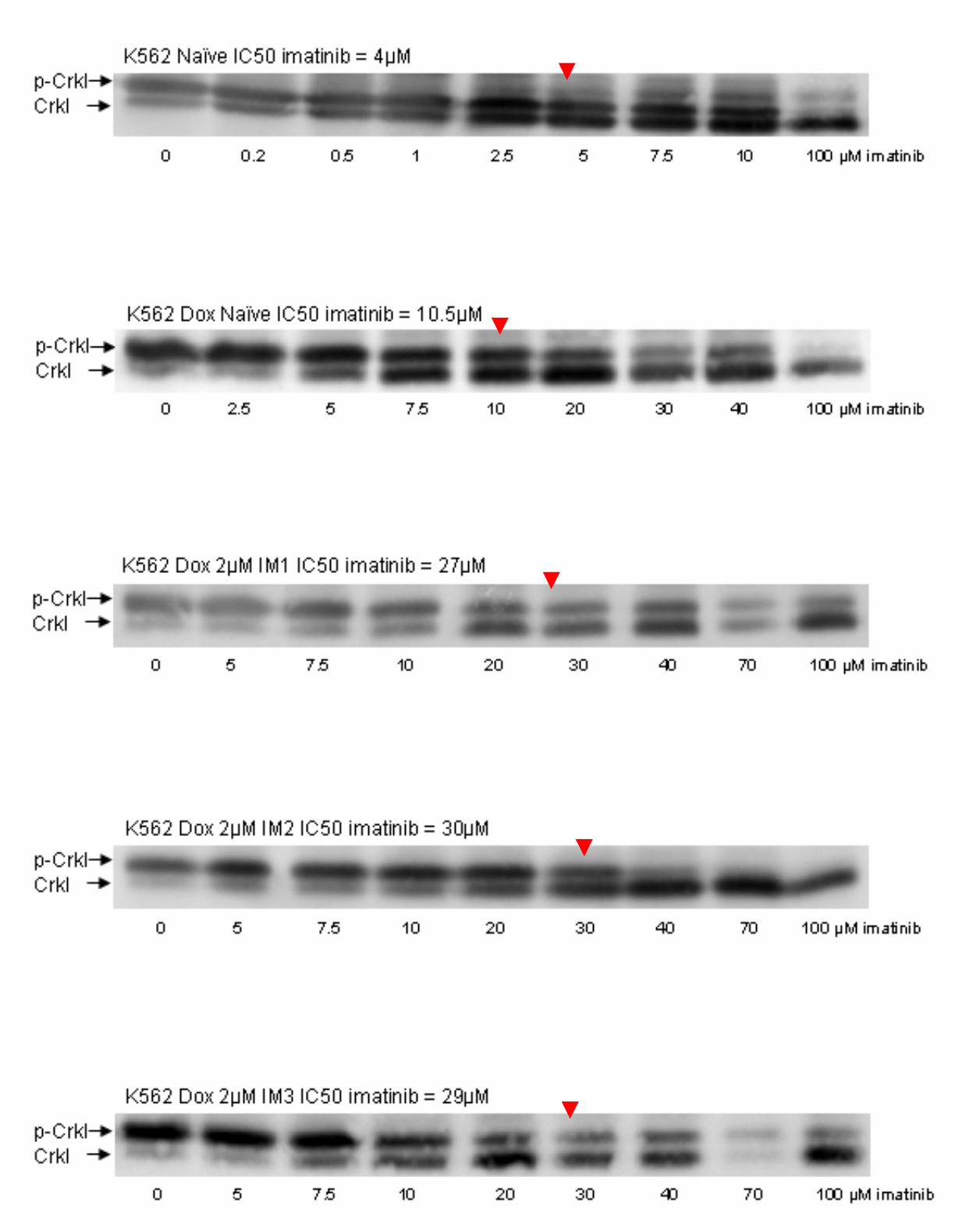
K562 Naïve IC50 imatinib = 4µM
p-Crkl
Crkl
0 0.2 0.5 1 2.5 5 7.5 10 100 µM imatinib
K562 Dox Naïve IC50 imatinib = 10.5µM
p-Crkl
Crkl
0 2.5 5 7.5 10 20 30 40 100 µM imatinib
K562 Dox 2µM IM1 IC50 imatinib = 27µM
p-Crkl
Crkl
0 5 7.5 10 20 30 40 70 100 µM imatinib
K562 Dox 2µM IM2 IC50 imatinib = 30µM
p-Crkl
Crkl
0 5 7.5 10 20 30 40 70 100 µM imatinib
K562 Dox 2µM IM3 IC50 imatinib = 29µM
p-Crkl
Crkl
0 5 7.5 10 20 30 40 70 100 µM imatinib

Figure 4.8: In the presence of PSC833, K562 Dox IM-resistant cell lines have similar $IC50^{imatinib}$ values compared to K562 Dox Naïve control cells

Cells were incubated for 2 hours at 37℃/5%CO_2 with IM concentrations ranging up to 100μM, in the presence of 10μM PSC833 – an ABCB1 inhibitor. Western blot analysis for p-Crkl was performed as previously described[36]. Signals were quantified using Image Quant software (Molecular Dynamics), and the ratio of p-Crkl to Crkl was determined using Image Quant analysis. The IC50 value for each blot (determined as the dose of drug required to reduce levels of p-Crkl by 50%) is indicated above each blot (and with red arrow). IC50 assays were performed at least four times. One representative blot is shown for each of the five cell lines.

Figure 4.8

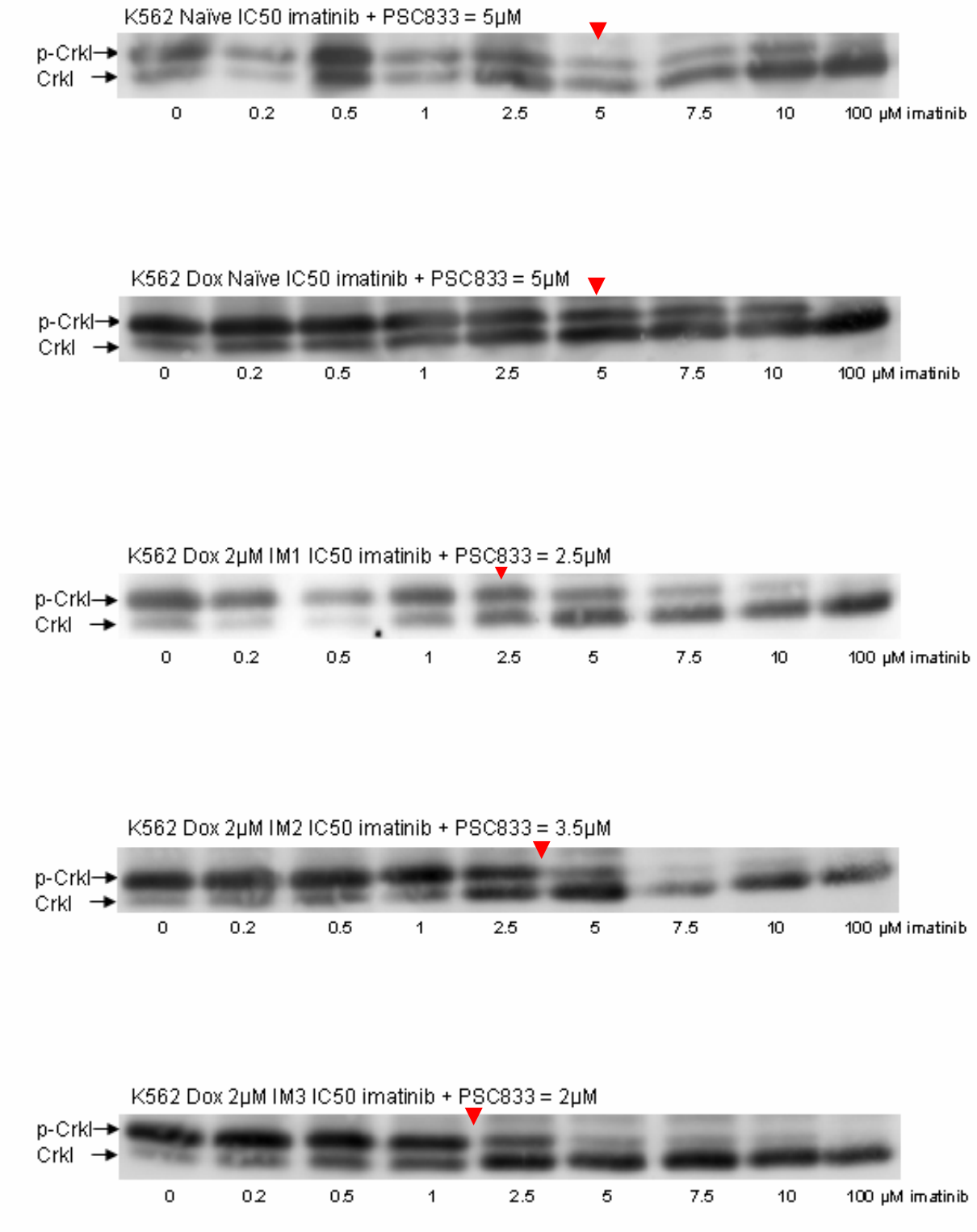
K562 Naïve IC50 imatinib + PSC833 = 5μM
p-Crkl
Crkl
0 0.2 0.5 1 2.5 5 7.5 10 100 μM imatinib
K562 Dox Naïve IC50 imatinib + PSC833 = 5μM
p-Crkl
Crkl
0 0.2 0.5 1 2.5 5 7.5 10 100 μM imatinib
K562 Dox 2μM IM1 IC50 imatinib + PSC833 = 2.5μM
p-Crkl
Crkl
0 0.2 0.5 1 2.5 5 7.5 10 100 μM imatinib
K562 Dox 2μM IM2 IC50 imatinib + PSC833 = 3.5μM
p-Crkl
Crkl
0 0.2 0.5 1 2.5 5 7.5 10 100 μM imatinib
K562 Dox 2μM IM3 IC50 imatinib + PSC833 = 2μM
p-Crkl
Crkl
0 0.2 0.5 1 2.5 5 7.5 10 100 μM imatinib

Figure 4.9

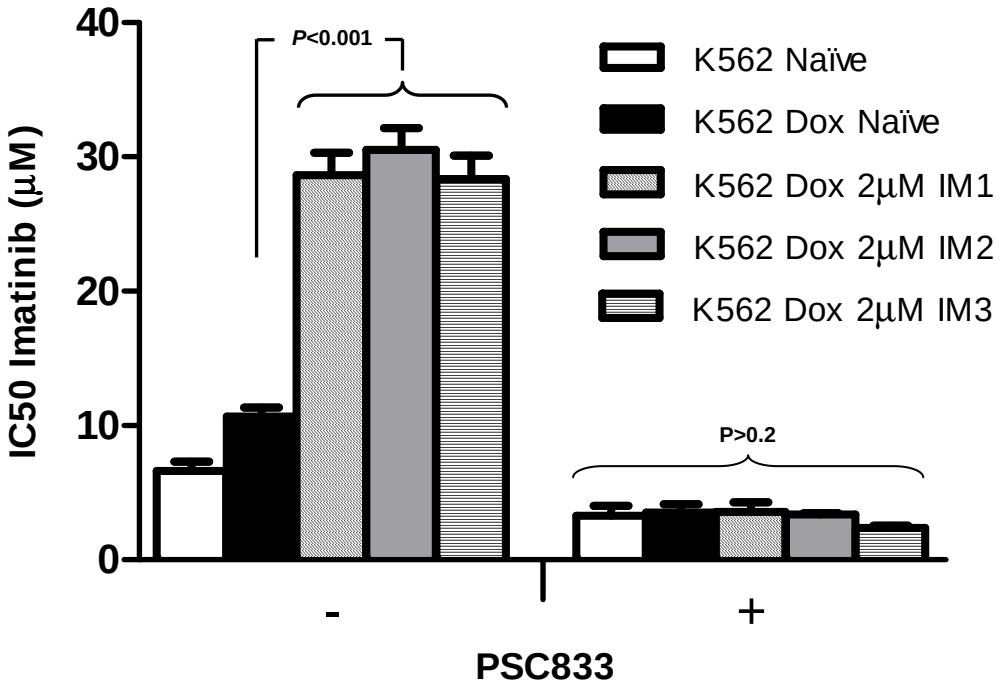

Figure 4.9: PSC833 removes the significant difference in IC50^{imatinib} values between the three IM-resistant K562 Dox lines and Naïve controls

Blocking ABCB1 with PSC833 (10µM) ablated the difference in IC50 between IM-resistant lines and K562 Dox Naïve, indicating ABCB1 overexpression is the primary mode of resistance in these cell lines. Data are presented as the mean +SEM from at least 4 independent experiments.

4.4 Discussion

Imatinib resistance in CML patients remains a significant clinical challenge. Currently defined mechanisms of resistance include mutations in the kinase domain of BCR-ABL[107,109,119,223], overexpression of BCR-ABL[127,139,224], and overexpression of imatinib efflux proteins such as ABCB1 and ABCG2[40,71,74,75]. ABCB1 overexpression as the major mode of imatinib resistance has been observed in several *in vitro* studies[71,74,195], while patient outcome has been shown to be affected by ABCB1 expression[211], inhibition[74] and ABCB1 polymorphisms[76]. One case study reports a BCR-ABL positive ALL patient who had relapsed 2 months after an allogeneic bone marrow transplant. DNA PCR revealed a 2-fold increase in ABCB1 expression after two weeks of imatinib treatment (to which the patient was not responding). It was found that rhodamine efflux by the patient's blast cells could be inhibited by cyclosporine A (CsA), an ABCB1 inhibitor. After treatment with a bolus of CsA, followed by continuous infusion for 72hr with CsA, the combined treatment with imatinib resulted in a reduction of blasts in the peripheral blood, as well as abolishing phosphorylation of Crkl, a direct BCR-ABL target[74]. Therefore it appeared that inhibition of ABCB1 with CsA allowed imatinib to affectively target BCR-ABL, impacting patient response. A study by Dulucq *et. al.*[76], of 90 CML patients treated with imatinib, found that 85% of patients homozygous for the 1236T ABCB1 allele achieved a major molecular response (MMR), compared with only 47.7% for other genotypes (P=0.003). Other ABCB1 haplotypes were statistically linked with less frequent MMR[76]. Together, these studies suggest a role for ABCB1 activity in imatinib response in CML patients. It has also been postulated that low imatinib intracellular concentrations (mediated by ABCB1 activity) may create an environment conducive to the emergence of more overt resistance mechanisms *e.g.* kinase domain mutations[165].

To investigate the kinetics of resistance mechanism emergence, specifically the interplay between drug-efflux protein expression and kinase domain mutations, an ABCB1-overexpressing cell line (K562 Dox) was cultured in gradually increasing concentrations of imatinib to generate resistance. It was already noted that KD mutations had not arisen when imatinib resistance was generated in two K562 cell lines. This time, by using the K562 Dox cell line, any differences in resistance mechanism emergence in the presence of an efflux pump (in this case, ABCB1) would be identified. Three IM-resistant K562 Dox cell lines were generated and characterised to determine the mechanism(s) of resistance.

The three K562 Dox 2µM imatinib-resistant cell lines were generated in much less time (4 months) than it took to generate imatinib resistance in the K562 cell lines (approximately 6.5 months on average). This observation again supported the findings that ABCB1 is involved in imatinib efflux and resistance *in vitro*[195] and *in vivo*[211]. It appeared that imatinib efflux, mediated by the ABCB1 protein, was conferring some resistance in the K562 Dox Naive cell line, making drug escalation quicker and easier than in the K562 cell line.

No BCR-ABL kinase domain mutations were detected when the K562 Dox 2µM IM1, IM2 and IM3 cell lines were sequenced. Therefore, ABCB1 overexpression does not appear to promote KD mutation development *in vitro*. This may be because the levels of ABCB1 expression achieved in the K562 Dox imatinib-resistant cell lines were sufficient to confer resistance to 2µM imatinib. If a threshold imatinib concentration was reached at which ABCB1 expression was no longer sufficient, the cell line may then have resorted to another resistance mechanism, such as a BCR-ABL kinase domain mutation.

Unlike the K562 IM-resistant cell lines, no BCR-ABL overexpression was observed in the three K562 Dox IM-resistant lines (**Figure 4.2**). Instead, the only detectable mechanism of resistance was a further increase in ABCB1 expression (**Figure 4.4**). As these cells were already overexpressing ABCB1, it seems this mechanism of resistance was 'primed' and therefore easily utilised by the cells to defend against imatinib exposure. Although the sample size is small (n = 3) it appears that this cell line will always rely on ABCB1 overexpression for resistance when exposed to imatinib, because ABCB1 is already being overexpressed and is therefore the easiest path for imatinib resistance.

Due to post-translational modifications, localisation and other regulation, increased ABCB1 expression does not always correlate with increased ABCB1 activity[56,225]. To demonstrate that the increased ABCB1 cell-surface expression in the K562 Dox 2µM IM-resistant cell lines caused imatinib efflux (and therefore contributed to imatinib resistance) IUR assays were conducted. In all three IM-resistant cell lines, the intracellular uptake and retention of imatinib was less than the Naïve control, and this decrease was significant in two of the cell lines (P>0.03) (**Figure 4.5**). Furthermore, blocking ABCB1 activity with PSC833 was able to increase the imatinib IUR in all three IM-resistant cell lines, and this increase was significant in the K562 Dox 2µM IM3 cell line (P<0.05). By inhibiting ABCB1, imatinib

was no longer being effluxed from the cells, and was therefore accumulating intracellularly – thus causing the increase in IUR. Furthermore, the ABCB1-mediated imatinib efflux (that is, the amount of imatinib being effluxed due to ABCB1 activity) was significantly increased in all three IM-resistant lines above that of the Naïve control (**Figure 4.5**). This demonstrates that the ABCB1 protein being overexpressed in the K562 Dox 2μM IM1, IM2 and IM3 cell lines was functionally active and able to reduce the intracellular concentrations of imatinib in these cell lines. However, it was necessary to demonstrate that ABCB1 overexpression was sufficient to cause resistance to 2μM imatinib.

Viability experiments with 10μM PSC833 were attempted in order to demonstrate that imatinib sensitivity could be restored by blocking ABCB1. This concentration of PSC833 is routinely used in the 2hr IUR and IC50 assays to inhibit ABCB1, and was therefore chosen for preliminary viability experiments. However, it was found that 10μM PSC833 alone resulted in cell death at 72hrs, thereby invalidating the experiment. Other studies have successfully used PSC833 in culture to measure reduced viability of ABCB1 expressing cells in the presence of imatinib and cyclosporine, but at much lower concentration ranges (0.1-1μM)[195,226]. Thus, these concentrations of PSC833 could be used for such an experiment with the K562 Dox IM-resistant cell lines. Nevertheless, restoration of imatinib sensitivity by blockade of ABCB1 was demonstrated with the IC50 assay.

In all three K562 Dox IM-resistant cell lines, the $IC50^{imaitnib}$ had significantly increased above that of the Naïve control ($P<0.001$) (**Figure 4.9**). If ABCB1 was the cause of imatinib resistance, then blocking ABCB1 should restore sensitivity of the resistant cell lines, back to the same level as the Naïve control. This is in fact what was observed, as in the presence of PSC833, there was no significant difference between the $IC50^{imatinib}$ values of the K562 Dox IM-resistant cell lines and the Naïve control ($P>0.2$) (**Figure 4.9**). If there were other unidentified resistance mechanisms besides ABCB1 expression, we would expect only partial restoration of the IC50 values when ABCB1 is blocked with PSC833. However, sensitivity was fully restored in all IM-resistant cell lines with PSC833. This indicates that ABCB1 overexpression was the only mechanism of resistance present in these cell lines. Notably, the three imatinib-resistant K562 Dox cell lines also displayed resistance to nilotinib and dasatinib. This is discussed in *Chapter 6: TKI cross-resistance*.

Chapter 5:

BCR-ABL kinase domain mutations arise in the setting of BCR-ABL overexpression, in imatinib- and dasatinib-resistant cell lines

5.1 Introduction

Despite the success of tyrosine kinase inhibitor (TKI) therapy in many CML patients, a proportion of patients acquire secondary resistance. Secondary resistance is defined as disease progression or the loss of an achieved response while on therapy. Specifically, this includes loss of haematologic response, loss of complete cytogenetic response (CCR), or an increase in BCR-ABL expression of 1 log or greater[196]. Approximately 10% of chronic phase patients treated with imatinib will relapse and this percentage is increased for patients in accelerated phase (40-50%) and blast crisis (80%)[7]. Approximately half the patients that switch to a second generation tyrosine kinase inhibitor (*e.g.* nilotinib or dasatinib) due to imatinib failure, are found to have BCR-ABL kinase domain (KD) mutations that confer imatinib resistance[120].

5.1.1 BCR-ABL kinase domain mutations

TKIs designed for CML treatment function by binding BCR-ABL in the ATP-binding pocket of the KD. Specifically, imatinib stabilises BCR-ABL in the inactive conformation, thus preventing the hydrolysis of ATP and the phosphorylation of downstream substrates[4,22]. Particular residues in the KD are essential for the imatinib-BCR-ABL interaction, providing hydrogen bonds and facilitating the correct protein conformation[22,105]. If the BCR-ABL kinase has a mutation in the KD, a specific residue required for imatinib binding may be lost, or prevent imatinib stabilising BCR-ABL in the inactive conformation[105,107]. KD mutations leading to resistance do not render the BCR-ABL protein kinase inactive[109]. Due to the specific nature of the TKI-BCR-ABL interaction, differential resistance may be observed for certain mutations *i.e.* different KD mutations will confer different levels of resistance to different TKIs. This is because imatinib, nilotinib and dasatinib all bind BCR-ABL utilising slightly different residues[119-121], however, a residue critical for binding for all three TKIs is the threonine molecule at position 315. When this residue is replaced with isoleucine, neither imatinib, nilotinib nor dasatinib can bind BCR-ABL[107,121]. This residue is called the 'gatekeeper' residue, and the T315I mutation is known as the 'gatekeeper' mutation[119,124]. To date, more than 50 mutation sites, and more than 70 individual mutations conferring varying TKI resistance have been identified in CML patients[227]. Of these, mutations at 15 residues account for more than 85% of mutations detected, including T315I, Y253F/H, E255D/K/R/V, M351T, G250A/E, F359C/L/V, H396P/R, M244V, E355A/G/K, F317C/L/V, M237I, Q252H/R, D276G, L248V and F486S[227].

5.1.2 BCR-ABL expression and kinase domain mutations

BCR-ABL expression itself is known to promote genomic instability and results in abnormalities such as mutations, chromosomal rearrangements and aneuploidy[97,98]. This is largely facilitated by increased production of reactive oxygen species (ROS; such as superoxide, hydrogen peroxide and hydroxyl free radicals[85,86]) due to BCR-ABL kinase activity[89-91]. The mechanisms by which BCR-ABL facilitates production of ROS is unclear, but one group has demonstrated the involvement of the T177 BCR-ABL residue and the PI3K/mTOR pathway[92]. ROS are intermediates of oxygen reduction, and are damaging to all molecules, including DNA[85,86]. Extensive DNA damage in cells normally leads to apoptosis[94], however, in BCR-ABL positive cells these apoptotic signals are overridden due to BCR-ABL-mediated activation of the JAK/STAT, Raf/MEK/ERK, and PI3K/Akt pathways[8]. Furthermore, DNA repair mechanisms such as mismatch repair are hindered by BCR-ABL expression[100], while error-prone repair mechanisms such as non-homologous end joining (NHEJ) are enhanced[93,102,103]. Thus, BCR-ABL expression is responsible for ROS production which damages DNA, as well as promoting survival in cells that would otherwise undergo apoptosis due to this damage. Finally, through hindering DNA repair mechanisms, genomic fidelity is compromised, resulting in the accumulation of genetic lesions and genomic instability.

A link between BCR-ABL overexpression and BCR-ABL KD mutations has been postulated by several groups[164]. In 2005, Barnes *et. al.*[161] generated IM-resistance in a murine myeloid cell line transfected with BCR-ABL (named 32Dp210[228,229]). Several clones expressing different levels of BCR-ABL were cultured in gradually increasing concentrations of IM at a rate of 100nM every 10 days until 1µM was reached. It was noted that BCR-ABL expression levels determined the rate of resistance development (*i.e.* the more BCR-ABL expressed, the faster imatinib resistance developed). It was also observed that BCR-ABL expression increased gradually in a step-wise fashion as imatinib concentration was escalated, and levels peaked before the emergence of KD mutations, after which BCR-ABL levels declined (in two cases, below the BCR-ABL expression levels in the 'naïve' controls)[161]. The uniform emergence of KD mutations in the setting of increased BCR-ABL expression has also been noted *in vivo*[162,163].

Most patients are routinely screened by RQ-PCR to monitor BCR-ABL expression levels, ensuring that achieved recovery benchmarks are maintained[162,163]. In one study of 214 IM-treated CML patients, BCR-ABL expression data were correlated with mutation status[162]. It was found that 56/214 patients had a greater than 2-fold rise in BCR-ABL mRNA while on imatinib therapy, and of these patients, 34 (61%) had detectable BCR-ABL KD mutations. In the majority of these patients (31/34) the mutation was present at the time of the rise in BCR-ABL expression, and in the remaining 3 patients the mutations became detectable within 3 months of the increase in BCR-ABL expression. Of the 158 patients with stable or decreasing BCR-ABL expression, only one developed a KD mutation (P>0.0001). Thus, this study suggested that a >2-fold rise in BCR-ABL expression identified 97% (34/35) of the patients who developed a KD mutation[162]. A study in 2009 involving 150 patients used a receiver operating characteristic (ROC) analysis to determine a 2.6-fold increase in BCR-ABL expression as the optimal rise that is predictive of KD mutation emergence[163]. It is difficult to determine whether a clinical observation of a rise in BCR-ABL is attributable to 1) an increase in the number of circulating leukaemic cells, or 2) increased expression of BCR-ABL per cell, or both. This is because conventional monitoring using RNA-based PCR (RQ-PCR) measures the number of BCR-ABL transcripts in a sample relative to a control gene. It is therefore a composite of leukaemic cell number and RNA expression level.

5.1.3 Conventional sequencing and the MassARRAY technique

The dideoxynucleotide system (dye-terminator sequencing) is commonly used for sequencing DNA and cDNA. This reaction is a PCR in which normal dNTPs and dideoxynucleotide triphosphate (ddNTP) chain terminators are present. ddNTPs lack a 3'-hydroxyl (-OH) group on their deoxyribose sugar, and therefore halt DNA chain elongation as no phosphodiester bond can be formed with the 5' phosphate of a subsequent nucleotide. As both dNTPs and ddNTPs are equally likely to be incorporated in the reaction, this PCR results in products of different lengths, each terminating at a different nucleotide of the sequence. Each of the four possible ddNTPs (adenine, guanine, thymine and cytosine) are labelled with fluorescent dyes, each of which emit light at different wavelengths. To obtain the sequence, gel electrophoresis is used to separate the PCR products by length (to a resolution of one nucleotide) before detection of the four fluorescent dyes which represent a particular base. This method (known as conventional sequencing) has a sensitivity of around 20%, as mutations

that represent less than 20% of the total transcript may not be detectable due to the vast majority of 'wild-type' sequence overwhelming the mutant sequence. The MassARRAY method is a much more sensitive sequencing technique, allowing detection of mutations as low as 0.5%. Rather than using a mixture of 4 ddNTPs in the primer extension reaction, specific mixes of 2 or 3 ddNTPs are used for each PCR. This restricts the generation of extension products to the mutant allele only, increasing assay sensitivity compared to conventional sequencing.

5.1.4 The KU812 cell line

The myeloblastic KU812 cell line was established in 1984 from the peripheral blood of a 38-year-old male with CML in blast crisis[167]. Karyotyping revealed this cell line carried two Ph chromosomes, as well as several other genomic abnormalities such as aneuploidy **(Figure 5.1)**. Chromosome number was found to vary from 50-60[**167**], and more recent studies confirm this karyotype has changed little over passage from the original cell line[230].

Figure 5.1

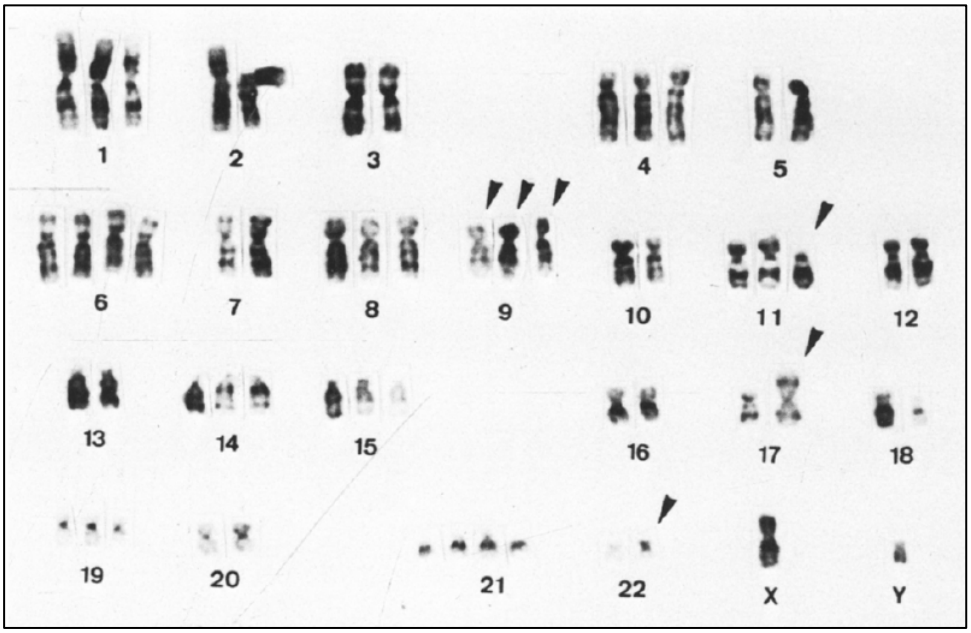

Figure 5.1: Karyotype of KU812 cell line when first established
Shown is the karyotype of the KU812 cell line by Kishi (Leukemia Research, 1985)[167] when the cell line was first established. Arrows show the common abnormalities of this cell line.
Described as: 58, XY, t(9;22)(q34;ql 1), i(17q), + 1, +4, + 6, + 6, + 8, + der(9)t(9;22), + der(9)t(9;22), + der(1 l)(ql 1), + 14, + 15, + 19, +21, +21, -9.

5.2 Approach

Due to clonal differences, not all cell lines for a particular model will behave in the same way or provide similar results[231,232]. To ensure that trends in resistance mechanism emergence were not merely cell-line specific, multiple cell lines were used in the generation of imatinib- and dasatinib-resistance in this study. The KU812, K562 and K562 Dox cell lines were chosen for several reasons. Firstly, all three were readily available and are widely accepted and used in *in vitro* CML studies[65,81,127,155,156,164,233]. Secondly, they are human CML cell lines and therefore provide a more relevant model over murine cell lines, or cell lines transfected with p210 BCR-ABL. Finally, none of these cell lines carry kinase domain mutations and BCR-ABL expression levels are comparable with CML patient cells.

5.2.1 Generating dasatinib resistance in the K562 and K562 Dox cell lines

Previously, BCR-ABL overexpression (in the K562 2μM IM1 and IM2 cell lines) and ABCB1 overexpression (in the K562 Dox 2μM IM1, IM2 and IM3 cell lines) was observed when these cell lines acquired resistance to imatinib (**Figure 3.11** and **Figure 4.4**). Therefore, resistance to dasatinib was generated in order to compare the resistance mechanisms that had previously emerged in response to imatinib. To our knowledge, this is the first instance of dasatinib-resistance generation in a human CML cell line. Notably, generation of dasatinib resistance was considerably harder than generating imatinib resistance. This may be because dasatinib is 300 times more potent than imatinib[33] and inhibits sarcoma (Src) family kinase members in addition to BCR-ABL[30,33], thus making it harder for the cells to survive and develop resistance. Src family kinases are involved in numerous signalling pathways regulating homeostasis, cell proliferation and survival, and are implicated in a variety of human cancers[234] (**Figure 5.2**).

In patient plasma, peak dasatinib concentrations reach 100nM[199], therefore 200nM dasatinib was chosen as the final 'resistant' concentration for this study, as cells thriving in this concentration would be comparably resistant (or even more resistant) than patient cells from a DAS-resistant patient. K562 cells were initiated in 0.5nM dasatinib, and subsequently escalated to 1nM, 2nM, 3.5nM, 5nM, 10nM, 15nM, 25nM, 50nM, 75nM, 100nM, 150nM until reaching 200nM (approximately 11 months). The final resistant cell line was named K562 200nM DAS.

Figure 5.2

Figure 5.2: Src-mediated pathways contribute to cancer progression
Src family kinases are involved in numerous signalling pathways governing cell proliferation and homeostasis. In tumour cells, association of Src with overexpressed and mutated receptor tyrosine kinases (RTK; *e.g.* BCR-ABL) leads to increased enzymatic activity of Src. This leads to the activation of pro-survival pathways (green), angiogenic pathways (blue), proliferation through the Ras/Raf pathway (gold) and decreased stromal adhesion through the focal adhesion kinase (FAK) (red). PI3K, phosphatidylinositol 3-kinase; STAT3, signal transducers and activators of transcription 3; IKK, IκB kinase; MAPK, mitogen-activated protein kinase; MEK, mitogen-activated protein kinase kinase; IL-8, interleukin-8; ERK, extracellular signal-regulated kinase; NF-κB, nuclear factor-κB (Summy *et. al.* 2006, Clinical Cancer Research)[234].

Next, one K562 Dox cell culture was initiated in 6nM dasatinib, and subsequently escalated to 12nM, 20nM, 30nM, 40nM, 55nM, 75nM, 100nM and 150nM until reaching 200nM (approximately 8 months). This cell line was named K562 Dox 200nM DAS1. A second K562 Dox DAS culture was initiated in 6nM, and subsequently escalated to 12nM, 20nM, 35nM, 55nM, 75nM, 100nM and 150nM until reaching 200nM (approximately 7 months). This cell line was named K562 Dox 200nM DAS2. In all cases of dasatinib-resistance generation, dasatinib concentration was escalated every 10-30 days, depending on cell proliferation and viability. Generating a KU812 DAS-resistant line was also attempted, however due to the extreme sensitivity of this cell line, dasatinib concentrations could not be increased above 1nM.

Serial dilutions of dasatinib (in DMSO) were made from 10mM stocks such that no more than 20µl of drug was ever added to a 50mL cell culture – thus DMSO concentration never exceeded 0.04% in dasatinib cultures. Parental, 'naïve' cell lines, and DMSO (0.1%) lines were maintained in parallel cultures as controls – the latter to confirm that DMSO itself does not generate TKI resistance.

5.2.2 Generating imatinib resistance in the KU812 cell line

Previous studies have failed to generate IM-resistant KU812 cells due to the inherent sensitivity of these cells to TKIs, and the rigidity of the 10-day-escalation method[127,164]. The method used in this study was more flexible, as drug concentrations were escalated more slowly if the cell cultures required. As a result, three IM-resistant KU812 cell lines were generated.

Cultures of the KU812 cell line were initiated in 100nM IM, and subsequently increased to 200nM, 300nM, 400nM, 500nM, 600nM, 700nM, 800nM, 1.4µM and 2µM. A second resistant cell line was generated as follows; 100nM, 200nM, 350nM, 450nM, 600nM, 800nM, 1.4µM, 2µM, 2.5µM, 3µM, and a third; 100nM, 200nM, 300nM, 400nM, 600nM, 800nM, 1.4µM, 2µM. These cell lines were named KU812 2µM IM1, KU812 3µM IM2 and KU812 2µM IM3. On average, it took 9 months to generate resistance to 2µM imatinib in the KU812 cell line. A drug 'naïve' KU812 culture was maintained in parallel as a control (named KU812 Naïve).

5.2.3 Re-escalation of intermediates in imatinib, dasatinib or nilotinib

When clinically relevant BCR-ABL kinase domain mutations were identified in these cell lines, two cell lines were chosen for 're-escalation' studies. The K562 Dox 200nM DAS1 cell line was found to harbour a KD mutation, which emerged in the 75nM DAS intermediate cell culture. To determine whether clones carrying the mutation were present at undetectable levels in earlier intermediates, the 40nM DAS and 55nM DAS intermediates were re-escalated in either dasatinib or nilotinib (NIL). Nilotinib escalation from the 55nM DAS1 intermediate was conducted as follows: 200nM, 250nM, 350nM, 500nM (escalating every ten-15 days) and the two nilotinib-resistant cell lines generated were named K562 Dox 500nM NIL1 RE55 and NIL2 RE55. Although the achievable plasma trough concentrations of nilotinib has been reported as 2000nM[235], it is difficult to know what concentration of nilotinib is pharmacologically relevant as plasma concentrations may not represent the effective/intracellular concentration. Nilotinib is highly lipophillic[236], and is therefore particularly susceptible to plasma protein binding which sequesters the drug away from leukaemic cells in the blood. *In vivo*, the effective dose may therefore be much lower than 2000nM, and for the purposes of this study, a concentration of 500nM for the final nilotinib resistant culture was deemed sufficient.

When the same KD mutation repeatedly emerged in dasatinib re-escalation cultures, it was hypothesised that a clone carrying this mutation was present in the K562 Dox Naïve culture (and would always be expanded under DAS selection). Dasatinib resistance was therefore generated 'from scratch', resulting in the K562 Dox 200nM DAS2 cell line.

Lastly, the KU812 2µM IM3 cell line was found to carry a KD mutation from the 300nM IM3 intermediate cell line onwards. The 200nM IM3 culture was therefore used in an imatinib re-escalation to determine if a KD-carrying clone was present in the 200nM intermediate, even though it was not detectable by MassARRAY sequencing. For all re-escalation studies, the intermediate of interest was thawed from frozen stocks and cultured in an escalated TKI concentration *i.e.* the KU812 200nM IM3 intermediate was thawed and immediately exposed to 300nM imatinib.

5.2.4 Analysis of dasatinib- and imatinib-resistant cell lines

Various assays were utilised in order to characterise the resistance mechanisms present in the dasatinib- and imatinib-resistant cell lines. To measure the level of kinase inhibition in response to particular TKIs, IC50 assays were performed as previously described[36]. Thus, by measuring the concentration of TKI required to reduce levels of p-Crkl (a BCR-ABL adaptor protein) by 50%, relative levels of TKI resistance were determined (**Figure 5.3**).

In order to demonstrate that resistance was not mediated by TKI efflux protein expression, flow cytometry was used to measure levels of ABCB1 and ABCG2 cell surface expression. Furthermore, the intracellular uptake and retention (IUR) assay was used to confirm that TKI transport (influx/efflux) was not involved in conferring resistance.

In all TKI-resistant cell lines, intermediate stages of resistance development were sampled for RNA and DNA isolation. These samples were later used for RQ-PCR to measure BCR-ABL mRNA expression, quantitative DNA PCR to measure Bcr-Abl copy number, and for sequencing of the BCR-ABL KD. If BCR-ABL expression and DNA copy number had increased, FISH and karyotyping was used to demonstrate the mode of amplification (*e.g.* whether by HSR or dmin carrying Bcr-Abl).

Figure 5.3: K562 DMSO IC50^{dasatinib} Western blot quantification
Cells were incubated for 2 hours at 37℃/5%CO_2 with DAS concentrations ranging up to 5000nM. Western blot analysis for p-Crkl was performed as previously described[36]. Signals were quantified using Image Quant software (Molecular Dynamics), and the ratio of p-Crkl to Crkl was determined using Image Quant analysis. **(A)** Top panel: Scanned Western blot image before analysis. Bottom panel: Polygons were drawn around each Crkl and p-Crkl band, and blank membrane was also sampled as a background control. **(B)** Bands of p-Crkl were measured and graphed as a percentage of the intensity of total Crkl (*i.e.* p-Crkl + Crkl intensity = 100%). **(C)** These percentages were normalised (0nM dasatinib is 100% p-Crkl, 5000nM dasatinib is 0% p-Crkl). The IC50 value was then taken as the concentration of dasatinib when normalised p-Crkl was reduced to 50% (*i.e.* IC50^{dasatinib} = 13.2nM in this case). This blot is shown again in Figure 5.4.

Figure 5.3

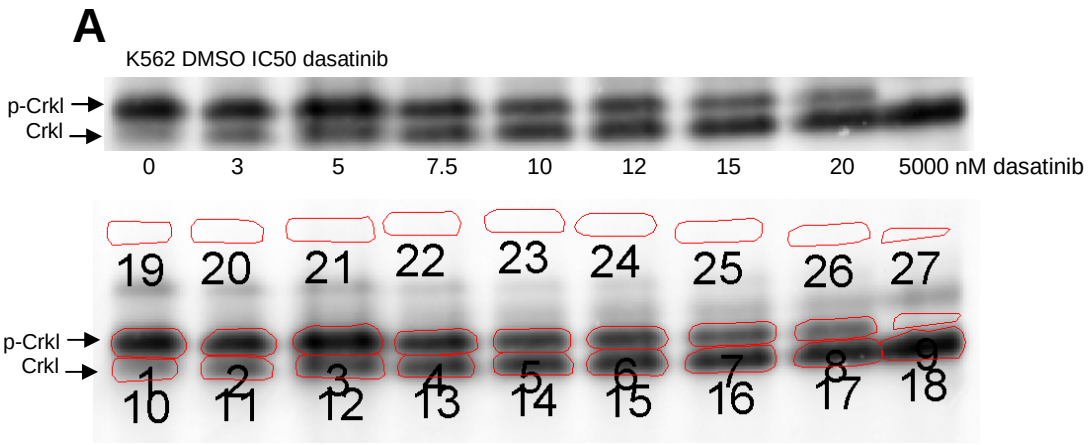
A
K562 DMSO IC50 dasatinib
p-Crkl
Crkl
0 3 5 7.5 10 12 15 20 5000 nM dasatinib
19 20 21 22 23 24 25 26 27
p-Crkl
Crkl
1 2 3 4 5 6 7 8 9
10 11 12 13 14 15 16 17 18

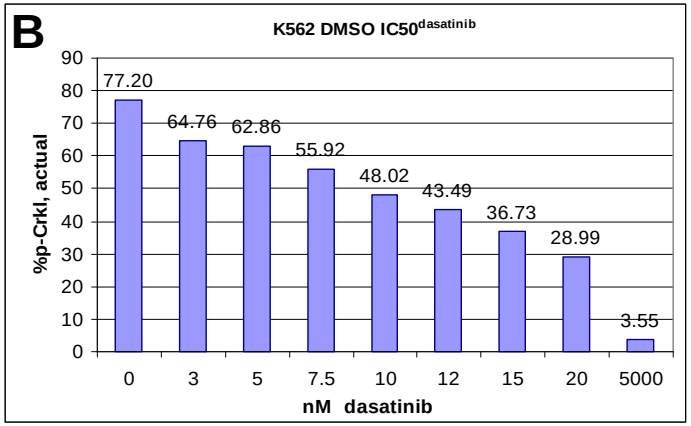
B
K562 DMSO IC50dasatinib
%p-Crkl, actual
77.20
64.76
62.86
55.92
48.02
43.49
36.73
28.99
3.55
0 3 5 7.5 10 12 15 20 5000
nM dasatinib

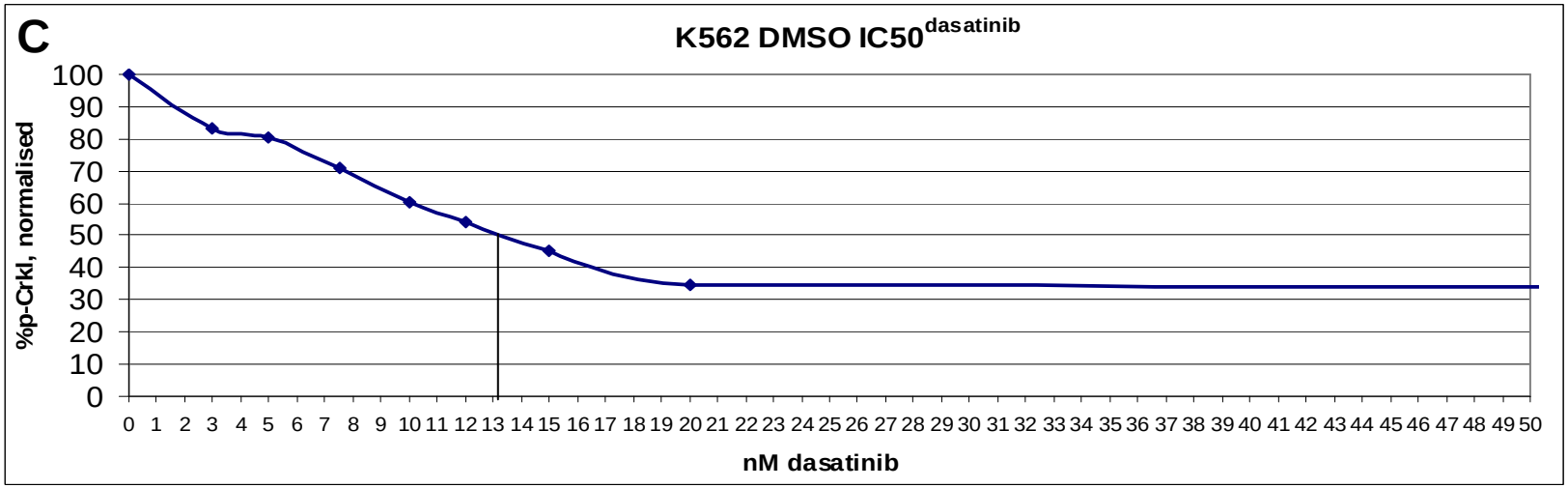
C
K562 DMSO IC50dasatinib
%p-Crkl, normalised
100 90 80 70 60 50 40 30 20 10 0
0 1 2 3 4 5 6 7 8 9 10 11 12 13 14 15 16 17 18 19 20 21 22 23 24 25 26 27 28 29 30 31 32 33 34 35 36 37 38 39 40 41 42 43 44 45 46 47 48 49 50
nM dasatinib

5.3 Results

In order to compare and contrast the different resistance mechanisms that arise in different cell lines exposed to different TKIs, the K562, K562 Dox and KU812 cell lines were exposed to imatinib or dasatinib. Previously it was observed that imatinib resistance in the K562 cell line was mediated by BCR-ABL overexpression (*Chapter 3*) while imatinib resistance in the K562 Dox cell line was mediated by overexpression of ABCB1 (*Chapter 4*). In this chapter, these resistance mechanisms were compared with one dasatinib-resistant K562 cell line and two dasatinib-resistant K562 Dox cell lines, as well as three imatinib-resistant KU812 cell lines.

5.3.1 Dasatinib resistance in the K562 cell line

To compare the level of dasatinib resistance in the K562 200nM DAS cell line, $IC50^{DAS}$ assays were conducted and compared with values for the K562 Naïve and K562 DMSO control cell lines. The K562 Naive and DMSO control cell lines had an average $IC50^{DAS}$ of 11.7nM and 10.7nM respectively, whereas the K562 200nM DAS cell line had an $IC50^{DAS}$ greater than 50,000nM **(Figure 5.4 and 5.5)**. To identify the mechanism(s) facilitating this overt dasatinib resistance, various assays were performed.

To exclude ABCB1 and ABCG2 cell surface expression, cells were analysed by flow cytometry. No expression of either of these efflux pumps was detected in the K562 200nM DAS cell line **(Figure 5.6)**. To further confirm that dasatinib uptake and retention did not play a role in dasatinib resistance, DAS IUR assays were conducted. At both 1µM and 2µM dasatinib, there was no significant difference in DAS IUR in the K562 200nM DAS cell compared with the K562 Naïve and DMSO control cell lines (**Figure 5.7**).

RQ-PCR for BCR-ABL revealed that expression had increased from 178% in the K562 Naive control, to 847% in the K562 200nM DAS cell line (**Figure 5.8**, *"200nM"*). Retrospective analysis of the intermediate stages of resistance revealed that BCR-ABL expression had increased gradually in a step-wise fashion, peaking at 1915% in the 3.5nM intermediate. BCR-ABL expression levels then dropped significantly to approximately 1000% in the 5nM intermediate (P=0.0003) **(Figure 5.8)**. Using a sensitive mutation detection technique (MassArray), it was found that the T315I gatekeeper mutation

Figure 5.4

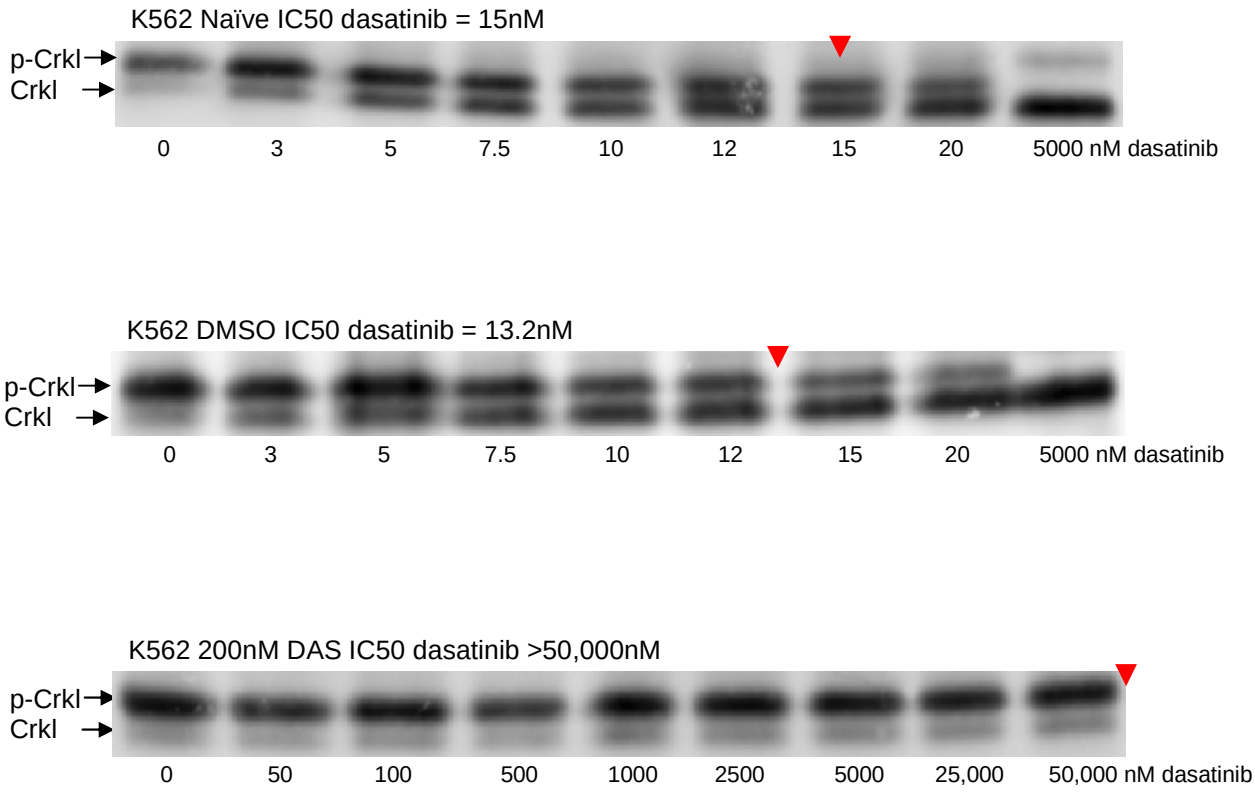

Figure 5.4: The K562 200nM DAS cell line has an increased IC50^{DAS} compared to the K562 Naïve and DMSO control cell lines
Cells were incubated for 2 hours at 37℃/5%CO_2 with DAS concentrations ranging up to 50,000nM. Western blot analysis for p-Crkl was performed as previously described[36]. The IC50 value for each blot (determined as the dose of drug required to reduce levels of p-Crkl by 50%) is indicated above each blot (and with red arrow). IC50 assays were performed at least four times. One representative blot is shown for each of the three cell lines.

Figure 5.5

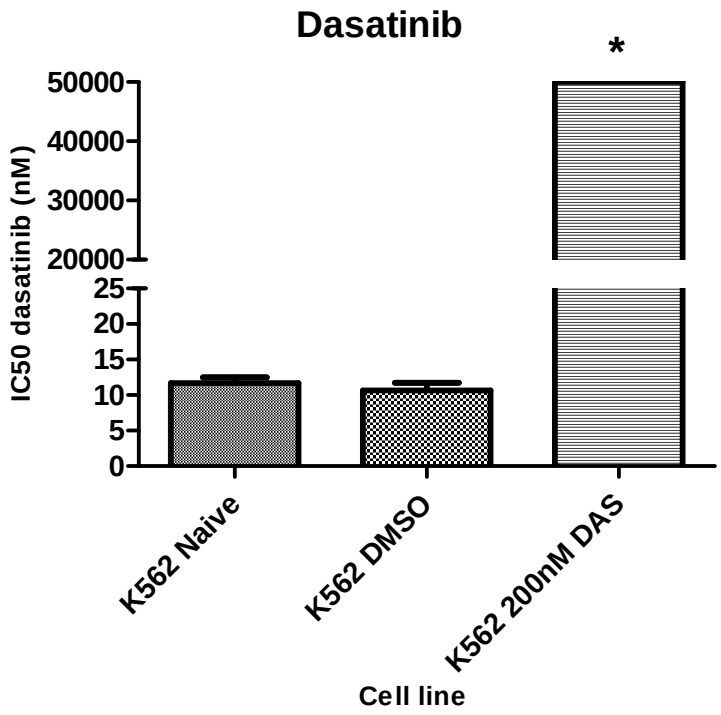

Figure 5.5: The average IC50^{DAS} for K562 200nM DAS was significantly greater than that of the K562 Naïve and DMSO control cell lines

Note that no exact value can be given for the K562 200nM DAS cell line, as p-Crkl could not be ablated even in the presence of 50,000nM DAS (see Figure 5.4). A higher IC50 value indicates greater resistance to dasatinib, while a lower IC50 value indicates more sensitivity. Data are presented as mean +SEM of data from at least 4 independent experiments. The K562 200nM DAS IC50^{DAS} was significantly greater than the K562 Naïve and DMSO control cell lines (*P<0.00001).

Figure 5.6

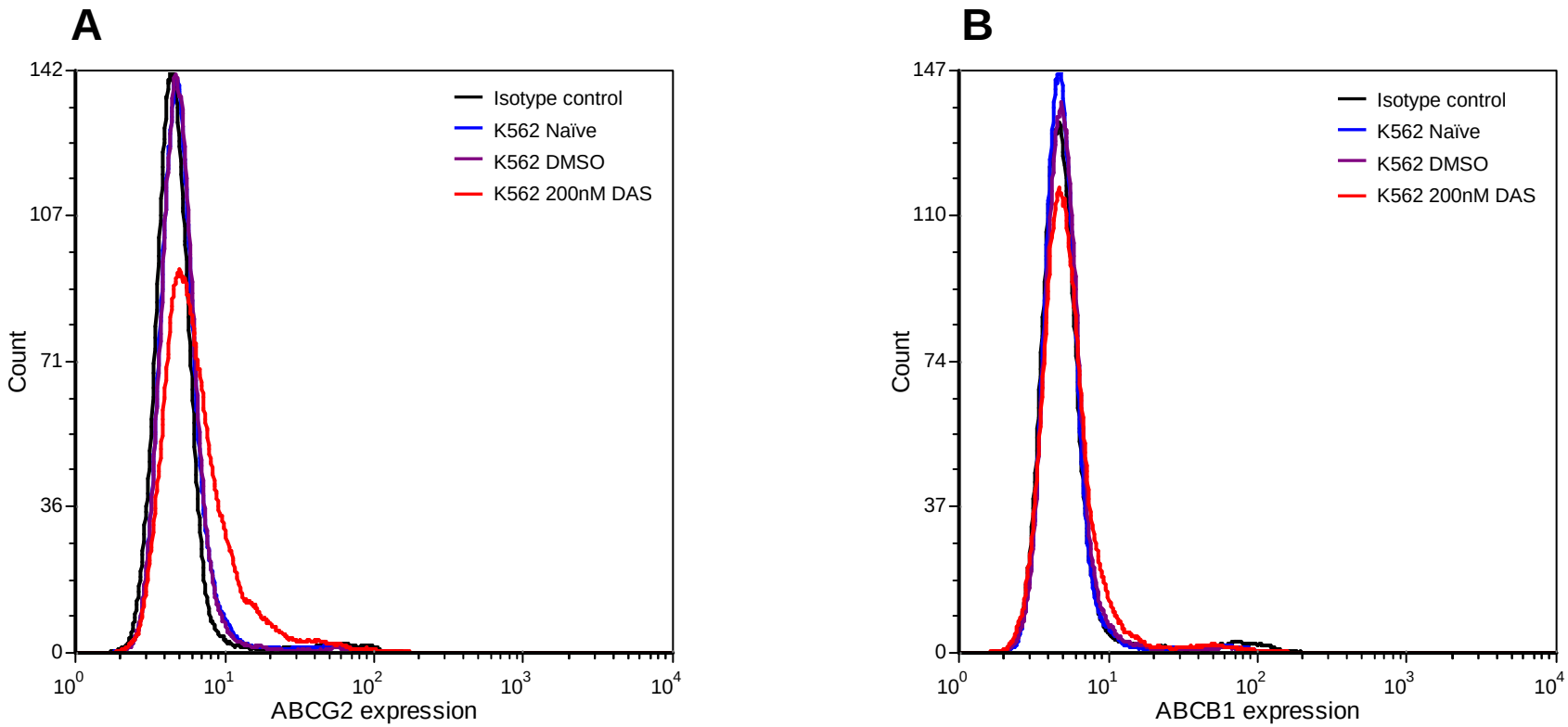

Figure 5.6: The K562 200nM DAS cell line does not express ABCB1 or ABCG2
K562 Naïve, DMSO, and 200nM DAS cells were harvested and stained with either an isotype control antibody or the corresponding PE ABCB1 or PE ABCG2 antibody. After a 45 minute incubation with the antibody, the cells were washed and analysed by flow cytometry. Neither ABCG2 **(A)** nor ABCB1 **(B)** expression could be detected in the K562 200nM DAS cell line. Histograms are representative of 3 experiments.

Figure 5.7

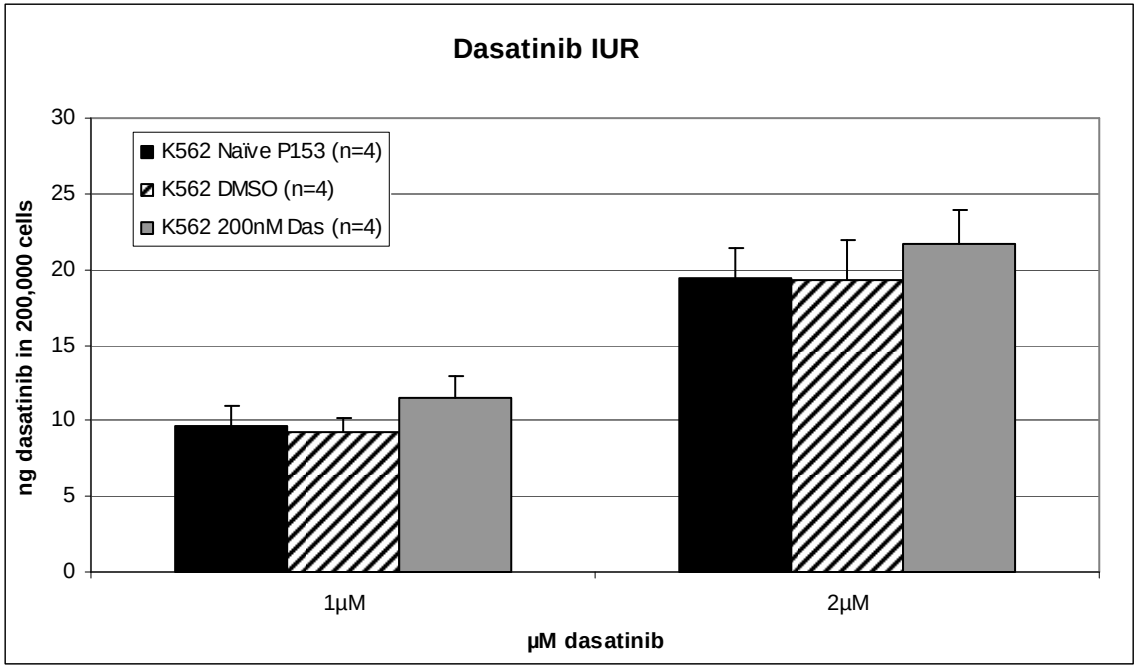

Figure 5.7: Dasatinib IUR does not differ between the K562 200nM DAS cell line and the K562 Naïve and DMSO control cell lines

The intracellular uptake and retention (IUR) assay was performed as previously described[172]. The K562 200nM DAS cell line had a similar IUR compared to the K562 Naïve and DMSO control cell lines (no significant difference). Data are presented as mean +SD calculated from at least four independent experiments.

Figure 5.8

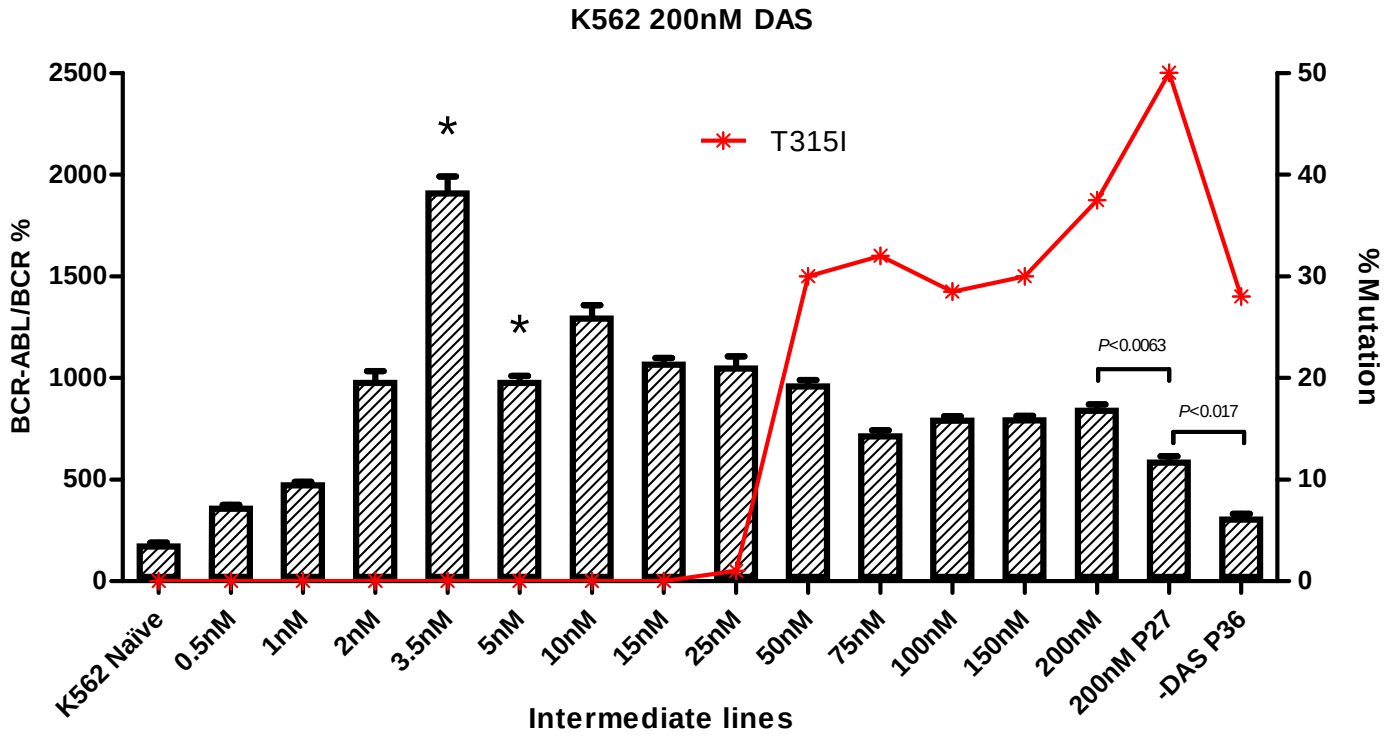

Figure 5.8: BCR-ABL expression levels and KD mutation status in the K562 200nM DAS cell line
BCR-ABL expression levels increased gradually in a step-wise fashion, peaking in the 3.5nM intermediate. Expression levels then significantly decreased (*P=0.0003) before the emergence of the T315I mutation, detectable by MassARRAY at 1% in the 25nM intermediate. Subsequently, conventional sequencing revealed the T315I% increased steadily over time in the presence of DAS. Note that the T315I% continued to rise after 27 passages in DAS while BCR-ABL expression decreased (200nM P27). When the 200nM P27 cells were grown in the absence of dasatinib for 36 passages (-DAS P36) both T315I% and BCR-ABL expression decreased. BCR-ABL expression levels are plotted as a ratio of BCR expression (% +SEM from at least 3 independent experiments).

had emerged in the 25nM intermediate cell line. The T315I percentage (relative to total BCR-ABL transcript) continued to increase and became detectable by conventional sequencing in the 50nM intermediate cell line. The T315I mutation reached a peak of 50% after 27 passages in 200nM dasatinib (200nM P27) (**Figure 5.8**). Conversely, BCR-ABL expression levels significantly decreased from 847% to approximately 590% after 27 passages in 200nM dasatinib (P<0.007) (**Figure 5.8**). To investigate whether BCR-ABL overexpression and mutation status would be maintained if the selective pressure was removed, frozen stocks of K562 200nM DAS cells (P27) were thawed and cultured in the absence of dasatinib. After 36 passages in the absence of dasatinib (-DAS P36) it was found that BCR-ABL expression levels had significantly decreased from ~590% to ~313% (P<0.02) and this was accompanied by a decrease in T315I% (**Figure 5.8**).

DNA PCR confirmed a significant increase in Bcr-Abl copy number from 115% in the K562 Naïve control cell line to 438% in the K562 200nM DAS cell line (P<0.0005), and that these levels significantly decreased to 305% after 27 passages in 200nM dasatinib (P<0.04) (**Figure 5.9**). Furthermore, when the K562 200nM DAS P27 cells were cultured in the absence of dasatinib for 36 passages, Bcr-Abl copy number again decreased to 210% (P<0.02) (**Figure 5.9**) but still remained significantly higher than in the K562 Naïve cell line (P<0.005).

5.3.2 Dasatinib-resistance in K562 Dox cell lines

Dasatinib-resistance generation in the K562 Dox cell line was noticeably easier than in the K562 cell line, as duration was ~7.5 months for the former compared to 11 months in the latter. This is likely due to the fact that dasatinib is transported by ABCB1[55,69], which is expressed at high levels in the K562 Dox cell line thereby facilitating some level of primary dasatinib resistance.

5.3.2.1 The K562 Dox 200nM DAS1 cell line

The K562 Dox 200nM DAS1 cell line was able to thrive in the presence of 200nM dasatinib. The mechanisms facilitating this resistance were investigated by a variety of methods. Firstly, flow cytometry was used to determine whether any changes in expression of ABCB1 or ABCG2 had occurred. It was found that expression levels of both these transporters had not changed in the K562 Dox 200nM DAS1 cell line compared to the parental K562 Dox cell line (**Figure 5.10**). This was unexpected, as ABCB1 overexpression was previously observed as a resistance mechanism in three

Figure 5.9

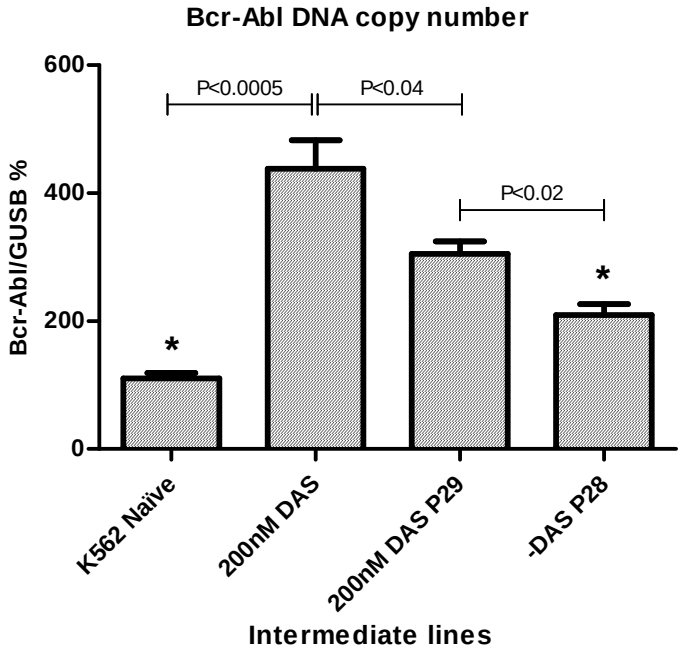

Figure 5.9: Bcr-Abl copy number in intermediates of the K562 200nM DAS cell line

Bcr-Abl copy number (with respect to the GUSB control gene) was significantly increased in the K562 200nM DAS cell line compared to the K562 Naïve control cell line. After 29 passages in 200nM DAS, the Bcr-Abl copy number significantly decreased (200nM DAS P29), and 28 passages in the absence of dasatinib (-DAS P28) resulted in a further significant decrease. These results mirror the values seen for BCR-ABL transcript expression (Figure 5.7). DNA was extracted using a High Pure PCR Template Preparation Kit (Roche Diagnostics, Mannheim, Germany). The DNA was used as a template in quantitative DNA PCR, performed in duplicate for each experiment. Data are presented as mean +SD from at least 3 independent experiments. *P<0.005.

Figure 5.10

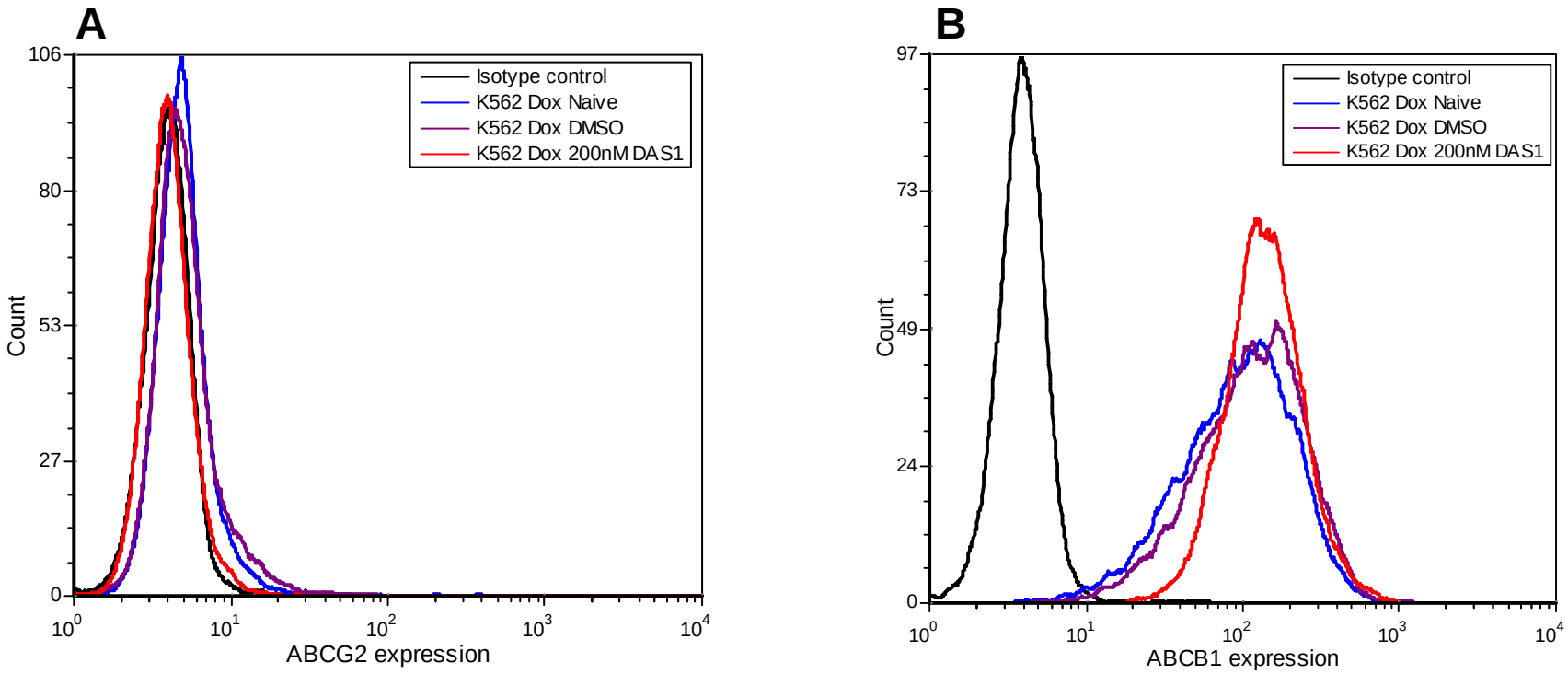

Figure 5.10: Cell surface expression of ABCB1 or ABCG2 in the K562 Dox 200nM DAS1 cell line
K562 Dox Naïve, K562 Dox DMSO and K562 Dox 200nM DAS1 cells were harvested and stained with either an isotype control antibody or the corresponding PE labelled ABCB1 or PE labelled ABCG2 antibody. After a 45 minute incubation with the antibody, the cells were washed and analysed by flow cytometry. Neither ABCG2 **(A)** nor ABCB1 **(B)** expression had increased in the K562 Dox 200nM DAS1 cell line compared to the dasatinib-naïve control cell lines. Histograms are representative of 3 experiments.

imatinib-resistant K562 Dox cell lines (**Figure 4.4**). Furthermore, the dasatinib intracellular uptake and retention (IUR) was not significantly different from the K562 Dox Naïve cell line, indicating that drug influx/efflux was not mediating dasatinib resistance (**Figure 5.11**).

RQ-PCR revealed that BCR-ABL expression had increased from 186% in K562 Dox Naïve cells to 540% in the final K562 Dox 200nM DAS1 cell line (**Figure 5.12**). Studies of the intermediate cultures revealed that BCR-ABL expression levels again increased gradually as the dasatinib concentration was escalated (as it did in the K562 200nM DAS cell line; **Figure 5.8**), reaching a peak in the 55nM DAS1 intermediate of ~850%. Notably, expression levels then dropped significantly to ~466% (P<0.004) coinciding with the appearance of the V299L BCR-ABL kinase domain mutation. BCR-ABL expression levels then appeared to plateau at around 500%, while the percent of V299L mutation (relative to total BCR-ABL transcript) steadily increased from ~40% to ~70% as dasatinib concentrations increased (**Figure 5.12**).

Quantitative DNA PCR demonstrated that the Bcr-Abl DNA copy number mirrored BCR-ABL mRNA expression in the 55nM DAS1, 75nM DAS1 and 200nM DAS1 cultures, again showing a significant decrease between the 55nM and 75nM intermediates (P<0.0001) (**Figure 5.13**). FISH revealed the presence of multiple copies of Bcr-Abl, although it is unclear whether this amplification was due to double minutes or homogeneously staining regions (**Figure 5.14**).

Using conventional sequencing, the V299L mutation first became detectable in the 75nM DAS1 intermediate cell line. However, this method is only sensitive to 20% (*i.e.* mutations present below this threshold are not detectable by conventional sequencing). To investigate whether the V299L mutant clone emerged at an earlier time-point, MassARRAY sequencing (sensitive to 1%) was utilised, but the mutation was not identified in any intermediate cell cultures prior to the 75nM condition.

5.3.2.1.1 Re-escalation of intermediates in DAS or NIL

If indeed the V299L clone was present in the 55nM DAS1 intermediate, it should again be selected for if this intermediate was re-escalated in dasatinib. Therefore, frozen stocks of the 55nM DAS1 intermediate were thawed and two separate cultures were re-escalated to 200nM dasatinib (named K562 Dox 200nM DAS 1RE55 and 2RE55 respectively). Neither dasatinib-re-escalated cell line

Figure 5.11

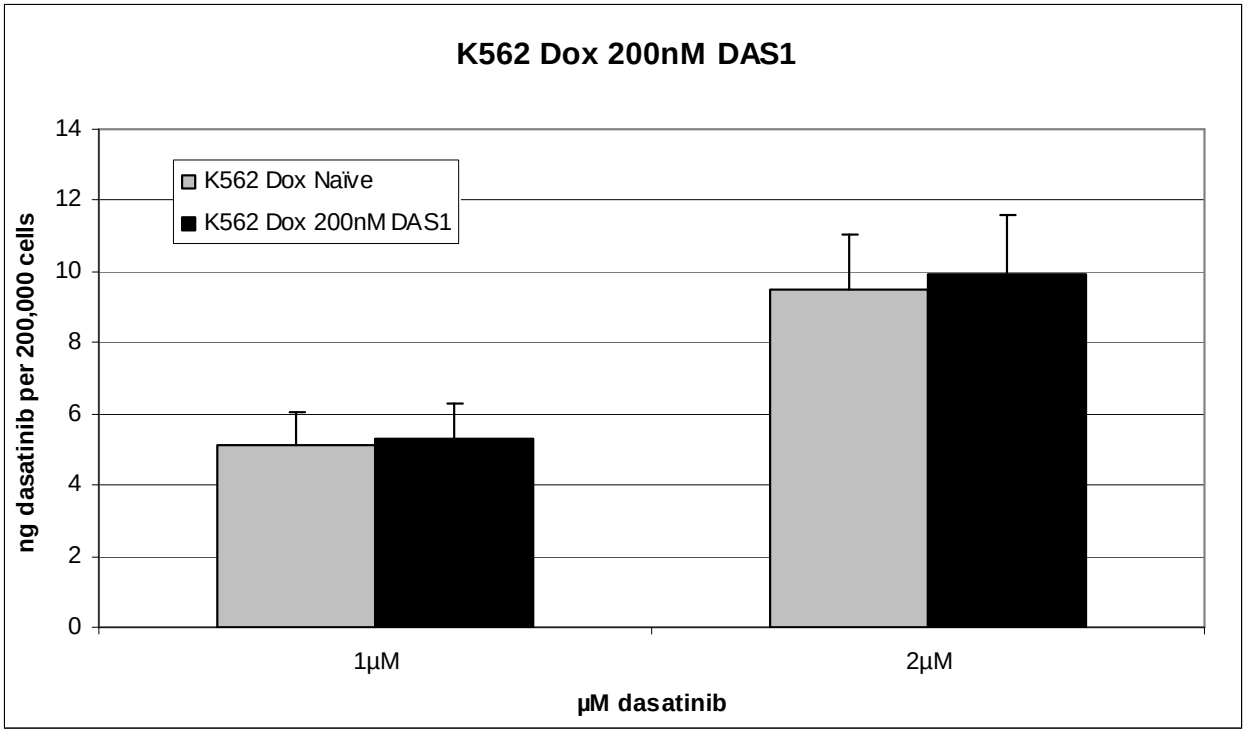

Figure 5.11: Dasatinib IUR does not differ between the K562 Dox 200nM DAS1 cell line and the K562 Dox Naïve control cell line

The intracellular uptake and retention (IUR) assay was performed as previously described[172]. The K562 Dox 200nM DAS1 cell line has a similar DAS IUR compared to the K562 Dox Naïve control cell line, in the presence of 1µM or 2µM DAS. Data are presented as mean +SD calculated from at least four independent experiments.

Figure 5.12

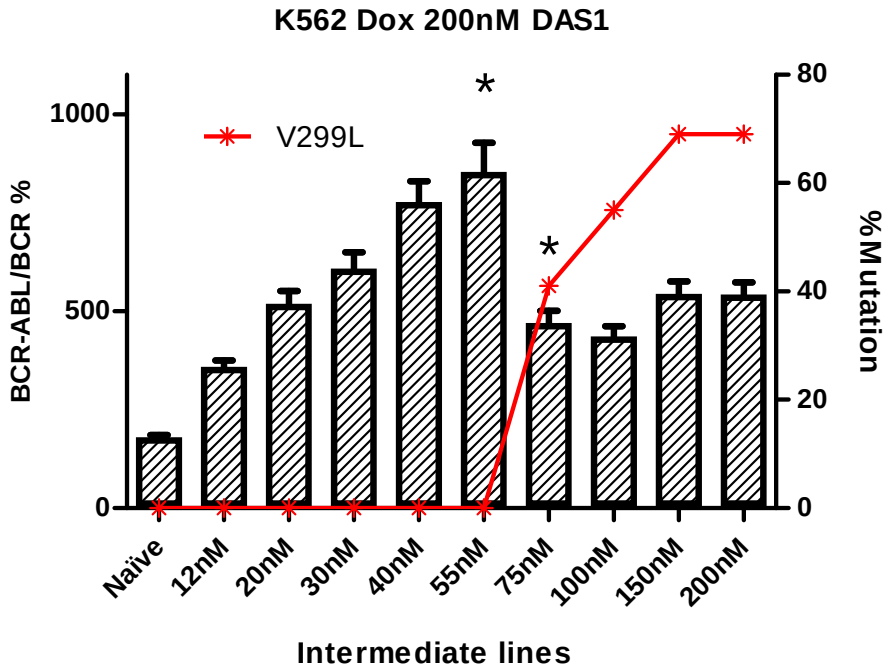

Figure 5.12: BCR-ABL expression increased until the emergence of the V299L mutation in a DAS-resistant K562 Dox cell line

BCR-ABL expression levels increased gradually, peaking in the 55nM DAS intermediate. Expression levels then significantly dropped (*P<0.004) coinciding with the appearance of the V299L mutation. Neither conventional sequencing nor MassARRAY could detect the mutation in the 55nM DAS intermediate. After the emergence of the V299L mutation, BCR-ABL expression levels appeared to plateau. BCR-ABL expression is plotted as a ratio of BCR expression % +SEM from at least 3 independent experiments.

Figure 5.13

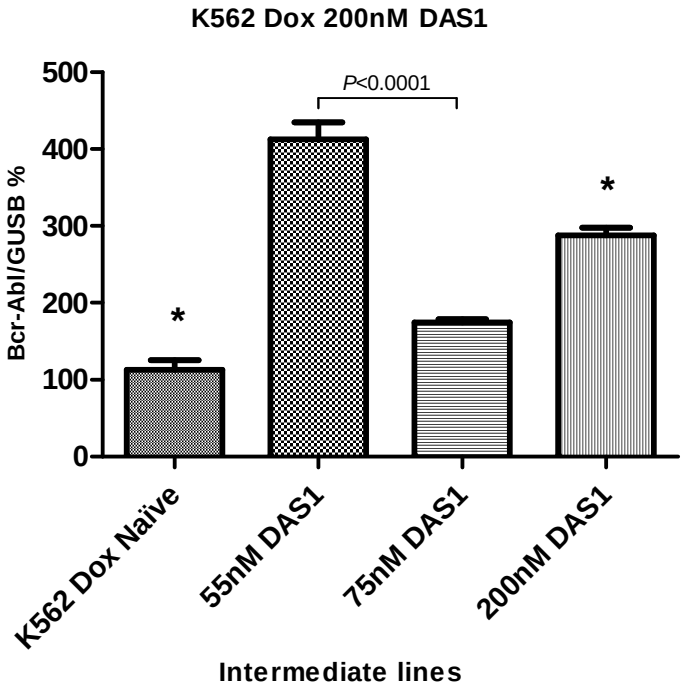

Figure 5.13: Bcr-Abl copy number in selected intermediates of the K562 Dox 200nM DAS1 cell line

Bcr-Abl copy number (with respect to the GUSB control gene) mirrored BCR-ABL expression levels (Figure 5.12) in the K562 Dox Naïve, 55nM DAS1, 75nM DAS1 and 200nM DAS1 cell lines. Again, note the significant decrease between the 55nM and 75nM intermediates. DNA was extracted from cells using a High Pure PCR Template Preparation Kit (Roche Diagnostics, Mannheim, Germany). The DNA was used as a template in quantitative DNA PCR and was performed in duplicate for each experiment. Data are presented as mean +SD from at least 3 independent experiments. (*P<0.0008).

Figure 5.14

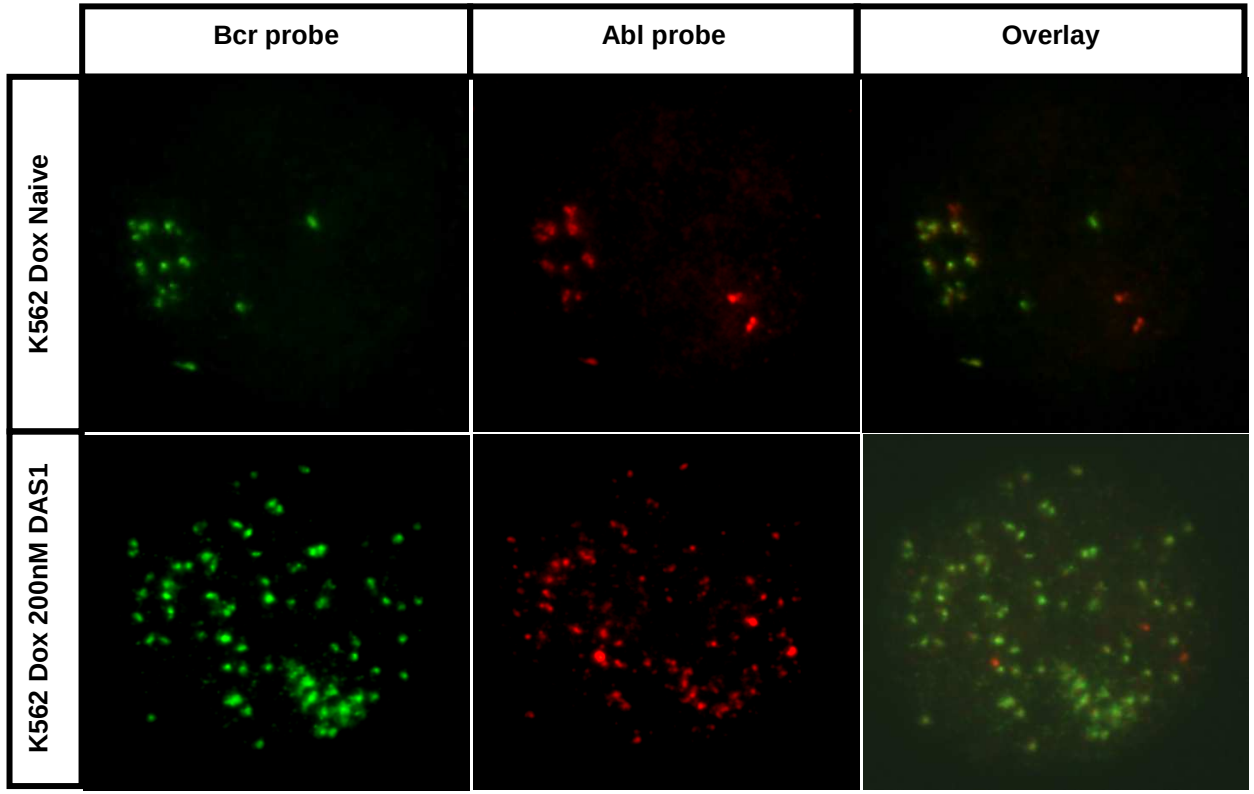

Figure 5.14: Interphase FISH to identify Bcr-Abl fusion genes
Shown above is a single, representative K562 Dox Naïve cell (top panel) and a K562 Dox 200nM DAS1 cell (bottom panel). Bcr-Abl amplification in the DAS-resistant cell line is evident due to numerous co-localising Bcr (green) and Abl (red) signals. 1×10^{6} cells were harvested from culture and incubated in 100µL colcemid before being fixed onto glass slides. After RNase treatment, cells were probed with a dual fusion probe and analysed with a fluorescence microscope.

exhibited overexpression of ABCB1 or ABCG2 above levels in the Naïve control cell line (**Figure 5.15**). The V299L mutation did emerge again in both cell lines in 75nM DAS, accompanied by a significant decrease in BCR-ABL expression levels (**Figure 5.16**). To determine whether even earlier intermediates harboured the V299L clone at undetectable levels, frozen stocks of the 40nM DAS1 intermediate were thawed and re-escalated in dasatinib to 200nM. This cell line was named K562 Dox 200nM DAS RE40, and also did not express ABCB1 or ABCG2 above control levels (**Figure 5.15**). Once more, the V299L mutation emerged at the 75nM condition, and the familiar pattern of BCR-ABL expression decrease was observed (**Figure 5.17**).

It was clear that, under the selective pressure of dasatinib, the dasatinib-resistant V299L-carrying clone would always expand, as this mutation is known to confer dasatinib resistance[120,121]. To investigate whether a different mutation would arise under a different selective pressure, the 55nM DAS1 intermediate cells were then re-escalated in nilotinib (as the V299L mutation is thought to be sensitive to nilotinib[121]). Stocks of the 55nM DAS1 cells were thawed and immediately cultured in 200nM nilotinib, before being escalated every 10-15 days to 250nM, 350nM and finally 500nM. The nilotinib-resistant cell lines (named K562 Dox 500nM NIL1 RE55 and NIL2 RE55) did not exhibit ABCB1 or ABCG2 overexpression (**Figure 5.18**), nor did they carry the V299L mutation. The NIL1 RE55 cell line developed the G250E mutation in the 350nM nilotinib intermediate, which was again associated with a significant decrease in BCR-ABL expression (from 853% in the 200nM NIL1 intermediate to 669% in the 350nM NIL1 intermediate; $P<0.02$), while the NIL2 RE55 cell line did not carry any BCR-ABL KD mutations but rather had a significant increase in BCR-ABL expression (from 851% in the 55nM DAS intermediate to 1213% in the 200nM NIL2 intermediate; $P<0.04$) (**Figure 5.19**).

5.3.2.2 The K562 Dox 200nM DAS2 cell line

To determine if the V299L clone was present in the K562 Dox Naïve cell line (though undetectable by available sequencing methods), a second dasatinib-resistant culture was generated, and named K562 Dox 200nM DAS2. Again, these cells did not demonstrate any increased ABCB1 or ABCG2 expression (**Figure 5.20**) and interestingly, no kinase domain mutations were detected in any intermediates. Rather, the only apparent resistance mechanism was a significant increase in BCR-ABL expression from 176% in the K562 Dox Naïve cell line, to 512% in the K562 Dox 200nM DAS2 cell line ($P<0.00001$) (**Figure 5.21**).

Figure 5.15

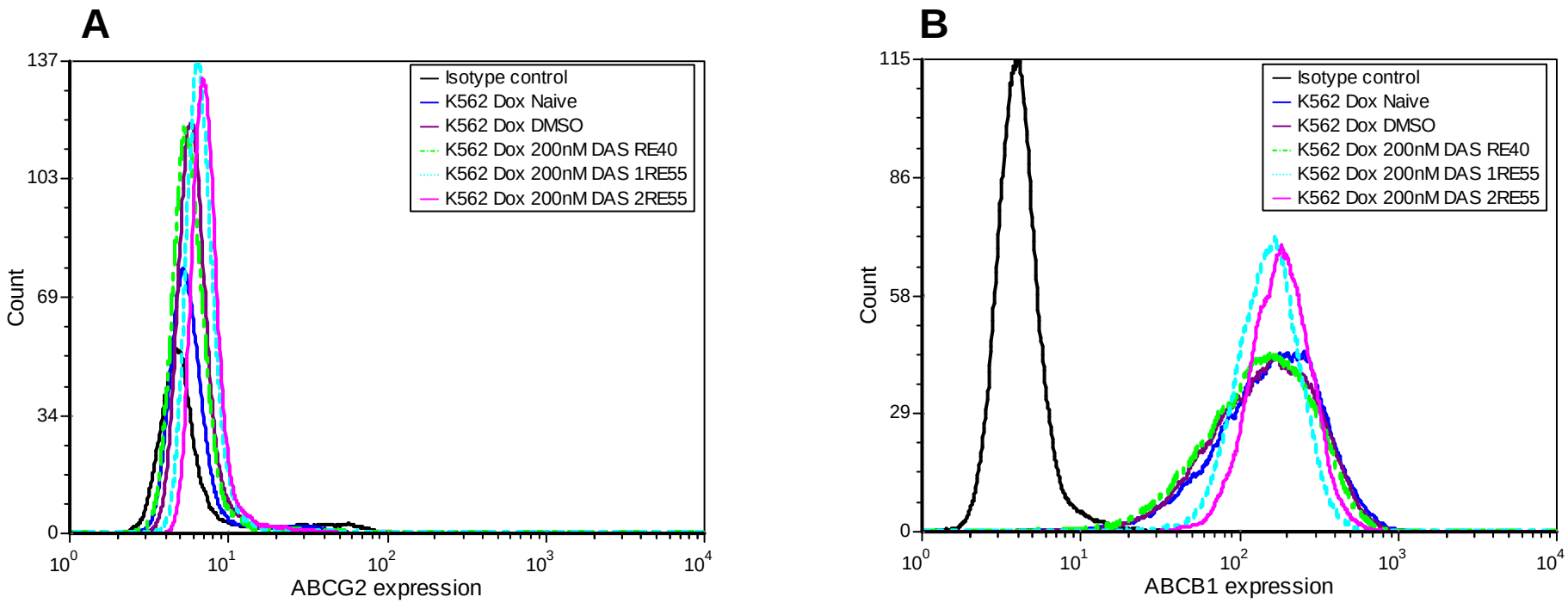

Figure 5.15: Cell surface expression of ABCB1 or ABCG2 in the K562 Dox 40nM and 55nM dasatinib re-escalation cell lines

K562 Dox Naïve, DMSO, 200nM DAS RE40, 200nM DAS 1RE55 and 200nM DAS 2RE55 cells were harvested and stained with either an isotype control antibody or the corresponding PE labelled ABCB1 or PE labelled ABCG2 antibody. After a 45 minute incubation with the antibody, the cells were washed and analysed by flow cytometry. Neither ABCG2 **(A)** nor ABCB1 **(B)** expression had increased in the dasatinib re-escalated cell lines compared to the Naïve or DMSO control cell lines. Histograms are representative of 3 experiments.

Figure 5.16

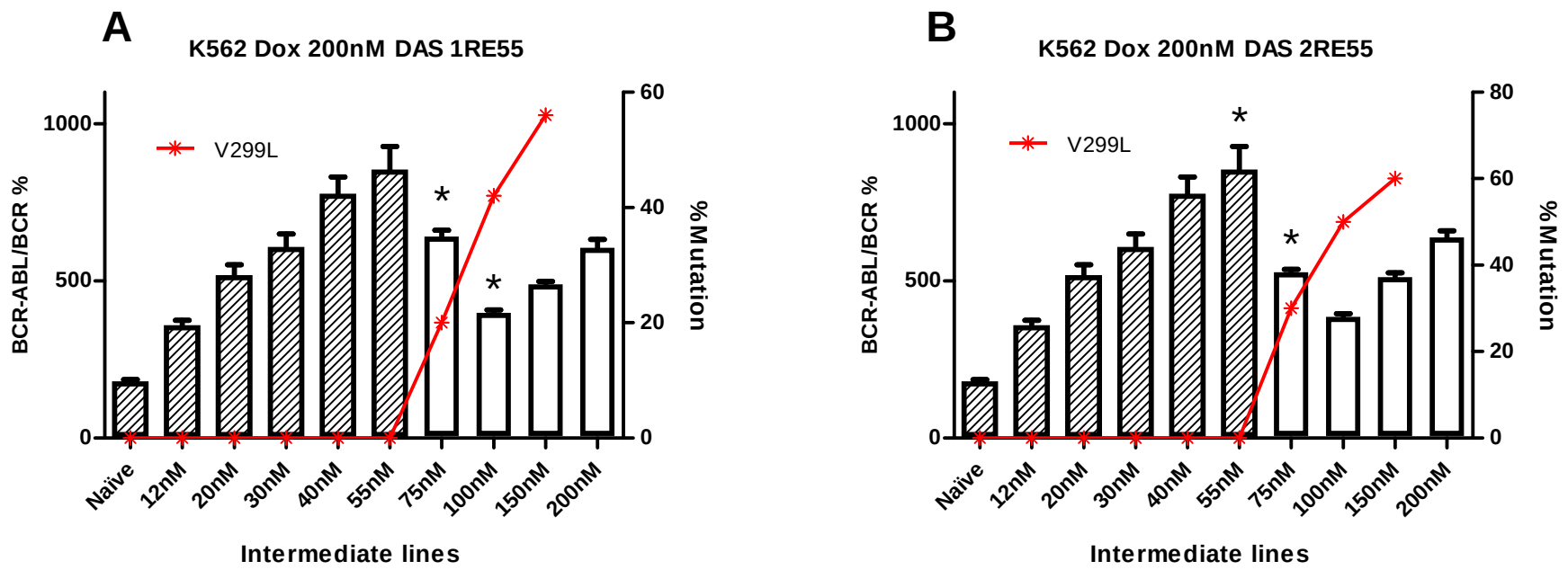

Figure 5.16: The V299L mutation emerged when the K562 Dox 55nM DAS1 intermediate was re-escalated in dasatinib
When the 55nM DAS intermediate of the K562 Dox 200nM DAS1 cell line was re-escalated in dasatinib, the V299L mutation again emerged as the dominant clone. The first re-escalation was named K562 Dox 200nM DAS 1RE55 **(A)**, and the second named K562 Dox 200nM DAS 2RE55 **(B)**. In both cases the emergence of the V299L mutation was accompanied by a significant decrease in BCR-ABL expression (*P<0.0005). BCR-ABL expression is plotted as a ratio of BCR expression % +SEM from at least 3 independent experiments. Patterned columns indicate results from the original K562 Dox 200nM DAS1 cell line (Figure 5.12) while white columns indicate results for the re-escalated cultures.

Figure 5.17

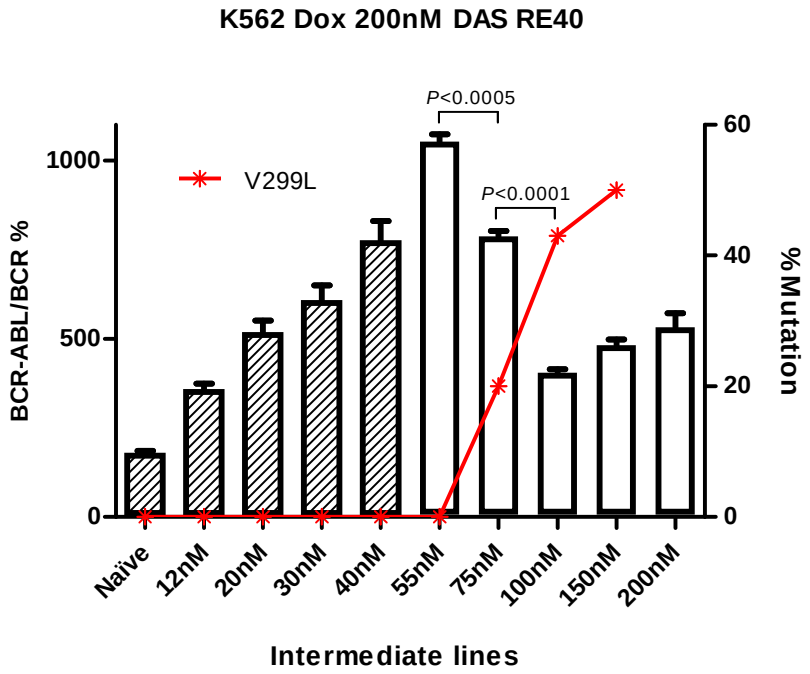

Figure 5.17: The V299L mutation emerged when the K562 Dox 40nM DAS1 intermediate was re-escalated in dasatinib
When the 40nM DAS intermediate of the K562 Dox 200nM DAS1 cell line was re-escalated in dasatinib, the V299L mutation again emerged (in the 75nM intermediate) as the dominant clone. Furthermore, the emergence of the V299L mutation was again accompanied by a significant decrease in BCR-ABL expression. BCR-ABL expression is plotted as a ratio of BCR expression % +SEM from at least 3 independent experiments. Patterned columns indicate results from the original K562 Dox 200nM DAS1 cell line (Figure 5.12) while white columns indicate results for the re-escalated cultures.

Figure 5.18

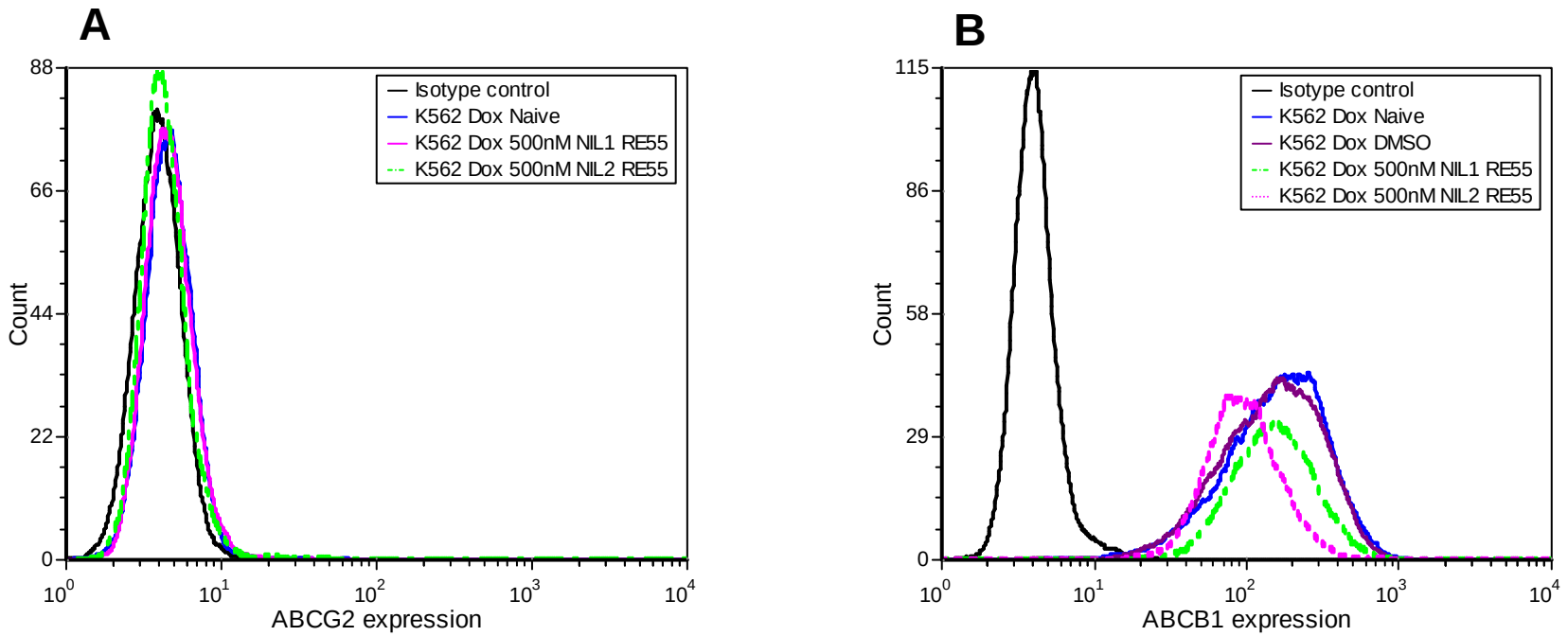

Figure 5.18: There was no change in cell surface expression of ABCB1 or ABCG2 in the K562 Dox 500nM NIL re-escalation cell lines

K562 Dox Naïve, DMSO, 500nM NIL1 RE55 and 500nM NIL2 RE55 cells were harvested and stained with either an isotype control antibody or the corresponding PE labelled ABCB1 or PE labelled ABCG2 antibody. After a 45 minute incubation with the antibody, the cells were washed and analysed by flow cytometry. Neither ABCG2 **(A)** nor ABCB1 **(B)** expression had increased in the nilotinib re-escalated cell lines compared to the Naïve or DMSO controls. Histograms are representative of 3 experiments.

Figure 5.19

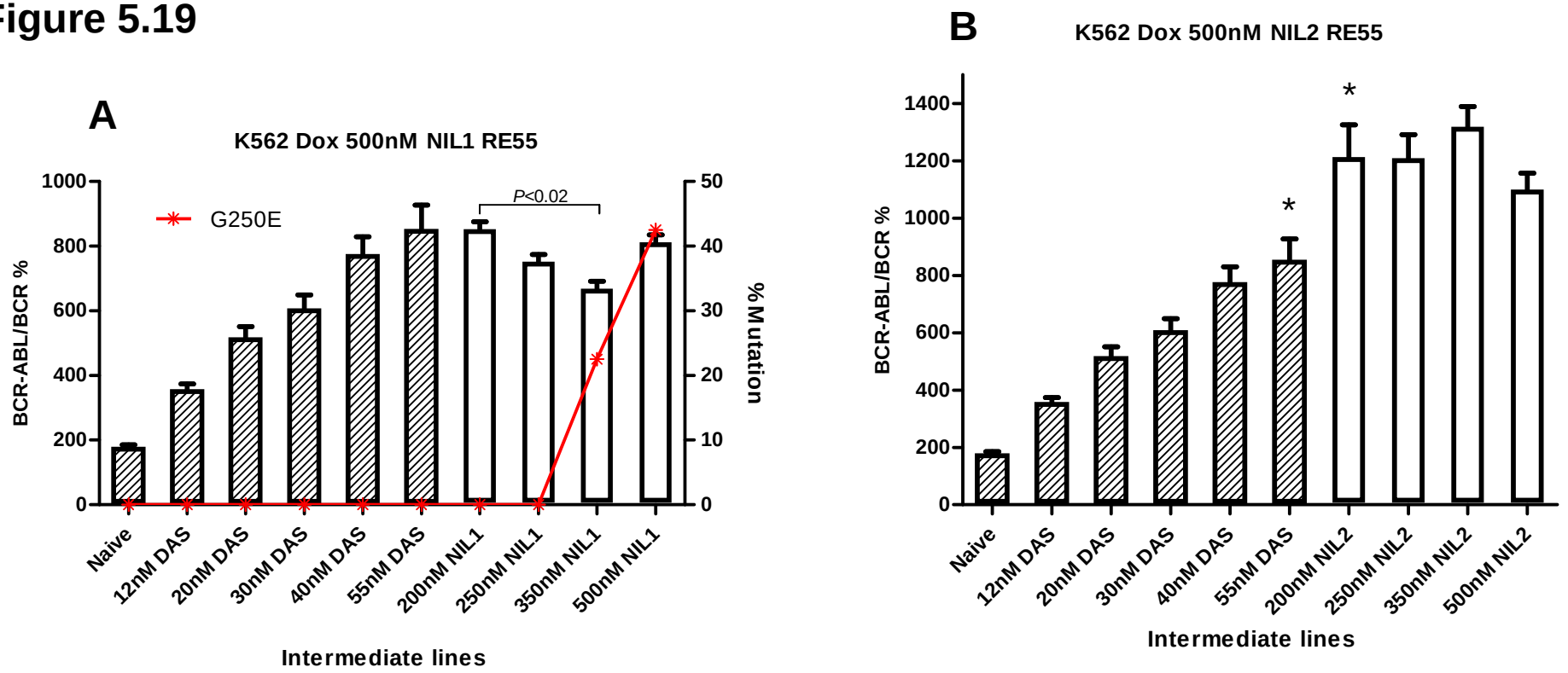

Figure 5.19: Re-escalation of the K562 Dox 55nM intermediate in NIL resulted in the emergence of the G250E mutation or increased BCR-ABL expression

Two nilotinib resistant cell lines were generated by re-escalating the K562 Dox 55nM DAS1 intermediate, and named K562 Dox 500nM NIL1 RE55 and NIL2 RE55 respectively. In the NIL1 cell line, the G250E mutation emerged **(A)**, while in the NIL2 cell line there was no KD mutation but instead a significant increase in BCR-ABL expression (**P*<0.04) **(B)**. BCR-ABL expression is plotted as a ratio of BCR expression % +SEM from at least 3 independent experiments. Patterned columns indicate results from the original K562 Dox 200nM DAS1 cell line (Figure 5.12) while white columns indicate results for the re-escalated cultures.

Figure 5.20

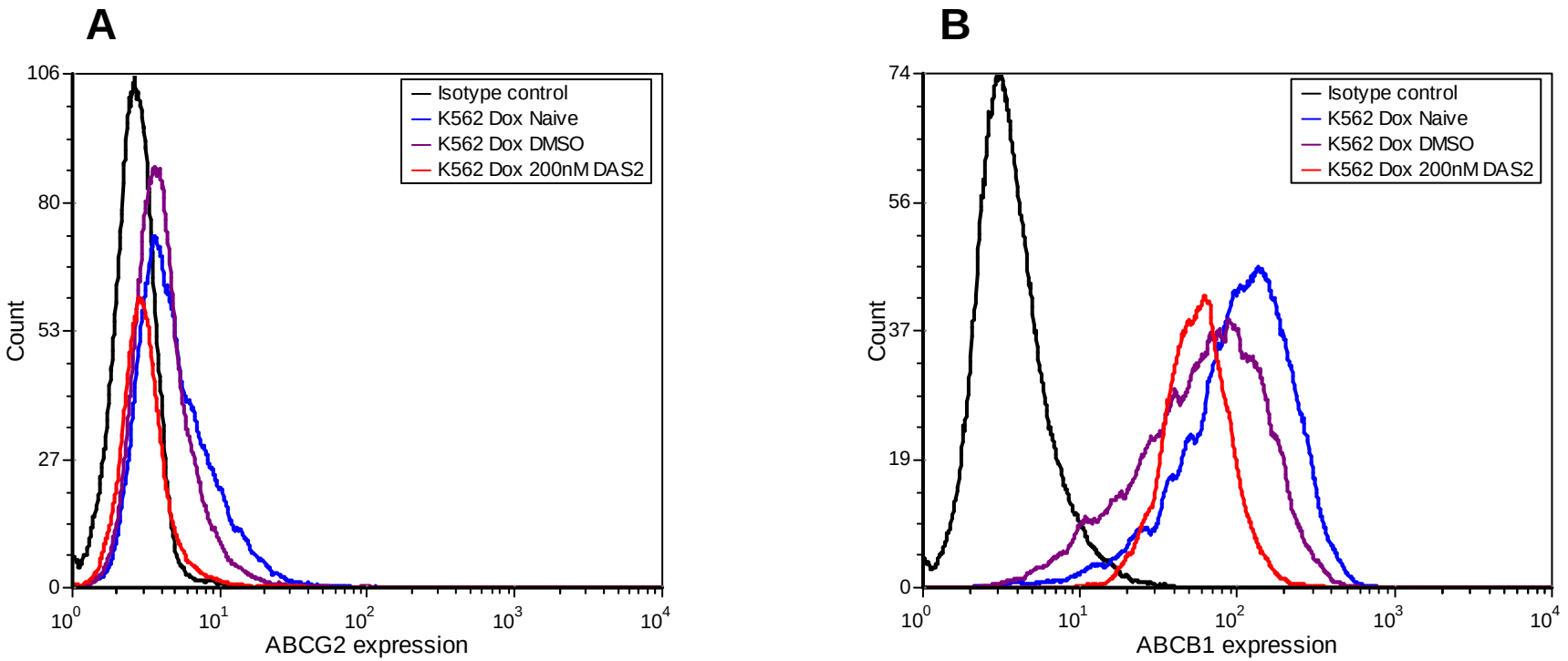

Figure 5.20: Cell surface expression of ABCB1 or ABCG2 in the K562 Dox 200nM DAS2 cell line
K562 Dox Naïve, DMSO and 200nM DAS2 cells were harvested and stained with either an isotype control antibody or the corresponding PE labelled ABCB1 or PE labelled ABCG2 antibody. After a 45 minute incubation with the antibody, the cells were washed and analysed by flow cytometry. Neither ABCG2 **(A)** nor ABCB1 **(B)** expression had increased in the K562 Dox 200nM DAS2 cell line. Histograms are representative of 3 experiments.

Figure 5.21

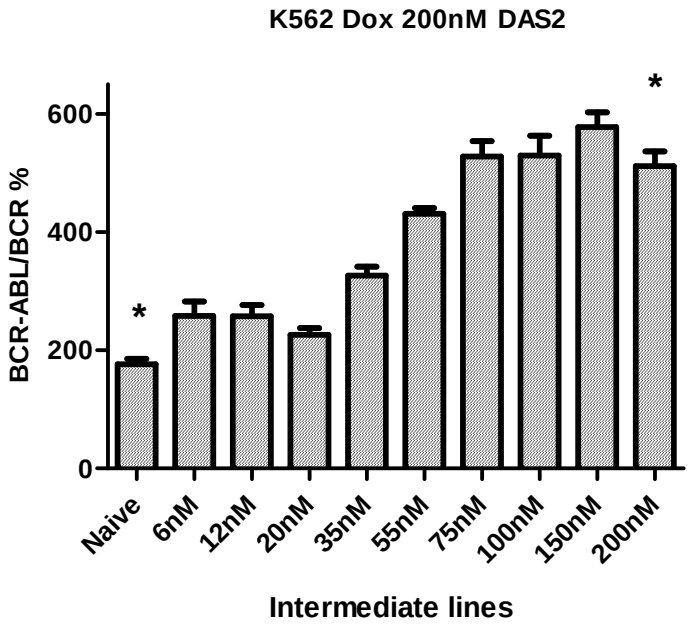

Figure 5.21: Intermediate BCR-ABL expression levels in the K562 Dox 200nM DAS2 cell line

BCR-ABL expression increased significantly as dasatinib concentration was escalated in the K562 Dox 200nM DAS2 cell line (**P*<0.00001). Unlike the DAS1 cell line, no BCR-ABL KD mutations emerged in the DAS2 cell line. Samples were taken at intermediate stages of resistance development, and cDNA was synthesised using the RNA extracted from 1×10^7 cells. RQ-PCR was conducted using cDNA as the template, and BCR-ABL expression was determined as a ratio of BCR expression. Data are presented as mean +SEM from at least 3 independent experiments.

5.3.3 Imatinib-resistance in KU812 cell lines

Imatinib resistance generation in the K562 and K562 Dox cell lines only took ~6 months and ~4 months respectively, however, the KU812 cell line was noticeably more sensitive, taking an average of 9 months to become resistant to 2µM IM. Furthermore, when dasatinib cultures of KU812 cells were initiated, drug concentration could not be escalated above 1nM, and proliferation was noticeably slowed. This TKI-sensitivity is likely due to the fact that the KU812 cell line is known to only harbour two copies of BCR-ABL, while the K562 cell line has in excess of 20 copies[230]. Therefore, in contrast to the KU812 cell line, the increased BCR-ABL expression in both the K562 and the derivative K562 Dox cell line (which also has ABCB1 overexpression) result in intrinsic TKI resistance, enabling escalation in dasatinib and faster resistance development in imatinib. This may explain why previous studies have failed to generate TKI resistance in the KU812 cell line[127,164]. In this study three imatinib-resistant KU812 cell lines were established, namely KU812 2µM IM1, IM2 and IM3.

5.3.3.1 The KU812 2µM IM1 cell line

Imatinib resistance was generated in the KU812 cell line to compare modes of imatinib-resistance with the K562 and K562 Dox cell lines. The KU812 2µM IM1 cell line was found to not have any ABCB1 overexpression, but flow cytometry indicated a very slight increase in ABCG2 expression (x-mean increased from 0.97 in the Naïve control to 2.18) (**Figure 5.22**). To determine whether this minimal increase was functionally relevant and contributing to imatinib resistance, IUR assays were conducted. Imatinib IUR was not significantly different in the presence of 1µM imatinib (9.7ng and 10.2ng imatinib per 200,000 cells in the Naïve and IM-resistant cell line respectively) or 2µM imatinib (20.2ng and 20.7ng imatinib in 200,000 cells in the Naïve and IM-resistant cell line respectively) (**Figure 5.23**). Furthermore, there was no significant difference in imatinib accumulation when cells were incubated with the ABCG2 inhibitor, Ko143, and there was no significant difference in OCT-1 activity (**Figure 5.23**). This indicated that neither the IM-Naïve nor the IM-resistant cell lines had any functional ABCG2, and that imatinib influx and efflux was not playing a role in IM-resistance.

RQ-PCR was conducted with available intermediate samples, revealing that BCR-ABL expression had significantly increased from 443% in the KU812 Naïve cell line to 5860% in the 600nM intermediate (P<0.0002), after which BCR-ABL mRNA reached a plateau of approximately 6000% (**Figure 5.24**).

Figure 5.22

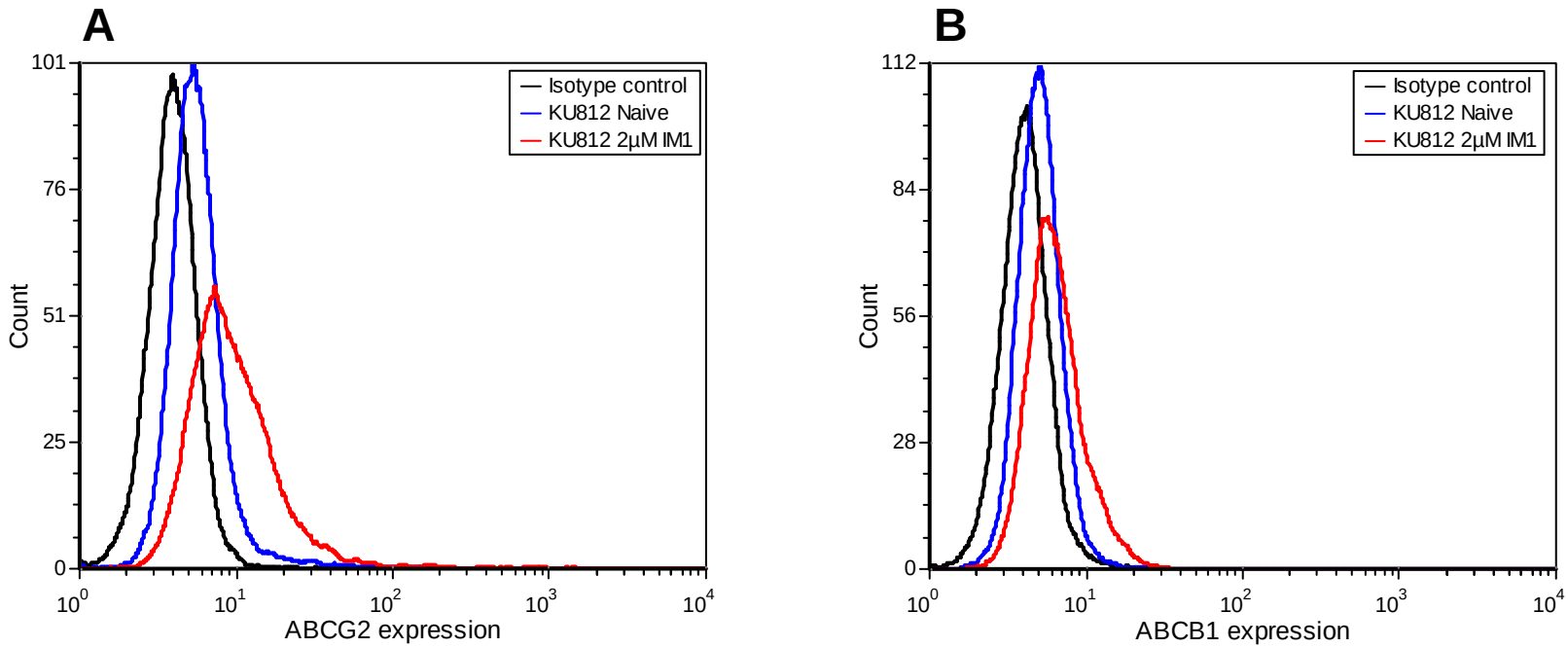

Figure 5.22: Cell surface expression of ABCB1 and ABCG2 in the KU812 2µM IM1 cell line
KU812 Naive and KU812 2µM IM1 cells were harvested and stained with either an isotype control antibody or the corresponding PE labelled ABCB1 or PE labelled ABCG2 antibody. After a 45 minute incubation with the antibody, the cells were washed and analysed by flow cytometry. **(A)** Minimal ABCG2 expression was detected (x-mean increased from 0.97 in the Naïve control to 2.18 in the KU812 2µM IM1 cell line). **(B)** No ABCB1 expression was detected. Histograms are representative of 3 experiments.

Figure 5.23

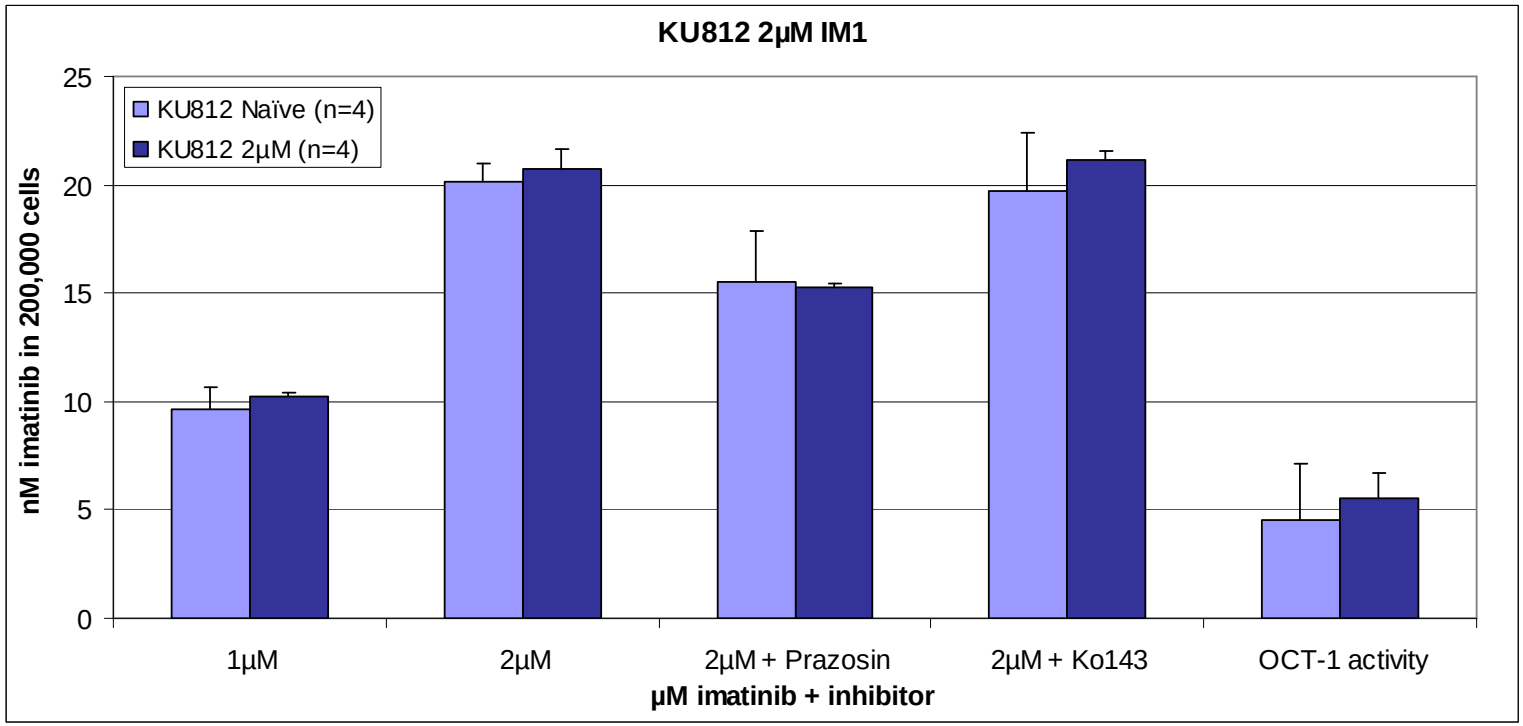

Figure 5.23: The imatinib IUR in the KU812 2µM IM1 cell line was not significantly different from the KU812 Naïve cell line, and was not affected by blocking ABCG2

The IUR assay was performed as previously described[172]. Ko143 (0.5µM) inhibits ABCG2, while prazosin (100µM) is a potent inhibitor of OCT-1. OCT-1 activity is calculated by subtracting the IUR in the presence of prazosin from the IUR in the absence of prazosin. The IM1-resistant cell line had neither a decreased IUR, nor a decreased OCT-1 activity compared to the KU812 Naïve control cell line. Furthermore, blocking ABCG2 did not result in an increased IUR for either cell line, indicating imatinib efflux by ABCG2 was not facilitating resistance. Data are presented as mean +SD calculated from four independent experiments.

Figure 5.24

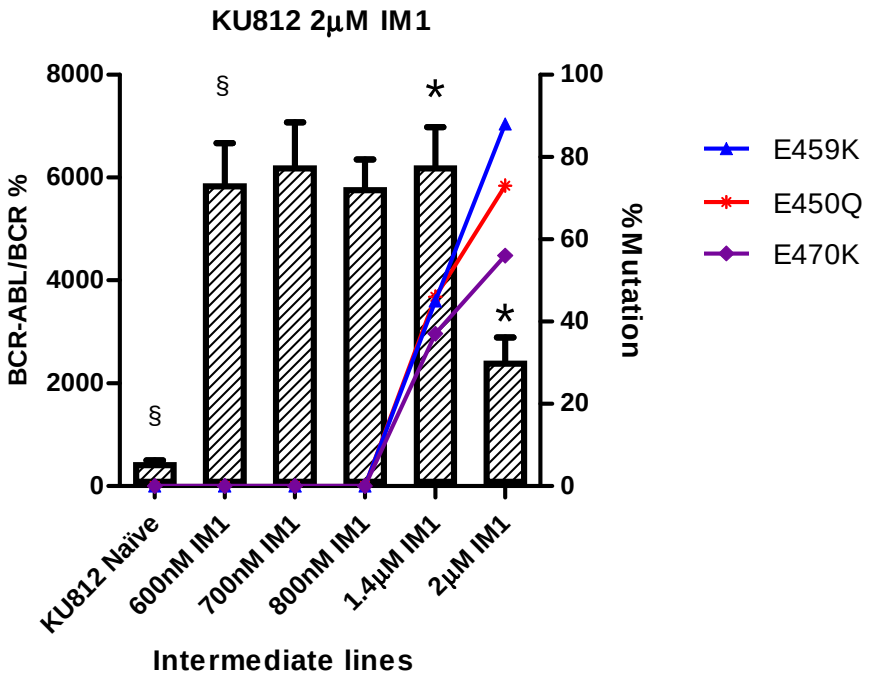

Figure 5.24: BCR-ABL expression increased until the emergence of three KD mutations in the KU812 2µM IM1 cell line
BCR-ABL mRNA expression levels significantly increased in the KU812 2µM IM1 cell line compared to the KU812 Naive cell line as imatinib concentration was escalated ($^{\S}P<0.0002$). Expression levels then significantly dropped coinciding with the appearance of the E459K, E450Q and E470K mutations (*$P<0.004$). BCR-ABL expression is plotted as a ratio of BCR expression % +SEM from at least 3 independent experiments. Conventional sequencing was used to determine the mutation status of the kinase domain of BCR-ABL.

Following the emergence of three kinase domain mutations (E459K, E450Q and E470K), BCR-ABL mRNA levels significantly decreased to 2414% (P<0.004). Bcr-Abl DNA copy number (with respect to the GUSB control gene) increased from 128% in the KU812 Naïve cell line, to 2426% in the KU812 2µM IM1 cell line - mirroring BCR-ABL mRNA levels (**Figure 5.25**).

To determine the mode of Bcr-Abl DNA amplification, karyotyping and FISH was conducted. The KU812 Naive cell line did not have any homogeneously staining regions or dmin (**Figure 5.26**) and confirmed that the karyotype had changed very little from the originally established KU812 cell line (**Figure 5.1**) despite over 100 passages. In contrast, the heterogeneous KU812 2µM IM1 population had a variable karyotype, with abnormalities of ploidy and additional structural rearrangements (**Figure 5.27**). Of note was the presence of dmin, which are observed in various human cancers and frequently carry oncogenes[146,148-150]. To determine whether the dmin in the KU812 2µM IM1 cell line harboured additional copies of Bcr-Abl, FISH was conducted. It was found that the KU812 2µM IM1 cell line had many more positive signals for BCR and ABL, which co-localised and indicated numerous copies of Bcr-Abl (**Figure 5.28**). Thus, the small, acentric fragments of DNA (dmin) were shown to carry Bcr-Abl and were therefore considered responsible for BCR-ABL overexpression.

5.3.3.2 The KU812 3µM IM2 cell line

A second imatinib-resistant KU812 cell line was generated and named KU812 3µM IM2. At the 2µM IM2 intermediate, sequencing and RQ-PCR showed that several kinase domain mutations had emerged, but that BCR-ABL expression had steadily increased and remained high (from ~440% in KU812 Naïve cells, to over 10,000% in the KU812 3µM IM2 cell line) (**Figure 5.29**). Previously, in the K562 200nM DAS cell line, the K562 Dox 200nM DAS1 cell line (and its dasatinib and nilotinib re-escalations) and the KU812 2µM IM1 cell line, KD mutation emergence was always accompanied by a significant decrease in BCR-ABL expression (**Figure 5.8, 5.12, 5.16, 5.17, 5.19 & 5.24**). To determine whether BCR-ABL expression levels in the KU812 2µM IM2 intermediate cell line would eventually decrease since KD mutations had emerged, this cell line was further escalated in imatinib to 3µM. It was found that BCR-ABL expression levels in the 2.5µM IM2 intermediate had indeed significantly decreased to 5266% (P<0.008), while the percentage of the E459K mutation continued to rise to 90% (**Figure 5.29**).

Figure 5.25

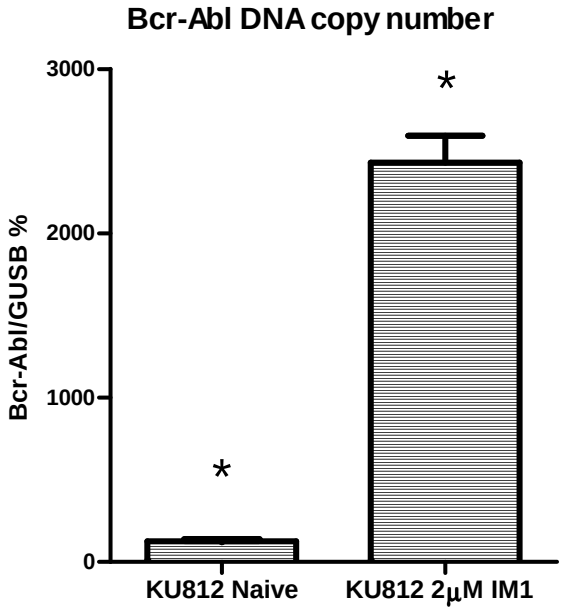

Figure 5.25: Bcr-Abl DNA copy number was significantly increased in the KU812 2μM IM1 cell line compared to the KU812 Naïve cell line

Bcr-Abl copy number (with respect to the GUSB control gene) was significantly increased in the IM-resistant cell line (**P*<0.00001). DNA was extracted from the three cell lines using a High Pure PCR Template Preparation Kit (Roche Diagnostics, Mannheim, Germany). The DNA was used as a template in quantitative DNA PCR, performed in duplicate for each experiment. Data are presented as mean +SD from at least 3 independent experiments.

Figure 5.26

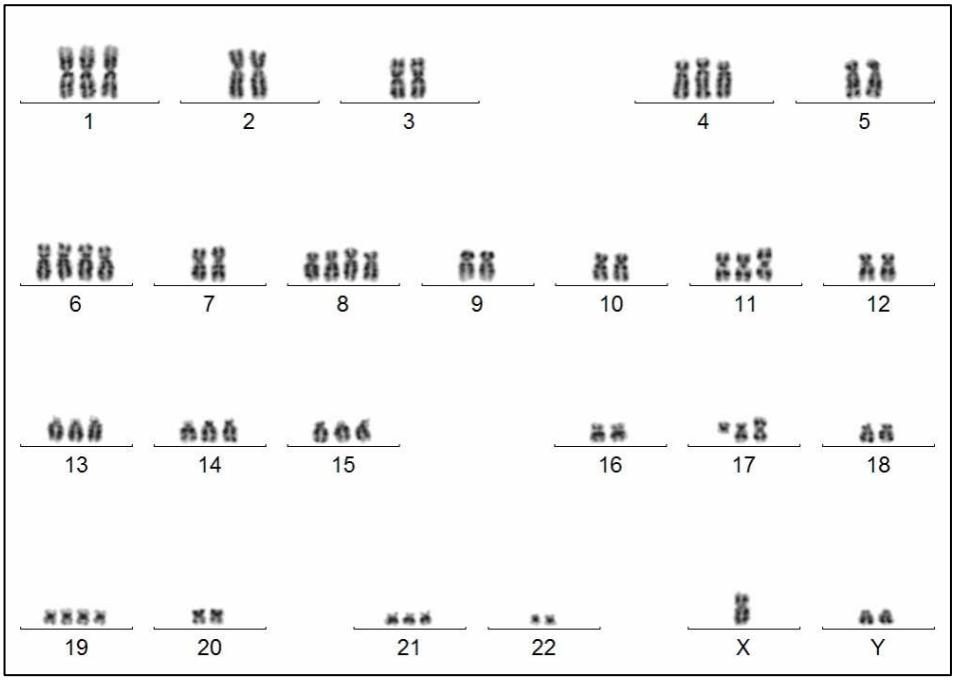

Figure 5.26: Karyotype of the KU812 Naïve cell line
Karyotype of the KU812 Naïve cell line after ~50 passages in our laboratory. The cell line showed a fairly constant, near triploid karyotype: 61,XYY,-2,-3,add(4)(p11),-5,+6,-7,+8,-9,t(9;22)(q34;q11.2) x2,-10,i(11) (q10),-12, 16,del(17)(q11.2q24),i(17)(q10), -18,+19,-20,-22
This karyotytpe is consistent with the originally published KU812 karyotype (see Figure 5.1). Karyotyping conducted by Sarah Moore.

Figure 5.27

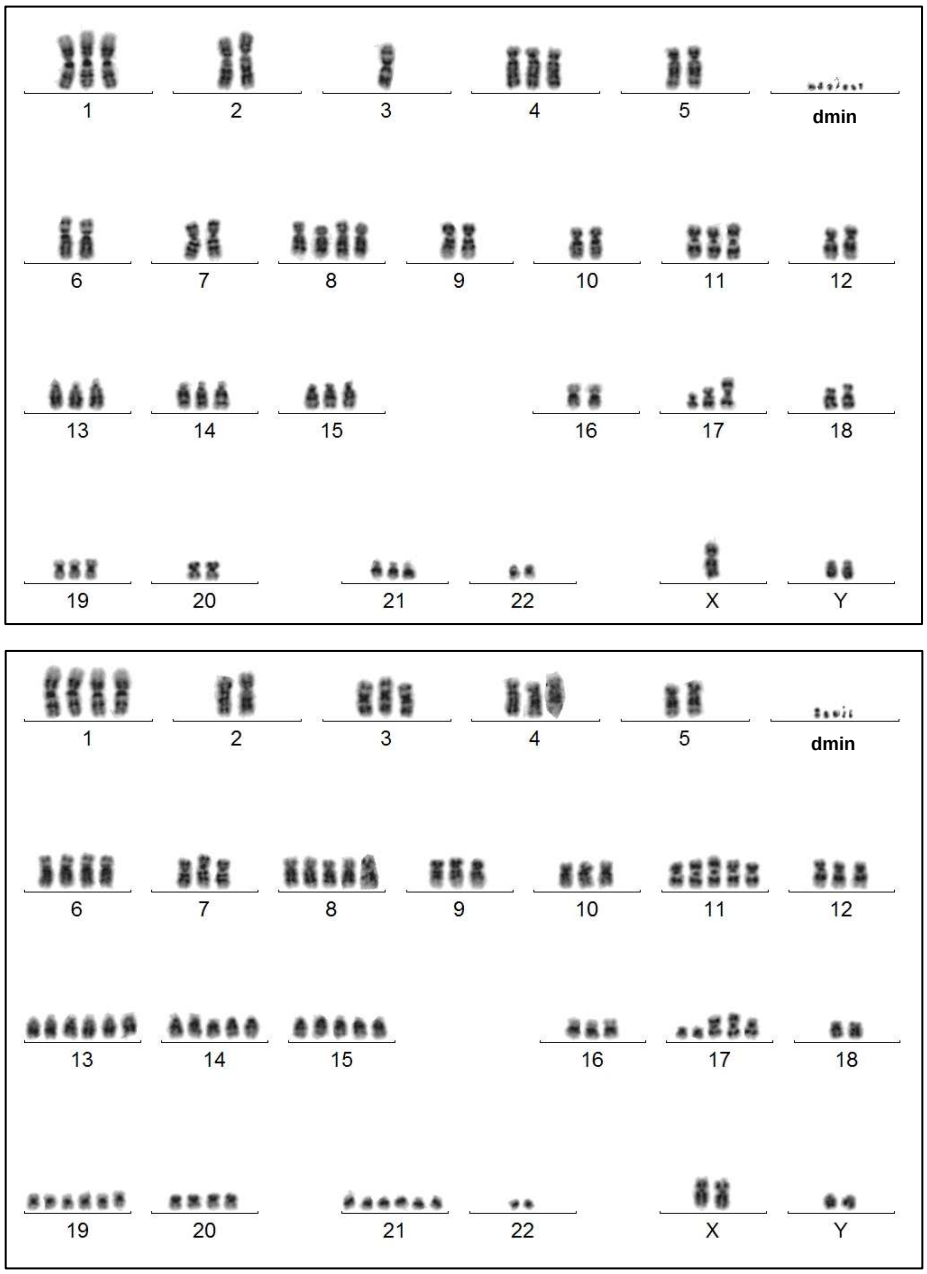

Figure 5.27: Karyotypes of the heterogeneous KU812 2μM IM1 population
These cells showed a variable karyotype, with abnormalities of ploidy and additional structural rearrangements including double minutes (dmin): 57~118<3n>,XYY,-2,-3,-4,-5,+6,-7,+8,-9,t(9;22)(q34;q11.2)x2,-10, i(11)(q10),-12,-16, del(17)(q11.2q24),i(17)(q10),-18,+19,-20,-22, +5~8dmin[cp]/57~58, idem,der(?)t(21;?)(q11;?). Two example karyotypes are shown. Karyotyping conducted by Sarah Moore.

Figure 5.28

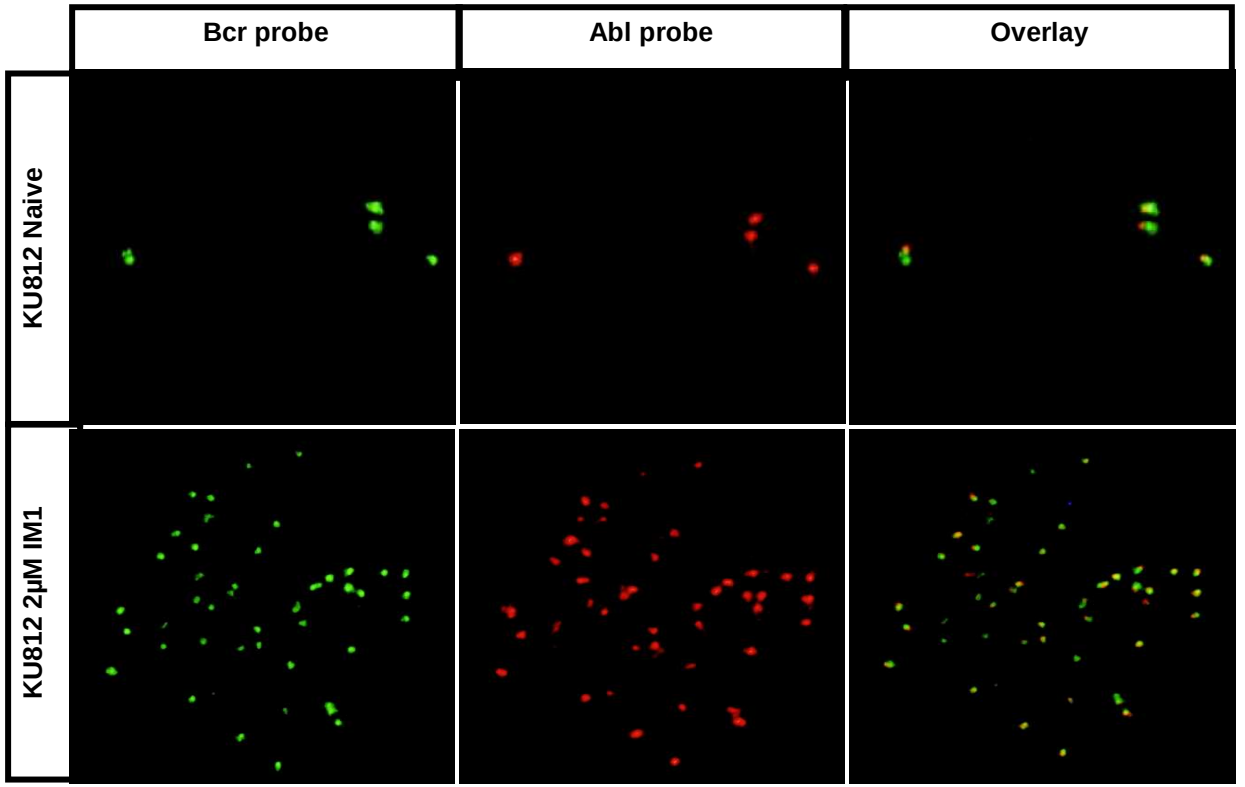

Figure 5.28: Interphase FISH to identify Bcr-Abl fusion genes
Shown above is a single, representative KU812 Naïve cell (top panel) and a single KU812 2µM IM1 cell (bottom panel). Bcr-Abl amplification in the KU812 2µM IM1 cell line is evident due to numerous co-localising Bcr (green) and Abl (red) signals, seen in the 'Overlay' panel. This indicates that the dmin (identified by karyotyping) carry Bcr-Abl. 1×10^6 cells were harvested from culture and incubated in 100µL colcemid before being fixed onto glass slides. After RNase treatment, cells were probed with a dual fusion probe and analysed with a fluorescence microscope.

Figure 5.29

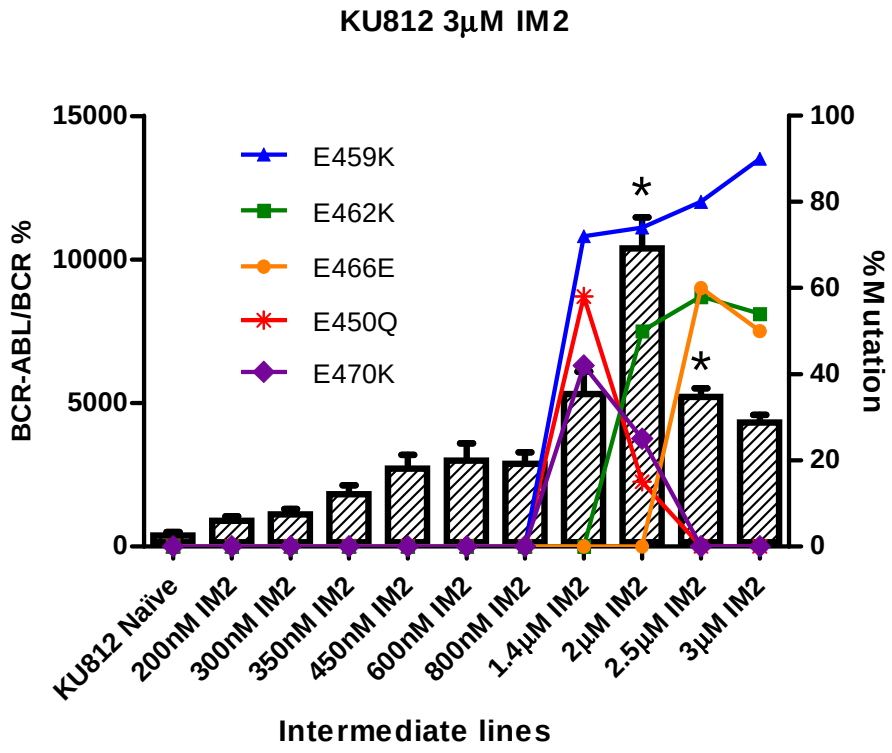

Figure 5.29: BCR-ABL expression and KD mutation status in the KU812 3µM IM2 cell line
BCR-ABL expression levels increased gradually, peaking in the 2µM intermediate at ~10,450%. BCR-ABL expression then significantly decreased to ~5,265% (*P<0.008), accompanied by the expansion of multiple KD mutant clones. BCR-ABL expression is plotted as a ratio of BCR expression % +SEM from at least 3 independent experiments. Conventional sequencing was used to determine the mutation status of the kinase domain of BCR-ABL.

Bcr-Abl DNA copy number had significantly increased in the KU812 3µM IM2 cell line (1732%) compared to the KU812 Naïve control (125%) (*P*<0.00001) (**Figure 5.30**). Furthermore, FISH results indicated multiple copies of the Bcr-Abl gene (**Figure 5.31**). This may again be evidence for the presence of dmin which are carrying the Bcr-Abl oncogene. Lastly, overexpression of ABCB1 and ABCG2 could be excluded as a resistance mechanism in the KU812 3µM IM2 cell line by flow cytometry (**Figure 5.32**).

5.3.3.3 The KU812 2µM IM3 cell line

In both the KU812 2µM IM1 and IM2 cell lines, the E459K, E450Q and E470K mutations emerged, and the E459K mutation reached approximately 90% in both cell lines (**Figure 5.24 & 5.29**). To determine whether these mutations were predisposed to emerge in the KU812 cell line, a third IM-resistant culture was established and named KU812 2µM IM3. Again, as with the previous IM-resistant KU812 cell lines, no ABCB1 or ABCG2 cell surface expression was detected (**Figure 5.33**), excluding drug efflux as a resistance mechanism. Instead, BCR-ABL expression levels steadily increased with imatinib concentration escalation, peaking at 990% in the 200nM IM3 intermediate before significantly decreasing to a plateau of approximately 660% in the 300nM IM3 intermediate (*P*<0.005)(**Figure 5.34**). Interestingly, this drop in BCR-ABL expression coincided with the appearance of the F359C KD mutation in the 300nM IM3 intermediate. The percentage of F359C mutation with respect to total BCR-ABL transcript reached 100% in the 2µM IM3 culture (**Figure 5.34**).

To determine whether the increase in BCR-ABL mRNA expression in the 200nM IM3 intermediate was mediated by an increased Bcr-Abl DNA copy number, quantitative DNA PCR was conducted. Strikingly, there was no significant difference in Bcr-Abl copy number when comparing the KU812 Naïve control (94%), the 200nM IM3 (86%) and 300nM IM3 (94%) intermediates, and the 2µM IM3 cell cultures (90%)(**Figure 5.35**). This was confirmed by FISH, as there were consistently only four overlaying Bcr and Abl signals in the KU812 Naïve cell line, and in the 200nM IM3, 300nM IM3 and 2µM IM3 cultures (**Figure 5.36**). Of the four signals, two represent the two copies of Bcr-Abl (the t(9:22) translocation) that the KU812 cell line is known to harbour[230], while the other two signals represent the reciprocal translocation (two copies of *der* 9).

Figure 5.30

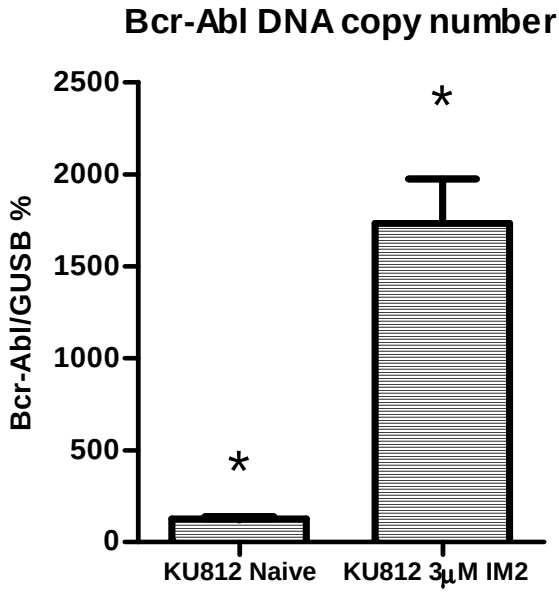

Figure 5.30: Bcr-Abl DNA copy number was significantly increased in the KU812 3µM IM2 cell line compared to the KU812 Naïve cell line
Bcr-Abl copy number (with respect to the GUSB control gene) was significantly increased in the KU812 3µM IM2 cell line (*P<0.00001). DNA was extracted from the three cell lines using a High Pure PCR Template Preparation Kit (Roche Diagnostics, Mannheim, Germany). The DNA was used as a template in quantitative DNA PCR, performed in duplicate for each experiment. Data are presented as mean +SD from at least 3 independent experiments.

Figure 5.31

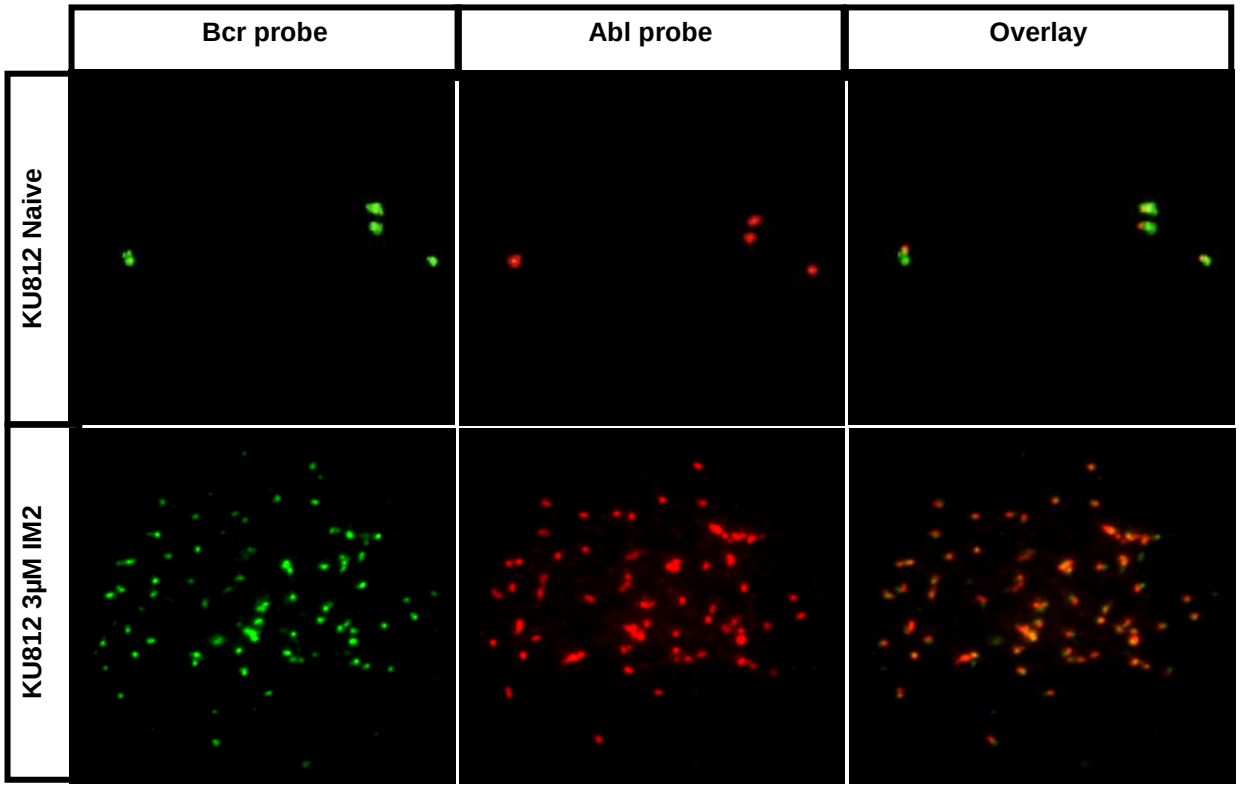

Figure 5.31: Interphase FISH to identify Bcr-Abl fusion genes
Shown above is a single, representative KU812 Naïve cell (top panel) and a single KU812 3µM IM2 cell (bottom panel). Bcr-Abl amplification in the IM-resistant cell line is evident due to numerous co-localising Bcr (green) and Abl (red) signals, seen in the 'Overlay' panel. 1×10^6 cells were harvested from cell cultures and incubated in 100µL colcemid before being fixed onto glass slides. After RNase treatment, cells were probed with a dual fusion probe and analysed with a fluorescence microscope.

Figure 5.32

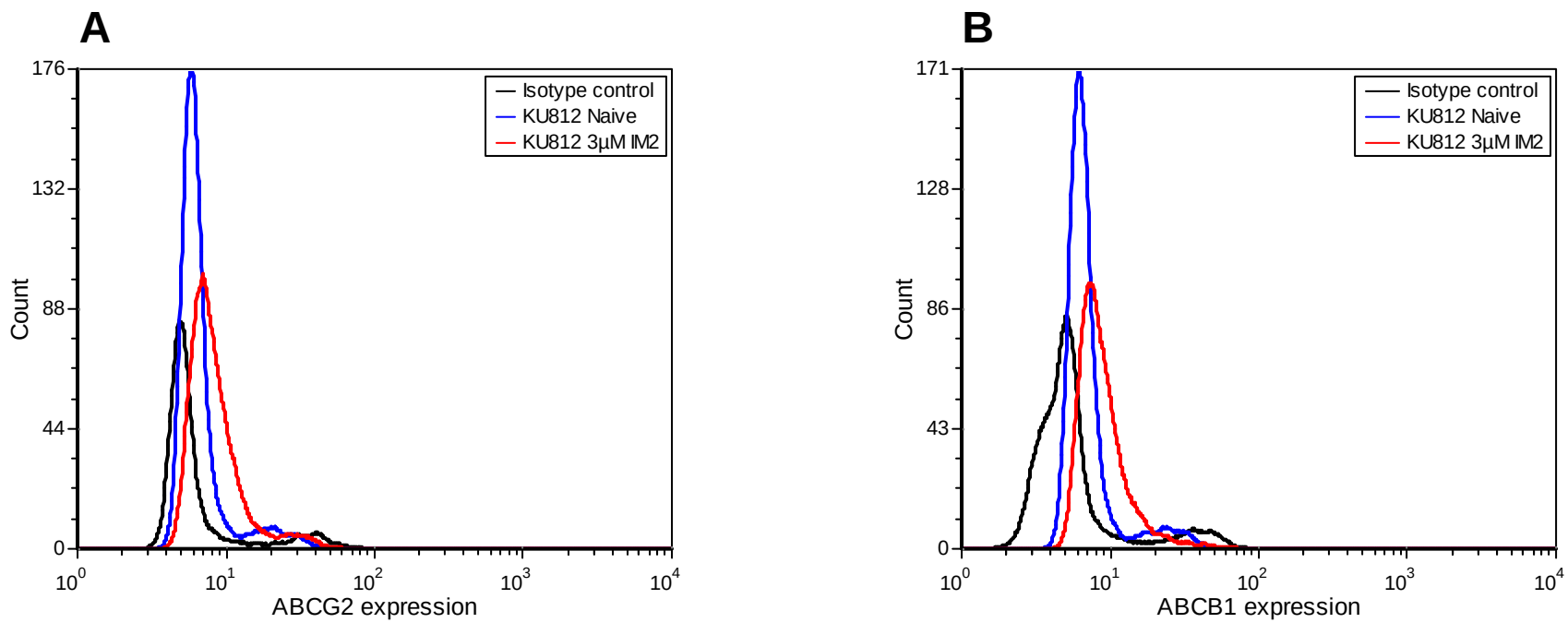

Figure 5.32: Cell surface expression of ABCB1 and ABCG2 in the KU812 3µM IM2 cell line
KU812 Naïve and KU812 3µM IM2 cells were harvested and stained with either an isotype control antibody or the corresponding PE ABCB1 or PE ABCG2 antibody. After a 45 minute incubation with the antibody, the cells were washed and analysed by flow cytometry. Neither ABCG2 **(A)** nor ABCB1 **(B)** expression could be detected in the KU812 3µM IM2 cell line. Histograms are representative of 3 experiments.

Figure 5.33

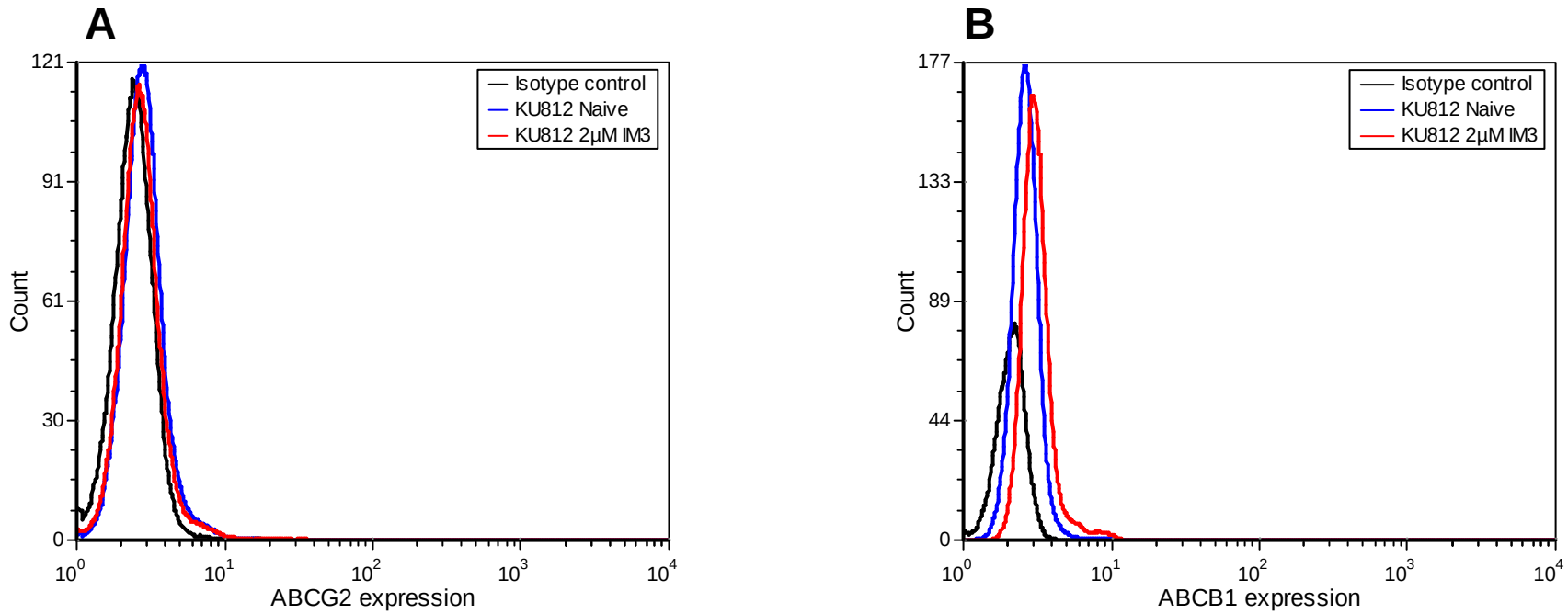

Figure 5.33: Cell surface expression of ABCB1 and ABCG2 in the KU812 2µM IM3 cell line
KU812 Naive and KU812 2µM IM3 cells were harvested and stained with either an isotype control antibody or the corresponding PE labelled ABCB1 or PE labelled ABCG2 antibody. After a 45 minute incubation with the antibody, the cells were washed and analysed by flow cytometry. Neither ABCG2 **(A)** nor ABCB1 **(B)** expression could be detected in the KU812 2µM IM3 cell line. Histograms are representative of 3 experiments.

Figure 5.34

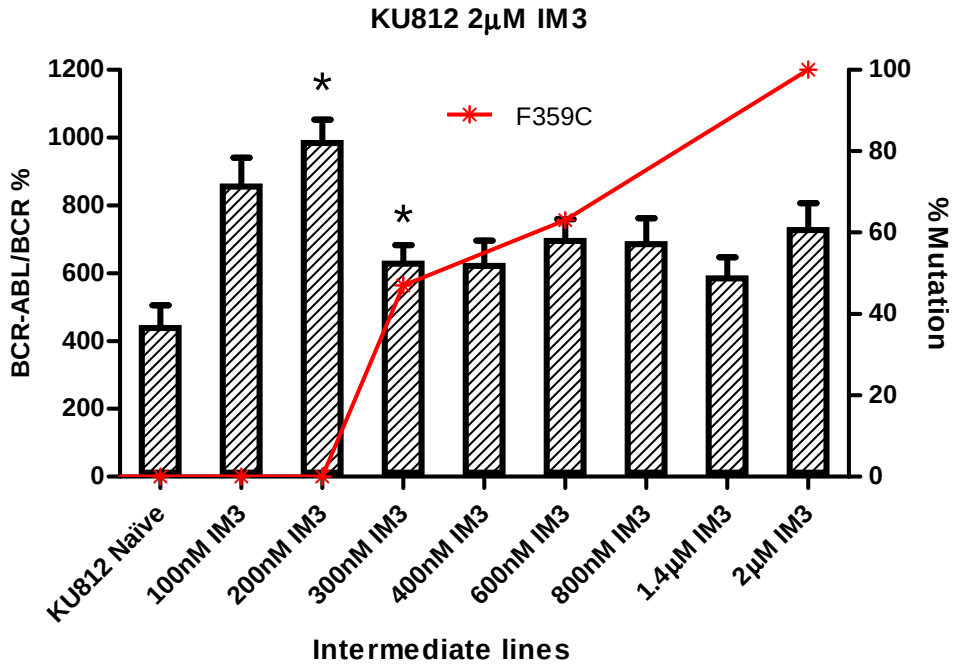

Figure 5.34: BCR-ABL expression increased until the emergence of the F359C mutation KU812 2µM IM3 cell line
BCR-ABL expression levels increased gradually in the KU812 2µM IM3 cell line, peaking in the 200nM intermediate at ~990%. Expression levels then significantly dropped (*P<0.005) coinciding with the appearance of the F359C mutation. Neither conventional sequencing nor MassARRAY analysis could detect the mutation in the 200nM IM3 intermediate. After the emergence of the F359C mutation, BCR-ABL expression levels reached a plateau. BCR-ABL expression is plotted as a ratio of BCR expression % +SEM from at least 3 independent experiments.

Figure 5.35

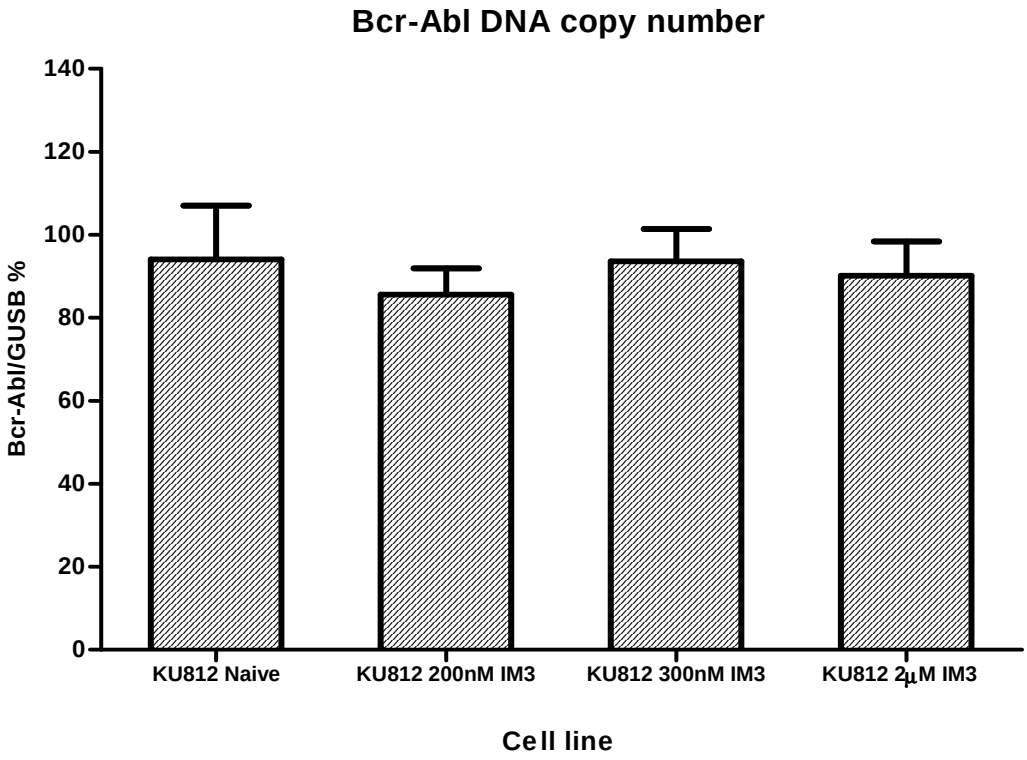

Figure 5.35: Bcr-Abl DNA copy number did not significantly change in the KU812 2μM IM3 intermediates or final cell line compared to the KU812 Naïve cell line

Bcr-Abl copy number (with respect to the GUSB control gene) was not significantly different to the KU812 Naïve control cell line in either the 200nM intermediate, 300nM intermediate, or in the final 2μM IM3 cell line. DNA was extracted using a High Pure PCR Template Preparation Kit (Roche Diagnostics, Mannheim, Germany). The DNA was used as a template in quantitative DNA PCR, performed in duplicate for each experiment. Data are presented as mean +SD from at least 3 independent experiments.

Figure 5.36

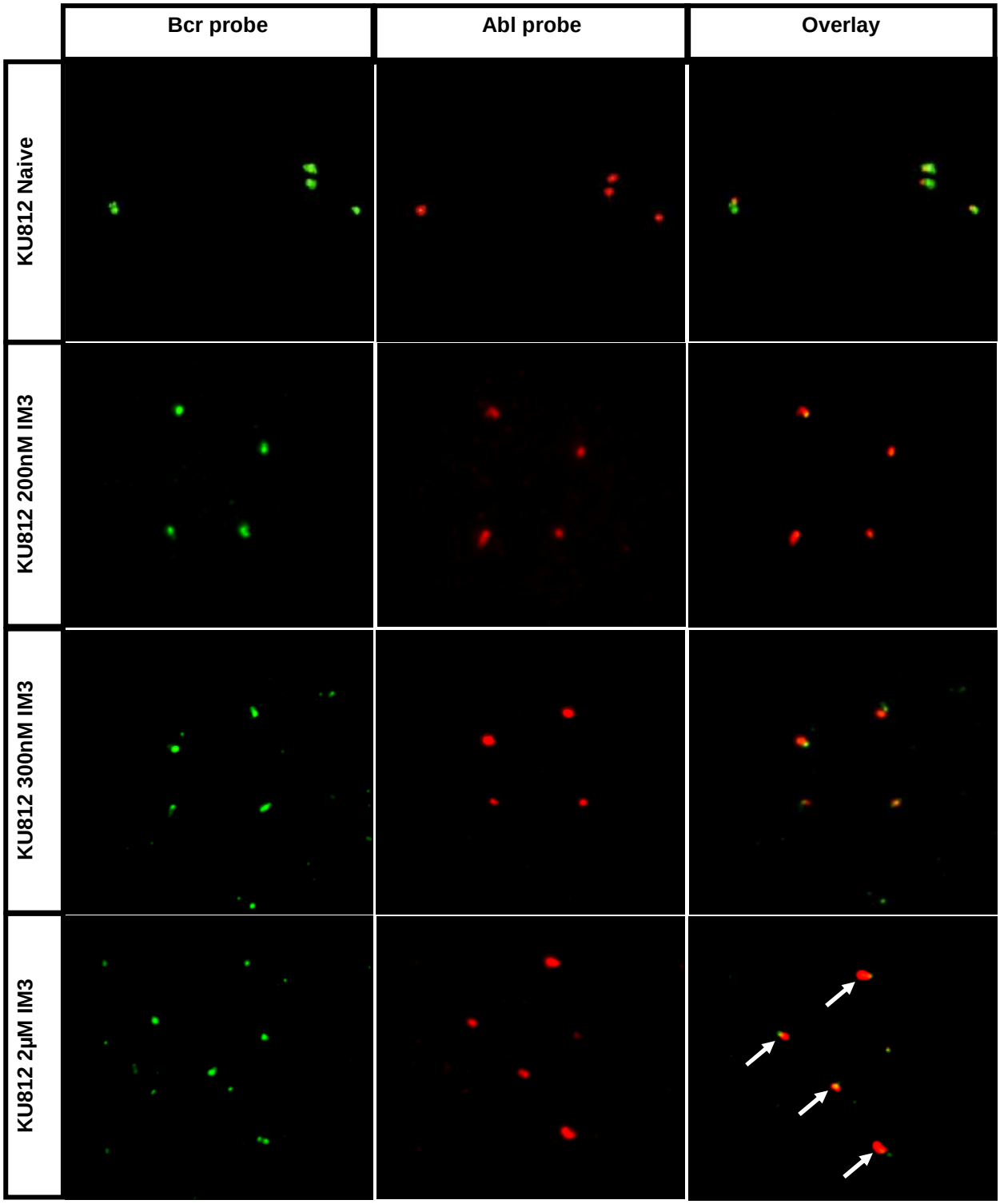

Figure 5.36: Interphase FISH to identify Bcr-Abl fusion genes
FISH analysis of a single, representative KU812 Naïve cell (top panel), a single KU812 200nM IM3 cell (second panel), a 300nM IM3 cell (third panel) and a 2µM IM3 cell (bottom panel). Overlaying Bcr (green) and Abl (red) signals confirms that Bcr-Abl amplification has not occurred in the IM-resistant cell line. There were consistently four signals in the four cell lines. White arrows indicate overlaying signals in the KU812 2µM IM3 panel.

Neither conventional sequencing nor the more sensitive MassARRAY technique could detect any mutations in the 200nM IM3 intermediate. In previous re-escalation studies with the K562 Dox 200nM DAS1 cell line, it was shown that the same KD mutation emerged and became the dominant clone, even when the re-escalated intermediate culture had no detectable mutation (**Figures 5.16 & 5.17**). To determine if this phenomenon would also be observed in the KU812 cell line in the context of imatinib resistance, the 200nM IM3 intermediate culture was thawed from frozen stocks, before being re-escalated in imatinib. It was found that the F359C again emerged in the presence of 300nM imatinib. As previously observed, the emergence of the KD mutation was accompanied by a significant decrease in BCR-ABL expression levels ($P<0.02$) (**Figure 5.37**).

Figure 5.37

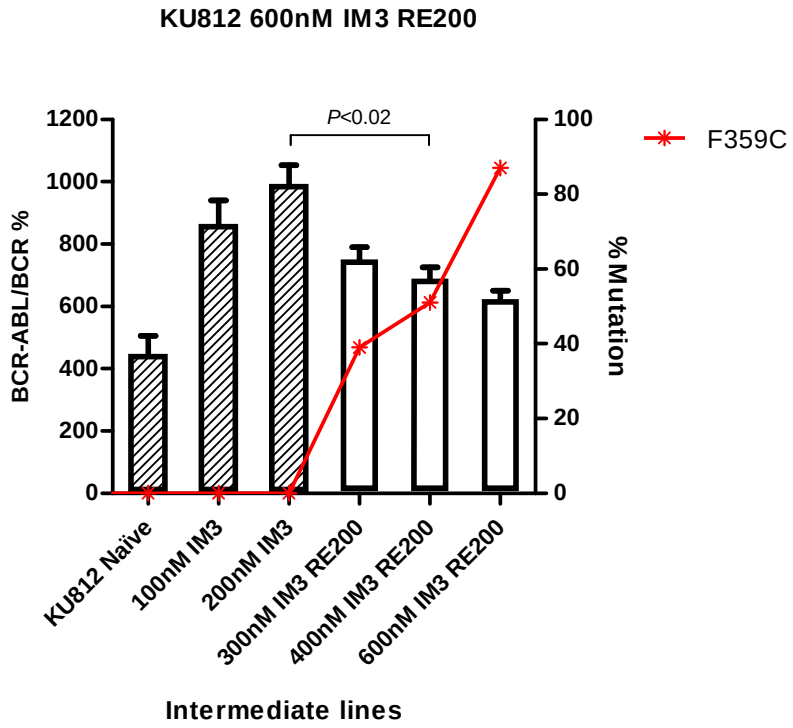

Figure 5.37: The F359C mutation emerged when the KU812 200nM IM3 intermediate was re-escalated in imatinib
When the 200nM IM3 intermediate of the KU812 2µM IM3 cell line was re-escalated in imatinib, the F359C mutation again emerged (in the 300nM intermediate) as the dominant clone. Furthermore, the emergence of the F359C mutation was again accompanied by a significant decrease in BCR-ABL expression. BCR-ABL expression is plotted as a ratio of BCR expression % +SEM from at least 3 independent experiments. Patterned columns indicate results from the original KU812 2µM IM3 cell line (Figure 5.33) while white columns indicate results for the re-escalated cultures.

5.4 Discussion

In order to investigate mechanisms of TKI resistance, several TKI-resistant cell lines were generated, including one dasatinib-resistant K562 cell line, two dasatinib-resistant K562 Dox cell lines, and five dasatinib or nilotinib re-escalated cultures. Imatinib resistance was also generated in three KU812 cell lines (**Table 5.1**).

5.4.1 BCR-ABL overexpression precedes the emergence of KD mutations

In the DAS-resistant K562 and K562 Dox DAS1 cell lines, and in all three KU812 IM-resistant cell lines, increased BCR-ABL expression was the first TKI resistance mechanism to emerge. This mechanism was then superseded by the emergence of one or more KD mutations. For all 10 cell lines that developed KD mutations, increased BCR-ABL expression always occurred first. In a study by Branford *et. al.*[162] (where the BCR-ABL mRNA expression and KD mutation data of 214 CML patients taking imatinib was correlated) it was found that in most patients with mutations (91% of patients with KD mutations), the mutations were detectable at the time of the ≥2-fold rise in BCR-ABL expression. However, in 47% of these patients, the mutations were also detectable from 1.5 to 8 months *before* the rise in BCR-ABL expression. Only 9% of patients exhibited mutations that were detectable at 2-3 months *after* the rise in BCR-ABL expression. Thus, most patients developed KD mutations followed by BCR-ABL overexpression – the opposite order observed in this study. In these patients, it appears that a leukaemic clone carrying a KD mutation emerges first, and is selected for by therapy which results in the measurable BCR-ABL rise *after* the mutation was detected. Thus, the rise in BCR-ABL expression may merely reflect a rise in the number of circulating leukaemic cells, rather than increased expression of BCR-ABL per cell (though these are not mutually exclusive). In the case of those patients where BCR-ABL overexpression emerged first and was followed by a KD mutation, it appears that leukaemic burden first increased, perhaps due to some other resistance mechanism (*e.g.* increased ABCB1 expression) and/or that BCR-ABL expression per cell increased as a partially protective resistance mechanism, and that the KD mutation followed due to the increased likelihood of mutation caused by increased BCR-ABL expression itself. This scenario most likely mimics the observations of this study.

It should also be noted that the cell lines in this study were effectively monitored every 10-30 days (whenever TKI escalation occurred), whereas the patients in the study by Branford *et. al.*[162] were

Table 5.1

	KU812				K562 Dox							K562
Cell line	IM1	IM2	IM3	IM3 RE200	DAS1	DAS RE40	DAS 1RE55	DAS 2RE55	NIL1 RE55	NIL2 RE55	DAS2	DAS
KD Mutation	**E450Q E459K E470K**	**E459K E462K E466E**	**F359C**	**F359C**	**V299L**	**V299L**	**V299L**	**V299L**	**G250E**	✗	✗	**T315I**
Increased ABCB1/ABCG2 cell-surface expression	✗	✗	✗		✗	✗	✗	✗	✗	✗	✗	✗
Increased BCR-ABL expression	✓	✓	✓	✓	✓	✓	✓	✓	✓	✓	✓	✓

Table 5.1: Summary of resistance mechanisms detected in three TKI-resistant cell lines exposed to IM or DAS, as well as those detected in the re-escalated cell cultures.

✓= yes; **x** = no. Greyed box indicates 'not tested'.

monitored between 1-6 month intervals. If intervals were consistent and shorter, more patients in which a rise in BCR-ABL expression occurred *before* the emergence of a KD mutation may have been identified.

In this study, FISH and DNA PCR confirmed that the K562 200nM DAS, K562 Dox 200nM DAS1, KU812 2µM IM1 and KU812 3µM IM2 cell lines all had increased Bcr-Abl DNA copy number, likely causing overexpression of BCR-ABL. The presence of dmin was confirmed by karyotyping as the mode of Bcr-Abl DNA amplification in the KU812 2µM IM1 cell line. FISH results and fluctuating copy number observed by DNA PCR in key intermediate cell lines indicate that dmin may also be present in the K562 200nM DAS, K562 Dox 200nM DAS1 and KU812 3µM IM2 cell lines. Rapid increase in BCR-ABL expression may have emerged as the first mechanism of resistance in these cell lines due to the ease of (dmin) amplification[146]. Dmin are small, circular, acentric[h] fragments of DNA[146] that frequently carry oncogenes (hence facilitating oncogene overexpression) in human cancers[145,146,148,149]. The number of dmin per cell varies, as they cannot attach to the mitotic spindle and are randomly segregated into the daughter cells following DNA replication. After mitosis, the daughter cell with the most dmin would have the selective advantage, and thus the number of dmin/cell in a population can rapidly increase[146]. BCR-ABL expression is known to increase DNA damage and genomic instability[33,34,117,223] via reactive oxygen species (ROS)[89]. This may in part explain why cells overexpressing BCR-ABL have an increased likelihood of developing a KD mutation[97,161]. Furthermore, increased levels of genomic Bcr-Abl (*e.g.* copies present on dmin) may also increase the likelihood of KD mutation development by virtue of the fact that more Bcr-Abl is being duplicated during mitosis, and the chance of an error in replication increases as copy number increases.

5.4.2 BCR-ABL expression levels significantly decrease upon the emergence of KD mutations

Barnes *et. al.*[161] hypothesised that excessive expression of active BCR-ABL may be detrimental to the cell. When imatinib was suddenly removed from cultures of BCR-ABL-overexpressing cells, their proliferation suddenly and significantly decreased, and apoptosis increased[161]. This may explain why a

[h] Acentric: Without a centromere.

clone carrying a KD mutation, yet with lower levels of BCR-ABL expression, has a selective advantage over a clone without a mutation that exhibits excessive expression of BCR-ABL. Thus, a drop in BCR-ABL expression accompanies the appearance of a KD mutation, as the mutation supersedes BCR-ABL overexpression as the preferred mechanism of resistance.

5.4.3 Kinetics of DAS-resistance development in the K562 200nM DAS cell line

The T315I mutation confers high level resistance to IM, DAS, and NIL[107,121]. The K562 200nM DAS cell line was found to harbour the T315I mutation. An $IC50^{DAS}$ value could not be obtained for this cell line, as no amount of dasatinib was able to reduce the amount of p-Crkl (a measure of BCR-ABL activity) even when challenged with 50,000nM dasatinib. IC50 values for IM and NIL are shown in *Chapter 6: TKI cross-resistance.* The IC50 assay also confirmed that long term culture in 0.1% DMSO did not generate resistance to dasatinib. Thus, any dasatinib resistance mechanisms observed are due only to dasatinib, and not the DMSO vehicle.

After 27 passages of the K562 200nM DAS cell line in dasatinib, BCR-ABL expression levels significantly decreased while T315I% continued to increase in the population as a whole (**Figure 5.8**). Without intensive clonal studies which are beyond the scope of this project, it remains unclear whether these resistance kinetics represent *A)* two separate clones which are competing for survival (one with low BCR-ABL expression carrying the T315I mutation, and the other with high BCR-ABL expression but no T315I mutation) *OR B)* one dominant clone carrying wild-type- and T315I-Bcr-Abl on double minutes, where the proportion of dmin carrying T315I-Bcr-Abl in that clone is increasing due to selection (**Figure 5.38**). Either of these theories may explain why T315I% continued to increase while BCR-ABL expression levels continued to decrease over time. Interestingly, when the K562 200nM DAS cell line was grown in the absence of dasatinib for over 30 passages, BCR-ABL mRNA expression continued to fall (as increased expression was no longer beneficial), as did the T315I% (**Figure 5.8**). This was not unexpected, as it has been documented in CML patients with KD mutations that mutation% decreases upon cessation of TKI therapy (as wild-type BCR-ABL outgrows)[114-116]. This indicates that the kinase activity of mutant BCR-ABL molecules may be slightly compromised compared to their wild-type counterparts. In conclusion, the removal of dasatinib as a source of selective pressure causes a reduction in BCR-ABL expression (as excess, active BCR-ABL activity is

Figure 5.38: Representations of possible clonal kinetics of resistance emergence
There are different explanations that account for the resistance kinetics of BCR-ABL expression and mutation% in the K562 200nM DAS, K562 Dox 200nM DAS1, KU812 2µM IM1, IM2 and IM3 cell lines. This figure shows possible mechanisms for how T315I% increased as BCR-ABL expression decreased in the K562 Dox 200nM DAS cell line. **Left panel:** Early in dasatinib escalation, two different cells may have mutated such that one acquired the T315I mutation only, while the other developed BCR-ABL overexpression only. At low dasatinib concentrations, both clones may have been equally viable and continued to grow. However, as dasatinib concentration was escalated, the T315I-carrying clone was able to survive and expanded, while BCR-ABL overexpression in the latter clone was not sufficient in such high dasatinib concentrations, causing this clone to decline. **Right panel:** Double minutes carrying wild-type and mutant Bcr-Abl are present in a single clone which populates the culture. As dasatinib concentration is increased, daughter cells that contain higher numbers of mutant Bcr-Abl (but not necessarily higher numbers of total Bcr-Abl) are selected and thrive. Both explanations provide plausible theories to explain the results obtained in this study. Dmin = double minutes; HSR = homogenously staining regions.

Figure 5.38

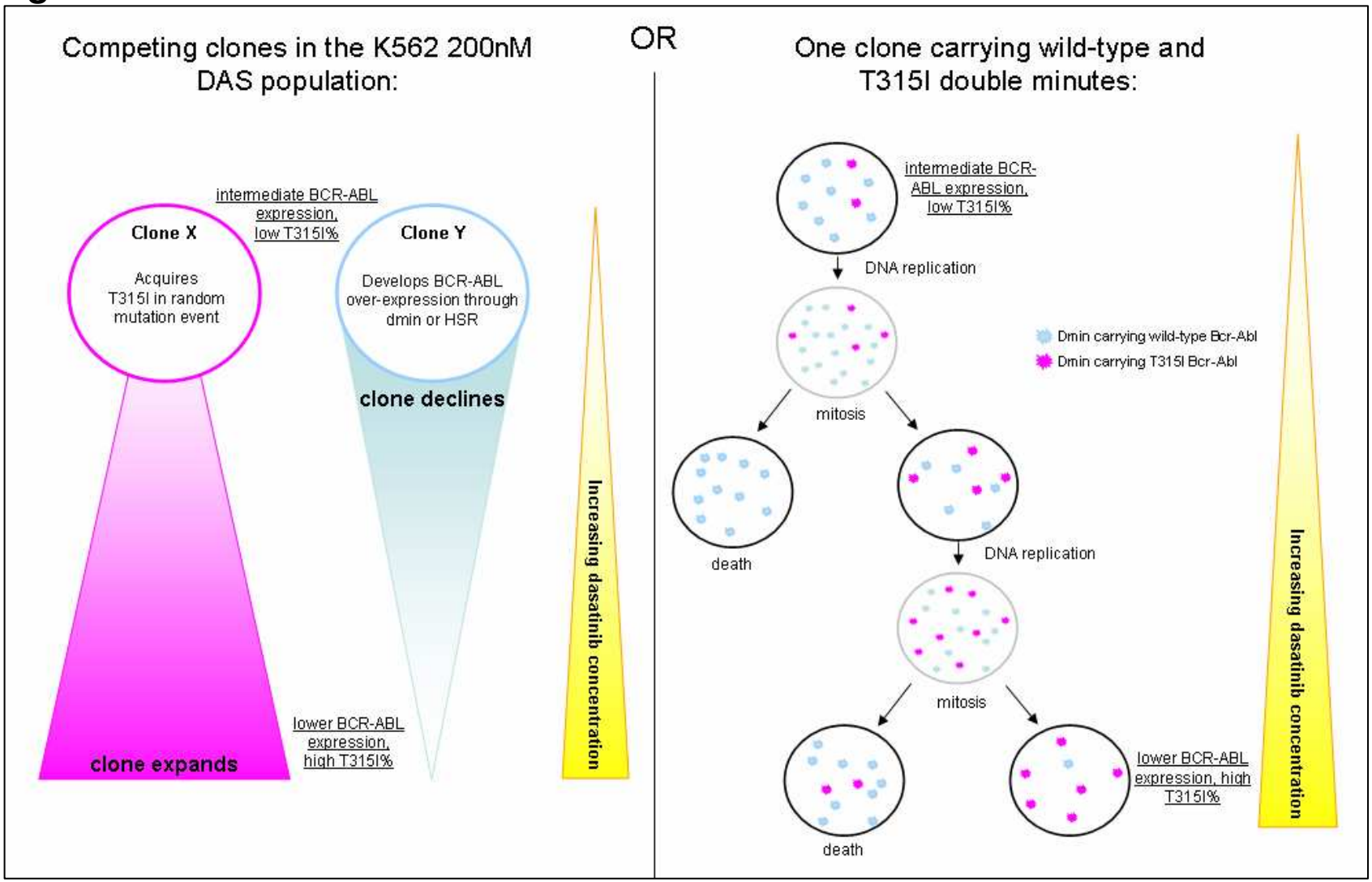
Competing clones in the K562 200nM DAS population:
OR
One clone carrying wild-type and T315I double minutes:
intermediate BCR-ABL expression, low T315I%
Clone X
Acquires T315I in random mutation event
Clone Y
Develops BCR-ABL over-expression through dmin or HSR
clone declines
clone expands
lower BCR-ABL expression, high T315I%
Increasing dasatinib concentration
intermediate BCR-ABL expression, low T315I%
DNA replication
Dmin carrying wild-type Bcr-Abl
Dmin carrying T315I Bcr-Abl
mitosis
death
DNA replication
mitosis
death
lower BCR-ABL expression, high T315I%
Increasing dasatinib concentration

detrimental[161]), as well as a reduction in T315I%, because this clone no longer has an advantage over un-mutated BCR-ABL.

5.4.4 A V299L-carrying clone emerged early on in DAS exposure in the K562 Dox cell line

Besides T315I, the V299L mutation is the most common KD mutation detected in CML patients treated with dasatinib[120]. The V299L mutation is known to confer dasatinib resistance *in vitro*[119,121] and *in vivo*[237].

When the K562 Dox cell line was exposed to gradually increasing concentrations of dasatinib, the V299L mutation emerged in the 75nM intermediate (**Figure 5.12**). It is possible that there were many different clones carrying different KD mutations in a previous intermediate culture that were all capable of emerging as the dominant clone. However, neither conventional sequencing nor more sensitive MassARRAY analysis could detect the presence of the V299L mutation (or any other of the 30 most common KD mutations found in CML patients; see *Appendix I.5*) in any prior intermediates, including the K562 Dox Naïve cell line. Despite this mutation being undetectable, two re-escalations of the 55nM DAS1 intermediate, and indeed even the 40nM DAS1 intermediate, resulted in the emergence of V299L again. Notably, the KD mutation always became detectable when cultures reached the 75nM dasatinib culture condition (**Figures 5.16 & 5.17**). The V299L-carrying clone must have emerged at an earlier intermediate (*i.e.* 40nM DAS1 or earlier), but did not have the selective advantage (to allow for detection) over cells only overexpressing BCR-ABL when dasatinib concentrations were relatively low. Only when dasatinib concentrations reached 75nM did BCR-ABL overexpression become insufficient to confer dasatinib resistance, allowing the V299L-carrying clone to dominate and become detectable. It seems likely that the V299L-carrying clone was present in intermediates prior to the 75nM DAS1 intermediate, yet it was not detectable by the sensitive MassARRAY detection method. Therefore, the presence of clones carrying different KD mutations prior to the 75nM intermediate cannot be excluded merely because none were detected by MassARRAY.

The V299L mutation is thought to be sensitive to both nilotinib and imatinib[119,121,237]. Therefore, it was hypothesised that re-escalation in nilotinib would not facilitate selection of the V299L mutation, but that

the population would have to resort to some other mutation/resistance mechanism. This hypothesis was correct, as nilotinib culture resulted in the emergence of the G250E mutation in the 350nM NIL1 intermediate (**Figure 5.19**). This mutation has been implicated in both *in vitro*[235] and *in vivo*[238] nilotinib resistance, however its emergence in the NIL1 cell line must have been a stochastic event as it did not emerge in the second nilotinib re-escalation (NIL2) (**Figure 5.19**). Instead, BCR-ABL overexpression appeared to be the major mode of NIL-resistance in the K562 Dox 500nM NIL2 RE55 cell line (**Figure 5.19**).

KD mutations have been found to be present in *de novo* CML patients, before TKI therapy is started[107,110-113]. Thus, in some cases of relapse where KD mutations are present, it appears that clones with advantageous mutations were already present before treatment and were merely selected for by the TKI therapy. It was noted that the V299L repeatedly emerged in dasatinib cultures related to the K562 Dox 200nM DAS1 cell line. To determine whether a clone carrying this mutation was already present in the K562 Dox Naïve cell line and will always be expanded under dasatinib selection, the K562 Dox cell line was escalated in dasatinib a second time. The resulting K562 Dox 200nM DAS2 cell line did not harbour the V299L mutation (instead only exhibiting BCR-ABL overexpression), indicating that the emergence of this mutation was a random event of the K562 Dox 200nM DAS1 cell line.

5.4.5 Multiple KD mutations emerged in imatinib-resistant KU812 cell cultures

When two imatinib-resistant KU812 cell lines were generated, it was observed that both cell lines (KU812 2µM IM1 and 3µM IM2) carried the E459K mutation (as well as several bystander mutations[9]) (**Figure 5.24 & Figure 5.29**). The E462K, E466E (a synonymous or 'silent' mutation), and E470K mutations have not previously been observed in CML patients, however, the E459K and E450Q mutations have been reported. A case study by Kim *et. al.*[239] discussed a male CML patient taking imatinib who developed the E459K mutation within two months of starting treatment. The patient was then switched to bosutinib (another second generation TKI), but developed a compound mutation of V299L and E459K within five months and entered blast crisis. The patient was subsequently switched to nilotinib and achieved a complete cytogenetic remission within four months[239].

[9] A bystander mutation refers to a mutation that does not confer selective advantage, but is present on the same molecule or in the same cell as a mutation that is advantageous. As a result, the 'bystander' mutation (along with the advantageous mutation) may dominate in a population, even though it confers no advantage.

As both the KU812 2µM IM1 and 3µM IM2 cell lines harboured the E459K, E450Q, and E470K mutations, it was hypothesised that these mutations were present at undetectable levels in the KU812 Naïve cell line, and were simply being expanded by imatinib selection. To confirm this, a third imatinib-resistant KU812 cell line was generated, and named KU812 2µM IM3. However, neither the E459K mutation nor the E450Q and E470K mutations emerged a third time, but instead the F359C mutation (**Figure 5.34**). It was therefore concluded that specific KD mutations were not inevitably destined to expand in the KU812 cell line, but emerged stochastically.

It is unclear whether the mutations seen in the IM1 and IM2 cell lines are compound mutations (*i.e.* all present on the same BCR-ABL molecule) or whether each mutation represents a different clone that is competing for survival in the population. The latter seems more plausible, as in both the IM1 and IM2 cell lines the E459K mutation appears to dominate, while the other mutations show a declining rate of growth (or disappearance all together) as the percent of E459K mutation continues to increase (**Figure 5.24 & Figure 5.29**). If another mutation was on the same BCR-ABL molecule as E459K, then one would expect that the percentages of them both would be equal, even if the 'bystander' mutation conferred no selective advantage. This question could be definitively answered by clonal studies, which is the focus of ongoing investigations in the laboratory. It appears that (in the KU812 cell line) the E450–E470 region of BCR-ABL may be some sort of 'mutation hot-spot', due to the clusters of mutations seen in this region in both the KU812 2µM IM1 and IM2 cell lines.

BCR-ABL overexpression was much more subtle in the KU812 2µM IM3 cell line, as the F359C KD mutation (previously reported in imatinib-resistant patients[240,241]) emerged early on in resistance development – after only three escalations in imatinib (**Figure 5.34**). Therefore, these cells never needed to resort to excessive BCR-ABL expression as the KU12 2µM IM1 and IM2 cell lines did, because the KD mutation (and its steadily increasing percentage up to 100%) was sufficient to promote survival in 300nM–2µM imatinib. Re-escalation studies showed that the clone carrying the F359C mutation must have been present as early as the 200nM intermediate (**Figure 5.37**), even though no KD mutations were detectable in this intermediate (or any prior intermediate, including KU812 Naïve) by conventional sequencing or MassARRAY analysis (see *Appendix I.5*).

In several cell lines in this study Bcr-Abl copy number mirrored BCR-ABL transcript expression (K562 200nM DAS, **Figure 5.8 & 5.9**; K562 Dox 200nM DAS1, **Figure 5.12 & 5.13**; KU812 2µM IM1, **Figure 5.24 & 5.25** and KU812 3µM IM2, **Figure 5.29 & 5.30**) suggesting that changes in BCR-ABL expression were not regulated by the Bcr-Abl promoter. However, DNA PCR and FISH results for key intermediates of the KU812 2µM IM3 cell line showed that no amplification of the Bcr-Abl gene had occurred despite a more than 2-fold increase in BCR-ABL expression levels (compare **Figure 5.34, 5.35 & 5.36**). DNA copy number of Bcr-Abl remained stable throughout imatinib-resistance generation, even though peak BCR-ABL expression reached 990% (KU812 Naïve expression was only 443%) suggesting altered regulation of the Bcr-Abl promoter in the KU812 200nM IM3 intermediate. It is interesting to note that the Branford *et. al.*[162] study identified a ≥2-fold rise in BCR-ABL mRNA expression as predictive of BCR-ABL KD mutations. Therefore, an increase in Bcr-Abl copy number may not be necessary to facilitate BCR-ABL expression levels which promote the emergence of KD mutations.

Chapter 6:

TKI cross-resistance and differential resistance in imatinib- and dasatinib-resistant CML cell lines

6.1 Introduction

Multi-drug resistance is a common theme of numerous human cancers, whereby resistance to one chemotherapeutic drug results in cross-resistance to a variety of agents[61,149,200,242]. Similarly, TKI cross-resistance has been observed in CML patients. However, differential TKI resistance also occurs, and is frequently the result of particular kinase domain mutations which may confer resistance to one TKI but not another.

6.1.1 TKI cross-resistance and differential resistance

Imatinib, nilotinib and dasatinib have been rationally designed to effectively bind and inhibit BCR-ABL kinase activity[20,30]. In order to facilitate this interaction, specific residues in the KD are required to form hydrogen bonds and maintain the BCR-ABL molecule in the correct conformation[22,105]. As different TKIs utilise different BCR-ABL residues to bind, various KD mutations may result in differential TKI resistance. For example, a valine residue at position 299 is critical for dasatinib binding, but not for imatinib or nilotinib. The V299L mutation therefore confers resistance to dasatinib, but not to imatinib or nilotinib[120]. Furthermore, a phenylalanine residue at position 359 is critical for imatinib and nilotinib binding, but not for dasatinib. The F359C mutation therefore confers resistance to imatinib and nilotinib, but not dasatinib[240,241]. Only the T315I mutation is reported to confer cross-resistance to all three TKIs, as this residue provides a critical hydrogen bond for all three TKI-BCR-ABL interactions[107,121]. The T315I mutation is therefore known as the 'gatekeeper' mutation[124]. Apart from this mutation, there is no single resistance mechanism that has been reported to cause pan-TKI-resistance in the clinical setting.

6.1.2 BCR-ABL independent resistance: Src family kinases

BCR-ABL kinase activity drives the CML phenotype[5], and most TKI-resistance mechanisms involve BCR-ABL evading inhibition (*i.e.* by increased TKI efflux, decreased TKI uptake, KD mutation or BCR-ABL overexpression)[109]. However, genetic instability results in the accumulation of numerous genetic lesions and mutations in Ph+ positive cells, which can lead to TKI-resistance mechanisms that are independent of BCR-ABL kinase activity[7,83]. One prominent mode of BCR-ABL independent resistance observed *in vitro* and *in vivo* is the overexpression of sarcoma (Src) family kinases, such as

haemopoietic cell kinase (Hck) and V-yes-1 Yamaguchi sarcoma viral related oncogene homolog (Lyn)[81,156,197,243,244].

The human Src family includes nine structurally related non-receptor tyrosine kinases that are expressed ubiquitously (Src, Fyn, Yes) or are restricted to haematopoietic lineages (Blk, Yrk, Fgr, Hck, Lck and Lyn)[244]. Src family kinase members are composed of four Src Homology (SH) domains, of which the first (SH1) is the catalytic kinase domain[245]. These proteins play critical roles in regulation of proliferation, differentiation, migration, adhesion, invasion, angiogenesis, and immune function (**Figure 5.2**) and are implicated in a variety of human tumours[234,246-248]. Through activation of the PI3K and Ras/Raf pathways, Src family kinases are able to promote survival and proliferation of tumour cells[247]. Additionally, Lyn (through currently unknown mechanisms) increases expression of Bcl-2 which inhibits apoptosis[155]. In the context of CML, Hck or Lyn overexpression is therefore considered to be a BCR-ABL independent resistance mechanism, as Src signalling may be sufficient to promote survival despite BCR-ABL kinase inhibition[155,249].

In 2003, Donato *et. al.*[156] noted that an imatinib-resistant K562 cell line had reduced BCR-ABL expression compared to the parental culture, and did not carry any kinase domain mutations. However, Lyn kinase was highly overexpressed and imatinib sensitivity could be restored by Src inhibitors[156]. Six imatinib-resistant patients were screened and found to have Lyn (and/or Hck) expression levels similar to that of the imatinib-resistant K562 cell line[156]. In a study by Mahon *et. al.*[81], Lyn overexpression was identified as a resistance mechanism in 2/7 nilotinib resistant patients without kinase domain mutations or BCR-ABL overexpression. Hayette *et. al.*[244] found that Lyn overexpression accounted for 24% of imatinib resistance in a study of 111 TKI-resistant/blast crisis/accelerated phase CML patients. Mahon *et. al.*[81] and others[155,156] have also identified Lyn overexpression in nilotinib- or imatinib-resistant K562 cell lines. Notably, dasatinib (a dual Src/BCR-ABL inhibitor[30,33]) was as effective at killing cultures of the Lyn-overexpressing imatinib-resistant[250] and nilotinib-resistant[81] K562 cell lines as it was in killing cultures of the parental K562 cell line. Thus, although Src kinase overexpression in BCR-ABL positive cells appears to confer resistance to imatinib and nilotinib, it seems that such cells remain sensitive to dasatinib.

6.2 Approach

As expected, all of the TKI-resistant cell lines generated in this study were overtly resistant to the TKI in which they were cultured. In total, eleven cell lines (eight imatinib-resistant and three dasatinib-resistant) were generated. To investigate whether these cell lines (or their intermediates) displayed TKI-cross resistance or differential resistance, several techniques were employed.

IC50 assays were conducted on resistant cell lines and intermediates of interest to determine the level of BCR-ABL kinase inhibition in the presence of a given TKI. It was previously demonstrated (see *Chapter 4*) that imatinib resistance in the K562 Dox 2µM IM1, IM2 and IM3 cell lines was due to ABCB1 overexpression, as PSC833 (a potent ABCB1 inhibitor) was able to reduce the IC50 back to the same level as the K562 Dox Naïve control (**Figure 4.9**). The same approach was therefore used when investigating these cell lines' resistance to nilotinib and dasatinib.

In the case of BCR-ABL-independent resistance, one would expect to see increased viability that is *not* accompanied by a rise in IC50. This is because the IC50 assay has a BCR-ABL-dependent readout (Crkl phosphorylation levels), and should therefore not reflect the actual resistance level in a BCR-ABL-independent cell line. Therefore, three-day viability experiments were used to confirm or exclude BCR-ABL-independent resistance.

Finally, when it appeared that BCR-ABL-independent resistance may have been playing a role in mediating resistance in the K562 2µM IM2 cell line, RQ-PCR was conducted to measure Lyn expression levels (as a ratio of the GUSB control gene).

6.3 Results

Of particular note in this study was the observation that all resistant cell lines displayed resistance (at least to some extent) to all three TKIs tested (IM, DAS and NIL) despite previous exposure to only one TKI.

6.3.1 TKI cross-resistance in the K562 200nM DAS cell line

The K562 200nM DAS cell line was found to carry the T315I mutation, so it was not unexpected that this cell line exhibited overt resistance to imatinib and nilotinib despite previous exposure to only dasatinib (**Figure 6.1**). The average $IC50^{IM}$ for the K562 Naïve and DMSO control cell lines was 6.6µM and 6.8µM respectively (no significant difference) while the $IC50^{IM}$ for the K562 200nM DAS cell line was significantly greater than both the controls (>100µM; *P*<0.00001) (**Figure 6.2**). Similarly, the average $IC50^{NIL}$ for the K562 Naïve and DMSO control cell lines was 454nM and 427nM respectively (no significant difference) while the $IC50^{NIL}$ for the K562 200nM DAS cell line was significantly greater than both the control cell lines (>50,000nM; *P*<0.00001) (**Figure 6.2**). No IC50 value could be calculated for the K562 200nM DAS cell line, as p-Crkl could not be ablated even at the highest TKI concentrations used (**Figure 5.4 & 6.1**).

6.3.2 Differential TKI resistance and cross-resistance in the K562 Dox 200nM DAS1 and 2 cell lines

The K562 Dox 200nM DAS1 cell line carried the V299L KD mutation which reportedly confers resistance to dasatinib, but is sensitive to nilotinib and imatinib[120,121]. Despite this, the $IC50^{NIL}$ value increased from 750nM in the K562 Dox Naïve cell line to 1600nM in the 200nM DAS1 cell line; and the $IC50^{IM}$ value had increased from 14.3µM in K562 Dox Naïve cells to 46µM in the 200nM DAS1 cell line (**Table 6.1**). As this V299L-carrying cell line displayed resistance to imatinib and nilotinib, it was hypothesised that a different resistance mechanism was responsible for the increased imatinib and nilotinib IC50s. The only other resistance mechanism identified was BCR-ABL overexpression, which peaked in the 55nM DAS1 intermediate (**Figure 5.12**). It was reasoned that, if BCR-ABL overexpression was responsible for conferring imatinib and nilotinib resistance in the K562 Dox 200nM DAS1 cell line, then the 55nM DAS1 intermediate would have the greatest imatinib and nilotinib IC50 values. This was, in fact, the observed result (**Table 6.1**). The 55nM DAS1 intermediate (in which

Figure 6.1

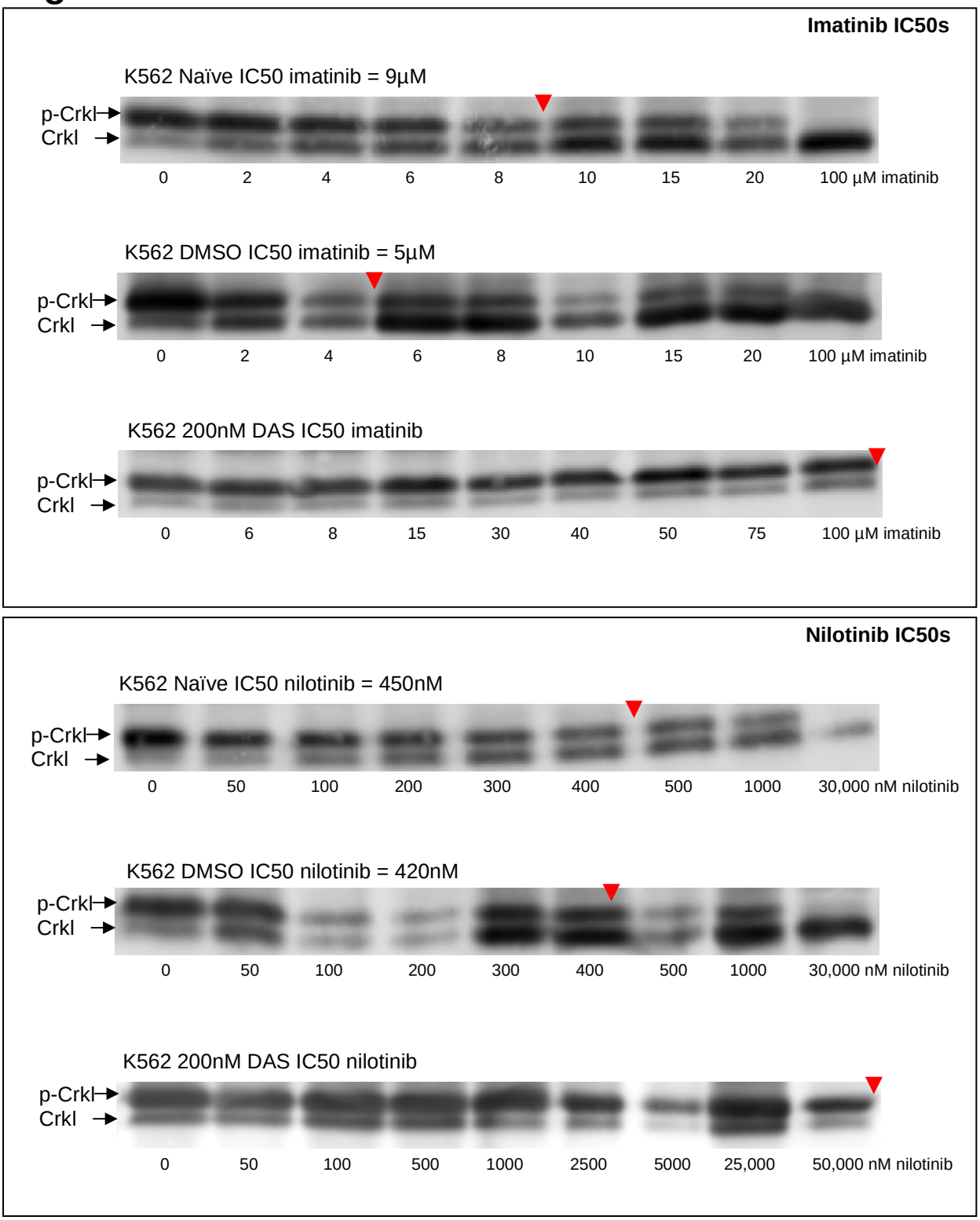

Figure 6.1: The K562 200nM DAS cell line displayed overt resistance to imatinib and nilotinib despite previous exposure to dasatinib only

One representative blot is shown for $IC50^{IM}$ (top) and $IC50^{NIL}$ (bottom) for the K562 Naïve, DMSO control and K562 200nM DAS cell lines. The K562 200nM DAS cell line carried the T315I mutation (~50%). Note that p-Crkl levels in the DAS-resistant cell line did not decrease as TKI concentration increased, therefore, no accurate IC50 value can be determined.

Figure 6.2

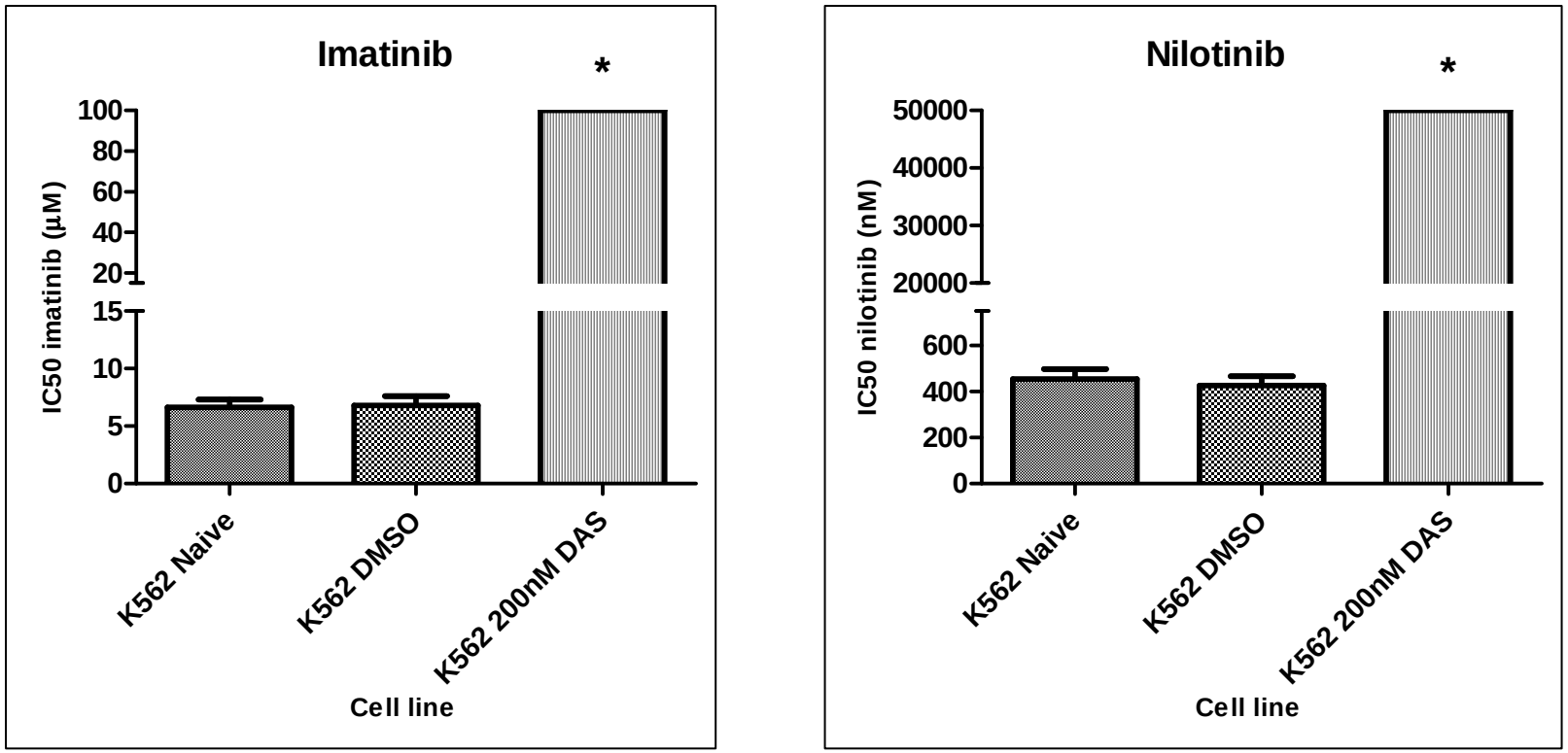

Figure 6.2: The average $IC50^{IM}$ and $IC50^{NIL}$ for K562 200nM DAS was significantly greater than that of the K562 Naïve and DMSO control cell lines

Quantification of IC50 Western blots for three cell lines. Note that no exact value can be given for the K562 200nM DAS cell line, as p-Crkl could not be ablated even in the presence of 100µM IM or 50,000nM NIL (see Figure 6.1). Data are presented as mean +SEM of data from at least 4 independent experiments. The K562 200nM DAS cell line had significantly greater IC50s than the K562 Naïve and DMSO control cell lines (*P<0.00001).

Table 6.1

	No mutation		V299L mutation	
	Naive	**55nM DAS1**	**75nM DAS1**	**200nM DAS1**
IC50 DAS (nM)	135	1700	4300	6800
IC50 NIL (nM)	750	4100	1680	1600
IC50 IM (μM)	14.3	115	40	46
BCR-ABL expression	186%	850%	470%	540%

Table 6.1: The K562 Dox 200nM DAS1 cell line has differential resistance to DAS, NIL and IM
IC50 values for DAS, NIL and IM compared with BCR-ABL expression in key intermediate lines of the K562 Dox 200nM DAS1 cell line. Note the highest BCR-ABL expression levels were accompanied by the highest $IC50^{IM}$ and $IC50^{NIL}$ values in the 55nM intermediate (pink). However, a significant decrease in BCR-ABL expression and the emergence of the V299L mutation accompanied a rise in $IC50^{DAS}$ in the 75nM intermediate (purple), while $IC50^{IM}$ and $IC50^{NIL}$ values decreased. For Western blots, see *Appendix I.7, I.8 and I.9.*

BCR-ABL expression was 850% and there was no KD mutation) had an $IC50^{NIL}$ of 4100nM, and an $IC50^{IM}$ of 115µM, while the $IC50^{DAS}$ was 1700nM. However, the 75nM DAS1 intermediate (in which BCR-ABL expression had dropped to 470%, but the V299L mutation had emerged) had a decreased $IC50^{NIL}$ and $IC50^{IM}$ of 1680nM 40µM respectively, while $IC50^{DAS}$ had increased to 4300nM (**Table 6.1**). It therefore appeared that the V299L mutation in the K562 Dox 200nM DAS1 cell line caused differential resistance to the three TKIs tested: BCR-ABL overexpression was primarily responsible for conferring nilotinib and imatinib resistance, while both BCR-ABL overexpression and the V299L mutation conferred overt resistance to dasatinib. In contrast, the K562 Dox 200nM DAS2 cell line (found to have BCR-ABL overexpression; see *Chapter 5*) displayed overt resistance to all three TKIs, despite previous exposure to dasatinib only (**Figure 6.3**). The $IC50^{DAS}$ had increased greater than 100-fold (from 79nM to >10,000nM), the $IC50^{IM}$ had increased 6-fold (from 10µM to 62µM) and the $IC50^{NIL}$ had increased 6-fold (from 790nM to >5,000nM) compared to the K562 Dox Naïve cell line.

6.3.3 ABCB1 overexpression confers TKI cross-resistance in the K562 Dox 2µM IM1, IM2 and IM3 cell lines

When the K562 Dox cell line was exposed to increasing concentrations of imatinib, the only identifiable resistance mechanism to emerge was a further increase in ABCB1 expression (**Figure 4.4**). It was found that the three cell lines generated were highly resistant to imatinib, but that blocking ABCB1 could restore the $IC50^{IM}$ back to levels of the Naïve control (**Figure 4.9**). IC50 analysis demonstrated that the K562 Dox 2µM IM-resistant cell lines were also resistant to nilotinib and dasatinib. The $IC50^{NIL}$ had significantly increased from 697nM in the K562 Dox Naïve cell line, to 1120nM, 1152nM and 1023nM in the K562 Dox 2µM IM1, IM2 and IM3 cell lines respectively (P<0.004) (**Figure 6.4**). Similarly, the $IC50^{DAS}$ had significantly increased from 112nM in the K562 Dox Naïve cell line, to 627nM, 638nM and 603nM in the K562 Dox 2µM IM1, IM2 and IM3 cell lines respectively (P<0.001) (**Figure 6.4**). To determine whether ABCB1 overexpression was responsible for conferring nilotinib and dasatinib resistance, IC50s were also conducted in the presence of PSC833 (a potent ABCB1 inhibitor). It was found that blocking ABCB1 removed the significant difference in $IC50^{NIL}$ and $IC50^{DAS}$ values between the K562 Dox IM-resistant cell lines and the K562 Dox Naïve cell line. In fact, values were restored back to the same level as the non-ABCB1 expressing K562 cell line (**Figure 6.4**).

Figure 6.3

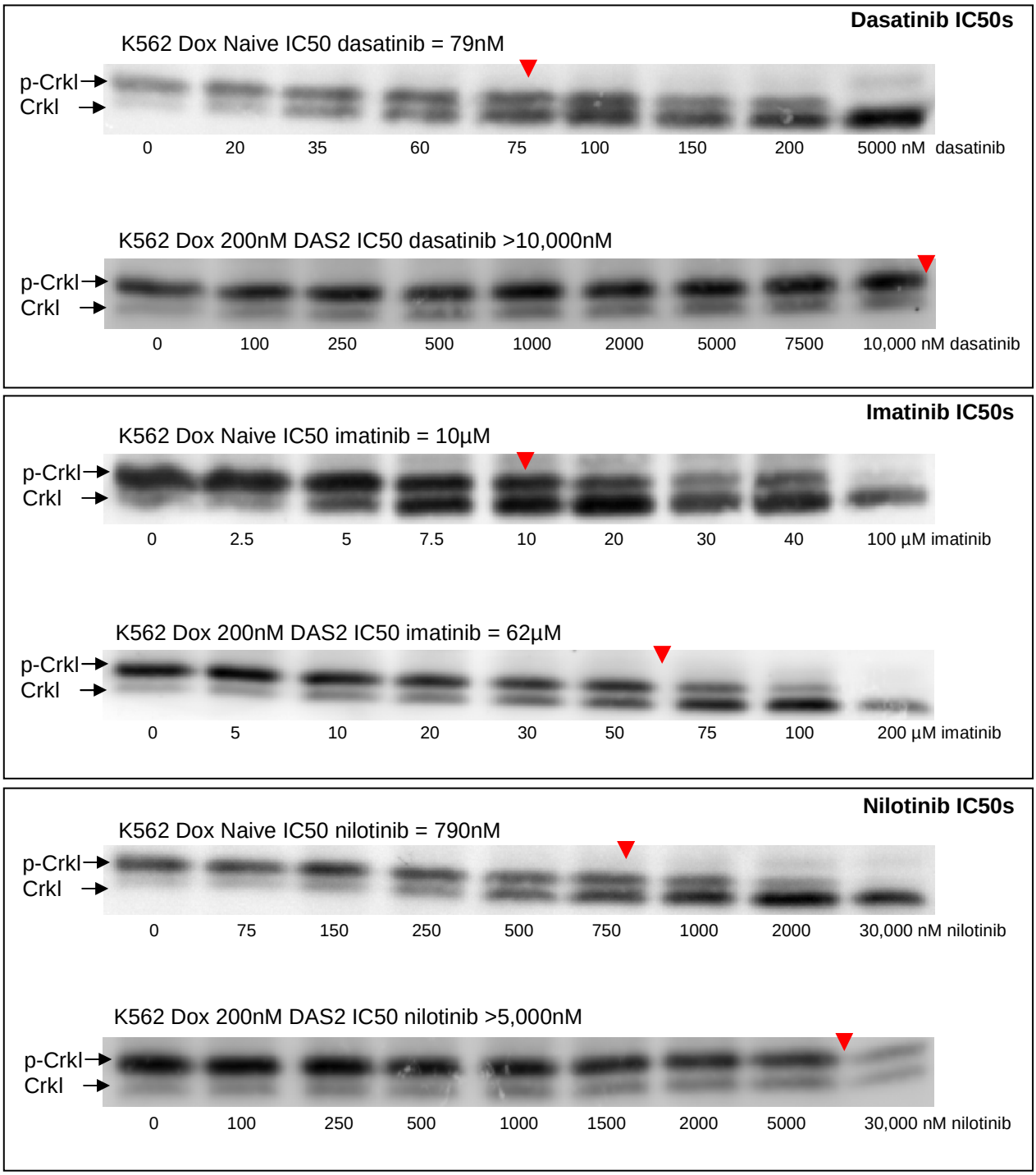

Figure 6.3: The K562 Dox 200nM DAS2 cell line displayed overt resistance to dasatinib, imatinib and nilotinib despite previous exposure to dasatinib only
One representative blot is shown for $IC50^{DAS}$ (top), $IC50^{IM}$ (middle) and $IC50^{NIL}$ (bottom) of the K562 Dox Naïve, DMSO control and K562 Dox 200nM DAS2 cell lines. The K562 Dox 200nM DAS2 cell line did not have any KD mutations, but did have BCR-ABL overexpression. The IC50 value for each blot (determined as the dose of drug required to reduce levels of p-Crkl by 50%) is indicated above each blot (and with red arrow).

Figure 6.4

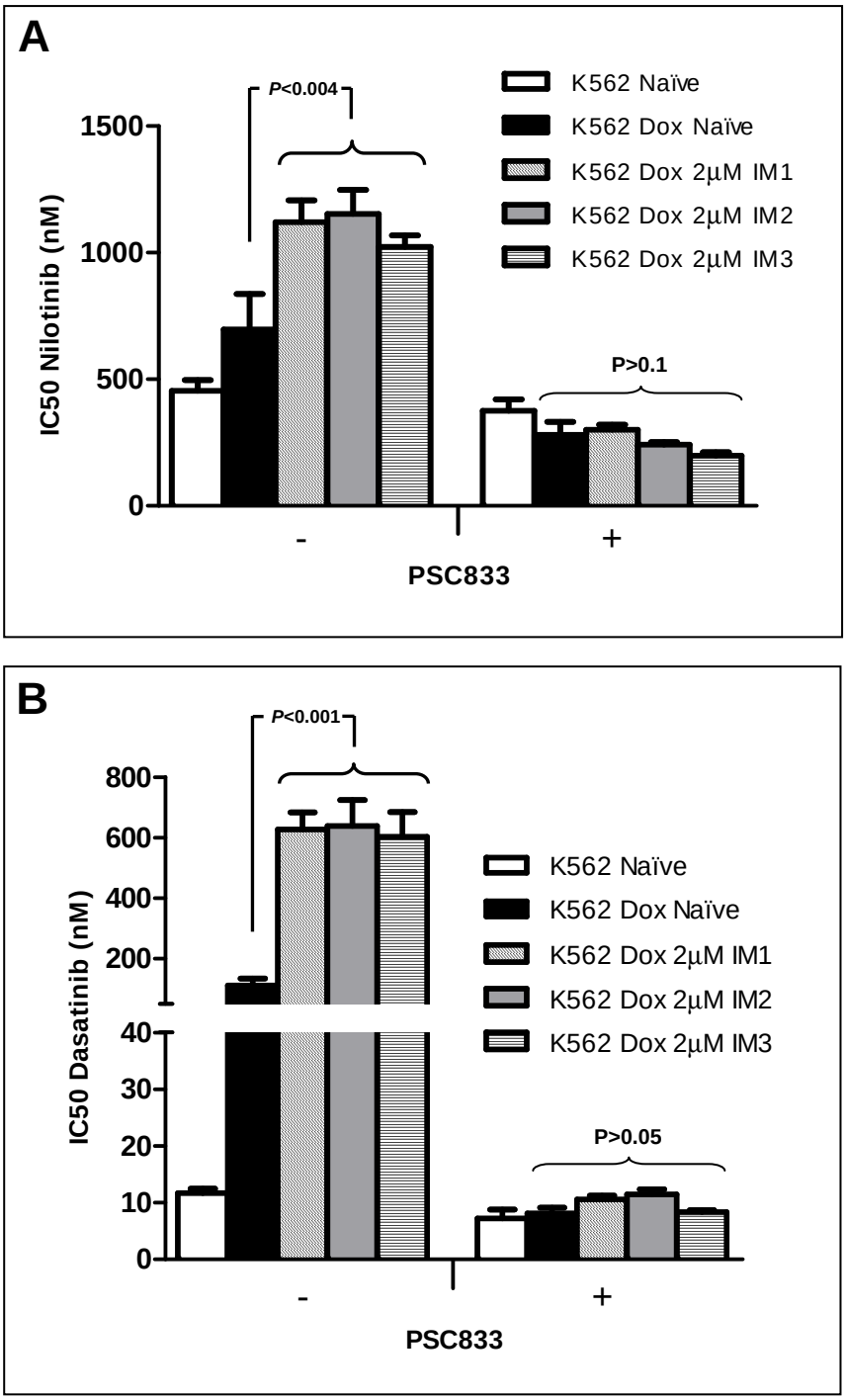

Figure 6.4: ABCB1 inhibition ablates NIL and DAS resistance in the three IM-resistant K562 Dox cell lines
Blocking ABCB1 with PSC833 (10µM) ablated the difference in **(A)** $IC50^{NIL}$ and **(B)** $IC50^{DAS}$ between IM-resistant cell lines and K562 Dox Naïve, indicating ABCB1 overexpression is the primary mode of resistance to nilotinib and dasatinib in these cell lines. Data are presented as the mean +SEM from at least 4 independent experiments. For Western blots, see *Appendix I.10, I.11, I.12, and I.13.*

6.3.4 BCR-ABL overexpression and KD mutations in the KU812 2μM IM1, 3μM IM2 and 2μM IM3 cell lines conferred differential or cross-resistance to TKIs

Three imatinib-resistant KU812 cell lines were generated, and all were found to carry kinase domain mutations. The KU812 2μM IM1 and 3μM IM2 cell lines harboured several mutations, including the E459K which has been previously implicated in clinical imatinib resistance[239]. Both of these cell lines had increased IC50 values for the three TKIs tested (**Table 6.2**). In contrast, the KU812 2μM IM3 cell line displayed differential resistance (**Table 6.3**). The 200nM IM3 intermediate (in which BCR-ABL expression peaked at 990% and there was no KD mutation, see **Figure 5.34**) had an $IC50^{DAS}$ of 25.3nM, while the $IC50^{IM}$ and $IC50^{NIL}$ were 24.2μM and 660nM respectively. However, the 300nM IM3 intermediate (in which BCR-ABL expression had decreased to 633%, but the F359C mutation had emerged) had a decreased $IC50^{DAS}$ of 16.5nM, while the $IC50^{IM}$ and $IC50^{NIL}$ had increased to 49μM and >10,000nM respectively (**Table 6.3**). It therefore appeared that BCR-ABL overexpression was primarily responsible for conferring dasatinib resistance in the KU812 2μM IM3 cell line, while the F359C mutation conferred resistance to imatinib and nilotinib.

6.3.5 BCR-ABL and Lyn overexpression in the K562 2μM IM1 and IM2 cell lines conferred differential or cross-resistance to TKIs

The two IM-resistant K562 cell lines both had increased BCR-ABL expression which was thought to be the sole resistance mechanism (**Figure 3.11**). IC50 assays were used to determine whether these cell lines were also resistant to nilotinib and dasatinib. The $IC50^{NIL}$ had significantly increased in both cell lines from 454nM in the K562 Naïve control to 2713nM and 2995nM in the K562 2μM IM1 and IM2 cell lines respectively (**Figure 6.5**). Furthermore, three-day viability experiments (both trypan blue cell counts and flow cytometry analysis) confirmed that in the presence of 250nM nilotinib, the IM-resistant cell lines had significantly increased survival above that of the Naïve cell line ($P<0.00002$ and $P<0.02$ by trypan blue count and flow cytometry respectively) (**Figure 6.5**). Interestingly, the K562 2μM IM2 cell line was significantly more resistant than the IM1 cell line ($P<0.03$ and $P<0.009$ by trypan blue count and flow cytometry respectively) (**Figure 6.5**).

Table 6.2

	KU812 Naive	KU812 2μM IM1	KU812 3μM IM2
IC50 IM (μM)	6.1	58	50
IC50 NIL (nM)	300	3500	4550
IC50 DAS (nM)	13.8	54	119

Table 6.2: The $IC50^{IM}$, $IC50^{NIL}$ and $IC50^{DAS}$ of the KU812 2μM IM1 and 2μM IM2 cell lines compared to the KU812 Naïve cell line
Both the KU812 2μM IM1 and 3μM IM2 cell lines have increased IC50s for all three TKIs compared to the Naïve control. IC50 assays determine the concentration of TKI required to reduce levels of p-Crkl (a BCR-ABL adapter protein) by 50%. For Western blots, see *Appendix I.14, I.15 and I.16.*

Table 6.3

	No mutation		F359C mutation	
	Naive	**200nM IM3**	**300nM IM3**	**2μM IM3**
IC50 IM (μM)	6.1	24.2	49	>100
IC50 NIL (nM)	300	660	>10,000	>10,000
IC50 DAS (nM)	12.3	25.3	16.5	16
BCR-ABL expression	443%	990%	633%	733%

Table 6.3: The KU812 2μM IM3 cell line exhibits differential resistance to IM, NIL and DAS
IC50 values for IM, NIL and DAS compared with BCR-ABL expression in key intermediate lines of the KU812 2μM IM3 cell line. Note the highest BCR-ABL expression levels were accompanied by the highest $IC50^{DAS}$ in the 200nM intermediate (pink). However, a significant decrease in BCR-ABL expression and the emergence of the F359C mutation accompanied a rise in imatinib and nilotinib IC50 in the 300nM intermediate (purple), while dasatinib IC50 decreased. For Western blots, see *Appendix I.17, I.18 and I.19.*

Figure 6.5: Nilotinib IC50 and viability of the K562 2µM IM1 and IM2 cell lines

The K562 2µM IM1 and IM2 cell lines are both significantly more resistant to nilotinib than the K562 Naïve control, and the IM2 cell line is significantly more resistant than the IM1 cell line.

(A) Average IC50 of the K562 Naïve and K562 2µM IM1 and IM2 cell lines. Data are presented as mean +SEM of data from at least 4 independent experiments. The $IC50^{IM}$ for both K562 2µM IM1 and IM2 were significantly greater than the Naïve control (**P*<0.00001). By IC50, the IM1 and IM2 cell lines were not significantly different, but a significant difference was seen in viability experiments.

(B) Nilotinib viability assay by trypan blue analysis. Cells were cultured in the presence of various nilotinib concentrations for three days before trypan blue cell counts were performed. Counts were normalised to viable cells in 0nM drug control well (100%). Data are presented as mean ±SD of at least 3 independent experiments. (**P*<0.00002; ***P*<0.03)

(C) Nilotinib viability by annexin V and 7AAD staining. Cells were treated as in part (B). Dying and apoptotic cells were stained with both annexin V and 7AAD, before being analysed by flow. Live cells were defined as those negative for both annexin V and 7AAD staining. Counts were normalised to live cells in the 0nM drug control (100%). Data are presented as mean ±SD of at least 3 independent experiments (**P*<0.02; ***P*<0.009). For Western blots, see *Appendix I.20.*

Figure 6.5

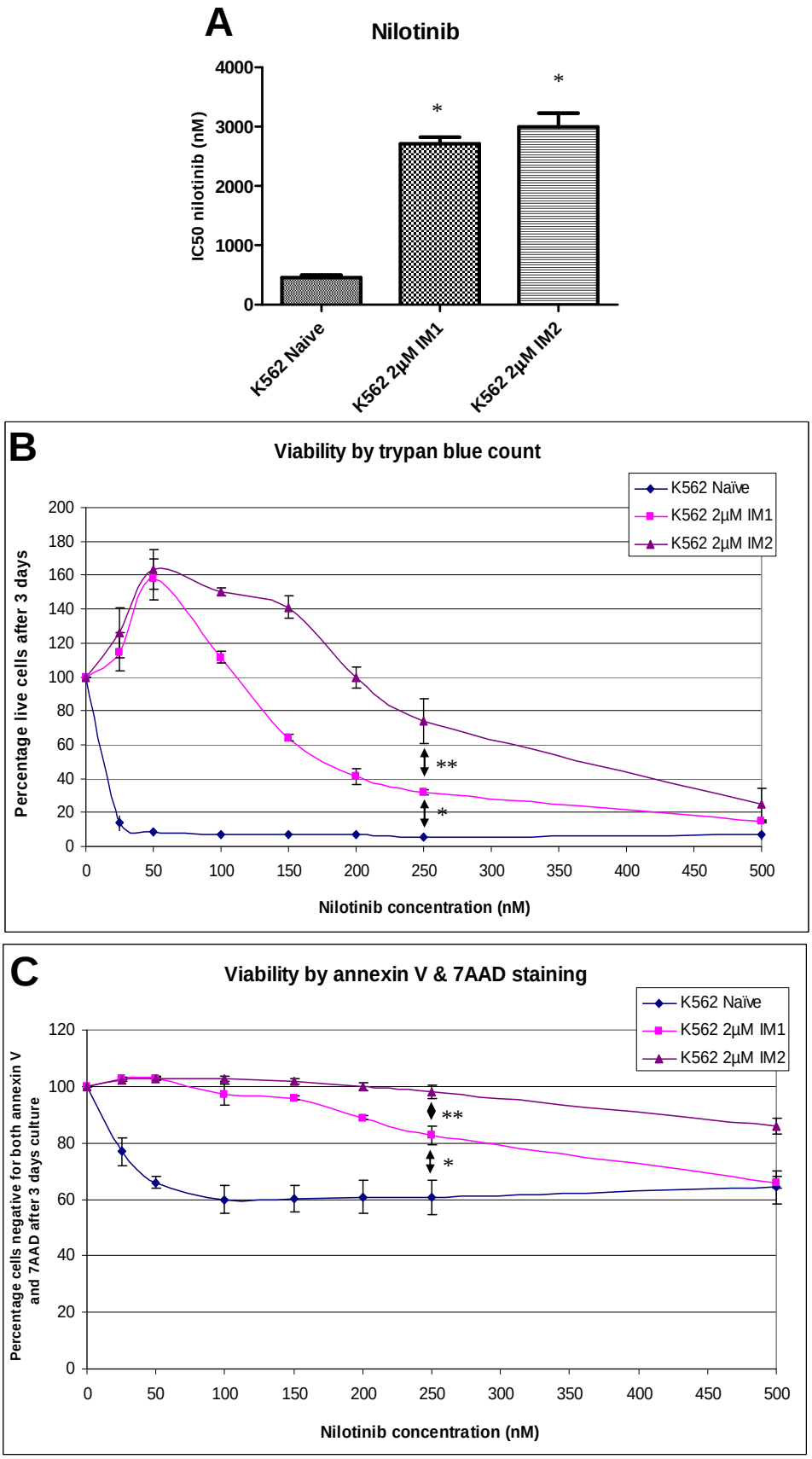
A
Nilotinib
IC50 nilotinib (nM)
4000
3000
2000
1000
0
*
*
K562 Naive
K562 2µM IM1
K562 2µM IM2
B
Viability by trypan blue count
K562 Naïve
K562 2µM IM1
K562 2µM IM2
Percentage live cells after 3 days
200
180
160
140
120
100
80
60
40
20
0
**
*
0
50
100
150
200
250
300
350
400
450
500
Nilotinib concentration (nM)
C
Viability by annexin V & 7AAD staining
K562 Naïve
K562 2µM IM1
K562 2µM IM2
Percentage cells negative for both annexin V and 7AAD after 3 days culture
120
100
80
60
40
20
0
**
*
0
50
100
150
200
250
300
350
400
450
500
Nilotinib concentration (nM)

The $IC50^{DAS}$ had significantly increased in both cell lines from 11.7nM in the K562 Naïve control to 34.8nM and 16.7nM in the K562 2µM IM1 and IM2 cell lines respectively (**Figure 6.6**). However, this time, the K562 2µM IM1 cell line had a significantly greater $IC50^{DAS}$ than the IM2 cell line (P<0.0005). Three-day viability experiments (both trypan blue cell counts and flow cytometry) confirmed that in the presence of 2-3nM dasatinib, the IM-resistant cell lines had significantly increased survival above that of the Naïve cell line (P<0.00001 by trypan blue count and flow cytometry) (**Figure 6.6**). However, in concordance with the IC50 results, the K562 2µM IM1 cell line was significantly more resistant than the IM2 cell line (P<0.00013 and P<0.000004 by trypan blue count and flow cytometry respectively) (**Figure 6.6**).

The K562 2µM IM2 cell line only had a third of the BCR-ABL expression evident in the K562 2µM IM1 cell line (**Figure 3.11**) and seemed to be more resistant to imatinib and nilotinib than the K562 2µM IM1 cell line (**Figure 3.4, 3.8 & 6.5**), but less resistant to dasatinib (**Figure 6.6**). The sensitivity of the K562 2µM IM2 cell line to dasatinib suggested a role for Src kinase overexpression in this cell line, even though the hypothesis of a BCR-ABL independent mechanism does *not* predict an *increased* imatinib or nilotinib IC50. Nevertheless, RQ-PCR was conducted on the K562 2µM IM2 cell line and all its intermediates to confirm or exclude Lyn involvement in mediating resistance. Interestingly, Lyn mRNA was found to be expressed at levels approximately 5-fold higher in the K562 2µM IM2 cell line than in the K562 Naïve control (P<0.0005), while the K562 2µM IM1 cell line exhibited no increased expression in Lyn mRNA (**Figure 6.7**). Lyn expression was already significantly increased in the 1.4µM IM2 intermediate (P<0.00003), and appeared to have an increasing trend in the earlier 600nM-800nM IM2 intermediates (**Figure 6.7**).

Figure 6.6: Dasatinib IC50 and viability of the K562 2μM IM1 and IM2 cell lines

The K562 2μM IM1 and IM2 cell lines are both significantly more resistant to dasatinib than the K562 Naïve control, and the IM1 cell line is significantly more resistant than the IM2 cell line.

(A) Average IC50 of the K562 Naïve and K562 2μM IM1 and IM2 cell lines. Data are presented as mean +SEM of data from at least 4 independent experiments. The $IC50^{IM}$ for both K562 2μM IM1 and IM2 were significantly greater than the Naïve control. **P*<0.01.

(B) Dasatinib viability assay by trypan blue analysis. Cells were cultured in the presence of various dasatinib concentrations for three days before trypan blue cell counts were performed. Counts were normalised to viable cells in 0nM drug control well (100%). Data are presented as mean ±SD of at least 3 independent experiments. (**P*<0.00001; ***P*<0.0002).

(C) Dasatinib viability by annexin V and 7AAD staining. Cells were treated as in part (B). Dying and apoptotic cells were stained with both annexin V and 7AAD, before being analysed by flow. Live cells were defined as those negative for both annexin V and 7AAD staining. Counts were normalised to live cells in the 0nM drug control (100%). Data are presented as mean ±SD of at least 3 independent experiments (**P*<0.00001). For Western blots, see *Appendix I.20.*

Figure 6.6

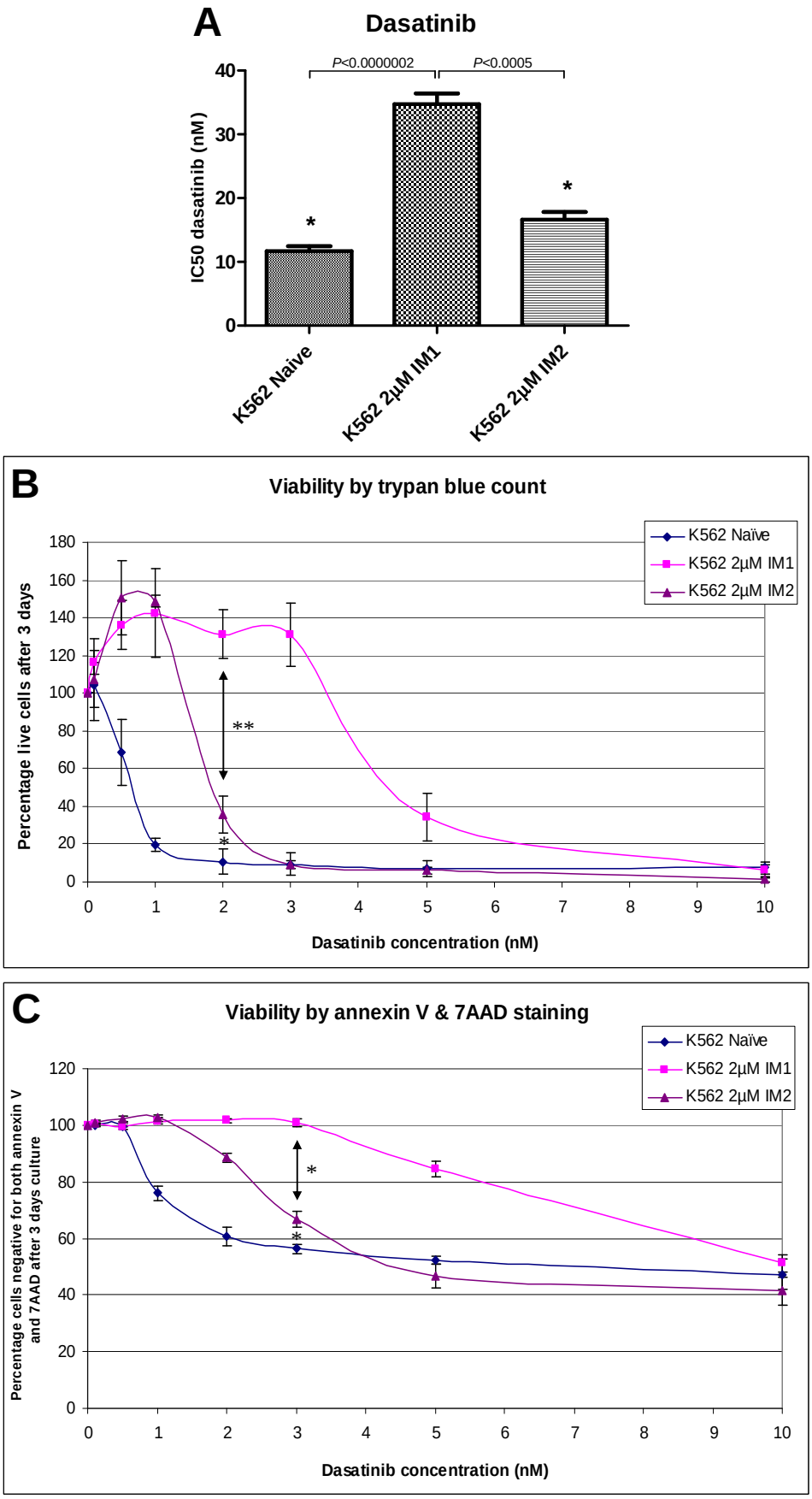
A
Dasatinib
P<0.0000002
P<0.0005
IC50 dasatinib (nM)
0
10
20
30
40
*
*
K562 Naïve
K562 2µM IM1
K562 2µM IM2
B
Viability by trypan blue count
K562 Naïve
K562 2µM IM1
K562 2µM IM2
Percentage live cells after 3 days
0
20
40
60
80
100
120
140
160
180
**
*
0
1
2
3
4
5
6
7
8
9
10
Dasatinib concentration (nM)
C
Viability by annexin V & 7AAD staining
K562 Naïve
K562 2µM IM1
K562 2µM IM2
Percentage cells negative for both annexin V and 7AAD after 3 days culture
0
20
40
60
80
100
120
*
*
0
1
2
3
4
5
6
7
8
9
10
Dasatinib concentration (nM)

Figure 6.7

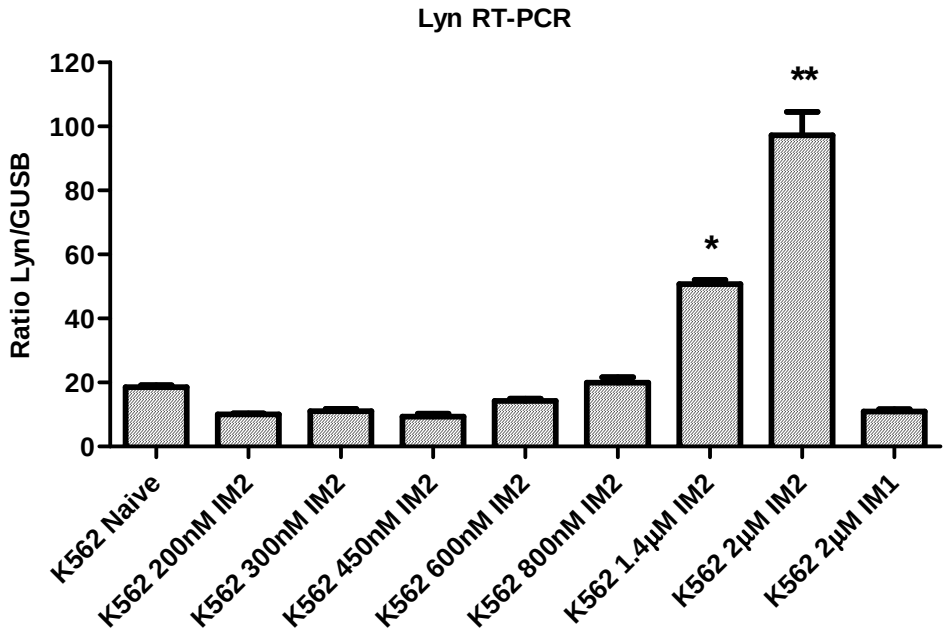

Figure 6.7: Lyn kinase expression was significantly increased in the K562 2µM IM2 cell line

Lyn expression was significantly greater in the K562 1.4µM IM2 intermediate and the 2µM IM2 cell line compared to the K562 Naïve control (**P*<0.00003; ***P*<0.0005). Samples were taken at intermediate stages of resistance development, and cDNA was synthesised using the RNA extracted from 1×10^7 cells. RQ-PCR was conducted using cDNA as the template, and Lyn mRNA expression was determined as a ratio of GUSB mRNA expression. Data are presented as mean +SEM from 3 independent experiments.

6.4 Discussion

In this study, eight imatinib- and three dasatinib-resistant cell lines were generated using the K562, K562 Dox and KU812 cell lines. While it was expected that each cell line would be resistant to the TKI in which it was cultured, it was not known whether these cell lines would also display resistance to other TKIs, and to what extent. In order to investigate TKI-cross resistance, IC50 analysis and viability studies were conducted, with interesting results.

6.4.1 TKI-cross resistance

Cell-lines displaying overt cross resistance to the three TKI's tested included the K562 200nM DAS cell line (harbouring the T315I mutation), K562 2µM IM1 and K562 Dox 200nM DAS2 (BCR-ABL overexpression), K562 Dox 2µM IM1, IM2 and IM3 (ABCB1 overexpression) and KU812 2µM IM1 and 3µM IM2 (BCR-ABL overexpression and kinase domain mutations) (**Table 6.4**). Thus, different cell lines exposed to different TKIs (imatinib or dasatinib) utilised various BCR-ABL-dependent resistance mechanisms that resulted in TKI-cross resistance. Of particular note was that both BCR-ABL overexpression and ABCB1 appeared to be sufficient to mediate resistance to all three drugs, even though ABCB1 has never been reported as a sole resistance mechanism in the clinical setting, nor has BCR-ABL overexpression been shown to be responsible for dasatinib or nilotinib resistance in patients.

One reason that BCR-ABL overexpression has not been observed to cause dasatinib or nilotinib resistance *in vivo*, may be that these drugs have only recently begun to be trialled as first line therapies. Hitherto, the second generation TKIs have predominantly been used in cases of imatinib therapy failure, where KD mutations have often already developed. It has been suggested that sequential TKI therapy merely selects for compound mutations[237], or that the presence of an imatinib-resistant KD mutations indicates a propensity to develop further mutations (as NIL and DAS resistant mutations were detectable at very low levels in 43/210 patients at the time of imatinib therapy failure[251]). Thus, when a patient is switched to dasatinib or nilotinib the 'preferred' resistance mechanism appears to be KD mutations rather than BCR-ABL overexpression. Due to the greater potency of nilotinib and dasatinib (compared to imatinib) BCR-ABL overexpression in imatinib-relapse

Table 6.4

	KU812			K562 Dox					K562		
Cell line	IM1	IM2	IM3	IM1	IM2	IM3	DAS1	DAS2	IM1	IM2	DAS
Overt resistance to IM, NIL and DAS	✓	✓	IM and NIL only	✓	✓	✓	DAS only	✓	✓	IM and NIL only	✓
KD Mutation	E450Q E459K E470K	E459K E462K E466E	F359C	x	x	x	V299L	x	x	x	T315I
Increased ABCB1 cell-surface expression	x	x	x	✓	✓	✓	x	x	x	x	x
Increased BCR-ABL expression	✓	✓	✓	x	x	x	✓	✓	✓	✓	✓
BCR-ABL 'independent' resistance	x	x	x	x	x	x	x	x	x	Lyn	x

Table 6.4: Summary of resistance mechanisms detected in the eleven imatinib- or dasatinib-resistant cell lines generated in this study

See Table 5.1 for results of the imatinib- nilotinib- and dasatinib-resistant 'Re-escalated' cultures. ✓= yes; **x** = no.

patients may be overcome in the first instance, as it may be below the threshold of expression required to confer NIL or DAS resistance.

It is unclear why ABCB1 overexpression is not observed more frequently in the clinical setting as a major resistance mechanism causing TKI-cross resistance. Intracellular uptake and retention of TKIs is influenced by various factors, including plasma protein binding[181] and OCT-1 activity in the case of imatinib[53]. As yet unidentified efflux transporters may also play a role.

6.4.2 Differential resistance

Differential resistance occurs when the resistance mechanism(s) that have emerged in response to one TKI do not confer resistance to the same extent in the presence of another TKI. In the context of CML, this is predominantly the result of specific KD mutations and is frequently observed in patients[33,120,121]. Here, the V299L mutation was identified in the K562 Dox 200nM DAS1 cell line – a mutation which is thought to confer resistance to dasatinib, yet is sensitive to nilotinib and imatinib[120,121]. Additionally, the KU812 2µM IM3 cell line was found to carry the F359C mutation which confers resistance to imatinib and nilotinib, yet is sensitive to dasatinib[120,240,241].

The marginal dasatinib resistance displayed by the KU812 2µM IM3 cell line ($IC50^{DAS}$ had increased from 12.3nM in the Naïve control, to 16nM) was likely due to the increase in BCR-ABL expression alone (from 443% in the KU812 Naïve cell line to 733% in the 2µM IM3 cell line; **Table 6.3**) rather than the F359C mutation. This hypothesis was supported by the finding that the 200nM IM3 intermediate (in which BCR-ABL expression peaked) displayed the highest $IC50^{DAS}$ of all intermediates. Similarly, the K562 Dox 200nM DAS1 cell line displayed modest increases in $IC50^{NIL}$ and $IC50^{IM}$ (2.1 and 3.2-fold increases respectively) compared with the large increase in $IC50^{DAS}$ (approximately 50-fold increase over the K562 Dox Naïve control). Again, the resistance to nilotinib and imatinib was likely the result of BCR-ABL overexpression (from 186% in K562 Dox Naïve cells, to 540% in the K562 Dox 200nM DAS1 cell line) as IC50 values for these TKIs peaked in the 55nM DAS1 intermediate in which BCR-ABL expression levels peaked at 850% (**Table 6.1**). The most intriguing case of differential resistance in this study was found in the K562 2µM IM2 cell line.

6.4.3 Lyn overexpression in the K562 2μM IM2 cell line: Is it really a BCR-ABL-independent resistance mechanism?

The IC50 assay measures the level of BCR-ABL kinase inhibition through the surrogate marker, p-Crkl. In cases of BCR-ABL independent resistance, one would expect that BCR-ABL may be efficiently inhibited by a TKI (*i.e.* low IC50 values, which normally indicate sensitivity) despite increased viability in that TKI. However, in the case of the K562 2μM IM2 cell line, it appeared that the IC50 results *correlated* with the viability experiment results. At first, this finding seemed counterintuitive, as a BCR-ABL independent resistant mechanism such as Lyn kinase overexpression was not expected to give a BCR-ABL dependent readout (*i.e.* an increased IC50 value). How, then, was Lyn kinase overexpression mediating an increased $IC50^{IM}$ and $IC50^{NIL}$?

In 2000, Schindler *et. al.*[22] found that Hck phosphorylates the kinase domain of Abl, and in 2003 Donato *et. al.*[156] suggested that Lyn may also mediate phosphorylation of BCR-ABL itself, as it is closely related to Hck. Some groups have demonstrated a role for Hck and Lyn phosphorylation of the BCR-ABL Y177 residue in regulating BCR-ABL transforming potential[250,252]. In 2006 Meyn *et. al.*[253] demonstrated that Fyn, Hck and Lyn strongly phosphorylate the SH3-SH2 region of BCR-ABL. Lyn predominantly phosphorylates the Y89 residue, and to a lesser extent, the Y191 and Y158 residues of c-Abl, all of which lie along the interface between the SH3-SH2 region and the Abl kinase domain. Thus, it was postulated that phosphorylation of residues along this interface could influence BCR-ABL kinase activity by stabilising it in the active conformation[253]. Indeed, it was more recently shown that Y89 phosphorylation by Src family kinases prevents the Abl SH3 domain from interacting with the SH2-kinase linker (*i.e.* prevents adoption of the inactive conformation), leading to enhanced Abl kinase activity and cellular signalling[254]. As imatinib and nilotinib can only bind BCR-ABL in the inactive conformation[255], it appears that Lyn phosphorylation of Y89 may be mediating BCR-ABL-dependent resistance. Thus, through direct phosphorylation and activation of BCR-ABL, Lyn overexpression mediated increased IC50 values (specifically for imatinib and nilotinib) as BCR-ABL was able to continue to phosphorylate Crkl at higher TKI concentrations. Therefore, it appears that Src kinase overexpression may not be a truly BCR-ABL-*independent* resistance mechanism. The K562 2μM IM2 cell line's sensitivity to dasatinib (as demonstrated with IC50 and viability experiments) was expected, as dasatinib is able to inhibit both BCR-ABL and Lyn molecules.

Chapter 7:

Discussion

7.1 Introduction

Chronic myeloid leukaemia is characterised by the presence of the Philadelphia chromosome in cells of haematopoietic lineage[256]. The Philadelphia chromosome results from the reciprocal translocation between chromosomes 9 and 22, and harbours the Bcr-Abl fusion gene[6]. The BCR-ABL protein is a constitutively active tyrosine kinase that activates signalling pathways promoting proliferation and inhibiting apoptosis[8]. Imatinib mesylate is a rationally designed tyrosine kinase inhibitor (TKI) that is able to bind and inhibit BCR-ABL and its introduction has revolutionised CML therapy and patient outcome[20].

Despite excellent overall responses, however, many patients develop resistance to imatinib treatment – approximately 10% of chronic phase patients, 40-50% of patients in accelerated phase and 80% of patients in blast crisis[7]. This led to the development of second generation TKIs, nilotinib and dasatinib. Although these drugs have proven effective in many cases of imatinib-resistance, resistance to nilotinib and dasatinib has also been noted in patients[120,237]. In particular, the T315I mutation in the BCR-ABL kinase domain (KD) is known to prevent all three TKIs binding to BCR-ABL, leading to overt TKI cross-resistance[107,119,121].

7.2 TKI resistance mechanisms

Primary resistance, where the patient fails to achieve any recovery benchmarks after starting imatinib therapy, is typically mediated by factors that are intrinsic to the patient. For example, gastrointestinal absorption of imatinib[257], polymorphisms in CYP3A4 (responsible for hepatic metabolism of imatinib[258]), protein plasma binding[259], and the expression and activity of the imatinib influx protein, OCT-1[40,52,53] and efflux transporters, ABCB1 and ABCG2[74,75] in haematopoietic cells may all contribute to primary resistance[227].

After two years of imatinib therapy, approximately 10% of patients in chronic phase, 40-50% of patients in accelerated phase and 80% of patients in blast crisis will exhibit secondary resistance[7]. Secondary resistance is defined as the loss of response milestones or disease progression while on treatment. This is most commonly the result of mutations in the BCR-ABL KD[107,119] BCR-ABL amplification (*e.g.* through duplication of the Philadelphia chromosome, homogeneously staining

regions or double minutes)[138,139,142], or the emergence of other genetic abnormalities that result in BCR-ABL independent oncogenicity[81,83,244]. These mechanisms are not mutually exclusive, and when combined with patient intrinsic factors (*e.g.* primary resistance mechanisms) may result in a disease that is refractory to TKI therapy. In such cases, allogeneic stem cell transplant may be the only treatment alternative, however, not all patients will be eligible.

7.3 Studying the kinetics of TKI resistance mechanism emergence

In order to identify patients who are at risk of developing overt TKI resistance, it is important to understand the kinetics of resistance mechanism emergence (*e.g.* whether some mechanisms tend to arise first and/or predispose the emergence of other mechanisms). This study focuses on secondary resistance mechanism emergence. Previously, several groups have generated imatinib-resistance *in vitro* however these studies either did not investigate the kinetics of resistance mechanism emergence[139,127], or used murine cell lines transfected with Bcr-Abl[161]. In the present study, three human, CML cell lines (KU812, K562 and its derivative K562 Dox) were exposed to gradually increasing concentrations of imatinib or dasatinib up to pharmacologically relevant concentrations (2μM and 200nM respectively). Critically, cultures were sampled at each intermediate stage of resistance generation to identify any resistance mechanisms that may have emerged and ultimately identify trends in resistance development. Furthermore, this study documents the first instance of imatinib resistance in the KU812 cell line, and the first time dasatinib-resistance has been generated in any human CML cell line. Thus, the kinetics of *in vitro* resistance mechanism emergence for both imatinib and dasatinib could be compared and contrasted for the first time.

There are inherent limitations in the use of cell lines for such a study. The CML cell lines used here originated from patients in blast crisis, and may have contained chromosomal abnormalities not usually present in patients with early chronic phase CML. Other genetic changes may also occur when primary patient cells are immortalised to make cell lines. It is therefore acknowledged that the findings of this study may more closely resemble the kinetics of resistance development observed in the more advanced stages of the disease. Regardless, the resulting imatinib- and dasatinib-resistant cell lines generated in this study displayed resistance mechanisms similar to those observed in TKI-resistant patients who may still be classified as chronic phase[127,139,161].

7.4 Major findings of this study

Eleven TKI-resistant cell lines were generated displaying various levels of resistance to different TKIs, and various resistance mechanisms (**Table 6.4**). Eight imatinib-resistant cell lines, one imatinib-resistant 're-escalated' cell line, three dasatinib-resistant cell lines, three dasatinib-resistant 're-escalated' cell lines, and two nilotinib-resistant 're-escalated' cell lines (**Table 5.1**) were established, for a total of 17 TKI resistant cell lines.

7.4.1 Kinase domain mutations arise in the setting of BCR-ABL overexpression

Of the original eleven TKI-resistant cell lines generated, five developed KD mutations as a mode of resistance. Of these, all five displayed BCR-ABL overexpression prior to the detection of the mutation. Furthermore, the re-escalated K562 Dox 500nM NIL1 RE55 cell line also exhibited gradually increasing BCR-ABL expression levels before the emergence of the G250E mutation (**Table 6.4**). The K562 2µM IM1 and IM2, K562 Dox 500nM NIL2 and K562 Dox 200nM DAS2 cell lines were the only exceptions, where BCR-ABL overexpression was not followed by a KD mutation (**Table 6.4**). However, if escalation was continued, as was the case in the KU812 3µM IM2 cell line, KD mutations may have eventually emerged. These results suggest that BCR-ABL overexpression may not always give rise to KD mutations, but that the emergence of KD mutations may require BCR-ABL overexpression.

Another interesting observation was that, upon the emergence of a KD mutation, BCR-ABL overexpression became redundant and diminished. These kinetics of resistance emergence may be explained by one of two clonal mechanisms. Firstly, it may be that early in TKI escalation, two different clones may have mutated such that one acquired a KD mutation only, while the other developed BCR-ABL overexpression only. At low TKI concentrations, both clones may have been equally viable and continued to grow. However, as TKI concentration was escalated, the mutation-carrying clone was able to survive and expanded, while BCR-ABL overexpression in the latter clone was not sufficient in higher TKI concentrations, causing this clone to decline. The sudden, significant decrease in BCR-ABL expression levels upon the emergence of the KD mutation may reflect a threshold concentration of TKI at which BCR-ABL overexpression (which must itself be just below levels that are toxic to the cell) becomes insufficient to allow survival in the presence of TKI. Therefore, this clone is rapidly lost, while the second clone is able to rapidly increase. The second possibility is that double minutes, some

carrying wild-type and some carrying mutant Bcr-Abl, are present in a single clone which populates the culture. As TKI concentration is increased, daughter cells that happen to contain higher numbers of mutant Bcr-Abl, but not necessarily higher numbers of total Bcr-Abl, are selected and thrive. Again, the sudden and significant decrease in BCR-ABL expression in KD-carrying cell lines may be due to reaching a threshold TKI concentration at which daughter cells with more total Bcr-Abl (but fewer mutant Bcr-Abl-carrying dmin) are no longer viable, leaving only those cells with lower total Bcr-Abl but carrying high percentages of mutant Bcr-Abl. Both explanations provide plausible theories to explain the results for the six cell lines in this study that developed BCR-ABL overexpression, followed by the emergence of a KD mutation(s) and a subsequent significant decrease in BCR-ABL expression levels (the K562 200nM DAS, K562 Dox 200nM DAS1, K562 Dox 500nM NIL1 RE55, KU812 2µM IM1, 3µM IM2 and 2µM IM3 cell lines) (see *Chapter 5*).

These findings are in agreement with clinical studies that have a found a 2–2.6 fold rise in BCR-ABL expression correlates with the emergence of KD mutations[162,163]. However, after acquiring a KD mutation, a subsequent *decrease* in BCR-ABL overexpression has not been noted in patients. This may be because the leukaemic burden is increasing in such cases (as the patient is relapsing), and a decrease in BCR-ABL expression per cell may be masked by an increase in the number of circulating leukaemic cells.

7.4.2 Resistance mechanism emergence is stochastic

Of particular note, was that different mutations and even different resistance mechanisms emerged in the same cell line each time it was cultured in a given TKI. For example, although all three IM-resistant KU812 cell lines developed KD mutations, these mutations were different for each cell line. In the KU812 2µM IM1 and 3µM IM2 cell lines the E459K mutation (along with several bystander mutations, different for each cell line) emerged, while in the KU812 2µM IM3 cell line the F359C mutation developed. Furthermore, the V299L mutation was detected in the K562 Dox 200nM DAS1 cell line, but no mutation at all was found in the K562 Dox 200nM DAS2 cell line. Additionally, the K562 Dox 500nM NIL1 RE55 cell line developed the G250E mutation, while the NIL2 cell line only displayed a further increase in BCR-ABL expression. Finally, the K562 2µM IM1 cell line had BCR-ABL overexpression as the only detectable resistance mechanism, while the K562 2µM IM2 cell line developed Lyn overexpression. Thus, the particular KD mutation and/or resistance mechanism to emerge was

different each time, even though the same cell line and TKI was used. These differences were likely due to the fact that drug escalation was not performed identically for each cell line – *i.e.* slightly different intermediate drug concentrations and/or different time periods between drug escalations. Thus, something as subtle as the confluency or temperature of a culture, or the rate at which TKI concentration was increased could have affected which mutations emerged and also which mutant clones thrived. The repeated emergence of the V299L mutation in re-escalation of K562 Dox 200nM DAS1 intermediates (and the F359C mutation upon re-escalation of the KU812 200nM IM3 culture) was likely due to the fact that clones carrying these mutations were already present at undetectable levels, and were merely yet to be expanded under the right selective pressure.

Some cell lines appeared to be predisposed to certain resistance mechanisms, for example when imatinib-resistant cultures of the K562 Dox cell line were generated (2μM IM1, IM2 and IM3) all uniformly displayed a further increase in ABCB1 expression. Thus, while resistance-mechanism emergence appears to be stochastic, there are cases where cells are predisposed to a particular mechanism due to prior selection. In fact, this result may be paralleled with the results of the re-escalation studies, where the emergence of the V299L or F359C mutations were predisposed due to the presence of unexpanded clones. Similarly, the K562 Dox cell line had been previously selected in doxorubicin, resulting in the emergence and expansion of an ABCB1-overexpressing clone. Further culture in a drug that is transported by ABCB1 would be expected to continue the selection process that had already been started. If dasatinib is also transported by ABCB1, why then did dasatinib cultures of K562 Dox not result in the same phenotype?

7.4.3 Different TKIs may foster different resistance mechanisms

In this study it was also noted that different TKIs resulted in the emergence of different resistant mechanisms even when using the same cell line. For example, when K562 Dox cells were exposed to imatinib on three separate occasions, further ABCB1 overexpression occurred. However, when the same cell line was exposed to dasatinib, BCR-ABL overexpression and KD mutations emerged, while ABCB1 expression did not change or decreased. This was a surprising observation, considering that dasatinib is transported by ABCB1, but may be explained by the potency of dasatinib compared to imatinib. Dasatinib is 300× more potent than imatinib, meaning that efflux of dasatinib may never reduce dasatinib IUR to levels low enough to allow survival. Thus, ABCB1 overexpression did not

become the dominant resistance mechanism when this cell line was exposed to dasatinib. A deficiency in this study was the failure to monitor ABCB1/ABCG2 expression at all intermediate time points in all cell lines. If it had been interrogated, it may have been found that ABCB1 expression initially increased in both DAS-resistant K562 Dox cell lines, but was superseded by BCR-ABL overexpression and KD mutations. Thus, by the time the final 200nM DAS resistant cell lines were characterised, ABCB1 overexpression was no longer the dominating mode of resistance and had declined. In order to test this, early intermediate cultures of the K562 Dox 200nM DAS1 and DAS2 cell lines could be thawed out, expanded, and analysed by flow cytometry for ABCB1 expression levels.

The K562 cell line also displayed different resistance mechanisms depending on which TKI it was exposed to. In the case of dasatinib exposure, the T315I mutation emerged, but in the case of imatinib exposure, BCR-ABL overexpression and/or Lyn overexpression was sufficient to promote survival. Again, these results may reflect the difference in potency of these two drugs – as the presence of imatinib could be overcome by simply increasing the number of targets (BCR-ABL overexpression in the K562 2µM IM1 cell line) while in the presence of the dasatinib (~300 times more potent) BCR-ABL expression levels had to peak much higher (and at an earlier intermediate) and even then was insufficient and eventually superseded. Thus, it is likely that a difference in TKI potency and dosage was responsible for the observation that different TKIs fostered the emergence of different resistance mechanisms *in vitro*.

7.4.4 Different cell lines responded differently to a given TKI

In this study, a variety of resistance mechanisms emerged in response to long-term imatinib exposure. The KU812 cell line developed kinase domain mutations, the K562 Dox cell line exhibited further ABCB1 overexpression, while BCR-ABL overexpression and Lyn overexpression were observed in the K562 cell line. The upregulation of ABCB1 in the K562 Dox cell line, as stated previously, is likely due to prior selection by doxorubicin already promoting this mechanism. This explains why imatinib-resistance in the parental K562 cell line would not necessarily follow the same path to resistance. As the KU812 and K562 cell lines were both established from two different patients, it was expected that these cell lines would have intrinsic differences which may contribute to the resistance mechanisms that emerged. For example, anecdotal evidence suggests the KU812 cell line is inherently the most TKI-sensitive cell line used in this study[127,164]. With different karyotypes present in every population,

and differences in OCT-1 activity, plasma protein binding *etc.* it is no surprise that different patients (and therefore different cell lines) respond differently to a given TKI. Despite the differences in imatinib-resistance mechanisms, both dasatinib and imatinib were able to induce BCR-ABL overexpression and KD mutations across all three cell lines.

7.4.5 TKIs share the same broad resistance susceptibilities

In this study it was found that cross-resistance to imatinib, nilotinib and dasatinib was shared by 8/11 cell lines (**Table 6.4**). The remaining 3 cell lines that did not display cross-resistance either harboured KD mutations that are known to cause differential resistance, or Lyn kinase expression that is known to be sensitive to dasatinib treatment. These results suggest that the three TKIs tested share common resistance mechanisms and are broadly susceptible to BCR-ABL overexpression, ABCB1/ABCG2 expression, and the T315I mutation, even though these mechanisms may not be selected for by a particular TKI.

In the clinical setting of imatinib resistance, switching to a second-line drug only results in a 40-50% rate of complete cytogenetic remission (CCR), even when detectable KD mutations are predicted to be sensitive to the second-line drug[120]. This is consistent with the findings of this study – that multiple resistance mechanisms are usually present in a TKI-resistant population and contribute to overt TKI resistance, and that different mechanisms in the one population may confer resistance to different TKIs.

7.4.6 Src kinase overexpression may not be a BCR-ABL *independent* resistance mechanism

Src kinase overexpression has previously been suggested to be a BCR-ABL independent resistance mechanism, as resistance is thought to be mediated through the survival signalling of other kinases (*e.g.* Lyn or Hck) regardless of BCR-ABL activity[155,125] . In the present study, it was shown that Lyn overexpression resulted in an increased imatinib and nilotinib IC50 in the K562 2μM IM2 cell line – unexpected if there is no involvement of BCR-ABL in Lyn's mode of activity. It has been suggested that Lyn actually phosphorylates BCR-ABL, maintaining BCR-ABL in the active conformation[253,254], thereby resulting in overt imatinib and nilotinib resistance (as these TKIs can only bind BCR-ABL in

the inactive conformation[255]). Notably, Wu *et. al.*[250] suggest that "Lyn regulates BCR-ABL…phosphorylation" and that "Lyn exists as a component of the BCR-ABL signalling complex". Therefore Lyn overexpression may not be acting *independently* of BCR-ABL, but rather, enhancing and conserving BCR-ABL kinase activity in the presence of TKIs.

7.5 Future directions

As a result of the findings of this study, other avenues of investigation have become apparent, and are being undertaken in our laboratory.

- Clonal studies of key intermediate cultures in the development of resistance to give an insight into the make-up of heterogeneous cell populations and the nature of the clones which may be competing for dominance.
- Lyn knockdown/inhibition in cells overexpressing this kinase. By measuring BCR-ABL phosphorylation and p-Crkl IC50 values it will be determined whether Lyn is acting directly on BCR-ABL as hypothesised.
- Screening CML patients for Lyn expression, and correlating these results with treatment outcome.
- The third generation TKI 'ponatinib' has recently become available. This drug has been rationally designed to inhibit both wild-type and T315I mutated BCR-ABL, and a study of resistance-mechanism generation using ponatinib has already been commenced.

7.6 Summary & Conclusion

This study has generated a total of 17 TKI-resistant human, CML cell lines in order to investigate resistance pathways and the kinetics of resistance mechanism emergence for both imatinib and dasatinib.

Of these 17 cell lines, six were re-escalated cultures of key intermediate stages of imatinib and dasatinib resistance in the KU812 and K562 Dox cell lines. This work demonstrated that clones carrying clinically relevant KD mutations may be present below the threshold of detection of even the most sensitive sequencing methods available. Of the remaining 11 cell lines, five developed KD mutations which only emerged in the setting of BCR-ABL overexpression. This finding highlights the

importance of routine monitoring of BCR-ABL expression levels in TKI-treated CML patients, as even modest increases in BCR-ABL expression may indicate the presence or imminent emergence of KD mutations. ABCB1 or BCR-ABL overexpression alone appeared to be responsible for resistance in another five cell lines, and were notably able to cause cross-resistance to the three TKIs tested in this study. Lastly, one cell line utilised a combination of BCR-ABL and Lyn overexpression which resulted in overt imatinib and nilotinib resistance. IC50 results suggested that Lyn activity (in the context of CML TKI-resistance) may operate in a BCR-ABL dependent manner.

Importantly, these studies suggest that KD mutation emergence is a stochastic event (in the absence of pre-selected clones) but may be stimulated by increased BCR-ABL expression levels. Notably, different TKIs elicited different resistant mechanisms, but all appeared to be (at least to some extent) BCR-ABL dependent. Furthermore, many resistant cell lines showed cross-resistance to imatinib, nilotinib and dasatinib, suggesting that currently available TKIs share the same broad susceptibilities to drug resistance.

Appendix I

AI.1 Quantitative DNA PCR setup sheet

Worksheet prepared by _____ Q-PCR run date

GUSB	1 sample	no.samp + 2
Master Mix	12.5	0
dH2O	9.35	0
F 50uM	0.2	0.0
R 50uM	0.2	0.0
GUS probe	0.25	0.00

BCRABL	1 sample	no.samp + 2
Master Mix	12.5	0
dH2O	8.85	0
F 50uM	0.2	0.0
R 50uM	0.2	0.0
Probe	0.75	0.00

	1	2	3	4	5	6	7	8	9	10	11	12
A	100000	100000	10000	10000	1000	1000	100	100	10	10	DIL	
B												
C												
D												
E	100	100	10	10	1	1	0.1	0.1	0.01	0.01	DIL	normal DNA mix
F												
G												
H												

AI.2 RQ-PCR for BCR-ABL quantitation setup sheet

Preparation date _____

Performed by _____

	Name or Number	Collection Date	Trans-cript type	RNA 1 or 2	OD 260	OD 280	260/280	µg/µl	2µl SS	2µg RNA µl	DEPC dH_2O (9.6µl total)	
1												1
2												2
3												3
4												4
5												5
6												6
7												7
8												8
9												9
10												10
11												11
12												12
13												13
14												14
15												15
16												16
17												17
18												18
19												19
20												20
21												21
22												22
23												23
24												24
25												25

	RT-PCR Buffer	1 sample (µl)	__ samples (n+1) (µl)	Repeat QPCR samples
Mix 1 (2.4ul)	25mM dNTP	0.4		
	Random Hexamers	2		
Mix 2 (6ul)	5 x 1st Strand Buffer	4		
	DTT	2		

SA PATH 1076/B

BCR-ABL Worksheet prepared by _____ date:_____

BCR	1 sample	no.samp + 2
Master Mix	12.5	0
dH2O	9.55	0
B8 50uM	0.1	0.0
B9 50uM	0.1	0.0
BCR probe	0.25	0.00

B3A2	1 sample	no.samp + 2
Master Mix	12.5	0
dH2O	9.55	0
B3 50uM	0.1	0.0
3A2 50uM	0.1	0.0
B3A2 probe	0.25	0.00

	1	2	3	4	5	6	7	8	9	10	11	12
A	BCR std 6.0e3	BCR std 6.0e4	BCR std 6.0e5	BCR std 6.0e6	Hela	Low control	High control	NTC				
B	NTC											
C												
D												
E	B3A2 std 3.2e1	B3A2 std 3.2e1	B3A2 std 3.2e2	B3A2 std 3.2e2	B3A2 std 3.2e3	B3A2 std 3.2e4	B3A2 std 3.2e5	B3A2 std 3.2e6	Hela	Low control	High control	NTC
F												
G												
H												

AI.4 DNA sequence of the Abl gene

Yellow highlighted section shows position of the kinase domain of Abl. Pink highlights indicate the forward and reverse primers used to sequence the kinase domain.

```
   1 aaaatgttgg agatctgcct gaagctggtg ggctgcaaat ccaagaaggg gctgtcctcg
  61 tcctccagct gttatctgga agaagccctt cagcggccag tagcatctga ctttgagcct
 121 cagggtctga gtgaagccgc tcgttggaac tccaaggaaa accttctcgc tggacccagt
 181 gaaaatgacc ccaacctttt cgttgcactg tatgattttg tggccagtgg agataacact
 241 ctaagcataa ctaaaggtga aaagctccgg gtcttaggct ataatcacaa tggggaatgg
 301 tgtgaagccc aaaccaaaaa tggccaaggc tgggtcccaa gcaactacat cacgccagtc
 361 aacagtctgg agaaacactc ctggtaccat gggcctgtgt cccgcaatgc cgctgagtat
 421 ctgctgagca gcgggatcaa tggcagcttc ttggtgcgtg agagtgagag cagtcctggc
 481 cagaggtcca tctcgctgag atacgaaggg agggtgtacc attacaggat caacactgct
 541 tctgatggca agctctacgt ctcctccgag agccgcttca acaccctggc cgagttggtt
 601 catcatcatt caacggtggc cgacgggctc atcaccacgc tccattatcc agccccaaag
 661 cgcaacaagc ccactgtcta tggtgtgtcc cccaactacg acaagtggga gatggaacgc
 721 acggacatca ccatgaagca caagctgggc gggggccagt acggggaggt gtacgagggc
 781 gtgtggaaga aatacagcct gacggtggcc gtgaagacct tgaaggagga caccatggag
 841 gtggaagagt tcttgaaaga agctgcagtc atgaaagaga tcaaacaccc taacctggtg
 901 cagctccttg gggtctgcac ccgggagccc ccgttctata tcatcactga gttcatgacc
 961 tacgggaacc tcctggacta cctgagggag tgcaaccggc aggaggtgaa cgccgtggtg
1021 ctgctgtaca tggccactca gatctcgtca gccatggagt acctggagaa gaaaaacttc
1081 atccacagag atcttgctgc ccgaaactgc ctggtagggg agaaccactt ggtgaaggta
1141 gctgattttg gcctgagcag gttgatgaca ggggacacct acacagccca tgctggagcc
1201 aagttcccca tcaaatggac tgcacccgag agcctggcct acaacaagtt ctccatcaag
1261 tccgacgtct gggcatttgg agtattgctt tgggaaattg ctacctatgg catgtcccct
1321 tacccgggaa ttgacctgtc ccaggtgtat gagctgctag agaaggacta ccgcatggag
1381 cgcccagaag gctgcccaga gaaggtctat gaactcatgc gagcatgttg gcagtggaat
1441 ccctctgacc ggccctcctt tgctgaaatc caccaagcct ttgaaacaat gttccaggaa
1501 tccagtatct cagacgaagt ggaaaaggag ctggggaaac aaggcgtccg tggggctgtg
1561 agtaccttgc tgcaggcccc agagctgccc accaagacga ggacctccag gagagctgca
1621 gagcacagag acaccactga cgtgcctgag atgcctcact ccaagggcca gggagagagc
1681 gatcctctgg accatgagcc tgccgtgtct ccattgctcc ctcgaaaaga gcgaggtccc
1741 ccggagggcg gcctgaatga agatgagcgc cttctcccca aagacaaaaa gaccaacttg
1801 ttcagcgcct tgatcaagaa gaagaagaag acagccccaa cccctcccaa acgcagcagc
1861 tccttccggg agatggacgg ccagccggag cgcagagggg ccggcgagga agagggccga
1921 gacatcagca acggggcact ggctttcacc cccttggaca cagctgaccc agccaagtcc
1981 ccaaagccca gcaatggggc tggggtcccc aatggagccc tccgggagtc cgggggctca
2041 ggcttccggt ctccccacct gtggaagaag tccagcacgc tgaccagcag ccgcctagcc
2101 accggcgagg aggagggcgg tggcagctcc agcaagcgct tcctgcgctc ttgctccgcc
2161 tcctgcgttc cccatggggc caaggacacg gagtggaggt cagtcacgct gcctcgggac
2221 ttgcagtcca cgggaagaca gtttgactcg tccacatttg gagggcacaa aagtgagaag
2281 ccggctctgc ctcggaagag ggcaggggag aacaggtctg accaggtgac ccgaggcaca
2341 gtaacgcctc cccccaggct ggtgaaaaag aatgaggaag ctgctgatga ggtcttcaaa
2401 gacatcatgg agtccagccc gggctccagc ccgcccaacc tgactccaaa acccctccgg
2461 cggcaggtca ccgtggcccc tgcctcgggc ctcccccaca aggaagaagc tggaaagggc
2521 agtgccttag ggacccctgc tgcagctgag ccagtgaccc ccaccagcaa agcaggctca
2581 ggtgcaccag ggggcaccag caagggcccc gccgaggagt ccagagtgag gaggcacaag
2641 cactcctctg agtcgccagg gagggacaag gggaaattgt ccaggctcaa acctgccccg
2701 ccgcccccac cagcagcctc tgcagggaag gctggaggaa agccctcgca gagcccgagc
2761 caggaggcgg ccggggaggc agtcctgggc gcaaagacaa aagccacgag tctggttgat
2821 gctgtgaaca gtgacgctgc caagcccagc cagccgggag agggcctcaa aaagcccgtg
2881 ctcccggcca ctccaaagcc acagtccgcc aagccgtcgg ggacccccat cagcccagcc
2941 cccgttccct ccacgttgcc atcagcatcc tcggccctgg caggggacca gccgtcttcc
3001 accgccttca tccctctcat atcaacccga gtgtctcttc ggaaaacccg ccagcctcca
3061 gagcggatcg ccagcggcgc catcaccaag ggcgtggtcc tggacagcac cgaggcgctg
3121 tgcctcgcca tctctaggaa ctccgagcag atggccagcc acagcgcagt gctggaggcc
3181 ggcaaaaacc tctacacgtt ctgcgtgagc tatgtggatt ccatccagca aatgaggaac
3241 aagtttgcct tccgagaggc catcaacaaa ctggagaata atctccggga gcttcagatc
3301 tgcccggcga cagcaggcag tggtccagcg gccactcagg acttcagcaa gctcctcagt
3361 tcggtgaagg aaatcagtga catagtgcag aggtagcagc agtcaggggt caggtgtcag
3421 gcccgtcgga gctgcctgca gcacatgcgg gctcgcccat acccgtgaca gtggctgaca
3481 agggactagt gagtcagcac cttggcccag gagctctgcg ccaggcagag ctgagggccc
3541 tgtggagtcc agctctacta cctacgtttg caccgcctgc cctcccgcac cttcctcctc
```

3601 cccgctccgt ctctgtcctc gaattttatc tgtggagttc ctgctccgtg gactgcagtc
3661 ggcatgccag gacccgccag ccccgctccc acctagtgcc ccagactgag ctctccaggc
3721 caggtgggaa cggctgatgt ggactgtctt tttcattttt ttctctctgg agcccctcct
3781 cccccggctg ggcctccttc ttccacttct ccaagaatgg aagcctgaac tgaggccttg
3841 tgtgtcaggc cctctgcctg cactccctgg ccttgcccgt cgtgtgctga agacatgttt
3901 caagaaccgc atttcgggaa gggcatgcac gggcatgcac acggctggtc actctgccct
3961 ctgctgctgc ccggggtggg gtgcactcgc catttcctca cgtgcaggac agctcttgat
4021 ttgggtggaa aacagggtgc taaagccaac cagcctttgg gtcctgggca ggtgggagct
4081 gaaaaggatc gaggcatggg gcatgtcctt tccatctgtc cacatcccca gagcccagct
4141 cttgctctct tgtgacgtgc actgtgaatc ctggcaagaa agcttgagtc tcaagggtgg
4201 caggtcactg tcactgccga catccctccc ccagcagaat ggaggcaggg gacaagggag
4261 gcagtggcta gtggggtgaa cagctggtgc caaatagccc cagactgggc ccaggcaggt
4321 ctgcaagggc ccagagtgaa ccgtcctttc acacatctgg gtgccctgaa agggcccttc
4381 ccctccccca ctcctctaag acaaagtaga ttcttacaag gccctttcct ttggaacaag
4441 acagccttca cttttctgag ttcttgaagc atttcaaagc cctgcctctg tgtagccgcc
4501 ctgagagaga atagagctgc cactgggcac ctgcgcacag gtgggaggaa agggcctggc
4561 cagtcctggt cctggctgca ctcttgaact gggcgaatgt cttatttaat taccgtgagt
4621 gacatagcct catgttctgt gggggtcatc agggagggtt aggaaaacca caaacggagc
4681 ccctgaaagc ctcacgtatt tcacagagca cgcctgccat cttctccccg aggctgcccc
4741 aggccggagc ccagatacgg gggctgtgac tctgggcagg gacccggggt ctcctggacc
4801 ttgacagagc agctaactcc gagagcagtg ggcaggtggc cgcccctgag gcttcacgcc
4861 gggagaagcc accttcccac cccttcatac cgcctcgtgc cagcagcctc gcacaggccc
4921 tagctttacg ctcatcacct aaacttgtac tttatttttc tgatagaaat ggtttcctct
4981 ggatcgtttt atgcggttct tacagcacat cacctctttg cccccgacgg ctgtgacgca
5041 gccggaggga ggcactagtc accgacagcg gccttgaaga cagagcaaag cgcccaccca
5101 ggtcccccga ctgcctgtct ccatgaggta ctggtccctt ccttttgtta acgtgatgtg
5161 ccactatatt ttacacgtat ctcttggtat gcatctttta tagacgctct tttctaagtg
5221 gcgtgtgcat agcgtcctgc cctgcccccc cgggggcctg tggtggctcc ccctctgctt
5281 ctcggggtcc agtgcatttt gtttctgtat atgattctct gtggtttttt ttgaatccaa
5341 atctgtcctc tgtagtattt tttaaataaa tcagtgttta catt

AI.5 Kinase domain mutations included in the MassARRAY sequencing screen

FR = fully resistant; PR = partially resistant; FS = fully sensitive; U = unknown

	Mutation	Nucleotide substitution		Imatinib sensitivity	Dasatinib sensitivity	Nilotinib sensitivity
1	M244V	730A>G	ATG>GTG	PR	FS	FS
2	L248V	742C>G	CTG>GTG	FR	U	FS
3	G250E	749G>A	GGG>GAG	FR	FS	PR
4	Q252H	756G>C	CAG>CAC	FR	PR	PR
5	Q252H	756G>T	CAG>CAT	FR	PR	PR
6	Y253H	757T>C	TAC>CAC	FR	FS	PR
7	Y253F	758A>T	TAC>TTC	FR	FS	PR
8	E255K	763G>A	GAG>AAG	FR	PR	PR
9	E255V	764A>T	GAG>GTG	FR	PR	PR
10	D276G	827A>G	GAC>GGC	FR	U	FS
11	E279K	835G>A	GAG>AAG	PR	U	U
12	V299L	895G>C	GTG>CTG	FS	PR	FS
13	V299L	895G>T	GTG>TTG	FS	PR	FS
14	T315A	943A>G	ACT>GCT	FS	FR	FS
15	T315I	944C>T	ACT>ATT	FR	FR	FR
16	F317I	949T>A	TTC>ATC	FS	PR	FS
17	F317L	949T>C	TTC>CTC	PR	PR	FS
18	F317L	951C>G	TTC>TTG	PR	PR	FS
19	F317L	951C>A	TTC>TTA	PR	PR	FS
20	F317C	950T>G	TTC>TGC	U	PR	FS
21	F317V	949T>G	TTC>GTC	FS	PR	FS
22	M351T	1052T>C	ATG>ACG	PR	FS	FS
23	E355G	1064A>G	GAG>GGG	PR	FS	FS
24	E355A	1064A>C	GAG>GAC	PR	FS	FS
25	F359I	1075T>A	TTC>ATC	PR	U	U
26	F359V	1075T>G	TTC>GTC	PR	FS	FR
27	F359C	1076T>G	TTC>TGC	PR	FS	PR
28	H396R	1187A>G	CAT>CGT	PR	FS	FS
29	H396P	1187A>C	CAT>CCT	PR	FS	FS
30	E459K	1375G>A	GAG>AAG	PR	U	U
31	F486S	1457T>C	TTT>TCT	PR	FS	FS

While conventional sequencing is inclusive, MassARRAY sequencing is exclusive, as the KD mutations being sought must be selected (and specific primers designed) before the method is performed. This table catalogues the 31 BCR-ABL kinase domain mutations that were chosen for inclusion in this study *i.e.* each time MassARRAY sequencing was performed in this study, all of the listed mutations were screened for. The mutations chosen for inclusion include all mutations reported to confer clinical resistance to nilotinib and dasatinib (including the rarely observed DAS-resistant F317V/C mutations), plus the most common imatinib-resistant mutations. Even the E355A and H396P mutations, which are extremely rare imatinib-resistant mutations (detected in less than 1% of patients with mutations analysed at our institution) are included. TKI sensitivity status was compiled from various studies.

AI.6 Lyn quantitation setup sheet

RT-PCR #						
tube	sample	oligo				
A1	H2O (NTC)	RANKL		F1	K562 450M IM2	GUSB
A2	H2O (NTC)	Lyn		F2		
A3	H2O (NTC)	GUSB		F3		
A4	STD			F4	K562 600M IM2	Lyn
A5	STD	RANKL		F5		
A6	STD	only 1uL cDNA		F6		
A7				F7	K562 600M IM2	GUSB
A8	K562 Lab	Lyn		F8		
B1				G1		
B2				G2	K562 800M IM2	Lyn
B3	K562 Lab	GUSB		G3		
B4				G4		
B5				G5	K562 800M IM2	GUSB
B6	K562 Naïve P108	Lyn		G6		
B7				G7		
B8				G8	K562 1.4uM IM2	Lyn
C1	K562 Naïve P108	GUSB		H1		
C2				H2		
C3				H3	K562 1.4uM IM2	GUSB
C4	K562 2uM IM1	Lyn		H4		
C5				H5		
C6				H6	K562 2uM IM2	Lyn
C7	K562 2uM IM1	GUSB		H7		
C8				H8		
D1				I1	K562 2uM IM2	GUSB
D2	K562 200nM IM2	Lyn		I2		
D3				I3		
D4				I4		
D5	K562 200M IM2	GUSB		I5		
D6				I6		
D7				I7		
D8	K562 300M IM2	Lyn		I8		
E1						
E2				8 uL	mix per tube	
E3	K562 300M IM2	GUSB		2 uL	cDNA	
E4						
E5						
E6	K562 450M IM2	Lyn				
E7						
E8						
		RANKL	***Lyn***	***GUSB***		
1 sample		5	33	33		
5	***SYBR Green Mix***	**25**	**165**	**165**		
0.5	***Fwd Primer***	**2.5**	**16.5**	**16.5**		
0.5	***Rev Primer***	**2.5**	**16.5**	**16.5**		
2	***Water***	**10**	**66**	**66**		

AI.7 Western blots for Table 6.1: Dasatinib IC50s for the K562 Dox 200nM DAS1 cell line and intermediates

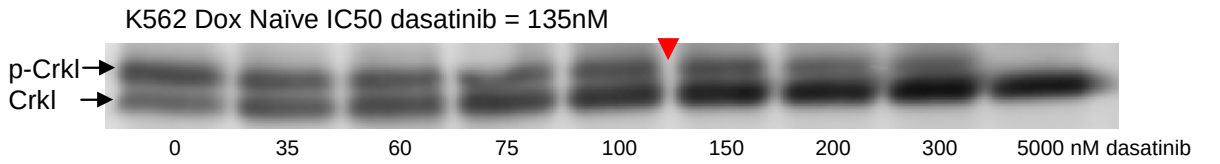

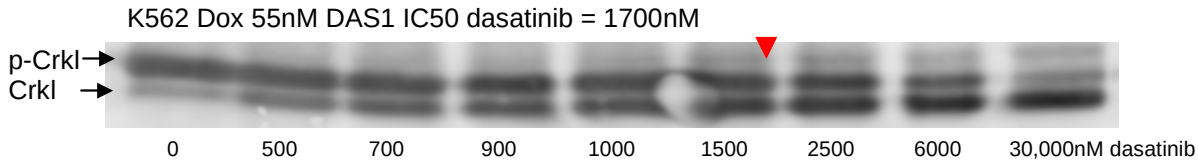

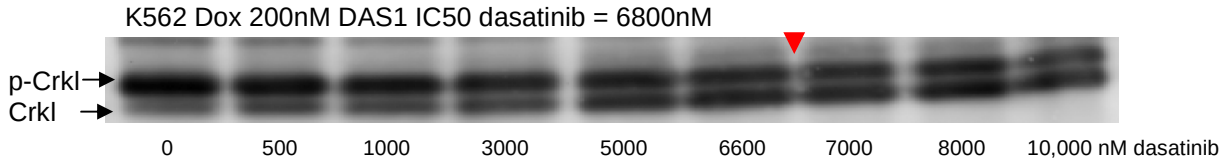

The IC50 value for each blot (determined as the dose of drug required to reduce levels of p-Crkl by 50%) is indicated above each blot (and with red arrow). IC50 assays were performed at least three times. Greyed concentrations indicated excluded lanes. One representative blot is shown for each cell line.

AI.8 Western blots for Table 6.1: Nilotinib IC50s for the K562 Dox 200nM DAS1 cell line and intermediates

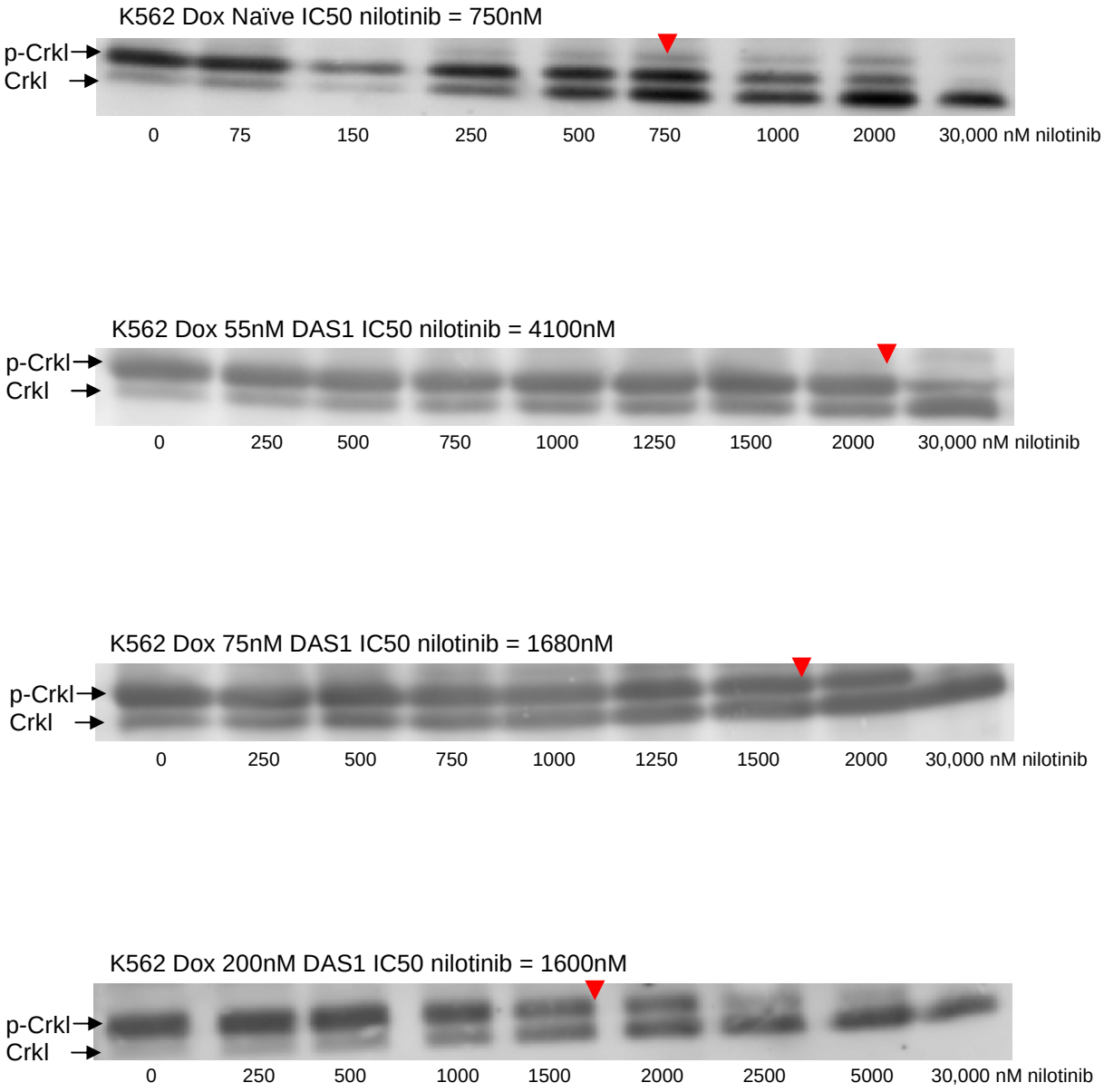

The IC50 value for each blot (determined as the dose of drug required to reduce levels of p-Crkl by 50%) is indicated above each blot (and with red arrow). IC50 assays were performed at least three times. One representative blot is shown for each cell line.

AI.9 Western blots for Table 6.1: Imatinib IC50s for the K562 Dox 200nM DAS1 cell line and intermediates

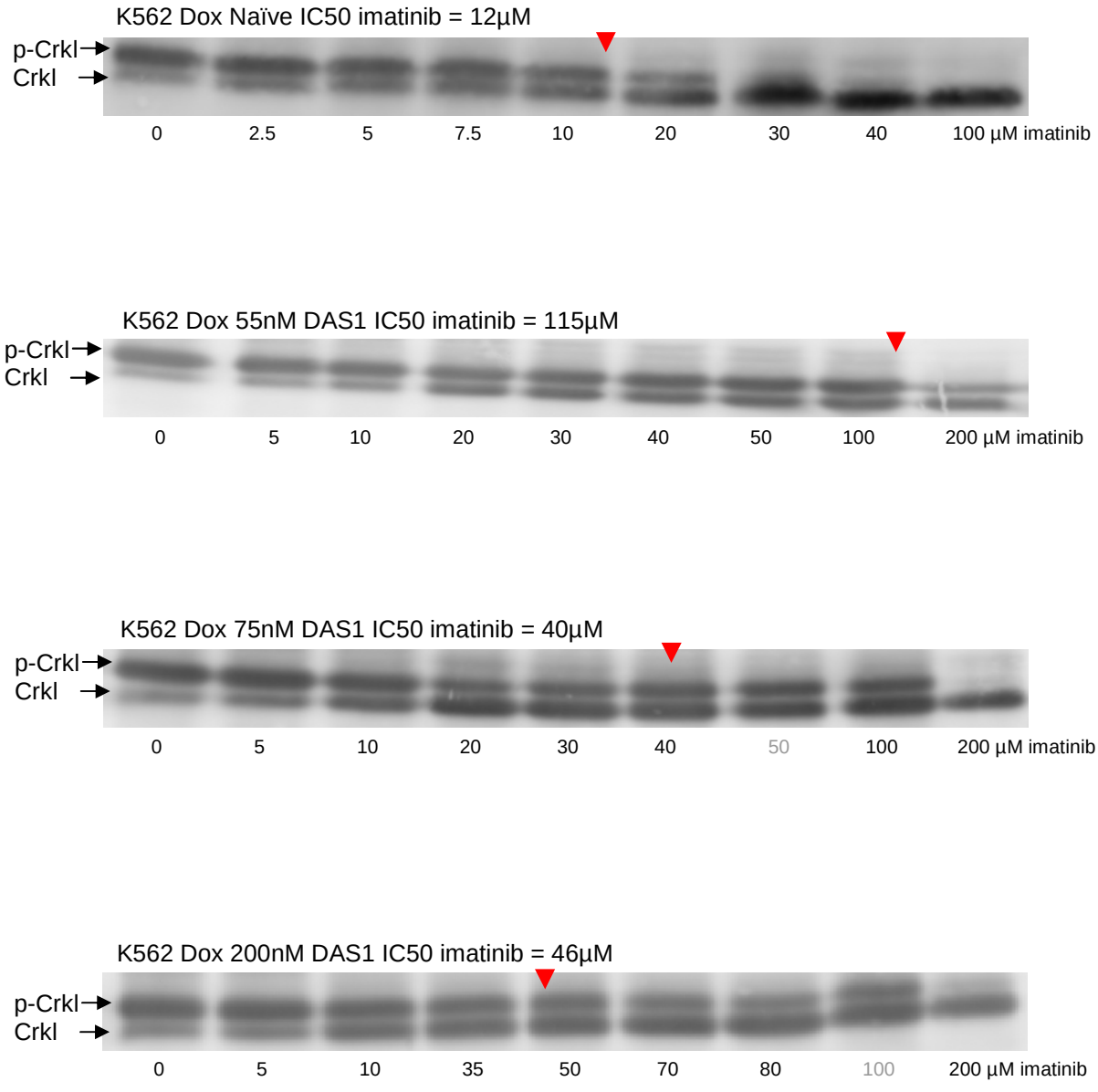

The IC50 value for each blot (determined as the dose of drug required to reduce levels of p-Crkl by 50%) is indicated above each blot (and with red arrow). IC50 assays were performed at least three times. One representative blot is shown for each cell line.

AI.10 Western blots for Figure 6.4: Nilotinib IC50s for the K562 Dox 2μM IM1, IM2 and IM3 cell lines and Naïve controls

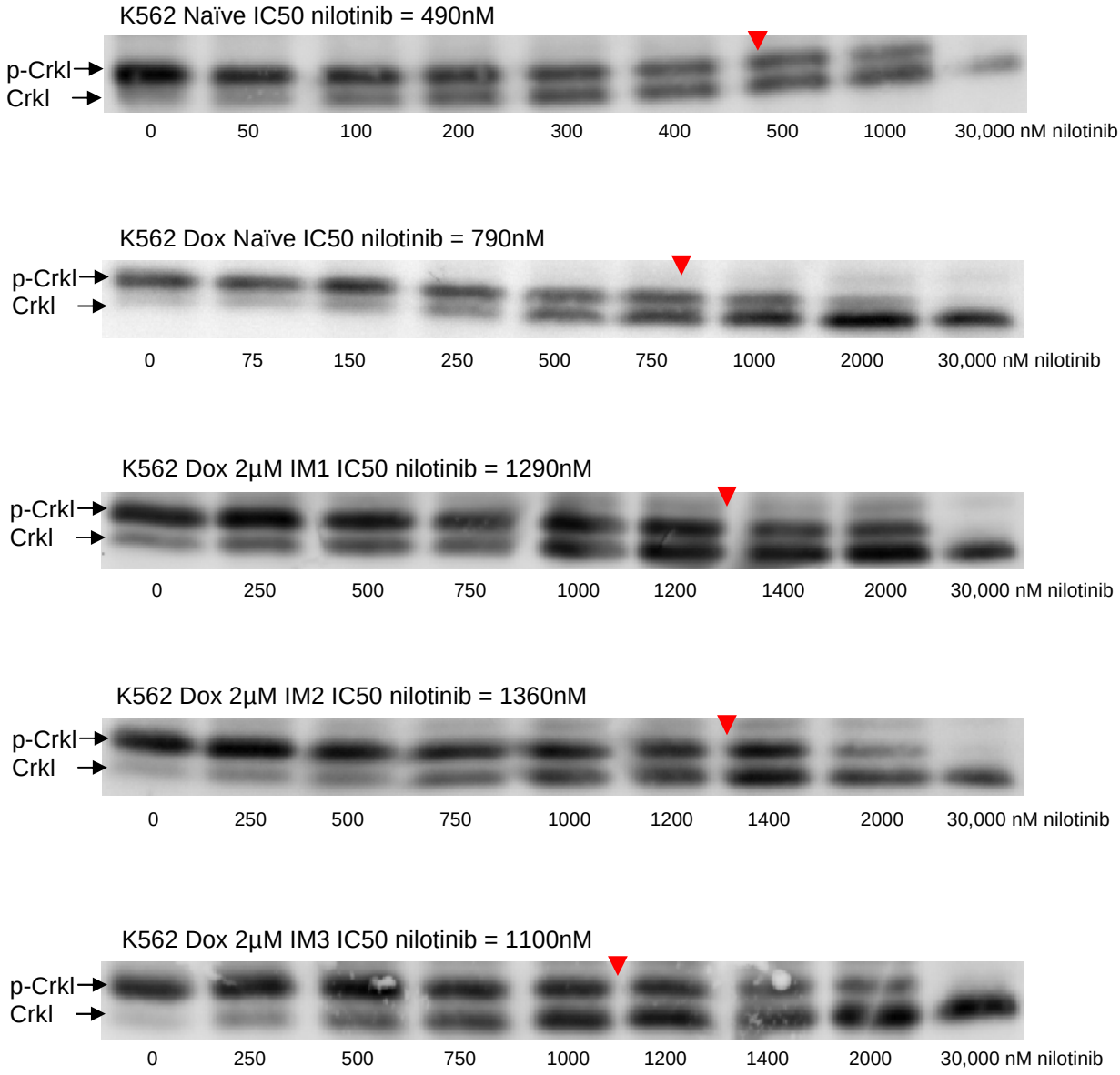

The IC50 value for each blot (determined as the dose of drug required to reduce levels of p-Crkl by 50%) is indicated above each blot (and with red arrow). IC50 assays were performed at least three times. One representative blot is shown for each cell line.

AI.11 Western blots for Figure 6.4: Nilotinib IC50s with PSC833 for the K562 Dox 2µM IM1, IM2 and IM3 cell lines and Naïve controls

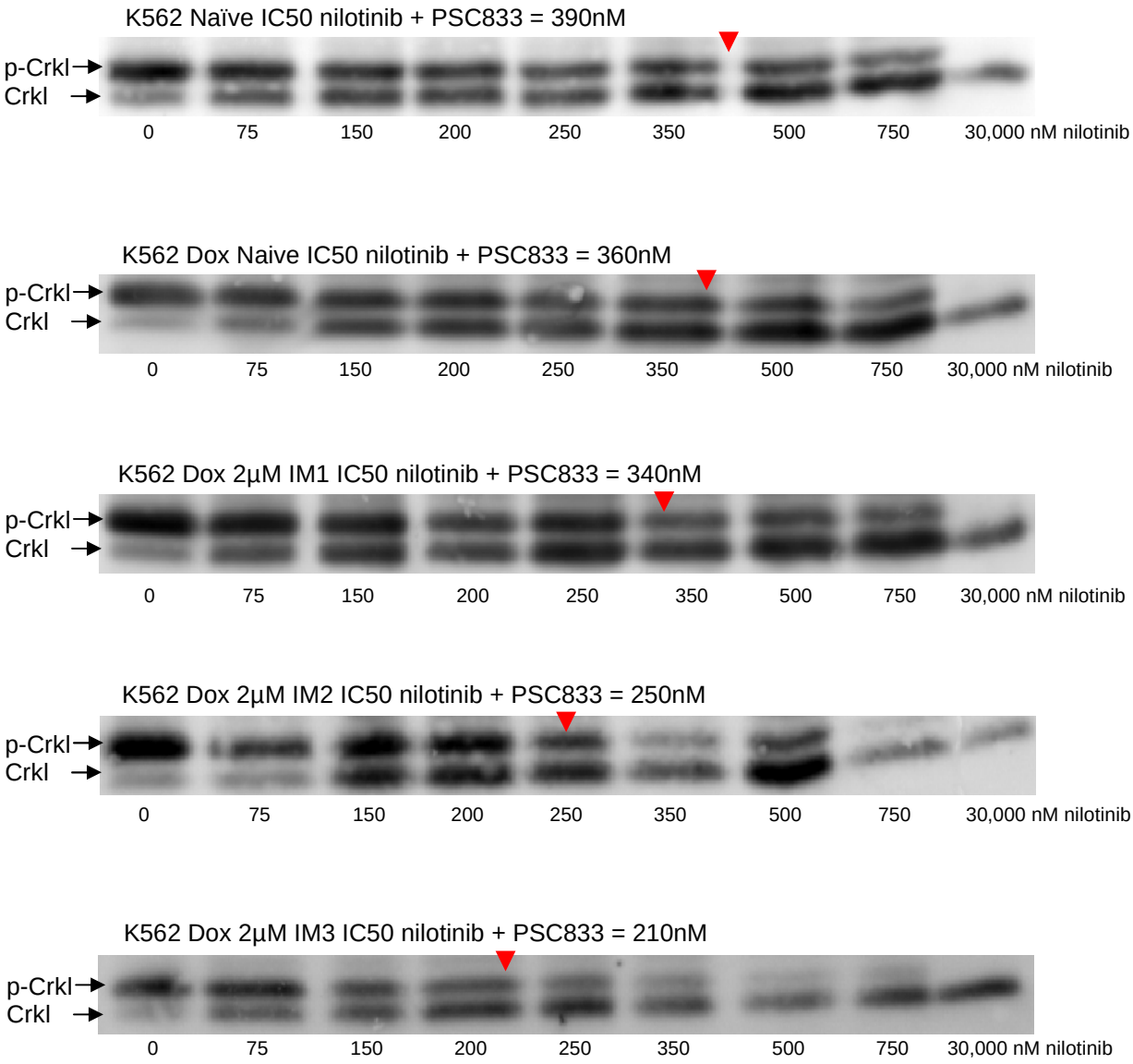

The IC50 value for each blot (determined as the dose of drug required to reduce levels of p-Crkl by 50%) is indicated above each blot (and with red arrow). IC50 assays were performed at least three times. One representative blot is shown for each of the five cell lines.

AI.12 Western blots for Figure 6.4: Dasatinib IC50s for the K562 Dox 2μM IM1, IM2 and IM3 cell lines and Naïve controls

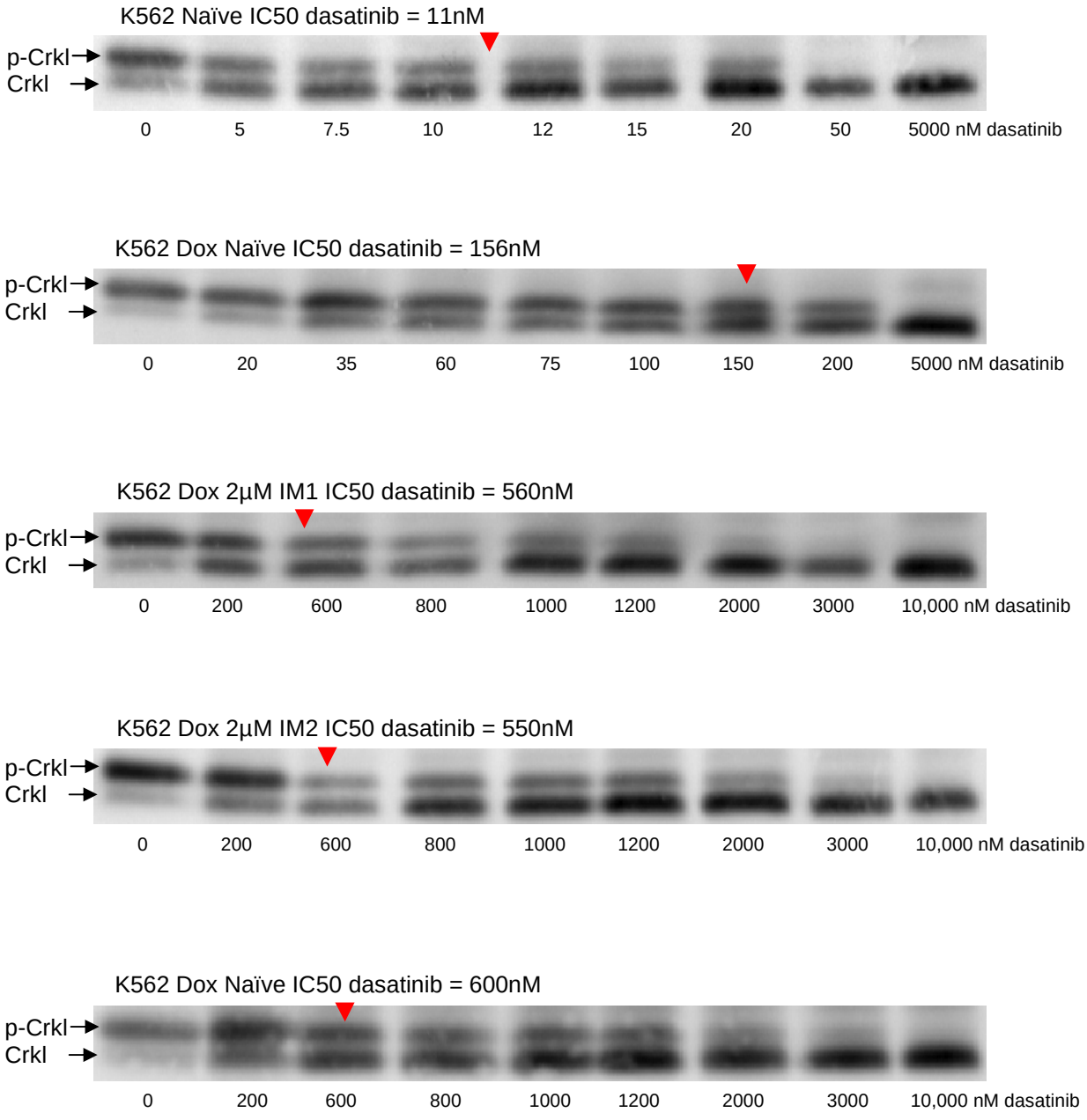

The IC50 value for each blot (determined as the dose of drug required to reduce levels of p-Crkl by 50%) is indicated above each blot (and with red arrow). IC50 assays were performed at least three times. One representative blot is shown for each cell line.

AI.13 Western blots for Figure 6.4: Dasatinib IC50s with PSC833 for the K562 Dox 2µM IM1, IM2 and IM3 cell lines and Naïve controls

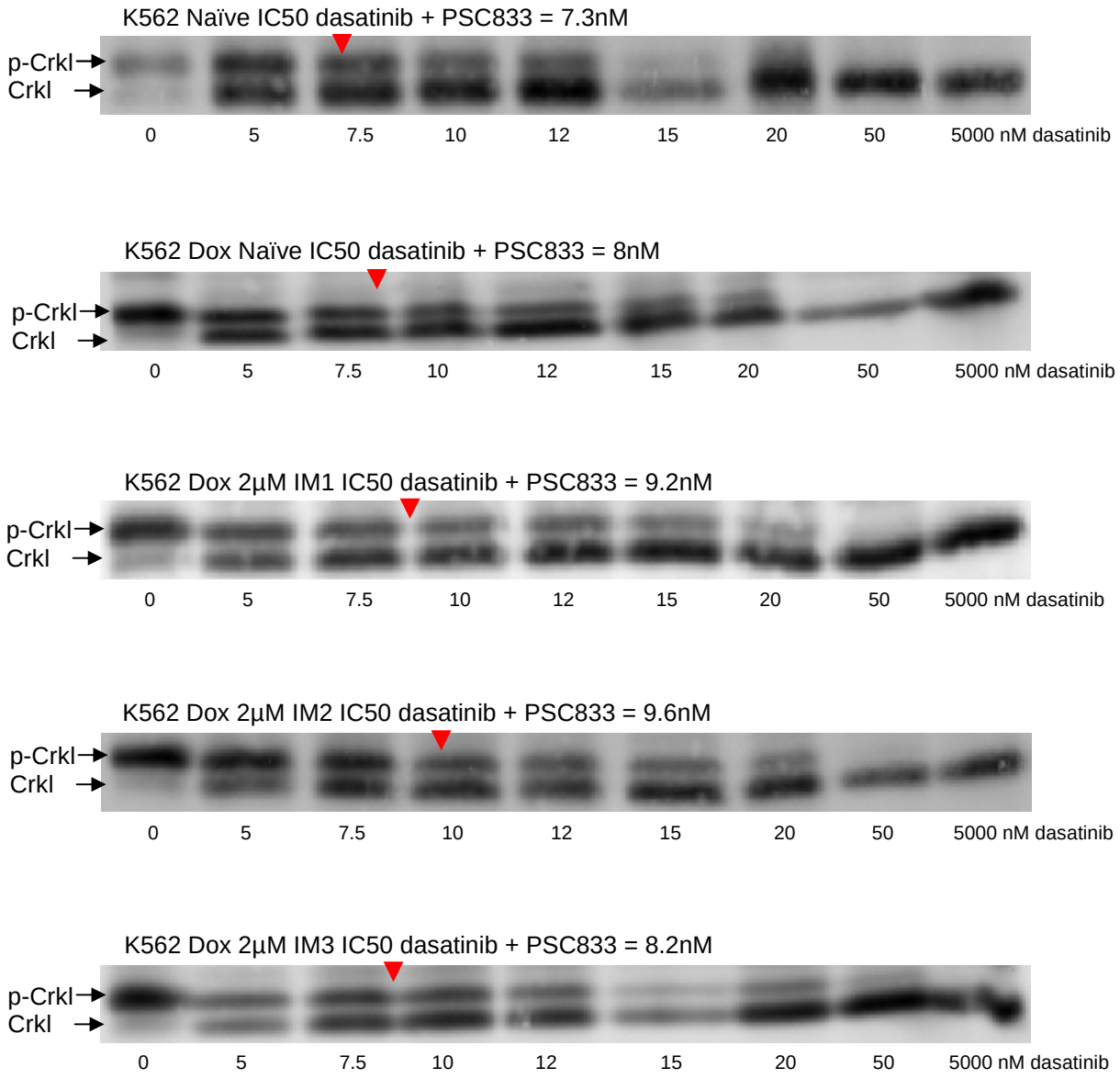

The IC50 value for each blot (determined as the dose of drug required to reduce levels of p-Crkl by 50%) is indicated above each blot (and with red arrow). IC50 assays were performed at least three times. One representative blot is shown for each of the five cell lines.

AI.14 Western blots for Table 6.2: Imatinib IC50s for the KU812 2μM IM1 and 3μM IM2 cell lines and KU812 Naïve control

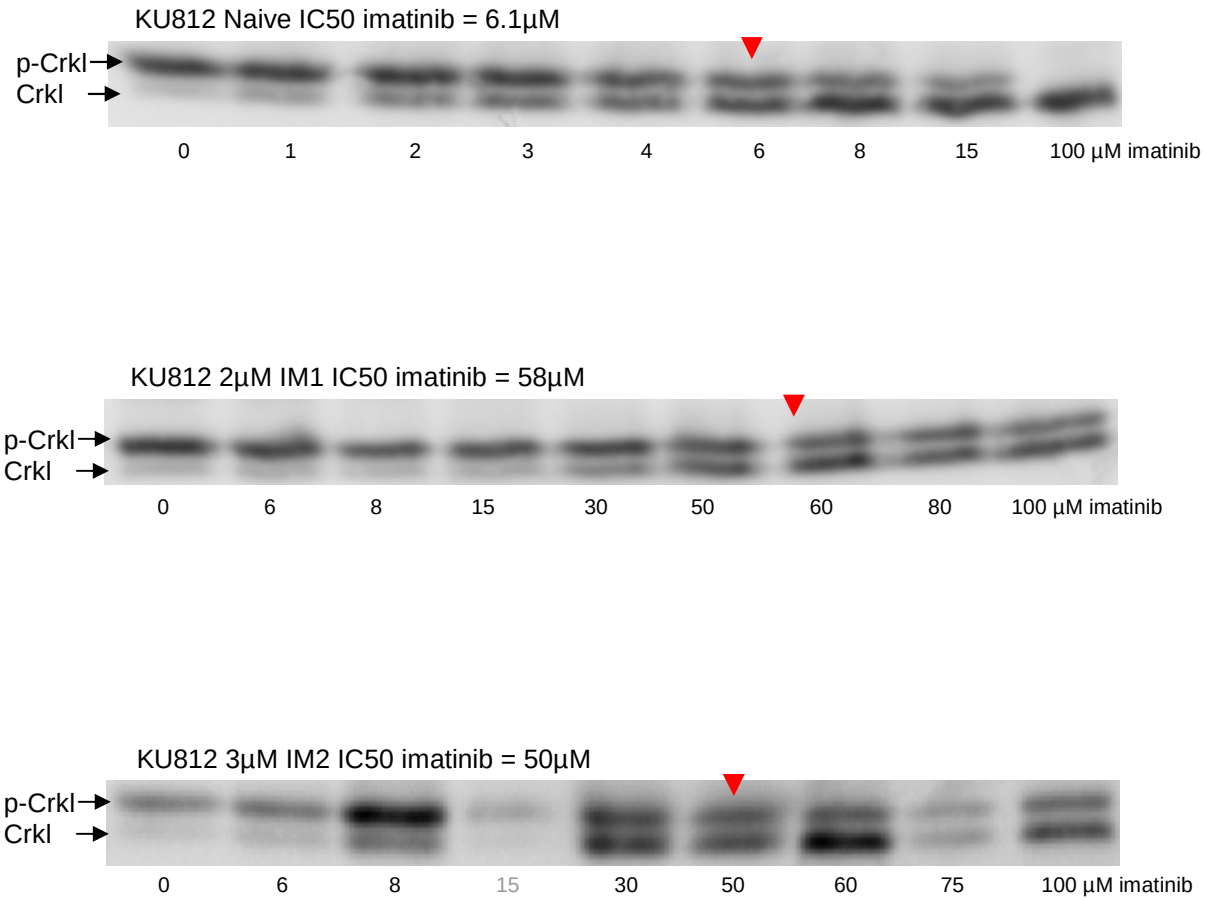

The IC50 value for each blot (determined as the dose of drug required to reduce levels of p-Crkl by 50%) is indicated above each blot (and with red arrow). IC50 assays were performed at least three times. Greyed concentrations indicate excluded lanes. One representative blot is shown for each cell line.

AI.15 Western blots for Table 6.2: Nilotinib IC50s for the KU812 2μM IM1 and 3μM IM2 cell lines and KU812 Naïve control

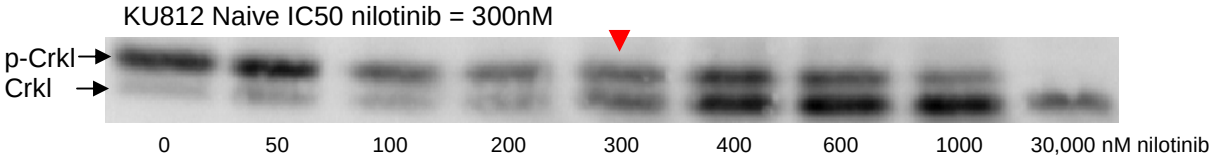

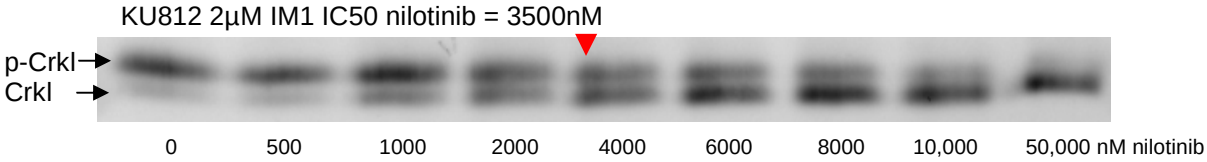

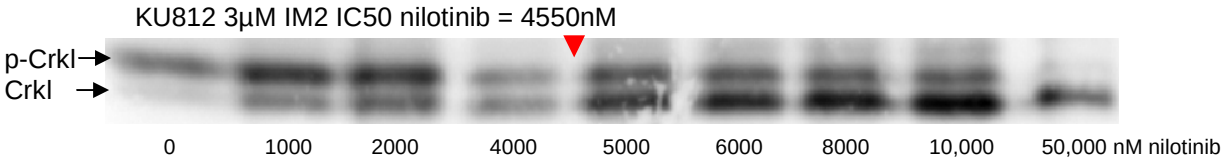

The IC50 value for each blot (determined as the dose of drug required to reduce levels of p-Crkl by 50%) is indicated above each blot (and with red arrow). IC50 assays were performed at least three times. One representative blot is shown for each cell line.

AI.16 Western blots for Table 6.2: Dasatinib IC50s for the KU812 2μM IM1 and 3μM IM2 cell lines and KU812 Naïve control

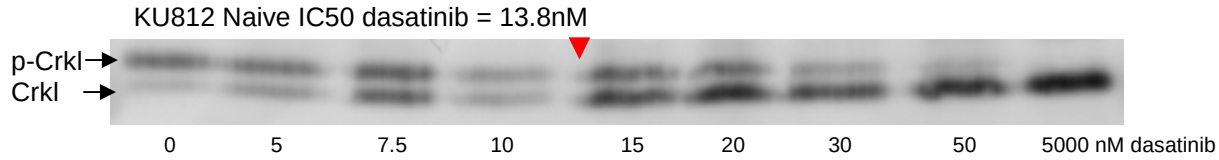

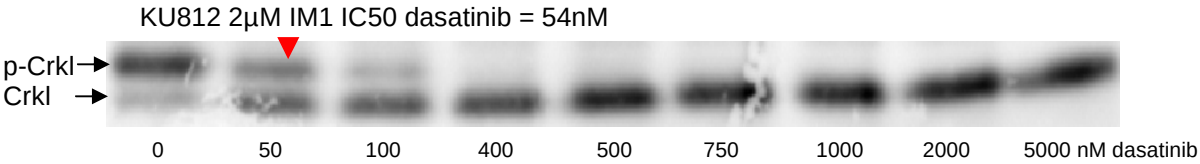

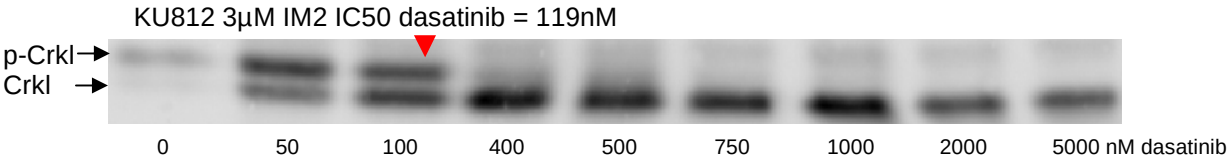

The IC50 value for each blot (determined as the dose of drug required to reduce levels of p-Crkl by 50%) is indicated above each blot (and with red arrow). IC50 assays were performed at least three times. One representative blot is shown for each cell line.

AI.17 Western blots for Table 6.3: Imatinib IC50s for the KU812 2µM IM3 cell line and intermediates

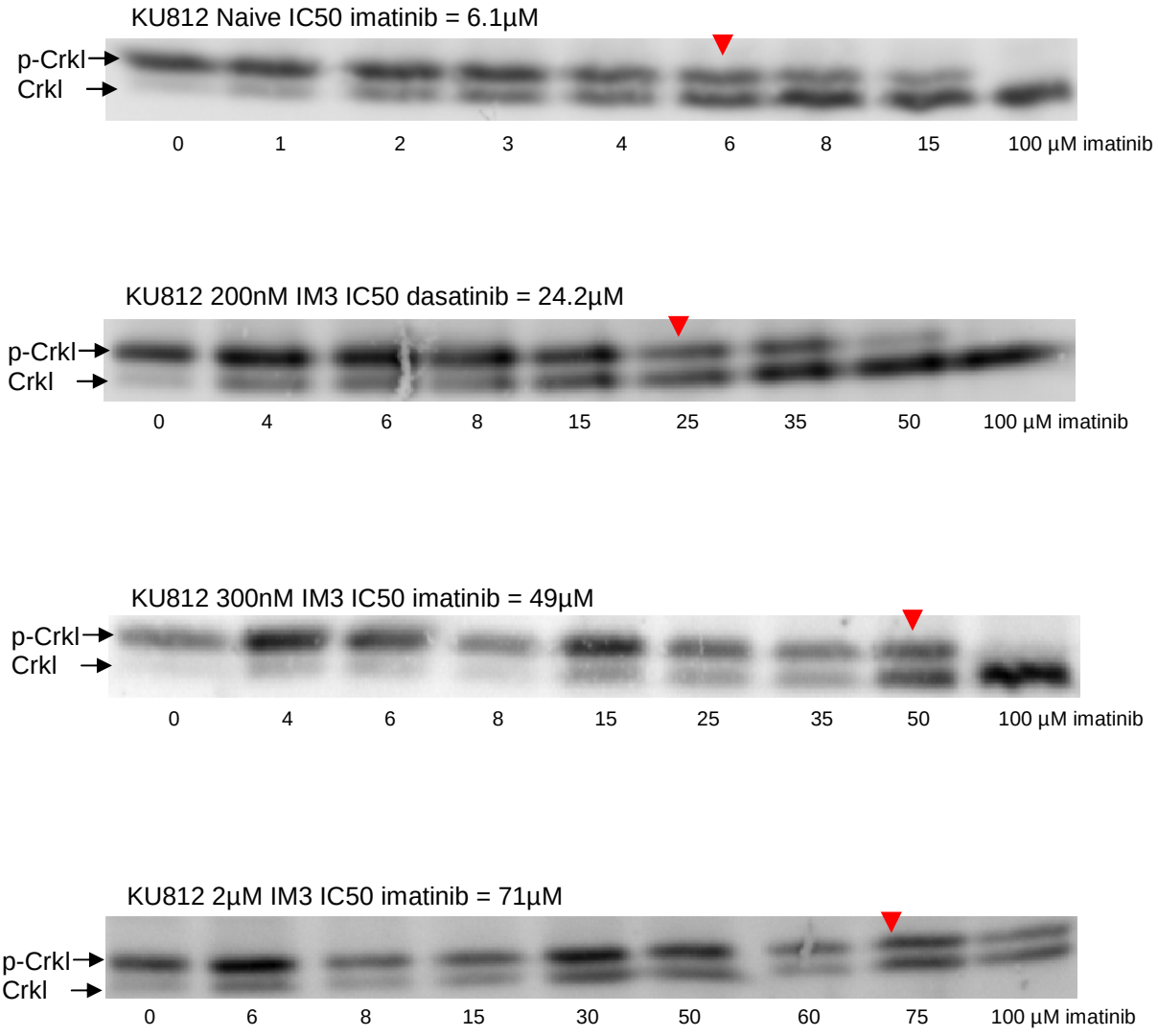

The IC50 value for each blot (determined as the dose of drug required to reduce levels of p-Crkl by 50%) is indicated above each blot (and with red arrow). IC50 assays were performed at least three times. One representative blot is shown for each cell line.

AI.18 Western blots for Table 6.3: Nilotinib IC50s for the KU812 2µM IM3 cell line and intermediates

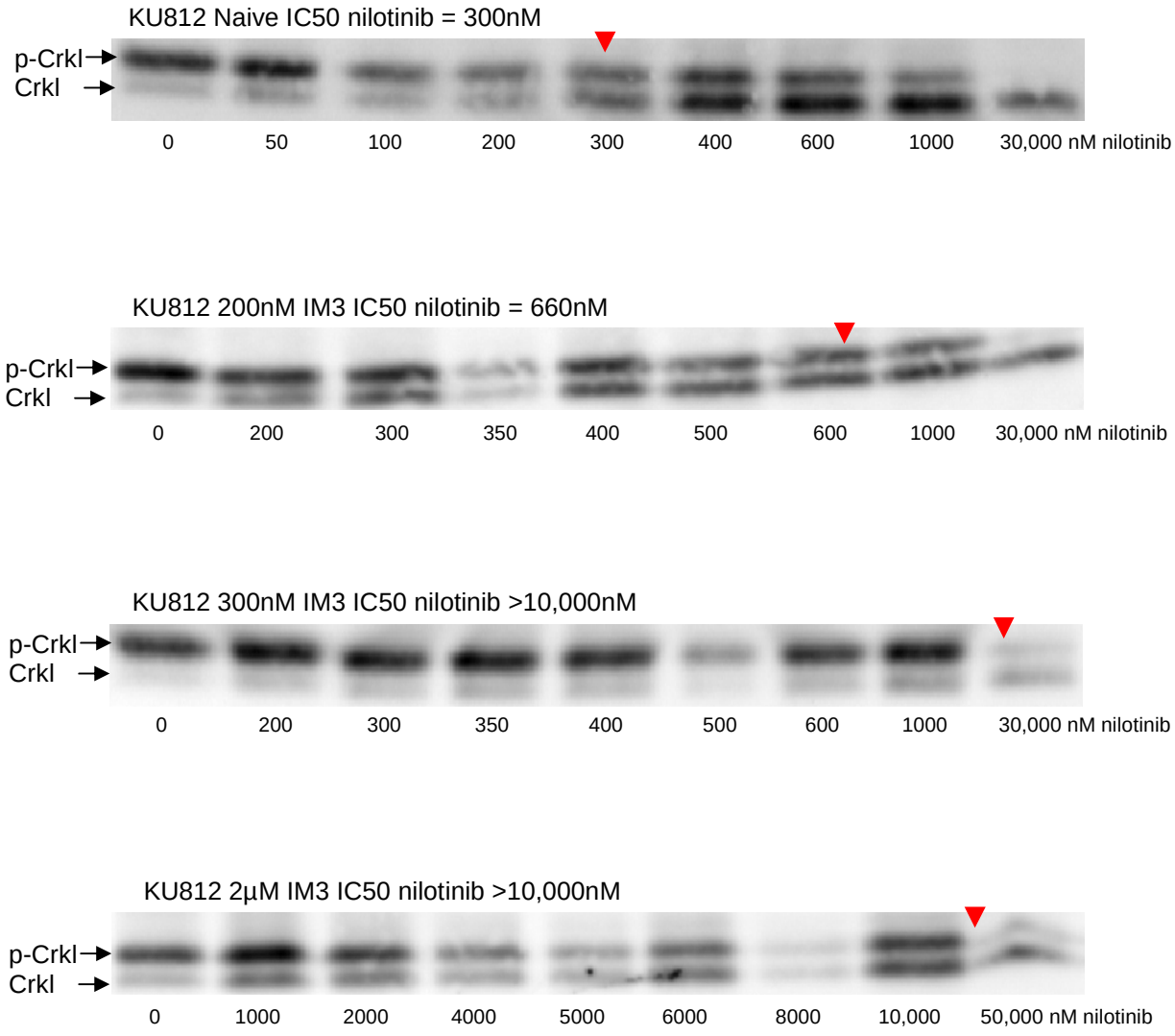

The IC50 value for each blot (determined as the dose of drug required to reduce levels of p-Crkl by 50%) is indicated above each blot (and with red arrow). IC50 assays were performed at least three times. One representative blot is shown for each cell line.

AI.19 Western blots for Table 6.3: Dasatinib IC50s for the KU812 2µM IM3 cell line and intermediates

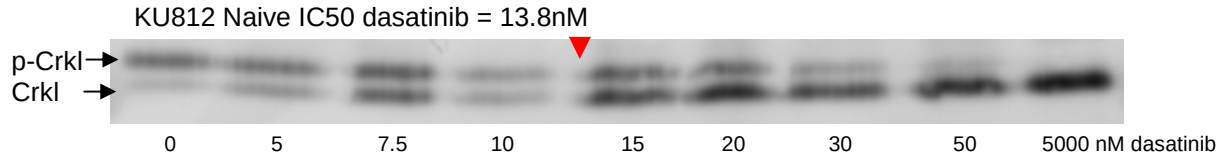

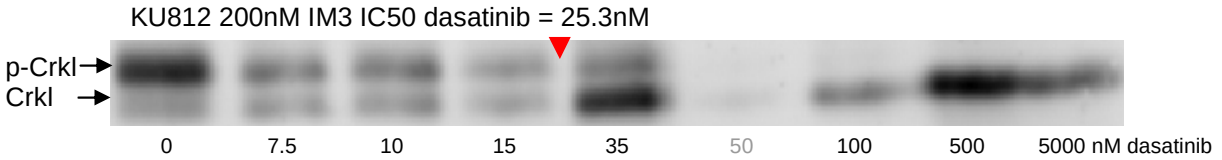

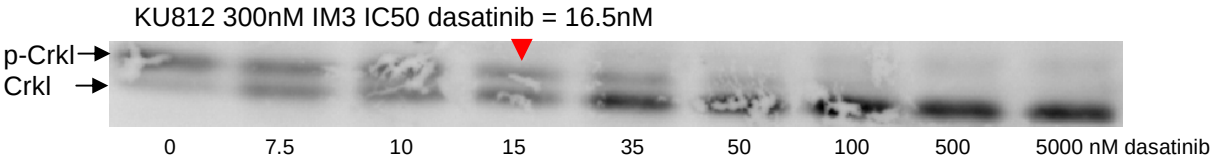

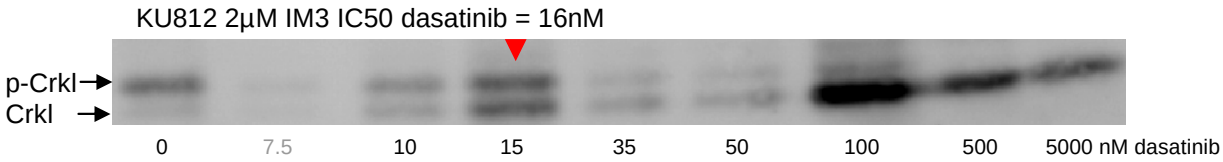

The IC50 value for each blot (determined as the dose of drug required to reduce levels of p-Crkl by 50%) is indicated above each blot (and with red arrow). IC50 assays were performed at least three times. Greyed concentrations indicate excluded lanes. One representative blot is shown for each cell line.

AI.20 Western blots for Figure 6.5 & 6.6: Nilotinib and dasatinib IC50s for the K562 2µM IM1 and IM2 cell lines

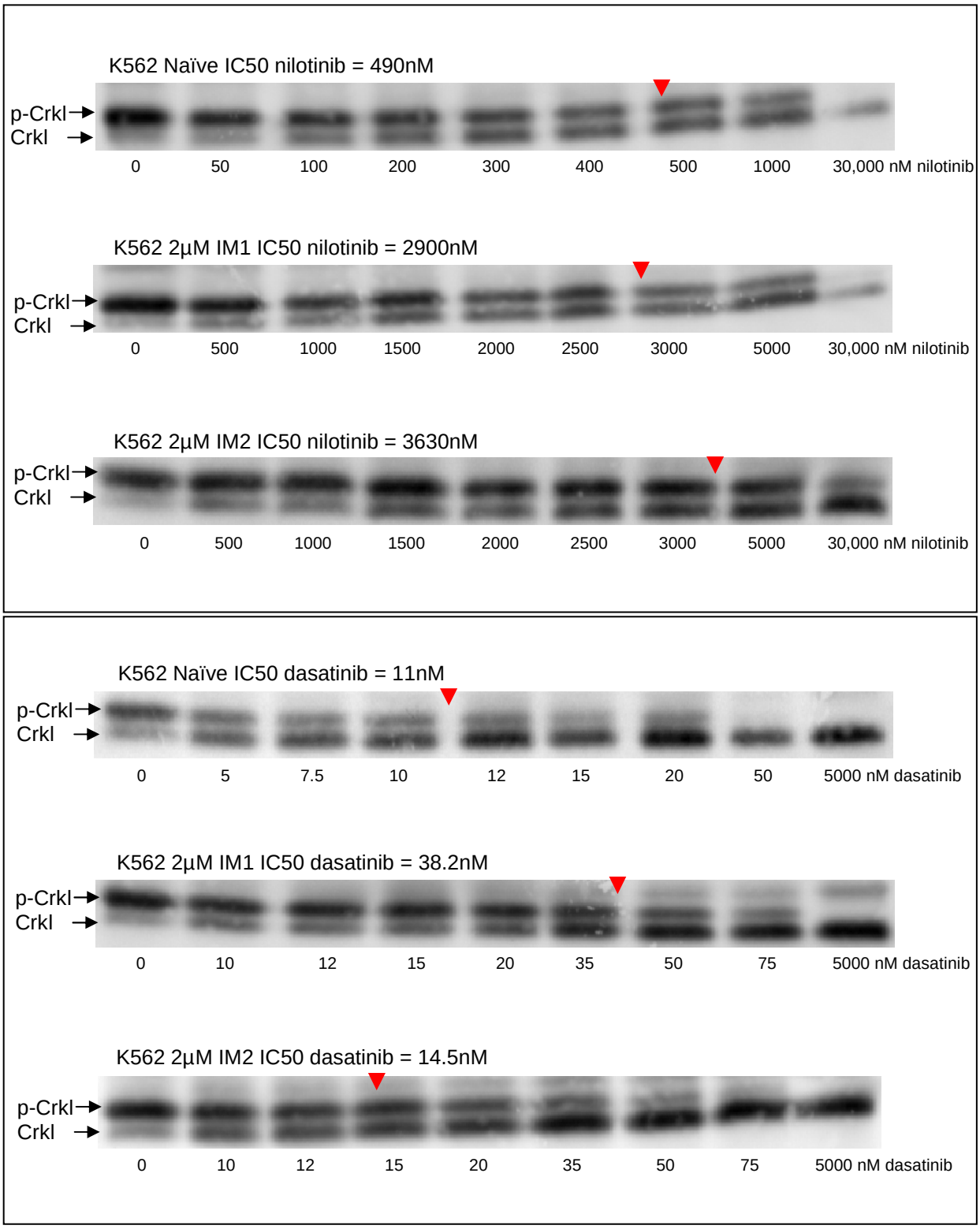

One representative blot is shown for $IC50^{nilotinib}$ (top) and $IC50^{dasatinib}$ (bottom) for the K562 Naïve, K562 2µM IM1 and IM2 cell lines. The IC50 value for each blot (determined as the dose of drug required to reduce levels of p-Crkl by 50%) is indicated above each blot (and with red arrow). IC50 assays were performed at least three times.

Appendix II

Tang, C., Schafranek, L., Watkins D., Parker, W., Moore, S., Prime, J., White, D. & Hughes, T. (2011) Tyrosine kinase inhibitor resistance in chronic myeloid leukemia cell lines: investigating resistance pathways.
Leukemia & Lymphoma, v 52 (11), pp. 2139 -2147

References

1. Faderl S, Talpaz M, Estrov Z, Kantarjian HM. Chronic myelogenous leukemia: biology and therapy. Ann Intern Med. 1999;131:207-219.

2. Coico R, Sunshine, G. & Benjamini, E. . Immunology: A Short Course (ed 5th). New Jersey: John Wiley & Sons Inc.; 2003.

3. Provan A, Provan, D., Ager, S., Duncombe, A., Evans, T. & Goldman, J.M. ABC of Clinical Haematology. Melbourne: Blackwell Publishing; 2003.

4. Clarkson B, Strife A, Wisniewski D, Lambek CL, Liu C. Chronic myelogenous leukemia as a paradigm of early cancer and possible curative strategies. Leukemia. 2003;17:1211-1262.

5. Mauro MJ, O'Dwyer M, Heinrich MC, Druker BJ. STI571: a paradigm of new agents for cancer therapeutics. J Clin Oncol. 2002;20:325-334.

6. Savona M, Talpaz M. Getting to the stem of chronic myeloid leukaemia. Nat Rev Cancer. 2008;8:341-350.

7. Marcucci G, Perrotti D, Caligiuri MA. Understanding the molecular basis of imatinib mesylate therapy in chronic myelogenous leukemia and the related mechanisms of resistance. Commentary re: A. N. Mohamed et al., The effect of imatinib mesylate on patients with Philadelphia chromosome-positive chronic myeloid leukemia with secondary chromosomal aberrations. Clin. Cancer Res., 9: 1333-1337, 2003. Clin Cancer Res. 2003;9:1248-1252.

8. Steelman LS, Pohnert SC, Shelton JG, Franklin RA, Bertrand FE, McCubrey JA. JAK/STAT, Raf/MEK/ERK, PI3K/Akt and BCR-ABL in cell cycle progression and leukemogenesis. Leukemia. 2004;18:189-218.

9. Huettner CS, Koschmieder S, Iwasaki H, et al. Inducible expression of BCR/ABL using human CD34 regulatory elements results in a megakaryocytic myeloproliferative syndrome. Blood. 2003;102:3363-3370.

10. Hariharan IK, Harris AW, Crawford M, et al. A bcr-v-abl oncogene induces lymphomas in transgenic mice. Mol Cell Biol. 1989;9:2798-2805.

11. Honda H, Fujii T, Takatoku M, et al. Expression of p210bcr/abl by metallothionein promoter induced T-cell leukemia in transgenic mice. Blood. 1995;85:2853-2861.

12. Voncken JW, Kaartinen V, Pattengale PK, Germeraad WT, Groffen J, Heisterkamp N. BCR/ABL P210 and P190 cause distinct leukemia in transgenic mice. Blood. 1995;86:4603-4611.

13. Daley GQ. Animal models of BCR/ABL-induced leukemias. Leuk Lymphoma. 1993;11 Suppl 1:57-60.

14. CML Society of Canada; 2007.

15. Goldman JM, Melo JV. Chronic myeloid leukemia--advances in biology and new approaches to treatment. N Engl J Med. 2003;349:1451-1464.

16. Buchdunger E, Zimmermann J, Mett H, et al. Inhibition of the Abl protein-tyrosine kinase in vitro and in vivo by a 2-phenylaminopyrimidine derivative. Cancer Res. 1996;56:100-104.

17. Sawyers CL. Chronic myeloid leukemia. N Engl J Med. 1999;340:1330-1340.

18. Silver RT, Woolf SH, Hehlmann R, et al. An evidence-based analysis of the effect of busulfan, hydroxyurea, interferon, and allogeneic bone marrow transplantation in treating the chronic phase of chronic myeloid leukemia: developed for the American Society of Hematology. Blood. 1999;94:1517-1536.

19. Carella AM, Daley GQ, Eaves CJ, Goldman JM, Hehlmann R. Chroinc Myeloid Leukaemia: Biology and Treatment. London: Martin Dunitz Ltd; 2001.

20. Druker BJ, Lydon NB. Lessons learned from the development of an abl tyrosine kinase inhibitor for chronic myelogenous leukemia. J Clin Invest. 2000;105:3-7.

21. Kantarjian HM, Talpaz M, O'Brien S, et al. Imatinib mesylate for Philadelphia chromosome-positive, chronic-phase myeloid leukemia after failure of interferon-alpha: follow-up results. Clin Cancer Res. 2002;8:2177-2187.

22. Schindler T, Bornmann W, Pellicena P, Miller WT, Clarkson B, Kuriyan J. Structural mechanism for STI-571 inhibition of abelson tyrosine kinase. Science. 2000;289:1938-1942.

23. Druker BJ, Tamura S, Buchdunger E, et al. Effects of a selective inhibitor of the Abl tyrosine kinase on the growth of Bcr-Abl positive cells. Nat Med. 1996;2:561-566.

24. Druker BJ, Guilhot F, O'Brien SG, et al. Five-year follow-up of patients receiving imatinib for chronic myeloid leukemia. N Engl J Med. 2006;355:2408-2417.

25. Branford S, Rudzki Z, Harper A, et al. Imatinib produces significantly superior molecular responses compared to interferon alfa plus cytarabine in patients with newly diagnosed chronic myeloid leukemia in chronic phase. Leukemia. 2003;17:2401-2409.

26. Copland M, Hamilton A, Elrick LJ, et al. Dasatinib (BMS-354825) targets an earlier progenitor population than imatinib in primary CML but does not eliminate the quiescent fraction. Blood. 2006;107:4532-4539.

27. Merante S, Orlandi E, Bernasconi P, Calatroni S, Boni M, Lazzarino M. Outcome of four patients with chronic myeloid leukemia after imatinib mesylate discontinuation. Haematologica. 2005;90:979-981.

28. Cortes J, O'Brien S, Kantarjian H. Discontinuation of imatinib therapy after achieving a molecular response. Blood. 2004;104:2204-2205.

29. Rousselot P, Huguet F, Rea D, et al. Imatinib mesylate discontinuation in patients with chronic myelogenous leukemia in complete molecular remission for more than 2 years. Blood. 2007;109:58-60.

30. Two new agents effective in Gleevec-resistant CML. Cancer Biol Ther. 2004;3:1198-1199.

31. NCBI Pubchem compound: http://www.ncbi.nlm.nih.gov/pccompound; 2011.

32. Mughal TI, Goldman JM. Molecularly targeted treatment of chronic myeloid leukemia: beyond the imatinib era. Front Biosci. 2006;11:209-220.

33. O'Hare T, Walters DK, Stoffregen EP, et al. In vitro activity of Bcr-Abl inhibitors AMN107 and BMS-354825 against clinically relevant imatinib-resistant Abl kinase domain mutants. Cancer Res. 2005;65:4500-4505.

34. Shah NP, Tran C, Lee FY, Chen P, Norris D, Sawyers CL. Overriding imatinib resistance with a novel ABL kinase inhibitor. Science. 2004;305:399-401.

35. Hu Y, Swerdlow S, Duffy TM, Weinmann R, Lee FY, Li S. Targeting multiple kinase pathways in leukemic progenitors and stem cells is essential for improved treatment of Ph+ leukemia in mice. Proc Natl Acad Sci U S A. 2006;103:16870-16875.

36. White D, Saunders V, Lyons AB, et al. In vitro sensitivity to imatinib-induced inhibition of ABL kinase activity is predictive of molecular response in patients with de novo CML. Blood. 2005;106:2520-2526.

37. ten Hoeve J, Arlinghaus RB, Guo JQ, Heisterkamp N, Groffen J. Tyrosine phosphorylation of CRKL in Philadelphia+ leukemia. Blood. 1994;84:1731-1736.

38. Oda T, Heaney C, Hagopian JR, Okuda K, Griffin JD, Druker BJ. Crkl is the major tyrosine-phosphorylated protein in neutrophils from patients with chronic myelogenous leukemia. J Biol Chem. 1994;269:22925-22928.

39. White DL, Saunders VA, Dang P, et al. OCT-1-mediated influx is a key determinant of the intracellular uptake of imatinib but not nilotinib (AMN107): reduced OCT-1 activity is the cause of low in vitro sensitivity to imatinib. Blood. 2006;108:697-704.

40. Thomas J, Wang L, Clark RE, Pirmohamed M. Active transport of imatinib into and out of cells: implications for drug resistance. Blood. 2004;104:3739-3745.

41. Koepsell H, Schmitt BM, Gorboulev V. Organic cation transporters. Rev Physiol Biochem Pharmacol. 2003;150:36-90.

42. Koepsell H, Lips K, Volk C. Polyspecific organic cation transporters: structure, function, physiological roles, and biopharmaceutical implications. Pharm Res. 2007;24:1227-1251.

43. Grundemann D, Gorboulev V, Gambaryan S, Veyhl M, Koepsell H. Drug excretion mediated by a new prototype of polyspecific transporter. Nature. 1994;372:549-552.

44. Ciarimboli G, Schlatter E. Regulation of organic cation transport. Pflugers Arch. 2005;449:423-441.

45. Cetinkaya I, Ciarimboli G, Yalcinkaya G, et al. Regulation of human organic cation transporter hOCT2 by PKA, PI3K, and calmodulin-dependent kinases. Am J Physiol Renal Physiol. 2003;284:293-302.

46. Ciarimboli G, Struwe K, Arndt P, et al. Regulation of the human organic cation transporter hOCT1. J Cell Physiol. 2004;201:420-428.

47. Crossman LC, Druker BJ, Deininger MWN, Pirmohamed M, Wang L, Clark RE. hOCT 1 and resistance to imatinib. Blood. 2005;106:1133-1134.

48. Wang L, Giannoudis A, Lane S, Williamson P, Pirmohamed M, Clark RE. Expression of the uptake drug transporter hOCT1 is an important clinical determinant of the response to imatinib in chronic myeloid leukemia. Clin Pharmacol Ther. 2008;83:258-264.

49. Kerb R, Brinkmann U, Chatskaia N, et al. Identification of genetic variations of the human organic cation transporter hOCT1 and their functional consequences. Pharmacogenetics. 2002;12:591-595.

50. Hayer M, Bonisch H, Bruss M. Molecular cloning, functional characterization and genomic organization of four alternatively spliced isoforms of the human organic cation transporter 1 (hOCT1/SLC22A1). Ann Hum Genet. 1999;63:473-482.

51. Jonker JW, Schinkel AH. Pharmacological and physiological functions of the polyspecific organic cation transporters: OCT1, 2, and 3 (SLC22A1-3). J Pharmacol Exp Ther. 2004;308:2-9.

52. White DL, Saunders VA, Dang P, et al. Most CML patients who have a suboptimal response to imatinib have low OCT-1 activity: higher doses of imatinib may overcome the negative impact of low OCT-1 activity. Blood. 2007;110:4064-4072.

53. White DL, Dang P, Engler J, et al. Functional activity of the OCT-1 protein is predictive of long-term outcome in patients with chronic-phase chronic myeloid leukemia treated with imatinib. J Clin Oncol. 2010;28:2761-2767.

54. Giannoudis A, Davies A, Lucas CM, Harris RJ, Pirmohamed M, Clark RE. Effective dasatinib uptake may occur without human organic cation transporter 1 (hOCT1): implications for the treatment of imatinib-resistant chronic myeloid leukemia. Blood. 2008;112:3348-3354.

55. Hiwase DK, Saunders V, Hewett D, et al. Dasatinib cellular uptake and efflux in chronic myeloid leukemia cells: therapeutic implications. Clin Cancer Res. 2008;14:3881-3888.

56. Sarkadi B, Homolya L, Szakacs G, Varadi A. Human multidrug resistance ABCB and ABCG transporters: participation in a chemoimmunity defense system. Physiol Rev. Vol. 86; 2006:1179-1236.

57. Borst P, Zelcer N, van de Wetering K, Poolman B. On the putative co-transport of drugs by multidrug resistance proteins. FEBS Lett. 2006;580:1085-1093.

58. Lin T, Islam O, Heese K. ABC transporters, neural stem cells and neurogenesis--a different perspective. Cell Res. 2006;16:857-871.

59. Viguié F. ABCB1 ATP-binding cassette, sub-family B (MDR/TAP), member 1: http://atlasgeneticsoncology.org//Genes/PGY1ID105.html; 1998.

60. Sorrentino BP. Gene therapy to protect haematopoietic cells from cytotoxic cancer drugs. Nat Rev Cancer. 2002;2:431-441.

61. Sarkadi B, Szakás G, Váradi A. Multi-Drug Resistance in Cancer - Role of ABC Transporter Proteins: Drug Metabolism Tech Review; Sigma-Aldrich; 2011.

62. Jordanides NE, Jorgensen HG, Holyoake TL, Mountford JC. Functional ABCG2 is overexpressed on primary CML CD34+ cells and is inhibited by imatinib mesylate. Blood. 2006;108:1370-1373.

63. Houghton PJ, Germain GS, Harwood FC, et al. Imatinib mesylate is a potent inhibitor of the ABCG2 (BCRP) transporter and reverses resistance to topotecan and SN-38 in vitro. Cancer Res. 2004;64:2333-2337.

64. White DL, Saunders VA, Quinn SR, Manley PW, Hughes TP. Imatinib increases the intracellular concentration of nilotinib, which may explain the observed synergy between these drugs. Blood. 2007;109:3609-3610.

65. Ferrao PT, Frost MJ, Siah S-P, Ashman LK. Overexpression of P-glycoprotein in K562 cells does not confer resistance to the growth inhibitory effects of imatinib (STI571) in vitro. Blood. 2003;102:4499-4503.

66. Brendel C, Scharenberg C, Dohse M, et al. Imatinib mesylate and nilotinib (AMN107) exhibit high-affinity interaction with ABCG2 on primitive hematopoietic stem cells. Leukemia. 2007;21:1267-1275.

67. Dohse M, Scharenberg C, Shukla S, et al. Comparison of ATP-binding cassette transporter interactions with the tyrosine kinase inhibitors imatinib, nilotinib, and dasatinib. Drug Metab Dispos. 2010;38:1371-1380.

68. Hiwase DK, White D, Zrim S, Saunders V, Melo JV, Hughes TP. Nilotinib-mediated inhibition of ABCB1 increases intracellular concentration of dasatinib in CML cells: implications for combination TKI therapy. Leukemia. 2010;24:658-660.

69. Hegedus C, Ozvegy-Laczka C, Apati A, et al. Interaction of nilotinib, dasatinib and bosutinib with ABCB1 and ABCG2: implications for altered anti-cancer effects and pharmacological properties. Br J Pharmacol. 2009;158:1153-1164.

70. Tiwari AK, Sodani K, Wang SR, et al. Nilotinib (AMN107, Tasigna) reverses multidrug resistance by inhibiting the activity of the ABCB1/Pgp and ABCG2/BCRP/MXR transporters. Biochem Pharmacol. 2009;78:153-161.

71. Burger H, van Tol H, Brok M, et al. Chronic imatinib mesylate exposure leads to reduced intracellular drug accumulation by induction of the ABCG2 (BCRP) and ABCB1 (MDR1) drug transport pumps. Cancer Biol Ther. 2005;4:747-752.

72. Burger H, van Tol H, Boersma AW, et al. Imatinib mesylate (STI571) is a substrate for the breast cancer resistance protein (BCRP)/ABCG2 drug pump. Blood. 2004;104:2940-2942.

73. Hamada A, Miyano H, Watanabe H, Saito H. Interaction of imatinib mesilate with human P-glycoprotein. J Pharmacol Exp Ther. 2003;307:824-828.

74. Illmer T, Schaich M, Platzbecker U, et al. P-glycoprotein-mediated drug efflux is a resistance mechanism of chronic myelogenous leukemia cells to treatment with imatinib mesylate. Leukemia. 2004;18:401-408.

75. Ozvegy-Laczka C, Hegedus T, Varady G, et al. High-affinity interaction of tyrosine kinase inhibitors with the ABCG2 multidrug transporter. Mol Pharmacol. 2004;65:1485-1495.

76. Dulucq S, Bouchet S, Turcq B, et al. Multidrug resistance gene (MDR1) polymorphisms are associated with major molecular responses to standard-dose imatinib in chronic myeloid leukemia. Blood. 2008;112:2024-2027.

77. Smith PJ, Furon E, Wiltshire M, et al. ABCG2-associated resistance to Hoechst 33342 and topotecan in a murine cell model with constitutive expression of side population characteristics. Cytometry A. 2009;75:924-933.

78. Davies A, Jordanides NE, Giannoudis A, et al. Nilotinib concentration in cell lines and primary CD34(+) chronic myeloid leukemia cells is not mediated by active uptake or efflux by major drug transporters. Leukemia. 2009;23:1999-2006.

79. Tsuruo T, Iida-Saito H, Kawabata H, Oh-hara T, Hamada H, Utakoji T. Characteristics of resistance to adriamycin in human myelogenous leukemia K562 resistant to adriamycin and in isolated clones. Jpn J Cancer Res. 1986;77:682-692.

80. Elkind NB, Szentpetery Z, Apati A, et al. Multidrug transporter ABCG2 prevents tumor cell death induced by the epidermal growth factor receptor inhibitor Iressa (ZD1839, Gefitinib). Cancer Res. 2005;65:1770-1777.

81. Mahon FX, Hayette S, Lagarde V, et al. Evidence that resistance to nilotinib may be due to BCR-ABL, Pgp, or Src kinase overexpression. Cancer Res. 2008;68:9809-9816.

82. Jiang X, Zhao Y, Smith C, et al. Chronic myeloid leukemia stem cells possess multiple unique features of resistance to BCR-ABL targeted therapies. Leukemia. 2007;21:926-935.

83. Mohamed AN, Pemberton P, Zonder J, Schiffer CA. The effect of imatinib mesylate on patients with Philadelphia chromosome-positive chronic myeloid leukemia with secondary chromosomal aberrations. Clin Cancer Res. 2003;9:1333-1337.

84. Mauro MJ. Defining and managing imatinib resistance. Hematology Am Soc Hematol Educ Program. 2006:219-225.

85. Liu Y, Fiskum G, Schubert D. Generation of reactive oxygen species by the mitochondrial electron transport chain. J Neurochem. 2002;80:780-787.

86. Wiseman H, Halliwell B. Damage to DNA by reactive oxygen and nitrogen species: role in inflammatory disease and progression to cancer. Biochem J. 1996;313 (Pt 1):17-29.

87. Krause DS, Van Etten RA. Tyrosine kinases as targets for cancer therapy. N Engl J Med. 2005;353:172-187.

88. Jackson AL, Loeb LA. The contribution of endogenous sources of DNA damage to the multiple mutations in cancer. Mutat Res. 2001;477:7-21.

89. Sattler M, Verma S, Shrikhande G, et al. The BCR/ABL tyrosine kinase induces production of reactive oxygen species in hematopoietic cells. J Biol Chem. 2000;275:24273-24278.

90. Penserga ET, Skorski T. Fusion tyrosine kinases: a result and cause of genomic instability. Oncogene. 2007;26:11-20.

91. Koptyra M, Falinski R, Nowicki MO, et al. BCR/ABL kinase induces self-mutagenesis via reactive oxygen species to encode imatinib resistance. Blood. 2006;108:319-327.

92. Kim JH, Chu SC, Gramlich JL, et al. Activation of the PI3K/mTOR pathway by BCR-ABL contributes to increased production of reactive oxygen species. Blood. 2005;105:1717-1723.

93. Nowicki MO, Falinski R, Koptyra M, et al. BCR/ABL oncogenic kinase promotes unfaithful repair of the reactive oxygen species-dependent DNA double-strand breaks. Blood. 2004;104:3746-3753.

94. Norbury CJ, Zhivotovsky B. DNA damage-induced apoptosis. Oncogene. 2004;23:2797-2808.

95. McGahon A, Bissonnette R, Schmitt M, Cotter KM, Green DR, Cotter TG. BCR-ABL maintains resistance of chronic myelogenous leukemia cells to apoptotic cell death. Blood. 1994;83:1179-1187.

96. Keeshan K, Cotter TG, McKenna SL. High Bcr-Abl expression prevents the translocation of Bax and Bad to the mitochondrion. Leukemia. 2002;16:1725-1734.

97. Burke BA, Carroll M. BCR-ABL: a multi-faceted promoter of DNA mutation in chronic myelogeneous leukemia. Leukemia. 2010;24:1105-1112.

98. Dierov J, Sanchez PV, Burke BA, et al. BCR/ABL induces chromosomal instability after genotoxic stress and alters the cell death threshold. Leukemia. 2008.

99. Deutsch E, Jarrousse S, Buet D, et al. Down-regulation of BRCA1 in BCR-ABL-expressing hematopoietic cells. Blood. 2003;101:4583-4588.

100. Stoklosa T, Poplawski T, Koptyra M, et al. BCR/ABL inhibits mismatch repair to protect from apoptosis and induce point mutations. Cancer Res. 2008;68:2576-2580.

101. Yun MH, Hiom K. Understanding the functions of BRCA1 in the DNA-damage response. Biochem Soc Trans. 2009;37:597-604.

102. Slupianek A, Nowicki MO, Koptyra M, Skorski T. BCR/ABL modifies the kinetics and fidelity of DNA double-strand breaks repair in hematopoietic cells. DNA Repair (Amst). 2006;5:243-250.

103. Gaymes TJ, Mufti GJ, Rassool FV. Myeloid leukemias have increased activity of the nonhomologous end-joining pathway and concomitant DNA misrepair that is dependent on the Ku70/86 heterodimer. Cancer Res. 2002;62:2791-2797.

104. Slupianek A, Poplawski T, Jozwiakowski SK, et al. BCR/ABL stimulates WRN to promote survival and genomic instability. Cancer Res. 2011;71:842-851.

105. Corbin AS, Buchdunger E, Pascal F, Druker BJ. Analysis of the structural basis of specificity of inhibition of the Abl kinase by STI571. J Biol Chem. 2002;277:32214-32219.

106. Hochhaus A, Kreil S, Corbin AS, et al. Molecular and chromosomal mechanisms of resistance to imatinib (STI571) therapy. Leukemia. 2002;16:2190-2196.

107. Gorre ME, Mohammed M, Ellwood K, et al. Clinical resistance to STI-571 cancer therapy caused by BCR-ABL gene mutation or amplification. Science. 2001;293:876-880.

108. Azam M, Latek RR, Daley GQ. Mechanisms of autoinhibition and STI-571/imatinib resistance revealed by mutagenesis of BCR-ABL. Cell. 2003;112:831-843.

109. Gambacorti-Passerini CB, Gunby RH, Piazza R, Galietta A, Rostagno R, Scapozza L. Molecular mechanisms of resistance to imatinib in Philadelphia-chromosome-positive leukaemias. Lancet Oncol. 2003;4:75-85.

110. Jiang X, Saw KM, Eaves A, Eaves C. Instability of BCR-ABL gene in primary and cultured chronic myeloid leukemia stem cells. J Natl Cancer Inst. 2007;99:680-693.

111. Willis SG, Lange T, Demehri S, et al. High-sensitivity detection of BCR-ABL kinase domain mutations in imatinib-naive patients: correlation with clonal cytogenetic evolution but not response to therapy. Blood. 2005;106:2128-2137.

112. Roche-Lestienne C, Soenen-Cornu V, Grardel-Duflos N, et al. Several types of mutations of the Abl gene can be found in chronic myeloid leukemia patients resistant to STI571, and they can pre-exist to the onset of treatment. Blood. 2002;100:1014-1018.

113. Flamant S, Turhan AG. Occurrence of de novo ABL kinase domain mutations in primary bone marrow cells after BCR-ABL gene transfer and Imatinib mesylate selection. Leukemia. 2005;19:1265-1267.

114. Muller MC, Lahaye T, Hochhaus A. [Resistance to tumor specific therapy with imatinib by clonal selection of mutated cells]. Dtsch Med Wochenschr. 2002;127:2205-2207.

115. Hayette S, Michallet M, Baille ML, Magaud JP, Nicolini FE. Assessment and follow-up of the proportion of T315I mutant BCR-ABL transcripts can guide appropriate therapeutic decision making in CML patients. Leuk Res. 2005;29:1073-1077.

116. Hanfstein B, Muller MC, Kreil S, et al. Dynamics of mutant BCR-ABL-positive clones after cessation of tyrosine kinase inhibitor therapy. Haematologica. 2011;96:360-366.

117. Weisberg E, Manley PW, Breitenstein W, et al. Characterization of AMN107, a selective inhibitor of native and mutant Bcr-Abl. Cancer Cell. 2005;7:129-141.

118. Tokarski JS, Newitt JA, Chang CY, et al. The structure of Dasatinib (BMS-354825) bound to activated ABL kinase domain elucidates its inhibitory activity against imatinib-resistant ABL mutants. Cancer Res. 2006;66:5790-5797.

119. O'Hare T, Eide CA, Deininger MW. Bcr-Abl kinase domain mutations, drug resistance, and the road to a cure for chronic myeloid leukemia. Blood. 2007;110:2242-2249.

120. Branford S, Melo JV, Hughes TP. Selecting optimal second-line tyrosine kinase inhibitor therapy for chronic myeloid leukemia patients after imatinib failure: does the BCR-ABL mutation status really matter? Blood. 2009;114:5426-5435.

121. Redaelli S, Piazza R, Rostagno R, et al. Activity of bosutinib, dasatinib, and nilotinib against 18 imatinib-resistant BCR/ABL mutants. J Clin Oncol. 2009;27:469-471.

122. Talpaz M, Shah NP, Kantarjian H, et al. Dasatinib in imatinib-resistant Philadelphia chromosome-positive leukemias. N Engl J Med. 2006;354:2531-2541.

123. Kantarjian H, Giles F, Wunderle L, et al. Nilotinib in imatinib-resistant CML and Philadelphia chromosome-positive ALL. N Engl J Med. 2006;354:2542-2551.

124. Noronha G, Cao J, Chow CP, et al. Inhibitors of ABL and the ABL-T315I mutation. Curr Top Med Chem. 2008;8:905-921.

125. Melo JV, Chuah C. Resistance to imatinib mesylate in chronic myeloid leukaemia. Cancer Lett. 2007;249:121-132.

126. Sherbenou DW, Hantschel O, Kaupe I, et al. BCR-ABL SH3-SH2 domain mutations in chronic myeloid leukemia patients on imatinib. Blood. 2010;116:3278-3285.

127. Mahon FX, Deininger MW, Schultheis B, et al. Selection and characterization of BCR-ABL positive cell lines with differential sensitivity to the tyrosine kinase inhibitor STI571: diverse mechanisms of resistance. Blood. 2000;96:1070-1079.

128. Knutsen T, Mickley LA, Ried T, et al. Cytogenetic and molecular characterization of random chromosomal rearrangements activating the drug resistance gene, MDR1/P-glycoprotein, in drug-selected cell lines and patients with drug refractory ALL. Genes Chromosomes Cancer. 1998;23:44-54.

129. Scotto KW. Transcriptional regulation of ABC drug transporters. Oncogene. 2003;22:7496-7511.

130. Krishnamurthy P, Ross DD, Nakanishi T, et al. The stem cell marker Bcrp/ABCG2 enhances hypoxic cell survival through interactions with heme. J Biol Chem. 2004;279:24218-24225.

131. Mayerhofer M, Valent P, Sperr WR, Griffin JD, Sillaber C. BCR/ABL induces expression of vascular endothelial growth factor and its transcriptional activator, hypoxia inducible factor-1alpha, through a pathway involving phosphoinositide 3-kinase and the mammalian target of rapamycin. Blood. 2002;100:3767-3775.

132. Nakanishi T, Shiozawa K, Hassel BA, Ross DD. Complex interaction of BCRP/ABCG2 and imatinib in BCR-ABL-expressing cells: BCRP-mediated resistance to imatinib is attenuated by imatinib-induced reduction of BCRP expression. Blood. 2006;108:678-684.

133. Arunasree KM, Roy KR, Anilkumar K, Aparna A, Reddy GV, Reddanna P. Imatinib-resistant K562 cells are more sensitive to celecoxib, a selective COX-2 inhibitor: role of COX-2 and MDR-1. Leuk Res. 2008;32:855-864.

134. Patel VA, Dunn MJ, Sorokin A. Regulation of MDR-1 (P-glycoprotein) by cyclooxygenase-2. J Biol Chem. 2002;277:38915-38920.

135. Zhang GS, Liu DS, Dai CW, Li RJ. Antitumor effects of celecoxib on K562 leukemia cells are mediated by cell-cycle arrest, caspase-3 activation, and downregulation of Cox-2 expression and are synergistic with hydroxyurea or imatinib. Am J Hematol. 2006;81:242-255.

136. Giles FJ, Kantarjian HM, Bekele BN, et al. Bone marrow cyclooxygenase-2 levels are elevated in chronic-phase chronic myeloid leukaemia and are associated with reduced survival. Br J Haematol. 2002;119:38-45.

137. Cisternino S, Mercier C, Bourasset F, Roux F, Scherrmann J-M. Expression, up-regulation, and transport activity of the multidrug-resistance protein Abcg2 at the mouse blood-brain barrier. Cancer Res. 2004;64:3296-3301.

138. Keeshan K, Mills KI, Cotter TG, McKenna SL. Elevated Bcr-Abl expression levels are sufficient for a haematopoietic cell line to acquire a drug-resistant phenotype. Leukemia. 2001;15:1823-1833.

139. le Coutre P, Tassi E, Varella-Garcia M, et al. Induction of resistance to the Abelson inhibitor STI571 in human leukemic cells through gene amplification. Blood. 2000;95:1758-1766.

140. Marega M, Piazza RG, Pirola A, et al. BCR and BCR-ABL regulation during myeloid differentiation in healthy donors and in chronic phase/blast crisis CML patients. Leukemia. 2010;24:1445-1449.

141. De Braekeleer E, Douet-Guilbert N, Le Bris MJ, Morel F, De Braekeleer M. Translocation 3;21, trisomy 8, and duplication of the Philadelphia chromosome: a rare but recurrent cytogenetic pathway in the blastic phase of chronic myeloid leukemia. Cancer Genet Cytogenet. 2007;179:159-161.

142. Morel F, Bris MJ, Herry A, et al. Double minutes containing amplified bcr-abl fusion gene in a case of chronic myeloid leukemia treated by imatinib. Eur J Haematol. 2003;70:235-239.

143. Bueno MJ, Perez de Castro I, Gomez de Cedron M, et al. Genetic and epigenetic silencing of microRNA-203 enhances ABL1 and BCR-ABL1 oncogene expression. Cancer Cell. 2008;13:496-506.

144. Biedler JL, Spengler BA. Metaphase chromosome anomaly: association with drug resistance and cell-specific products. Science. 1976;191:185-187.

145. Hahn PJ. Molecular biology of double-minute chromosomes. Bioessays. 1993;15:477-484.

146. Schwab M. Oncogene amplification in solid tumors. Semin Cancer Biol. 1999;9:319-325.

147. Storlazzi CT, Lonoce A, Guastadisegni MC, et al. Gene amplification as double minutes or homogeneously staining regions in solid tumors: origin and structure. Genome Res. 2010;20:1198-1206.

148. Vogt N, Lefevre SH, Apiou F, et al. Molecular structure of double-minute chromosomes bearing amplified copies of the epidermal growth factor receptor gene in gliomas. Proc Natl Acad Sci U S A. 2004;101:11368-11373.

149. Schoenlein PV, Shen DW, Barrett JT, Pastan I, Gottesman MM. Double minute chromosomes carrying the human multidrug resistance 1 and 2 genes are generated from the dimerization of submicroscopic circular DNAs in colchicine-selected KB carcinoma cells. Mol Biol Cell. 1992;3:507-520.

150. Balaban-Malenbaum G, Gilbert F. Double minute chromosomes and the homogeneously staining regions in chromosomes of a human neuroblastoma cell line. Science. 1977;198:739-741.

151. Bignell GR, Santarius T, Pole JC, et al. Architectures of somatic genomic rearrangement in human cancer amplicons at sequence-level resolution. Genome Res. 2007;17:1296-1303.

152. Campbell PJ, Stephens PJ, Pleasance ED, et al. Identification of somatically acquired rearrangements in cancer using genome-wide massively parallel paired-end sequencing. Nat Genet. 2008;40:722-729.

153. Coquelle A, Toledo F, Stern S, Bieth A, Debatisse M. A new role for hypoxia in tumor progression: induction of fragile site triggering genomic rearrangements and formation of complex DMs and HSRs. Mol Cell. 1998;2:259-265.

154. Quentmeier H, Eberth S, Romani J, Zaborski M, Drexler HG. BCR-ABL1-independent PI3Kinase activation causing imatinib-resistance. J Hematol Oncol. 2011;4:6.

155. Dai Y, Rahmani M, Corey SJ, Dent P, Grant S. A Bcr/Abl-independent, Lyn-dependent form of imatinib mesylate (STI-571) resistance is associated with altered expression of Bcl-2. J Biol Chem. 2004;279:34227-34239.

156. Donato NJ, Wu JY, Stapley J, et al. BCR-ABL independence and LYN kinase overexpression in chronic myelogenous leukemia cells selected for resistance to STI571. Blood. 2003;101:690-698.

157. Wang Y, Cai D, Brendel C, et al. Adaptive secretion of granulocyte-macrophage colony-stimulating factor (GM-CSF) mediates imatinib and nilotinib resistance in BCR/ABL+ progenitors via JAK-2/STAT-5 pathway activation. Blood. 2007;109:2147-2155.

158. Saudemont A, Hamrouni A, Marchetti P, et al. Dormant tumor cells develop cross-resistance to apoptosis induced by CTLs or imatinib mesylate via methylation of suppressor of cytokine signaling 1. Cancer Res. 2007;67:4491-4498.

159. Liu J, Joha S, Idziorek T, et al. BCR-ABL mutants spread resistance to non-mutated cells through a paracrine mechanism. Leukemia. 2008;22:791-799.

160. Burchert A, Wang Y, Cai D, et al. Compensatory PI3-kinase/Akt/mTor activation regulates imatinib resistance development. Leukemia. 2005;19:1774-1782.

161. Barnes DJ, Palaiologou D, Panousopoulou E, et al. Bcr-Abl expression levels determine the rate of development of resistance to imatinib mesylate in chronic myeloid leukemia. Cancer Res. 2005;65:8912-8919.

162. Branford S, Rudzki Z, Parkinson I, et al. Real-time quantitative PCR analysis can be used as a primary screen to identify patients with CML treated with imatinib who have BCR-ABL kinase domain mutations. Blood. 2004;104:2926-2932.

163. Press RD, Willis SG, Laudadio J, Mauro MJ, Deininger MW. Determining the rise in BCR-ABL RNA that optimally predicts a kinase domain mutation in patients with chronic myeloid leukemia on imatinib. Blood. 2009;114:2598-2605.

164. Yuan H, Wang Z, Gao C, et al. BCR-ABL gene expression is required for its mutations in a novel KCL-22 cell culture model for acquired resistance of chronic myelogenous leukemia. J Biol Chem. 2010;285:5085-5096.

165. White D, Dang P, Venables A, et al. ABCB1 overexpression may predispose imatinib treated CML patients to the development of Abl kinase domain mutations, and may be an important contributor to acquired resistance. ASH annual meeting abstracts. 2006;108.

166. Lozzio CB, Lozzio BB. Human chronic myelogenous leukemia cell-line with positive Philadelphia chromosome. Blood. 1975;45:321-334.

167. Kishi K. A new leukemia cell line with Philadelphia chromosome characterized as basophil precursors. Leuk Res. 1985;9:381-390.

168. Branford S, Hughes TP, Rudzki Z. Monitoring chronic myeloid leukaemia therapy by real-time quantitative PCR in blood is a reliable alternative to bone marrow cytogenetics. Br J Haematol. 1999;107:587-599.

169. Branford S, Rudzki Z, Walsh S, et al. Detection of BCR-ABL mutations in patients with CML treated with imatinib is virtually always accompanied by clinical resistance, and mutations in the ATP phosphate-binding loop (P-loop) are associated with a poor prognosis. Blood. 2003;102:276-283.

170. Ding C, Chiu RW, Lau TK, et al. MS analysis of single-nucleotide differences in circulating nucleic acids: Application to noninvasive prenatal diagnosis. Proc Natl Acad Sci U S A. 2004;101:10762-10767.

171. Miller E. Apoptosis measurement by annexin v staining. Methods Mol Med. 2004;88:191-202.

172. White DL, Saunders VA, Dang P, et al. OCT-1-mediated influx is a key determinant of the intracellular uptake of imatinib but not nilotinib (AMN107): reduced OCT-1 activity is the cause of low in vitro sensitivity to imatinib. Blood. 2006;108:697-704.

173. Dewar AL, Zannettino AC, Hughes TP, Lyons AB. Inhibition of c-fms by imatinib: expanding the spectrum of treatment. Cell Cycle. 2005;4:851-853.

174. Carroll M, Ohno-Jones S, Tamura S, et al. CGP 57148, a tyrosine kinase inhibitor, inhibits the growth of cells expressing BCR-ABL, TEL-ABL, and TEL-PDGFR fusion proteins. Blood. 1997;90:4947-4952.

175. Fraunfelder FW, Solomon J, Druker BJ, Esmaeli B, Kuyl J. Ocular side-effects associated with imatinib mesylate (Gleevec). J Ocul Pharmacol Ther. 2003;19:371-375.

176. van Oosterom AT, Judson I, Verweij J, et al. Safety and efficacy of imatinib (STI571) in metastatic gastrointestinal stromal tumours: a phase I study. Lancet. 2001;358:1421-1423.

177. Scheinfeld N. Imatinib mesylate and dermatology part 2: a review of the cutaneous side effects of imatinib mesylate. J Drugs Dermatol. 2006;5:228-231.

178. Burkhart PV, Sabate E. Adherence to long-term therapies: evidence for action. J Nurs Scholarsh. 2003;35:207.

179. Noens L, van Lierde MA, De Bock R, et al. Prevalence, determinants, and outcomes of nonadherence to imatinib therapy in patients with chronic myeloid leukemia: the ADAGIO study. Blood. 2009;113:5401-5411.

180. Peng B, Lloyd P, Schran H. Clinical pharmacokinetics of imatinib. Clin Pharmacokinet. 2005;44:879-894.

181. Gambacorti-Passerini C, Zucchetti M, Russo D, et al. Alpha1 acid glycoprotein binds to imatinib (STI571) and substantially alters its pharmacokinetics in chronic myeloid leukemia patients. Clin Cancer Res. 2003;9:625-632.

182. White DL, Dang P, Engler J, et al. Functional activity of the OCT-1 protein is predictive of long-term outcome in patients with chronic-phase chronic myeloid leukemia treated with imatinib. J Clin Oncol;28:2761-2767.

183. Appelbaum PC. Antimicrobial resistance in Streptococcus pneumoniae: an overview. Clin Infect Dis. 1992;15:77-83.

184. Carey B, Cryan B. Antibiotic misuse in the community--a contributor to resistance? Ir Med J. 2003;96:43-44, 46.

185. Witte W. Medical consequences of antibiotic use in agriculture. Science. 1998;279:996-997.

186. Watson MB, Lind MJ, Cawkwell L. Establishment of in-vitro models of chemotherapy resistance. Anticancer Drugs. 2007;18:749-754.

187. Akiyama S, Fojo A, Hanover JA, Pastan I, Gottesman MM. Isolation and genetic characterization of human KB cell lines resistant to multiple drugs. Somat Cell Mol Genet. 1985;11:117-126.

188. Yan XD, Li M, Yuan Y, Mao N, Pan LY. Biological comparison of ovarian cancer resistant cell lines to cisplatin and Taxol by two different administrations. Oncol Rep. 2007;17:1163-1169.

189. Bosmann HB. Mechanism of cellular drug resistance. Nature. 1971;233:566-569.

190. Passamonti F, Lazzarino M. Treatment of polycythemia vera and essential thrombocythemia: the role of pipobroman. Leuk Lymphoma. 2003;44:1483-1488.

191. Valdez BC, Andersson BS. Interstrand crosslink inducing agents in pretransplant conditioning therapy for hematologic malignancies. Environ Mol Mutagen. 2010;51:659-668.

192. Selden JR, Emanuel BS, Wang E, et al. Amplified C lambda and c-abl genes are on the same marker chromosome in K562 leukemia cells. Proc Natl Acad Sci U S A. 1983;80:7289-7292.

193. Naumann S, Reutzel D, Speicher M, Decker HJ. Complete karyotype characterization of the K562 cell line by combined application of G-banding, multiplex-fluorescence in situ hybridization, fluorescence in situ hybridization, and comparative genomic hybridization. Leuk Res. 2001;25:313-322.

194. Lozzio BB, Lozzi CB, Machado E. Human myelogenous (Ph+) leukemia cell line: transplantation into athymic mice. J Natl Cancer Inst. 1976;56:627-629.

195. Mahon FX, Belloc F, Lagarde V, et al. MDR1 gene overexpression confers resistance to imatinib mesylate in leukemia cell line models. Blood. 2003;101:2368-2373.

196. Hughes T, Deininger M, Hochhaus A, et al. Monitoring CML patients responding to treatment with tyrosine kinase inhibitors: review and recommendations for harmonizing current methodology for detecting BCR-ABL transcripts and kinase domain mutations and for expressing results. Blood. 2006;108:28-37.

197. Pene-Dumitrescu T, Smithgall TE. Expression of a Src family kinase in chronic myelogenous leukemia cells induces resistance to imatinib in a kinase-dependent manner. J Biol Chem. 2010;285:21446-21457.

198. Hiwase DK, White DL, Powell JA, et al. Blocking cytokine signaling along with intense Bcr-Abl kinase inhibition induces apoptosis in primary CML progenitors. Leukemia. 2010;24:771-778.

199. Shah NP, Kasap C, Weier C, et al. Transient potent BCR-ABL inhibition is sufficient to commit chronic myeloid leukemia cells irreversibly to apoptosis. Cancer Cell. 2008;14:485-493.

200. Juliano RL, Ling V. A surface glycoprotein modulating drug permeability in Chinese hamster ovary cell mutants. Biochim Biophys Acta. 1976;455:152-162.

201. Hochhauser D, Harris AL. Drug resistance. Br Med Bull. 1991;47:178-196.

202. Linn SC, Giaccone G. MDR1/P-glycoprotein expression in colorectal cancer. Eur J Cancer. 1995;31A:1291-1294.

203. Schneider J, Bak M, Efferth T, Kaufmann M, Mattern J, Volm M. P-glycoprotein expression in treated and untreated human breast cancer. Br J Cancer. 1989;60:815-818.

204. Liu Q, Ohshima K, Kikuchi M. High expression of MDR-1 gene and P-glycoprotein in initial and re-biopsy specimens of relapsed B-cell lymphoma. Histopathology. 2001;38:209-216.

205. Schadendorf D, Herfordt R, Czarnetzki BM. P-glycoprotein expression in primary and metastatic malignant melanoma. Br J Dermatol. 1995;132:551-555.

206. Giles FJ, Kantarjian HM, Cortes J, et al. Multidrug resistance protein expression in chronic myeloid leukemia: associations and significance. Cancer. 1999;86:805-813.

207. Kobayashi Y, Seino K, Hosonuma S, et al. Side population is increased in paclitaxel-resistant ovarian cancer cell lines regardless of resistance to cisplatin. Gynecol Oncol. 2011;121:390-394.

208. Kuwazuru Y, Yoshimura A, Hanada S, et al. Expression of the multidrug transporter, P-glycoprotein, in chronic myelogenous leukaemia cells in blast crisis. Br J Haematol. 1990;74:24-29.

209. Carulli G, Petrini M, Marini A, Ambrogi F. P-glycoprotein in acute nonlymphoblastic leukemia and in the blastic crisis of myeloid leukemia. N Engl J Med. 1988;319:797-798.

210. Herweijer H, Sonneveld P, Baas F, Nooter K. Expression of mdr1 and mdr3 multidrug-resistance genes in human acute and chronic leukemias and association with stimulation of drug accumulation by cyclosporine. J Natl Cancer Inst. 1990;82:1133-1140.

211. Galimberti S, Cervetti G, Guerrini F, et al. Quantitative molecular monitoring of BCR-ABL and MDR1 transcripts in patients with chronic myeloid leukemia during Imatinib treatment. Cancer Genet Cytogenet. 2005;162:57-62.

212. Dietel M, Arps H, Lage H, Niendorf A. Membrane vesicle formation due to acquired mitoxantrone resistance in human gastric carcinoma cell line EPG85-257. Cancer Res. 1990;50:6100-6106.

213. Futscher BW, Abbaszadegan MR, Domann F, Dalton WS. Analysis of MRP mRNA in mitoxantrone-selected, multidrug-resistant human tumor cells. Biochem Pharmacol. 1994;47:1601-1606.

214. Hazlehurst LA, Foley NE, Gleason-Guzman MC, et al. Multiple mechanisms confer drug resistance to mitoxantrone in the human 8226 myeloma cell line. Cancer Res. 1999;59:1021-1028.

215. Taylor CW, Dalton WS, Parrish PR, et al. Different mechanisms of decreased drug accumulation in doxorubicin and mitoxantrone resistant variants of the MCF7 human breast cancer cell line. Br J Cancer. 1991;63:923-929.

216. Nakagawa M, Schneider E, Dixon KH, et al. Reduced intracellular drug accumulation in the absence of P-glycoprotein (mdr1) overexpression in mitoxantrone-resistant human MCF-7 breast cancer cells. Cancer Res. 1992;52:6175-6181.

217. Doyle LA, Ross DD. Multidrug resistance mediated by the breast cancer resistance protein BCRP (ABCG2). Oncogene. 2003;22:7340-7358.

218. Doyle LA, Yang W, Abruzzo LV, et al. A multidrug resistance transporter from human MCF-7 breast cancer cells. Proc Natl Acad Sci U S A. 1998;95:15665-15670.

219. Scharenberg CW, Harkey MA, Torok-Storb B. The ABCG2 transporter is an efficient Hoechst 33342 efflux pump and is preferentially expressed by immature human hematopoietic progenitors. Blood. 2002;99:507-512.

220. Le Gal JM, Morjani H, Manfait M. Ultrastructural appraisal of the multidrug resistance in K562 and LR73 cell lines from Fourier transform infrared spectroscopy. Cancer Res. 1993;53:3681-3686.

221. Marie JP, Faussat-Suberville AM, Zhou D, Zittoun R. Daunorubicin uptake by leukemic cells: correlations with treatment outcome and mdr1 expression. Leukemia. 1993;7:825-831.

222. Watanabe T, Tsuge H, Oh-Hara T, Naito M, Tsuruo T. Comparative study on reversal efficacy of SDZ PSC 833, cyclosporin A and verapamil on multidrug resistance in vitro and in vivo. Acta Oncol. 1995;34:235-241.

223. Hochhaus A, Rosee PL, Muller MC, Ernst T, Cross NC. Impact of BCR-ABL mutations on patients with chronic myeloid leukemia. Cell Cycle. 2011;10:250-260.

224. Campbell LJ, Patsouris C, Rayeroux KC, Somana K, Januszewicz EH, Szer J. BCR/ABL amplification in chronic myelocytic leukemia blast crisis following imatinib mesylate administration. Cancer Genet Cytogenet. 2002;139:30-33.

225. Vasconcelos FC, Silva KL, de Souza PS, et al. Variation of MDR proteins expression and activity levels according to clinical status and evolution of CML patients. Cytometry B Clin Cytom. 2011;80:158-166.

226. Lehne G, Rugstad HE. Cytotoxic effect of the cyclosporin PSC 833 in multidrug-resistant leukaemia cells with increased expression of P-glycoprotein. Br J Cancer. 1998;78:593-600.

227. Apperley JF. Part I: mechanisms of resistance to imatinib in chronic myeloid leukaemia. Lancet Oncol. 2007;8:1018-1029.

228. Greenberger JS, Sakakeeny MA, Humphries RK, Eaves CJ, Eckner RJ. Demonstration of permanent factor-dependent multipotential (erythroid/neutrophil/basophil) hematopoietic progenitor cell lines. Proc Natl Acad Sci U S A. 1983;80:2931-2935.

229. Laneuville P, Heisterkamp N, Groffen J. Expression of the chronic myelogenous leukemia-associated p210bcr/abl oncoprotein in a murine IL-3 dependent myeloid cell line. Oncogene. 1991;6:275-282.

230. Ross DM, Schafranek L, Hughes TP, Nicola M, Branford S, Score J. Genomic translocation breakpoint sequences are conserved in BCR-ABL1 cell lines despite the presence of amplification. Cancer Genet Cytogenet. 2009;189:138-139.

231. Sughrue ME, Rutkowski MJ, Kane AJ, Parsa AT. Human glioma demonstrates cell line specific results with ATP-based chemiluminescent cellular proliferation assays. J Clin Neurosci. 2010;17:1573-1577.

232. Tsuji K, Kawauchi S, Saito S, et al. Breast cancer cell lines carry cell line-specific genomic alterations that are distinct from aberrations in breast cancer tissues: comparison of the CGH profiles between cancer cell lines and primary cancer tissues. BMC Cancer. 2010;10:15.

233. Gleixner KV, Ferenc V, Peter B, et al. Polo-like kinase 1 (Plk1) as a novel drug target in chronic myeloid leukemia: overriding imatinib resistance with the Plk1 inhibitor BI 2536. Cancer Res. 2010;70:1513-1523.

234. Summy JM, Gallick GE. Treatment for advanced tumors: SRC reclaims center stage. Clin Cancer Res. 2006;12:1398-1401.

235. Bradeen HA, Eide CA, O'Hare T, et al. Comparison of imatinib mesylate, dasatinib (BMS-354825), and nilotinib (AMN107) in an N-ethyl-N-nitrosourea (ENU)-based mutagenesis screen: high efficacy of drug combinations. Blood. 2006;108:2332-2338.

236. Mountford J, Davies A, Jordanides NE, et al. Nilotinib concentration in Cell Lines and CML CD34+ Cells Is Not Mediated by Active Uptake or Efflux by Major Drug Transporters. ASH Annual Meeting Abstracts. 2008;3205.

237. Shah NP, Skaggs BJ, Branford S, et al. Sequential ABL kinase inhibitor therapy selects for compound drug-resistant BCR-ABL mutations with altered oncogenic potency. J Clin Invest. 2007;117:2562-2569.

238. Garg RJ, Kantarjian H, O'Brien S, et al. The use of nilotinib or dasatinib after failure to 2 prior tyrosine kinase inhibitors: long-term follow-up. Blood. 2009;114:4361-4368.

239. Kim D, Kim DW, Cho BS, et al. Structural modeling of V299L and E459K Bcr-Abl mutation, and sequential therapy of tyrosine kinase inhibitors for the compound mutations. Leuk Res. 2009.

240. Nicolini FE, Chabane K, Tigaud I, Michallet M, Magaud JP, Hayette S. BCR-ABL mutant kinetics in CML patients treated with dasatinib. Leuk Res. 2007;31:865-868.

241. Ustun C, Jillella AP, Salama ME. Dasatinib induces complete cytogenetic response and loss of F359C in an imatinib resistant chronic myelocytic leukemia patient. Am J Hematol. 2009;84:386-387.

242. Persidis A. Cancer multidrug resistance. Nat Biotechnol. 1999;17:94-95.

243. Chen Y. Are SRC family kinases responsible for imatinib- and dasatinib-resistant chronic myeloid leukemias? Leuk Res. 2010;35:27-29.

244. Hayette S, Chabane K, Michallet M, et al. Longitudinal studies of SRC family kinases in imatinib- and dasatinib-resistant chronic myelogenous leukemia patients. Leuk Res. 2011;35:38-43.

245. Cohen DM. SRC family kinases in cell volume regulation. Am J Physiol Cell Physiol. 2005;288:C483-493.

246. Taylor SJ, Shalloway D. Src and the control of cell division. Bioessays. 1996;18:9-11.

247. Thomas SM, Brugge JS. Cellular functions regulated by Src family kinases. Annu Rev Cell Dev Biol. 1997;13:513-609.

248. Frame MC. Newest findings on the oldest oncogene; how activated src does it. J Cell Sci. 2004;117:989-998.

249. Sharma SV, Gajowniczek P, Way IP, et al. A common signaling cascade may underlie "addiction" to the Src, BCR-ABL, and EGF receptor oncogenes. Cancer Cell. 2006;10:425-435.

250. Wu J, Meng F, Lu H, et al. Lyn regulates BCR-ABL and Gab2 tyrosine phosphorylation and c-Cbl protein stability in imatinib-resistant chronic myelogenous leukemia cells. Blood. 2008;111:3821-3829.

251. Parker WT, Ho M, Lawrence RM, et al. Detection of Low Level Nilotinib or Dasatinib Resistant BCR-ABL Mutations by Mass Spectrometry In CML Patients Who Fail Imatinib Is Highly Predictive of Their Subsequent Clonal Expansion When Treated with the Drug for Which Their Mutation Confers Resistance. ASH annual meeting abstracts. 2010;116.

252. Warmuth M, Bergmann M, Priess A, Hauslmann K, Emmerich B, Hallek M. The Src family kinase Hck interacts with Bcr-Abl by a kinase-independent mechanism and phosphorylates the Grb2-binding site of Bcr. J Biol Chem. 1997;272:33260-33270.

253. Meyn MA, 3rd, Wilson MB, Abdi FA, et al. Src family kinases phosphorylate the Bcr-Abl SH3-SH2 region and modulate Bcr-Abl transforming activity. J Biol Chem. 2006;281:30907-30916.

254. Chen S, O'Reilly LP, Smithgall TE, Engen JR. Tyrosine phosphorylation in the SH3 domain disrupts negative regulatory interactions within the c-Abl kinase core. J Mol Biol. 2008;383:414-423.

255. Weisberg E, Manley PW, Cowan-Jacob SW, Hochhaus A, Griffin JD. Second generation inhibitors of BCR-ABL for the treatment of imatinib-resistant chronic myeloid leukaemia. Nat Rev Cancer. 2007;7:345-356.

256. Gordon MY. Biological consequences of the BCR/ABL fusion gene in humans and mice. J Clin Pathol. 1999;52:719-722.

257. Peng B, Dutreix C, Mehring G, et al. Absolute bioavailability of imatinib (Glivec) orally versus intravenous infusion. J Clin Pharmacol. 2004;44:158-162.

258. Floyd MD, Gervasini G, Masica AL, et al. Genotype-phenotype associations for common CYP3A4 and CYP3A5 variants in the basal and induced metabolism of midazolam in European- and African-American men and women. Pharmacogenetics. 2003;13:595-606.

259. Gambacorti-Passerini C, le Coutre P, Zucchetti M, D'Incalci M. Binding of imatinib by alpha(1)-acid glycoprotein. Blood. 2002;100:367-368; author reply 368-369.